Diss. ETH NO. 22557

# Characterization of individual steryl ferulates: occurrence in rice, antioxidant and Caco-2 cell permeation properties

A thesis submitted to attain the degree of

DOCTOR OF SCIENCES of ETH ZURICH

(Dr. sc. ETH Zurich)

presented by

## DAN ZHU

Master of Agriculture, Zhejiang University

born on 18.12.1985

citizen of China

accepted on the recommendation of

Prof. Dr. Laura Nyström, examiner

Prof. Dr. Jean-Christophe Leroux, co-examiner

Prof. Dr. Zhimin Xu, co-examiner

2015

One never notices what has been done;
one can only see what remains to be done.

Marie Curie

# Abstract

Steryl ferulates, esters of ferulic acid and phytosterols, are secondary plant metabolites present in the bran layers of cereal grains. They are a subclass of bioactive lipids, contributing to the health promoting effects of whole grains. So far the mixture of steryl ferulates in rice, γ-oryzanol, has mostly been studied, but there are indications that individual steryl ferulates may vary in their bioactivity. This study aims to provide a better understanding on the occurrence and properties of individual steryl ferulates. First, differentiation of various rice varieties was achieved by analysing the profiles of these minor lipids in rice. Further focus was put on the comparison of antioxidant activity of individual steryl ferulates. Moreover, the permeation of individual steryl ferulates using an *in vitro* intestinal barrier model was studied to explore their intestinal absorption mechanism.

The analysis of steryl ferulates was enabled through the new analytical techniques ultra performance liquid chromatography with high-resolution quadrupole time-of-flight mass spectrometric detection (UPLC-HR-Q-TOF-MS). With OMIC-technologies, we were able to find the characteristic markers that enable the differentiation of rice varieties based on their profiles of steryl ferulate and other small lipids. This study provides a targeted method for rice differentiation, which could be a new approach for rice authentication. Furthermore, these results could also be applied for the selection of rice varieties with optimal profiles of bioactive lipids.

Antioxidant activity of individual steryl ferulates was compared in different radical scavenging models. Eight individual steryl ferulates were obtained by purification from various cereal grain sources or by chemical synthesis. Our study demonstrates that individual steryl ferulates exhibit DPPH radical, hydroxyl radical, and superoxide anion radical scavenging abilities with subtle differences that are highly dependent on the kind of reaction taking place. Additionally, molecular simulations were carried out to identify correlations between molecular properties and their antioxidant activity. The grouping of steryl ferulates by principle component analysis was mainly attributed to molecular

i

properties, not antioxidant activities. Moreover, solvation energy was significantly correlated with some experimental observations. Results of this work demonstrate the differences in the antioxidant activities of steryl ferulates are very small.

Furthermore, the antioxidant effect of individual steryl ferulates on the kinetics of methyl linoleate autoxidation was also investigated. This was achieved by measuring the consumption rate of oxygen in peroxidating methyl linoleate in the presence and absence of different steryl ferulates by electron spin resonance spectroscopy. No induction period was observed for steryl ferulates even if they could retard lipid peroxidation. In the applied experimental conditions, the rate constant for hydrogen-atom transfer from steryl ferulate to lipid peroxyl radical was determined and no significant differences in antioxidant effect were found among individual steryl ferulates.

Finally, we investigated the permeation of individual steryl ferulates using an *in vitro* Caco-2 cell monolayer model that mimicked the intestinal barrier. A highly sensitive and accurate quantification method of individual steryl ferulates based on UPLC-HR-Q-TOF-MS was developed, which is a useful tool to investigate steryl ferulates in extremely low concentrations, bypassing the requirement of radioactivity handling. Although only a negligible amount of steryl ferulates ($< 0.5\%$) permeated across the Caco-2 cell monolayer, some differences in the permeability coefficients were observed between individual steryl ferulates. Permeation mechanism was mainly passive diffusion. This work demonstrates that the permeation of steryl ferulates across the gut is very low. Therefore, their cholesterol lowering and antioxidant activity related health benefits most likely occur in the gut independently from absorption.

Overall, this study shows that steryl ferulates are potent dietary antioxidants available from whole grains. The results obtained in this work provide better insight into the metabolism and bioactivities of individual steryl ferulates. The highly sensitive analytical methods developed in this study can further be applied to the analysis of steryl ferulates and their bioactivities in biological samples in further explorations of their mechanisms of action in the gut.

# Zusammenfassung

Sterylferulate, Ferulasäurepflanzensterylester, sind sekundäre Pflanzenmetabolite und kommen in der Kleie von Getreiden vor. Sie sind bekannt als bioaktive Lipide, welche zum gesundheitsfördernden Effekt von Vollkorn beitragen. Die Mischung von Sterylferulaten, welche im Reis vorkommt (γ-Oryzanol), ist bis jetzt am meisten untersucht worden. Weiter gibt es Hinweise auf eine unterschiedliche Bioaktivität zwischen den indiviuellen Sterylferulaten. Ziel dieser Doktorarbeit war es, ein besseres Verständnis vom Auftreten und der Eigenschaften dieser individuellen Sterylferulate zu gewinnen. Zuerst wurden verschiedene Reissorten anhand ihrer Sterylferulat-Profile differenziert. Weiter wurde der Vergleich der Antioxidanswirkung der individuellen Sterylferulate analysiert. Die Permeation der individuellen Sterylferulate wurde in einem *in vitro* Modell der intestinalen Barriere analysiert um ihren Absorptionsmechanismus im Darm zu ermitteln.

Die Analyse der Sterylferulate wurde möglich durch eine neue analytische Methode basierend auf Ultrahochleistungsflüssigkeitschromatographie gekoppelt mit einem hochauflösenden Flugzeitquadrupol-Massenspektrometer (UPLC-HR-Q-TOF-MS). Durch Metabolomik waren wir in der Lage prominente Marker zu identifizieren, welche eine Differenzierung der verschiedenen Reissorten basierend auf ihren Profilen der verschiedenen Sterylferulate und anderer kleiner Lipide zuliessen. Diese Studie bietet eine informative Methode für die Differenzierung von Reissorten, welche ein neuer Ansatz für die Reisauthentifizierung sein könnte. Weiter könnte diese Methode angewandt werden um Reissorten mit optimalen Profilen der bioaktiven Lipide auszuwählen.

Die antioxioxidative Wirkung der individuellen Sterylferulate wurde in verschiedenen Radikalfängermodellen verglichen. Acht unterschiedliche Sterylferulate wurden durch Aufreinigung von diversen Getreiden und durch Synthese gewonnen. Unsere Studie zeigt, dass individuelle Sterylferulate kleine Unterschiede in ihrer Antioxidanswirkung zeigen, abhängig von der Reaktion, welche im jeweiligen Test (DPPH-Assay,

Hydroxyl-Radikal-Assay und Superoxid-Anion-Radikal-Assay) abläuft. Zusätzlich wurden durch Computersimulation Korrelationen zwischen den molekularen Eigenschaften und deren Antioxidanswirkung identifiziert. Die Gruppierung, welche durch Hauptkomponentenanalyse erfolgte, war hauptsächlich auf die molekularen Eigenschaften zurückzuführen und weniger auf ihre Wirkung als Antioxidantien. Die Lösungsenergie war signifikant korrelierend mit einigen experimentellen Beobachtungen. Die Resultate dieser Arbeit zeigen, dass die Differenzen der antioxidativen Wirkung zwischen den individuellen Sterylferulaten eher klein sind.

Ausserdem wurde die Antioxidanswirkung der individuellen Sterylferulate anhand der Kinetik der Linolsäuremethylester-Autooxidation bestimmt. Die Saurestoffkonsumrate durch die Peroxidation der Linolsäuremethylester wurde mit und ohne Sterylferulatzusatz durch Elektronenspinresonanz bestimmt. Mit Sterylferulaten konnte zwar keine Verzögerung beobachtet werden, die Peroxidation wurde jedoch verlangsamt. In diesem Versuchsaufbau wurde die Geschwindigkeitskonstante für den Wasserstoffatomtransfer vom Sterylferulat zum Peroxylradikal des Lipids bestimmt. Es konnte keinen signifikanten Unterschiede der Antioxidanswirkung zwischen den individuellen Sterylferulaten festgestellt werden.

Zuletzt haben wir die Permeation der individuellen Sterylferulate in einem einschichtigen *in vitro* Caco-2-Zellmodell untersucht, welches die intestinale Barriere imitiert. Eine höchst sensitive und präzise Quantifizierungsmethode basierend auf dem HR-Q-TOF-MS wurde dazu entwickelt. Diese ermöglichte die Untersuchung der Sterylferulaten bei extrem tiefen Konzentrationen, was die Vermeidung von Radioaktivität erlaubte. Auch wenn nur ein verschwindend kleiner Anteil (<0.5%) die einschichtigen Caco-2-Zellen passierte, konnten Unterschiede in den Permeationskoeffizienten zwischen den individuellen Sterylferulaten beobachtet werden. Der Permeationsmechanismus war hauptsächlich mittels passiver Diffusion. Diese Arbeit zeigt, dass die Permeation der Sterylferulaten durch den Darm sehr klein ist. Folglich muss ihre cholesterinsenkende Wirkung und die antioxidativen

Gesundheitsnutzen wahrscheinlich im Darm stattfinden, unabhängig von der Absorption.

Insgesamt zeigt diese Studie, dass Sterylferulate potente Antioxidantien in Vollkornmahlzeiten sind. Die gewonnen Resultate stellen eine vertiefte Einsicht in den Metabolismus und Bioaktivität der individuellen Sterylferulate dar. Die hoch sensitiven Analysemethoden, welche im Rahmen dieser Doktorarbeit entwickelt wurden, können angewendet werden, um Sterylferulate und ihre Bioaktivität in biologischen Proben vertiefter zu untersuchen und ihren Wirkungsmechanismus im Darm weiter zu entschlüsseln.

# List of abbreviations

| | |
|---|---|
| ACN | Acetonitrile |
| BSA | Bovine Serum Albumin |
| DMEM | Dulbecco's Modified Eagle Medium |
| DMPO | 5,5-Dimethyl-1-pyrroline N-oxide |
| DPPH$^\bullet$ | 2,2-Diphenyl-1-picrylhydrazyl Radical |
| ESI | Electrospray Ionisation |
| ESR | Electron Spin Resonance |
| HBSS | Hank's Balanced Salt Solution |
| HPLC | High Performance Liquid Chromatography |
| HPX | Hypoxanthine |
| LOD | Limit of Detection |
| LOQ | Limit of Quantification |
| LY | Lucifer Yellow |
| MS | Mass Spectrometry |
| NBT | Nitrotetrazolium Blue chloride |
| $^\bullet$OH | Hydroxyl Radical |
| $O_2^{\bullet-}$ | Superoxide Anion Radical |
| OPLS-DA | Observed Partial Least Squares-Discriminant Analysis |
| $P_{app}$ | Apparent Permeability Coefficient |
| PCA | Principle Component Analysis |
| RP | Reverse Phase |
| RT | Retention Time |
| SF | Steryl Ferulate |
| SPE | Solid Phase Extraction |
| TEER | Transepithelial Electrical Resistance |
| TOF | Time-of-Flight |
| UPLC | Ultra Performance Liquid Chromatography |
| UV-VIS | Ultraviolet-Visible Spectroscopy |
| XOD | Xanthine Oxidase |

# Acknowledgements

First of all, I would like to warmly thank my supervisor Prof. Dr. Laura Nyström for giving me the opportunity to do my PhD in this very interesting field. I'm very grateful for your excellent guidance and support throughout the work. I would also like to express my gratitude to Prof. Dr. Jean-Christophe Leroux, for his valuable support and advice concerning the permeation study. I thank him and Prof. Dr. Zhimin Xu from Louisiana State University for accepting to be the co-examiners of this dissertation. Many thanks go to Dr. Antoni Sánchez-Ferrer who synthesized three types of steryl ferulates and provided the knowledge of simulation. Very special thanks to Dr. Davide Brambilla who introduced the cell experiment and always gave valuable suggestions and comments. I also thank Prof. Dr. Shana J. Sturla for inspiring discussions.

I owe many thanks to Eleni Dimitriadou who made valuable contribution to the oxygen consumption study. Many thanks go to Aline Schär, who helped to translate the abstract in German and is willing to provide help and share knowledge anytime. I thank Dr. Audrey Faure who introduced me the EPR instrument. Many thanks also to Linda Münger for her nice help and suggestions. I wish to thank Dr. Anja Rahn for her valuable feedbacks on my writing. My thanks also go to Samy Boulos and Attila Bagdi for always giving me good suggestions. I thank all the current and former lab members, especially Daniela Kalbermatter, Nadja Romano, Aida Huber, Dr. Eszter Mandak, Teresa Angst. I also want to thank the members of Leroux's group, who are always very friendly and kind. All of you broaden my vision in many ways. Working with you is very great.

# Contents

# Introduction

Steryl ferulates are esters of phytosterols and phenolic acids, namely ferulic acid. They are commonly found in cereal grains and have been extensively studied due to their proven and various suggested beneficial properties on human health. Best known of these properties are the cholesterol lowering and antioxidant functions (Ghatak and Panchal, 2011). Until now most studies have been performed using γ-oryzanol, which is a mixture of steryl ferulates from rice, and used as an antioxidant in cosmetic and food products in some counties. Furthermore, brans of cereal grains, *e.g.*, rice, wheat and corn, which are excellent sources of steryl ferulates (Mandak and Nyström, 2012), are also very abundant by-products of the food industry. Cereal bran fractions could be used as sources for extraction of steryl ferulates thus adding value to the industrial side stream and providing a source of an important natural bioactives. If beneficial health effects and other properties of the steryl ferulates were better known, bran fractions could be further processed to take full nutritional and financial benefit of the valuable natural components available in these grains.

The total content of individual steryl ferulates, as well as their composition, vary depending on the grain source, genotype, and environmental factors (Bergman and Xu, 2003). In rice most sterols esterified to ferulic acid are 4,4'-dimethylsterols, whereas in wheat and corn, for example, the sterols found are mostly 4-desmethylsterols (no methyl groups on C4 of the sterol structure) (Nyström, 2012). These differences are known to affect the cholesterol lowering properties of these sterols in their free (non-esterified) form (Ling and Jones, 1995), as well as to affect the affinity of various enzymes (esterases and lipases) on the hydrolysis of steryl ferulates (Miller et al., 2004). This suggests that the sterol composition is a prime matter in defining the bioactive properties of steryl ferulates and therefore highlights the importance of the source and species of steryl ferulates. All these factors demonstrate that detailed information on individual steryl ferulates is essential in understanding their functional properties.

The bioactive properties of steryl ferulates have been a focus of research for decades and there are some indications that individual steryl ferulates may vary in their bioactivities. So far their antioxidant activity is the one property that is well established, though there are still several discrepancies in the data and the links between structure and function are not fully understood (Nyström, 2012). Furthermore, γ-oryzanol has been reported to be poorly absorbed in rat (Fujiwara et al., 1983) and rabbit (Fujiwara et al., 1980). In a recent clinical study, nearly 80% of intact γ-oryzanol was recovered in the feces after consumption of γ-oryzanol-rich yogurt (Lubinus et al., 2013). Nevertheless, none of these studies provide clear evidence regarding the exact intestinal absorption of individual steryl ferulates.

The overall aim of this project was to evaluate the variation of individual steryl ferulates in different rice varieties, to compare their antioxidant activity in different models to shed light on the links between structure and function, and to investigate their permeation through Caco-2 cell monolayers to explore their intestinal absorption mechanism. In the first part of this thesis, the available literature on steryl ferulates is reviewed, and in the second part, four research papers written in the framework of this PhD project are presented.

# PART 1 - Review of Literature

## 1 Occurrence of steryl ferulates

### 1.1 Structures

Steryl ferulates are ferulic acid esters of various sterols (Figure 1). These compounds were first purified from rice bran oil by Kaneko and Tsuchiya (1954). The mixture of steryl ferulates in rice is known as γ-oryzanol. Their structural differences occur in and on the rings and in the side chain of the sterol moiety (Table 1). Sterols with a saturated steroid skeleton are called stanols, while the ones containing a double bond between C5 and C6 or between C7 and C8 are called sterols. In this thesis, "steryl ferulate" is used to describe both unsaturated and saturated sterol esters of ferulic acid.

Steryl ferulates are further structurally classified according to the number of methyl groups on C4, namely, 4-desmethyl, 4-monomethyl, and 4,4'-dimethylsteryl ferulates. The 4,4'-dimethylsterol moiety contains a cyclopropyl ring at C9/C10 and a methyl group at C14. In addition to the rings, the branched alkyl chain on C17 varies between different steryl ferulates. Furthermore, due to the presence of an unsaturation in the ferulic acid side chain, steryl ferulate can occur in *cis-* or *trans-* form. The *trans-* form is the naturally occurring and more abundant one. UV-irradiation can cause its isomerization from *trans-* form to *cis-* form (Nyström, 2012).
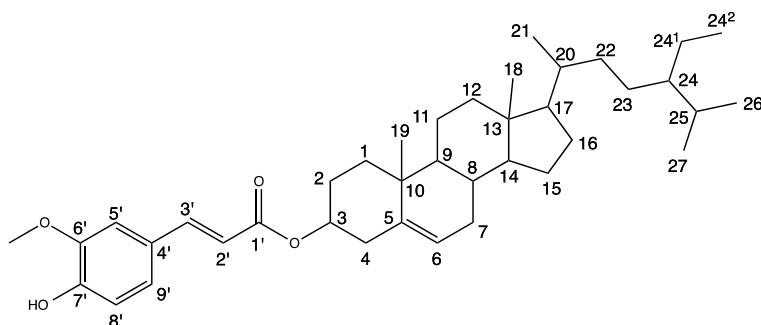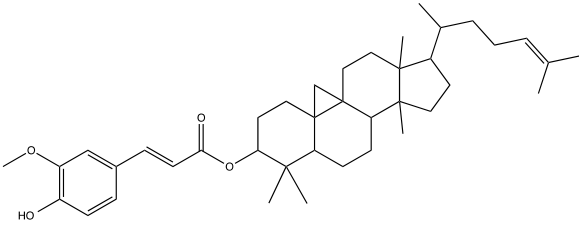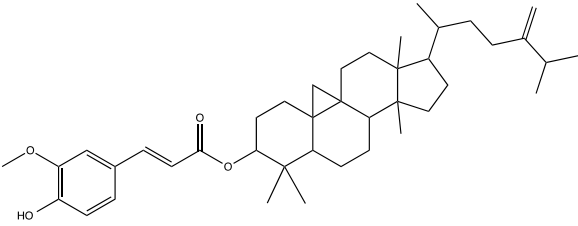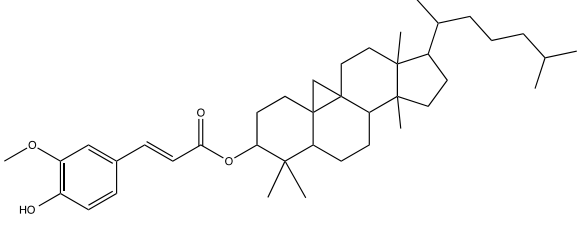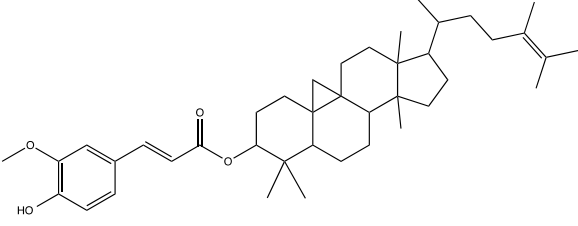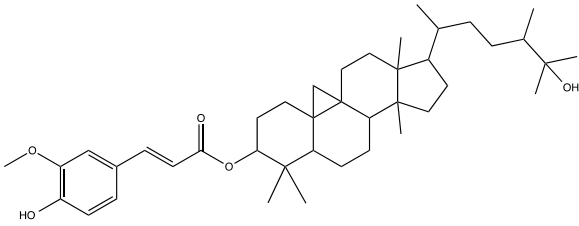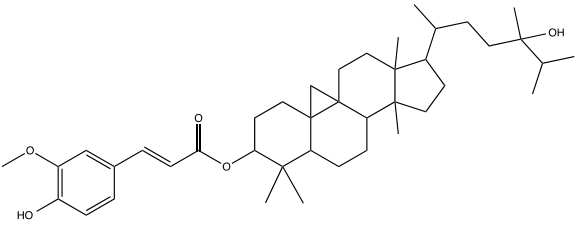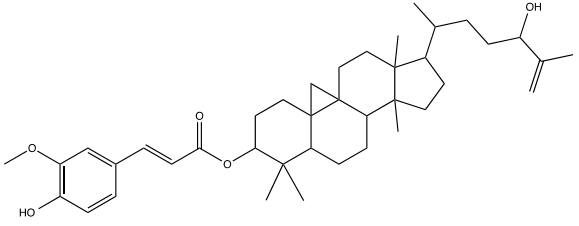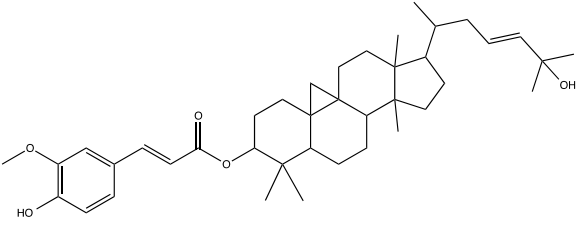


**Figure 1**: Molecular structure of a steryl ferulate (sitosteryl ferulate).

To date, at least 21 different steryl ferulates (Table 1) have been detected in various studies (Akihisa et al., 2000; Aladedunye et al., 2013; Fang et al., 2003; Luo et al., 2005; Nagy et al., 2013; Nakayama et al., 1987; Xu and Godber, 1999).

**Table 1**: Structure formulas of steryl ferulates.

| **4,4'-dimethylsteryl ferulate:** |
|---|



Cycloartenyl ferulate

24-Methylenecycloartanyl ferulate

Cycloartanyl ferulate

Cyclobranyl ferulate

25-Hydroxy-24-methylcycloartanyl ferulate

24-Hydroxy-24-methylcycloartanyl ferulate

24-Hydroxy-cycloart-25-enyl ferulate

25-Hydroxy-cycloart-23-enyl ferulate

**4-monomethylsteryl ferulate:**
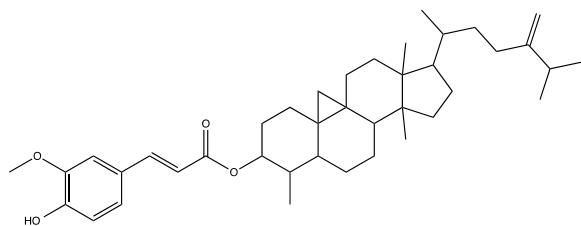
Cycloeucalenyl ferulate
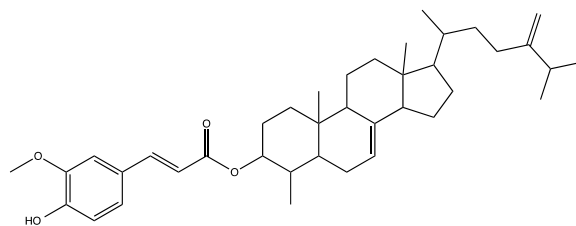
Gramisteryl ferulate
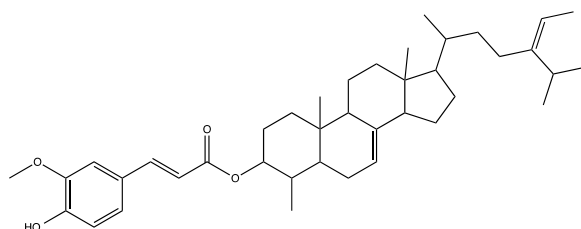
Citrostadienyl ferulate

**4-desmethylsteryl ferulate:**
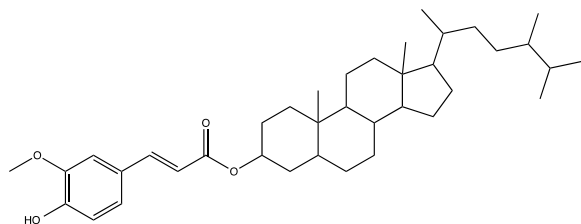
Campestanyl ferulate
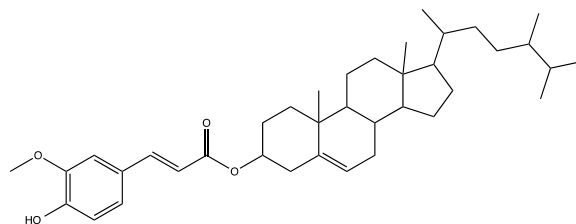
Campesteryl ferulate
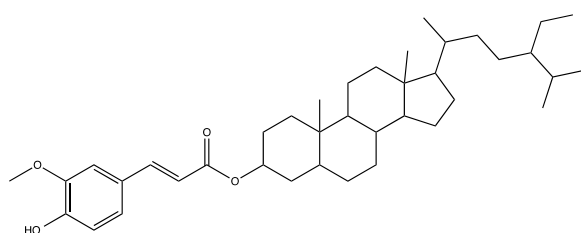
Sitostanyl (stigmastanyl) ferulate
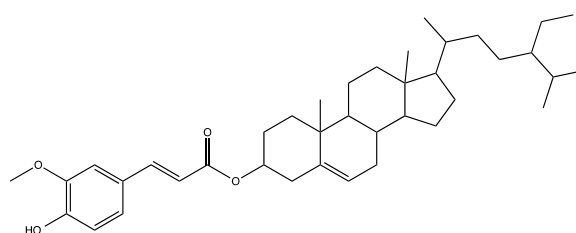
Sitosteryl ferulate
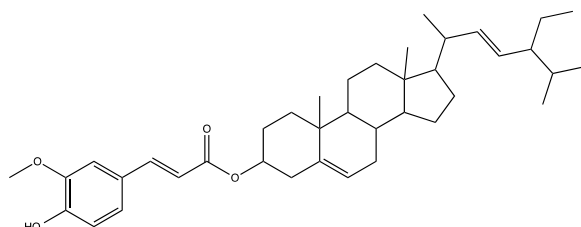
Stigmasteryl ferulate
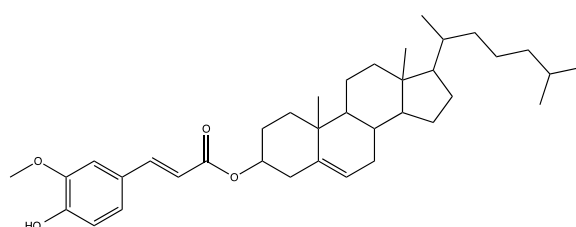
Cholesteryl ferulate
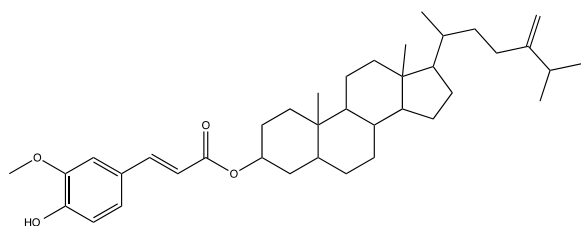
24-Methylenecholestanyl ferulate
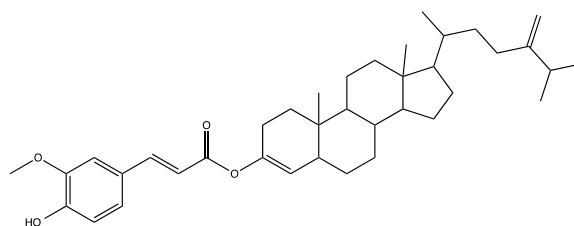


24-Methylenecholesteryl ferulate
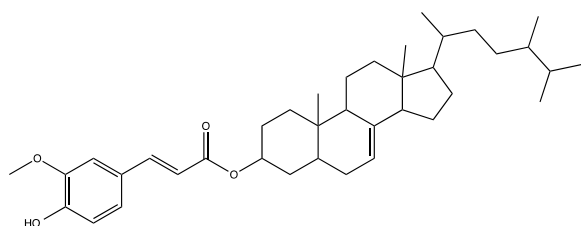


$\Delta^7$-Campestenyl (24-epifungisteryl) ferulate
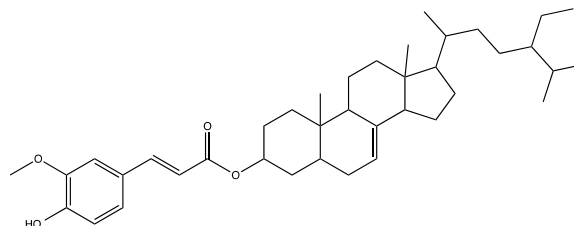


$\Delta^7$-Sitostenyl (schottenyl) ferulate

## 1.2 Occurrence in plants

### 1.2.1 Rice

The mixture of steryl ferulates in rice (*Oryza sativa L.*) is known as γ-oryzanol, which is mostly studied so far. The total content of γ-oryzanol shows huge variation among the different milling fractions of rice. Most of the γ-oryzanol is found in the bran layer, in which it ranges from 390 to 25200 μg/g (calculated based on dry matter, unless stated otherwise) in different studies (Huang and Ng, 2011; Imsanguan et al., 2008; Rohrer and Siebenmorgen, 2004; Sirikul et al., 2009). The rice bran oil products are reported to contain 415-55000 μg/g (oil weight basis) of γ-oryzanol (Anwar et al., 2005; Krishna et al., 2006). After dehulling of rice grains, the obtained brown rice has around 60-1700 μg/g γ-oryzanol (Finocchiaro et al., 2007; Huang and Ng, 2011). Furthermore, after complete milling of brown rice, the remaining part, known as polished rice, only contains 30-630 μg/g γ-oryzanol (Huang and Ng, 2011). The rice germ also contains γ-oryzanol, with the content of 580 μg/g (Fang et al., 2003). Content variation of steryl ferulates occurs not only within different fractions of the kernel, but also among different rice cultivars and genotypes. Moreover, their contents also vary depending on

environmental factors, growing locations, years and methods (Bergman and Xu, 2003; Cho et al., 2012; Miller and Engel, 2006; Sirikul et al., 2009).

Most of γ-oryzanol is removed in milling (polishing) of rice. Some other types of processing also affect their content. For instance, one study reported that the germination led to a significant increase of γ-oryzanol content (Moongngarm and Saetung, 2010). In another study, after the germination, γ-oryzanol in the pigmented brown rice increased, whereas it decreased in the unpigmented brown rice (Ng et al., 2013). Furthermore, heat treatment also has an impact on steryl ferulates; after steam-extrusion, a 26% decrease of steryl ferulates in rice bran was observed by Lloyd and colleagues (2000). Moreover, Shin and Godber (1996) studied the effects of irradiation on steryl ferulate in rice bran, and observed that the γ-irradiation at 5-15 kGy resulted in its decrease by 11-22%. In a recent study by Pascual and colleagues (2013), it was observed that the parboiling also led to an average γ-oryzanol loss of 20%.

The composition of steryl ferulates in different rice fractions or cultivars varies significantly (Table 2). The most abundant compounds of γ-oryzanol are 4,4'-dimethylsteryl ferulates, cycloartenyl ferulate (32-51% of total steryl ferulates in brown rice) and 24-methylenecycloartanyl ferulate (23-37%). Apart from these two compounds γ-oryzanol is composed of mainly 4-desmethylsteryl ferulates: campesteryl ferulate (5-18%), sitosteryl ferulate (5-10%) and campestanyl ferulate (3-14%) (Miller and Engel, 2006). In addition, other steryl ferulates, *e.g.,* 4-monomethylsteryl ferulates and hydroxylated steryl ferulates, are also detected in rice. Furthermore, cyclobranyl ferulate, a 4,4'-dimethylsteryl ferulate, which is only detected in trace in rice bran, ranges from 2 to 20% in some commercial rice bran oils (Berger et al., 2005; Norton, 1995).

**Table 2** Steryl ferulates composition (µg/g) [a] in rice

| Rice | Cycloartenyl ferulate | 24-Methylene cycloartanyl ferulate | Campesteryl ferulate | Campestanyl ferulate | Sitosteryl ferulate | Sitostanyl ferulate | Other steryl ferulate | Reference |
|---|---|---|---|---|---|---|---|---|
| Bran | 1000 | 983 | 745 | 479 | - | - | 194 | |
| Rice bran oil 1 [b] | 54 | 21 | 141 | 39 | - | - | 146 | (Norton, 1995) |
| Rice bran oil 2 [b] | 822 | 144 | 726 | 318 | - | - | 990 | |
| Bran | 59 | 63 | 61 | - | 33 | - | - | (Parrado et al., 2003) |
| Rice bran oil [b] | 17000 | 14000 | 12000 | - | 6000 | - | 2000 | (Berger et al., 2005) |
| Thaibonnet brown rice | 154 | 87 | 32 | 24 | 27 | - | - | |
| Savio brown rice | 172 | 109 | 26 | 50 | 27 | - | - | |
| Sigalon brown rice | 173 | 95 | 22 | 45 | 26 | - | - | (Miller and Engel, |
| Helene brown rice | 125 | 73 | 16 | 12 | 34 | - | - | 2006) |
| Elio brown rice | 196 | 147 | 33 | 58 | 30 | - | - | |
| Ambra brown rice | 173 | 119 | 26 | 41 | 27 | - | - | |
| Conventional brown rice [c] | 182 | 259 | 76 | 85 | - | - | - | (Cho et al., 2012) |
| Organic brown rice [c] | 212 | 269 | 78 | 98 | - | - | - | |
| Caroline polished rice | 18 | 14 | 4 | 3 | 6 | 2 | - | |
| S.Andrea polished rice | 15 | 16 | 7 | 3 | 6 | 2 | - | |
| S.Andrea cargo rice | 63 | 63 | 28 | 8 | 24 | 10 | - | (Mandak and |
| Perfume cargo rice | 34 | 115 | 29 | 21 | 6 | 5 | - | Nyström, 2012) |
| Camargue cargo rice | 85 | 54 | 26 | 10 | 29 | 12 | - | |
| Bran | 1088 | 1369 | 402 | 269 | 460 | 312 | - | |
| Dehusked black-purple rice seed [d] | 77 | 90 | 79 | - | 33 | - | - | (Pereira-Caro et al., 2013) |

**Note:** -: Not detected. [a]: Steryl ferulates composition is given on dry matter basis. [b]: Calculated based on oil weight, oil from commercial companies. [c]: Not reported with dry matter or fresh weight basis. [d]: Calculated based on fresh weight.

**1.2.2 Wheat**

In whole grain wheat (*Triticum aestivum L.*), 6 to 10 % of the total phytosterols are esterified with ferulic acid (Hakala et al., 2002; Nurmi et al., 2012; Nyström et al., 2007b). Analogously to rice, steryl ferulates in wheat are mostly located in the bran. Steryl ferulate content in wheat bran ranges from 300 to 600 µg/g, in whole flour from 66 to 126 µg/g (Nurmi et al., 2012). In another study by Hakala and colleagues (2002), in the refined flour with low ash content, only trace of steryl ferulates was found (< 5 µg/g, based on fresh weight), whereas the enriched flour with high ash content had relatively high levels of steryl ferulates, approximately 200 µg/g (based on fresh weight). Furthermore, it was reported that the total contents in bran fractions were 424 to 438 µg/g, 24 µg/g in the germ and 17-81 µg/g in wheat milling fractions (Nyström et al., 2007b). Moreover, commercial wheat bran oil was reported with 2 mg/g steryl ferulates (Iwatsuki et al., 2003).

Contents of steryl ferulates in wheat are similarly as rice dependent on genotypes, growth locations and weather. Seitz and colleagues (1989) observed that their total content varied from 62 to 123 µg/g in bread wheat varieties (six winter types and one spring type), and the highest content was found in the spring wheat genotype. Furthermore, in the study by Nurmi and colleagues (2010), various wheat genotypes were grown at different locations in Europe in different years. The genotype significantly affected the content of wheat steryl ferulates, ranging from 75 to 114 µg/g. Moreover, the growing locations also affected their steryl ferulate levels; the content in the same wheat genotype was detected with 79, 81, 94 and 101 µg/g in France, UK, Poland and Hungary, respectively. Finally, it was also found that the wheat grown in the wet year often possessed the lower steryl ferulate contents than the dry and warm year, indicating that the high temperature and low precipitation might result in high steryl ferulate content (Nurmi et al., 2010).

The composition of steryl ferulates in different wheat fractions or cultivars also varies (Table 3). Campestanyl ferulate and sitostanyl ferulate are dominating steryl ferulates in wheat, which account for 40-50% and 25-35% of total steryl ferulates, respectively. Moreover, campesteryl ferulate (10-20%) and sitosteryl ferulate (around 5%) are also found in wheat (Esche et al., 2012; Mandak and Nyström, 2012; Nurmi et al., 2010).

Wheat was reported to contain only 4-desmethylsteryl ferulate. However, in a recent study traces of 24-methylenecycloartanyl ferulate, a type of 4,4'-dimethylsteryl ferulates, was also detected in wheat (Esche et al., 2012). Additionally, $\Delta^7$-campesteryl and $\Delta^7$-sitosteryl ferulates have been found in wheat and spelt as minor compounds (Esche et al., 2012). Furthermore, the composition of steryl ferulate varies in different wheat cultivars (Nurmi et al., 2010).

**Table 3** Steryl ferulates composition (µg/g) [a] in wheat

| Wheat | 24-Methylene cycloartanyl ferulate | Campesteryl ferulate | Campestanyl ferulate | Sitosteryl ferulate | Sitostanyl ferulate | Other steryl ferulate | Reference |
|---|---|---|---|---|---|---|---|
| Winter wheat [b] | - | 6-9 | | 35-53 [c] | 19-32 | - | |
| Spring wheat [b] | - | 12 | | 66 [c] | 44 | - | (Seitz, 1989) |
| Durum wheat [b] | - | 5 | | 44 [c] | 20 | - | |
| Grain [d] | - | 11-12 | | 32-33 [c] | 18-19 | - | (Hakala et al., |
| Bran [d] | | 57-79 | | 148-200 [c] | 91-114 | - | 2002) |
| Whole grain | - | 9 | | 26 [c] | 17 | - | |
| Coarse bran | - | 44 | | 157 [c] | 98 | - | (Nyström et al., |
| Fine bran | - | 44 | | 161 [c] | 103 | - | 2007b) |
| Milling fractions | - | 2-9 | | 6-30 [c] | 4-18 | - | |
| Germ | - | 3 | | 9 [c] | 5 | - | |
| Cultivar Estica whole grain | - | 16 | | 40 [c] | 18 | - | (Nurmi et al., |
| Chinese Spring whole grain | - | 10 | | 46 [c] | 32 | - | 2010) |
| Cultivar Tommi whole grain | - | 15 | | 60 [c] | 37 | - | |
| Whole grain flour | - | 14 | | 53 [c] | 34 | - | |
| Peeling fraction | - | 13 | | 61 [c] | 35 | - | (Nurmi et al., |
| Bran fraction after peeling | - | 79 | | 326 [c] | 203 | - | 2012) |
| Pearling fraction | - | 51 | | 208 [c] | 129 | - | |
| Aleurone | - | 52-55 | | 218-217 [c] | 134-138 | | |
| Kernel | 2 | 13 | 56 | 6 | 42 | 4 | (Esche et al., |
| Spelt kernel | - | 8 | 40 | 4 | 36 | 3 | 2012) |
| Bran | - | 94 | 18 | 206 | 135 | - | (Mandak and Nyström, 2012) |

**Note:**  -: Not detected. [a]: Steryl ferulate composition is given on dry matter basis. [b]: Not reported with dry matter or fresh weight basis. [c]: Sum of campestanyl ferulate and sitosteryl ferulate. [d]: Calculated based on fresh weight.

**1.2.3 Corn**

In corn (*Zea mays L.*), 6-18% of sterols occur as esters of phenolic acids, mostly with ferulic acid (Esche et al., 2013a). Similar to rice and wheat, steryl ferulates are also located in the corn bran. In corn bran, 96% of steryl ferulates are located in the aleurone layer, and the remaining 4% are located in the pericarp (Singh et al., 2001). Seitz (1989) reported that steryl ferulates in different corn kernels range from 31 to 70 μg/g. Esche and colleagues (2013a) found that their contents in kernels varied among 25 types of corn cultivars from 46 to 240 μg/g. Moreover, the same group reported that the total steryl ferulates content was 34-112 μg/g in commercial sweet corn, and 164-187 μg/g in commercial popcorn (Esche et al., 2013b). Singhand and colleagues (2000) observed that steryl ferulate levels in corn were significantly affected by the corn hybrid as well as by growing locations. Moreover, commercial corn bran oil and corn fiber oil was reported with 5.6 mg/g (Iwatsuki et al., 2003) and 2.95 mg/g (Jiang and Wang, 2005) of steryl ferulates, respectively.

The composition of steryl ferulates in different corn fractions or cultivars has been reported in many studies (Table 4). Sitostanyl ferulate is the dominating steryl ferulate in corn. Studies have shown that the composition of steryl ferulates in corn is 55-85% sitostanyl ferulate, 8-30% campestanyl ferulate, 2-14% sitosteryl ferulate, 0-9% campesteryl ferulate and 1% stigmasteryl ferulate (Esche et al., 2013a; Iwatsuki et al., 2003; Jiang and Wang, 2005; Norton, 1995; Seitz, 1989). Like wheat, corn was also considered to only have 4-desmethylsteryl ferulate; however, Esche and colleagues (2013a) recently have detected 24-methylenecycloartanyl ferulate in some corn cultivars. Additionally, they also found other 4-desmethylsteryl ferulates, *e.g.*, $\Delta^7$-campesteryl and $\Delta^7$-sitosteryl ferulates, in corn kernels.

**Table 4** Steryl ferulate composition (μg/g) [a] in corn

| Corn | 24-Methylene cycloartanyl ferulate | Campesteryl ferulate | Campestanyl ferulate | Sitosteryl ferulate | Sitostanyl ferulate | Other steryl ferulate | Reference |
|---|---|---|---|---|---|---|---|
| Whole grain, cultivar BoJac [b] | - | 2 | 9 | - | 24 | - | |
| Whole grain, cultivar Stauffer [b] | - | 2 | 11 | - | 29 | - | (Seitz, 1989) |
| Whole grain, cultivar unknown [b] | - | 4 | 19 | - | 48 | - | |
| Standard bran | - | - | 47 | - | 342 | 8 | |
| Raw bran | - | - | 61 | - | 140 | 15 | |
| Corn bran flour | - | - | 5 | - | 60 | 2 | (Norton, 1995) |
| Unrefined corn oil [c] | - | - | 289 | - | 700 | 125 | |
| Unrefined corn oil [c] | - | - | 224 | - | 734 | 78 | |
| Bran | - | 29 | 15 | 93 | 194 | - | (Mandak and Nyström, 2012) |
| Kernel | - | 3 | 45 | 6 | 94 | 6 | (Esche et al., 2012) |
| Sweet corn 1 | 2 | 2 | 10 | 4 | 14 | - | (Esche et al., 2013b) |
| Sweet corn 2 | - | 11 | 41 | 11 | 47 | 2 | |
| Popcorn 1 | 1 | 7 | 47 | 5 | 100 | 4 | |
| Dent corn, cultivar MAS31a | - | 6 | 60 | 6 | 153 | 10 | |
| Dent corn, cultivar Herkuli | 3 | 4 | 34 | 3 | 83 | 2 | |
| Dent corn, cultivar Amanda | - | 5 | 30 | 3 | 73 | 2 | (Esche et al., 2013a) |
| Flint corn, cultivar Crazi | - | 5 | 12 | 2 | 25 | 2 | |
| Flint corn, cultivar Symbol | 3 | 4 | 18 | 3 | 54 | 3 | |
| Flint corn, cultivar Zidane | 3 | 11 | 30 | 6 | 73 | 8 | |

**Note:**  -: Not detected. [a]: Steryl ferulate composition is given on dry matter basis. [b]: Not reported with dry matter or fresh weight basis. [c]: Calculated based on oil weight, products from Spectrum Naturals Inc.

**1.2.4 Other sources**

A few other sources of steryl ferulates have been reported. Seitz (1989) reported that the content of steryl ferulates in triticale (×*Triticosecale Wittmack*) was 52 μg/g. Moreau and colleagues (1998) analyzed the levels of steryl ferulates in other seeds, and they found that their contents were 4 μg/g in barley (*Hordeum vulgare L.*), 50 μg/g in Job's tears (*Coix lacryma-jobi L.*) and 91 μg/g in wild rice (*Zizania palustris L.*). Recently, Aladedunye and colleagues (2013) reported that the amount of steryl ferulates in the wild rice samples from North American were generally higher compared to regular brown rice samples (1352 *vs.* 688 μg/g). However, Mandak and colleagues (2012) only detected 94 μg/g steryl ferulates in the whole grain of wild rice. Furthermore, in oat (*Avena sativaL.*) bran oil, the content of steryl ferulates detected was 270 μg/g (Moreau et al., 1996). But in their another study, steryl ferulates were not detected in oat kernels (Moreau et al., 1998).

Steryl ferulates have also been found in rye (*Secale cereale L.*), mostly in the bran part, and their content was reported as 44 μg/g in the whole grain rye and 199 μg/g in the rye bran (Nyström et al., 2007b). Nurmi and colleagues (2010) investigated 5 types of rye cultivars, and they found that the contents of steryl ferulates among the cultivars were not statistically significantly different (65-74 μg/g). Recently, Esche and colleagues (2012) detected 91 μg/g steryl ferulates in the rye kernel.

The composition of steryl ferulates in these cereal grains and seeds are less studied than in rice, wheat and corn (Table 5). In triticale, only 4-desmethylsteryl ferulates are detected (Seitz, 1989); whereas in wild rice, both 4-desmethylsteryl and 4,4'-dimethylsteryl ferulates are found and the growth locations have effects on their composition (Aladedunye et al., 2013). In the case of rye, the detected steryl ferulates are mostly 4,4'-dimethylsteryl ferulates, in which campestanyl ferulate and sitostanyl ferulate are dominating.

**Table 5** Steryl ferulate composition (μg/g) [a] in rye, wild rice and triticale

| Grain source | Cycloartenyl ferulate | 24-Methylene cycloartanyl ferulate | Campesteryl ferulate | Campestanyl ferulate | Sitosteryl ferulate | Sitostanyl ferulate | Other steryl ferulate | Reference |
|---|---|---|---|---|---|---|---|---|
| **Rye** | | | | | | | | |
| Whole kernel, Cultivar Rymin [b] | - | - | 4 | 16 | - | 9 | - | (Seitz, 1989) |
| Grain | - | - | 8-11 | 29-33 [c] | | 18-21 | - | (Hakala et al., |
| Bran | - | - | 25-54 | 76-127 [c] | | 49-70 | | 2002) |
| Whole grain | - | - | 8 | 22 [c] | | 14 | - | (Nyström et al., |
| Bran | - | - | 34 | 106 [c] | | 59 | - | 2007b) |
| Haute Loire Pop | - | - | 14 | 36 [c] | | 19 | - | (Nurmi et al., |
| Cultivar Nikita | - | - | 13 | 40 [c] | | 20 | - | 2010) |
| Cultivar Rekrut | - | - | 13 | 40 [c] | | 22 | - | |
| Kernel | - | 3 | 8 | 40 | 6 | 28 | 6 | (Esche et al., 2012) |
| **Wild rice** | | | | | | | | |
| Wild rice USA [b, d] | 329-643 [e] | 75-96 | 88-125 | - | 111-140 | 1-2 | 200-378 | (Aladedunye et |
| Wild rice Canada [b, d] | 372-642 [e] | 79-94 | 89-125 | - | 197-139 | 1-2 | 196-362 | al., 2013) |
| Wild rice Canada | 18 | 23 | 23 | 6 | 14 | 11 | - | (Mandak and Nyström, 2012) |
| **Triticale** | | | | | | | | |
| Whole grain [b] | - | - | 4 | 28 | - | 20 | - | (Seitz, 1989) |

**Note:**  -: Not detected. [a]: Steryl ferulate composition is given on dry matter basis. [b]: Not reported with dry matter or fresh weight basis. [c]: Sum of campestanyl ferulate and sitosteryl ferulate. [d]: Wild rice from different companies and grown in USA or Canada. [e]: Including unidentified isomers of cycloartenyl ferulate.

## 1.3 Other steryl phenolates identified in plants

Steryl ferulates are the most abundant compounds in steryl phenolates, and by far, they are also the most extensively studied compared to other steryl phenolates. However, in addition to steryl ferulates, the occurrence of other phenolic acid esters of phytosterols has been reported (Table 6). Steryl caffeate was identified in rice bran (Fang et al., 2003). Moreover, steryl *p*-coumarate was detected in corn as minor component (Norton, 1994; Norton, 1995; Seitz, 1989), representing less than 7% of total steryl phenolates (Esche et al., 2013a). The composition of these coumarates was significantly affected by the genotype of corn (Esche et al., 2013a). In a recent study, campestanyl and sitostanyl coumarates were detected in rye, wheat and spelt (Esche et al., 2012). Furthermore, cinnamic acid and caffeic acid esters of phytosterols were found with a significant amount in wild rice (Aladedunye et al., 2013). In general, their contents are very low.

**Table 6** Other steryl phenolates identified in various grain sources.

| Grain sources | Other steryl phenolates identified | Composition (%) [a] | Content of total steryl phenolates (µg/g) [b] | Reference |
|---|---|---|---|---|
| Rice | | | | |
| Bran | Cycloartenyl caffeate Campesteryl caffeate | Trace [c] | n.r. [d] | (Fang et al., 2003) |
| Corn | | | | |
| Whole grain | Campestanyl and Sitostanyl coumarates | 1.5-6 µg/g [e] | n.r. | (Seitz, 1989) |
| Bran flour | $\Delta^7$-campesteryl coumarate Campesteryl coumarate Campestanyl coumarate Sitostanyl coumarate | 1.7 Trace 0.9 1.3 | 93 [f] | (Norton, 1994) |
| Bran and related fractions | Campestanyl coumarate Sitostanyl coumarate Other coumarates | 0.4-3.9 1-7.6 trace-1.5 | 70-540 | (Norton, 1995) |
| Kernel, 25 different cultivars | Campestanyl coumarate Sitostanyl coumarate Campesteryl coumarate Sitosteryl coumarate | 0-2.4 0-4.5 Trace 0-0.7 | 46-240 | (Esche et al., 2013a) |

| | | | | |
|---|---|---|---|---|
| **Rye** | | | | |
| Kernel | Campestanyl coumarate | 0.5 | 92 | (Esche et al., |
| | Sitostanyl coumarate | 0.3 | | 2012) |
| **Wheat** | | | | |
| Kernel | Campestanyl coumarate | 1.4 | 124 | (Esche et al., |
| | Sitostanyl coumarate | 0.2 | | 2012) |
| **Spelt** | | | | |
| Kernel | Campestanyl coumarate | Trace | 92 | (Esche et al., |
| | Sitostanyl coumarate | Trace | | 2012) |
| **Wild rice** | | | | |
| Kernel | Cycloartenyl caffeate | 7-10 | 867-1352 [e] | (Aladedunye |
| | Campesteryl caffeate | 2-3 | | et al., 2013) |
| | Cycloartenyl cinnamate | 4-6 | | |
| | Campesteryl cinnamate | 4-8 | | |

**Note:** [a]: The composition is given as the percentage of total steryl phenolates. [b]: The content of total steryl phenolates (including steryl ferulates) is given on dry matter basis. [c]: Not quantified. [d]: Not reported. [e]: Not indicated with fresh weight or dry matter basis. [f]: Calculated based on fresh weight.

# 2 Biosynthetic pathway and biological function in plants

## 2.1 Location in plants

Steryl ferulates are secondary plant metabolites belonging to the lipid family. They are mainly found in certain cereal grains and seeds, especially in the outer layers of kernel. An uneven distribution of steryl ferulates within the bran layers was found, for instance, they were in the wheat aleurone and inner pericarp tissues, but not in the outer pericarp tissue (Seitz 1989). Buri and colleagues (2004) reported that high levels of phytosterol and steryl ferulate were found in aleurone layer of wheat. Moreover, Nurmi and colleagues (2012) reported that steryl ferulates were accumulated in the intermediate layers of wheat, whereas the phytosterols were more evenly distributed in the intermediate layers and aleurone cell contents; and the phytosterol composition varied within the wheat kernel, while the steryl ferulate composition was similar in different fractions.

Furthermore, Lloyd and colleagues (2000) demonstrated that γ-oryzanol was predominantly present in the outer pericarp, seedcoat and nucellus layers, which are the outermost layers of a brown rice kernel. Rohrer and colleagues (2004) found that the content of γ-oryzanol could vary depending on the thickness of kernel. Recently, Nantiyakuland and colleagues reported that 91% of γ-oryzanol were found in the oil bodies in rice bran (2012).

However, the exact location and distribution of steryl ferulates in plant or plant cells are still not clearly determined. According to their structural information, steryl ferulates most probably originate from the esterification of ferulic acid and sterols in those cells in bran layer where ferulic acid and sterol are available. Once the distribution of steryl ferulate is well determined, it will shed light on their biosynthesis and function in plants.

## 2.2 Biosynthetic pathway

The biosynthetic pathways of steryl ferulates are still not clearly understood. With regard to the structure, their biosynthesis in plants may initiate with the biosynthesis of phytosterol, biosynthesis of ferulic acid and then the esterification of ferulic acid and sterols.

Phytosterol is one of the important plant membrane components regulating the fluidity as well as the permeability of phospholipids bilayers, and it also serves as a precursor or substrate of other steroid compounds, such as brassinosteroids and steroidal saponins in plants (Piironen et al., 2000; Schaller, 2003). Phytosterol is the product of isoprenoid biosynthetic pathway. It is synthesized from cytoplasmic mevalonate via a sequence of enzyme-catalyzed reactions, which was summarized by Suzuki and colleagues (2007). Generally, the mevalonate is firstly converted to squalene, then epoxided to oxidosqualene, and further converted to cycloartenol and other sterols. The enzyme sterol methyltransferase converts cycloartenol to 24-methylenecycloartenol by introducing the methyl group onto C24, and the enzyme cyclopropyl sterol isomerase is required to open the cyclopropane ring at C9/C10. The 4,4'-dimethyl- and

4-monomethyl-sterols are the part of this biosynthetic pathway. Moreover, the 4-desmethylsterols (*e.g.*, campesterol and sitosterol) in plants are produced from cycloartenol that serves as the key intermediate (Nes et al., 2003; Piironen et al., 2000).

Ferulic acid is also a secondary plant metabolite, and it is one of the most abundant phenolic acids in various vegetables, cereals and fruits (Zhao and Moghadasian, 2008), playing essential roles in growth, reproduction and defense against pathogens due to its antioxidant activity (Graf, 1992). In plants, ferulic acid is rarely found in the free form. It is found with the highest levels in the aleurone and hyaline layers in wheat bran; and approximately 1% of ferulic acid is in free form, 7% is conjugated (*e.g.* phytosterols) and 92% is bound to cell wall polysaccharides (Li et al., 2008; Saulnier et al., 2012). The biosynthesis of ferulic acid is known to occur in the cytoplasm, and it is one of the metabolites of the biosynthesis of lignin in plants. Biogenetically, phenylalanine and tyrosine ammonialyases convert phenylalanine and tyrosine to cinnamic acid and *p*-coumaric acid, respectively. Cinnamic acid can be further converted to *p*-coumaric acid, and the latter can be converted to caffeic acid through hydroxylation. Ferulic acid derives from the methylation of caffeic acid with methionine acting as the methyl donor, and further the ferulic acid can be converted to sinapic acid (Graf, 1992; Rosazza et al., 1995). This suggests that the enzyme involved in the biosynthesis of steryl ferulate might also accept other phenolic acid, *e.g.*, caffeic acid or *p*-coumaric acid, as a substrate, and thus explains the presence of steryl caffeate in γ-oryzanol and steryl *p*-coumarate in corn.

Although the esterification of ferulic acid and sterol is suggested, the enzymatic system involved is not yet known. From the literature, the esterification is suggested to be associated with the microsomal fraction that is able to convert phytosterols into steryl esters; however, this esterification by a plant sterol acyltransferase takes place only with acyl donors including phospholipid, diacylglycerol and triacylglycerol, but not yet has been reported with phenolic acid (Benveniste, 2002; Chen et al., 2007). Furthermore, no ferulic acid esterases have been characterized for esterification of ferulic acid and

sterol in plant. Therefore, the esterification of ferulic acid and sterol as well as the regulation of their biosynthesis in plants needs to be studied in more depth.

## 2.3 Biological function in plants

The accumulation of steryl ferulates in the cereal grain bran may be related to its function in the kernel. Their function in plants may be related to the protection against elevated environmental temperature (Britz et al., 2007), antioxidant property (Nantiyakul et al., 2012) and regulation of microbial activity in the grains (Seitz, 1989). Recently, Kumar and colleagues reported that higher level of γ-oryzanol was observed in the drought-tolerant cultivar compared to the drought-susceptible cultivar, suggesting its role in drought tolerance (2014). To summarize, very little is known about the biological function of steryl ferulates in plants, and more research is needed.

## 3 Health promoting properties

The health promoting properties of steryl ferulates have been mostly studied with γ-oryzanol other than with individual steryl ferulates. Steryl ferulates combine the health promoting effects of phytosterols and ferulic acid. γ-Oryzanol is well known for its cholesterol lowering activity. Further, the antioxidant activity of γ-oryzanol is another property that has been widely studied. Steryl ferulates are furthermore suggested to have anti-inflammatory, anti-cancer, anti-allergic effects, *etc*., but knowledge on these properties is still scarce. Moreover, there are very few data available on the differences of bioactivity of individual steryl ferulates.

## 3.1 Cholesterol lowering property

Cardiovascular disease is one of the leading causes of death worldwide. It is well known that regular intake of phytosterols can reduce total cholesterol and low-density lipoprotein cholesterol, and further reduce the risk of cardiovascular disease (European Food Safety Authority, 2010). Like phytosterols, steryl ferulates also show high

potential to reduce cholesterol level. Early studies on the bioactivity of steryl ferulates started with the work regarding the influence of γ-oryzanol on hepatic cholesterol biosynthesis in the 1960s. Since then, many studies about their cholesterol lowering activity have been reported (Table 7).

**Table 7** Studies on the cholesterol-lowering effect of steryl ferulates.

| Test subject | Treatment | Effect | Reference |
|---|---|---|---|
| Animal or cell models | | | |
| Mice | Injection of 1 mg/kg ORY daily for 2 weeks. | TC ↓, biosynthesis of hepatic cholesterol ↓, feces excretion of bile salts and cholesterol ↑. | (Nakamura, 1966) |
| Male Sprague-Dawley rats fed with HCD for 2 weeks | Oral intake of ORY (1&2) [a] 100, 500 and 1000 mg/kg b.w. for 1-2 weeks. | ORY 1 and ORY 2 have no effects on liver lipid contents. Effect: ORY 2 > 1. | (Nakayama et al., 1987) |
| Male Sprague-Dawley rats fed with HCD for 2 weeks | ORY and cycloartenyl ferulate, Treat 1: 100 mg/kg b.w. daily (oral) for 1-2 weeks. Treat 2: 10 mg/kg daily (intravenous) for 1 week. | Treat 1: no effect. Treat 2: TC, LDL-C, VLDL-C, TG and PL ↓, HDL-C ↑. | (Sakamoto et al., 1987) |
| Rats fed with HCD | 0.5% ORY in diet for 7 weeks. | Serum TC and LDL-C ↓, Liver TC, TG and PL ↓. | (Seetharama-iah and Chandrasek-hara, 1988) |
| 32 hamsters fed with HCD for 7 weeks | 1% ORY in diet. | TC ↓, TG ↓, the sum of IDL-C, LDL-C and VLDL-C ↓, cholesterol absorption ↓, aortic fatty streak formation ↓, no influence on endogenous cholesterol synthesis. | (Rong et al., 1997) |
| 240 male F1B hybrid hamsters | Total phytosterols extract from soybean, rice bran or shea nut (including sterol conjugates) with 5 g/kg in diet for 1-4.5 weeks. | Cholesterol lowering effect: 1) soybean sterols > rice bran sterols > shea nut sterols; 2) 4-desmethylsterols > 4,4'-dimethylsterols > | (Meijer et al., 2003) |

| | | pentacyclic triterpene alcohols; 3) phytosterol fatty acid esters = free phytosterols > steryl phenolates. | |
|---|---|---|---|
| 10 male hamsters fed with HCD for 10 weeks | 0.09% ORY in diet. | LDL-C ↓, LDL-C/HDL-C ↓. | (Yokoyama, 2004) |
| 48 hamsters fed with HCD for 2 weeks | 0.5% ferulic acid, 0.5% ORY or 10% rice bran oil in HCD for additional 10 weeks. | Non-HDL ↓. HDL ↑. Excretion of cholesterol ↑. Cholesterol lowering effect: γ-oryzanol > ferulic acid. Antioxidant capacity: ferulic acid > rice bran oil and γ-oryzanol. | (Wilson et al., 2007) |
| 7 male hamsters | 10% steryl ferulates rich-corn fibre oil, diet with 0.5% sitostanol, 0.23% ferulic acid or 0.73% steryl ferulates for 4 weeks. | TC ↓: corn fibre oil > steryl ferulates > sitostanol > ferulic acid. Cholesterol absorption ↓: corn fibre oil = sitostanol > steryl ferulates > ferulic acid. No change of the intestinal gene expression of ABCG5, ABCG8 and NPC1L1. | (Jain et al., 2008) |
| 36 Triton WR-1339-induced acute hyperlipidemic albino rats | Oral intake of 50 or 100 mg/kg b.w. ORY daily for 3 weeks. | TC and TG ↓, LDL-C and VLDL-C ↓ (dose-dependently). HDL-C ↑ (with high dose). Hepatic antioxidant enzymes ↑ (dose-dependently). Atherogenic index and LDL-C/HDL-C ↓ (with high dose). | (Ghatak and Panchal, 2012a) |
| Coupled *in vitro* simulated digestion and Caco-2 human intestinal cell model | Incubation with 13 or 26 μM ORY. | Incorporation of cholesterol into synthetic micelles ↓, apical uptake of cholesterol into Caco-2 cells ↓, HMG-CoA reductase activity ↓. | (Mäkynen et al., 2012) |

| | | | |
|---|---|---|---|
| 24 mice fed with HCD over 2 weeks, 40 acute dyslipidemia induced mice | In HCD model: oral intake of 5, 25 and 50 mg/kg b.w. ORY for 2 months. In acute model: oral intake of 5, 25 and 50 mg/kg b.w. ORY 1h before induction, 22 h and 46 h after induction. | Only 50 mg/kg dosage had protective effects. In HCD model: TC and glucose ↓. In acute model: TC and TG ↓. No adverse effects. | (Arruda Filho et al., 2014) |
| **Human studies** | | | |
| 50 healthy young women | Oral intake of 60 g blended oil (70% rice bran oil and 30% safflower oil) daily for 7 days. | TC ↓. | (Suzuki and Oshima, 1970) |
| Hyperlipoproteinemic human | Oral intake of ORY, 4-8 treatments of 300 mg daily. | TC, LDL-C and TG ↓. HDL-C ↑. No side effects. | (Ishihara et al., 1982) |
| 67 patients with hyperlipidemia | Oral intake of 300 mg ORY daily for 3 months. | A mild but significant hypocholesterolemic effect: TC, LDL-C and TG ↓, HDL-C ↑. | (Yoshino et al., 1989) |
| 20 chronic schizophrenic patients with dyslipidemia who received neuroleptics for about ten years | Oral intake of 100 mg ORY 3 times daily for 16 weeks. | TC, LDL-C and apo B ↓, apo A-II ↑. No side effects. | (Sasaki et al., 1990) |
| 30 mildly hypercholesterolemic men | 50 g rice bran oil containing 50 mg ORY or 800 mg ORY daily for 4 weeks. | TC, LDL-C and LDL-C/HDL-C ratio ↓. No significant difference between two addition levels. | (Berger et al., 2005) |

**Abbreviations**: apo B: apolipoprotein B; b.w.: body weight; HCD: hypercholesterolemic diet; HDL-C: high-density lipoprotein cholesterol; IDL-C: intermediate-density lipoprotein cholesterol; LDL-C: low-density lipoprotein cholesterol; ORY: γ-oryzanol; PL: phospholipids; TC: total cholesterol; TG: triglyceride; VLDL-C: very low-density lipoprotein cholesterol; ↓: decrease; ↑: increase.

**Note**: [a]: γ-oryzanol 1 consisted 35% of cycloartenyl ferulate, 45% of 24-methylenecycloartanyl ferulate, 10% of cyclobranyl ferulate and 10% of other steryl ferulates; γ-oryzanol 2 consisted 60% of cycloartenyl ferulate, 30% of 24-methylenecycloartanyl ferulate and 10% of cyclobranyl ferulate.

Although a lot of data showed that γ-oryzanol could lower the cholesterol level, the exact mechanism is still unclear. Generally, steryl ferulates have been observed with the potential to lower total serum cholesterol and low-density lipoprotein cholesterol, and to increase the high-density lipoprotein cholesterol, by reducing absorption of dietary cholesterol and enhancing the excretion of cholesterol. Some studies suggested that hydrolysis of γ-oryzanol by cholesterol esterase during digestion could liberate free phytosterols (Fujiwara et al., 1983; Mandak and Nyström, 2012). Phytosterols are known as cholesterol lowering agent by inhibiting cholesterol absorption into the systemic circulation with several proposed mechanism: they may (1) block cholesterol ester hydrolysis; (2) co-precipitate with cholesterol and form nonabsorbable mixed crystals; (3) compete with cholesterol in the incorporation into dietary mixed micelles; (4) play a role on the sterol transporters localized in the membranes of enterocytes; (5) inhibit cholesterol esterification inside enterocyte further the incorporation into chylomicrons (De Smet et al., 2012; Gylling et al., 2014). However, the hydrolysis mechanism of γ-oryzanol *in vivo* is still unknown. It also seems that intact steryl ferulates possess cholesterol lowering potential. Recently, Mäkynen and colleagues (2012) showed that γ-oryzanol significantly inhibited the incorporation of cholesterol into synthetic micelles, and γ-oryzanol had ability to significantly reduce the apical uptake of cholesterol into Caco-2 cells. Nevertheless, the exact cholesterol lowering mechanism of steryl ferulates is still not clearly understood. Furthermore, due to the lack of individual steryl ferulates on the market, to date, there is almost no study available on the cholesterol lowering activity of individual steryl ferulates. Therefore, it still needs further studies.

## 3.2 Antioxidant activity

Steryl ferulates have been shown to prevent oxidation in various biological systems (Table 8). The mechanism of their antioxidant activity results from the phenolic proton in the ferulic acid moiety, which can be abstracted by any radical present in the media, and the resulting SF radical is stabilized by resonance along the π-electron system constituted by the aromatic ring and the conjugated unsaturation in the carboxylate in

*para* position to the phenol group (Graf, 1992; Nyström, 2012). Some researchers have suggested that the steryl ferulate radical might still influence oxidation, for example, by interfering with the chain reaction of lipid oxidation as alkyl radicals (Kochhar, 2000).

**Table 8** Studies on the antioxidant activity of steryl ferulates.

| Model | Method | Effect | Reference |
|---|---|---|---|
| Linoleic acid | Monitoring diene formation at 30°C for 0-30 h. | Campesteryl ferulate > 24-methylenecycloartanyl ferulate > cycloartenyl ferulate. | (Yagi and Ohishi, 1979) |
| Cytochrome P-450 | Scavenging effect on $O_2^{\bullet-}$ using ESR. | ORY scavenged $O_2^{\bullet-}$. | (Tajima et al., 1983) |
| Triacylglycerols of lard | Formation of lipid hydroperoxides at 100°C. | Ferulic acid > cholesteryl ferulate > cholesteryl ferulate isomers; Caffeic acid > cholesteryl caffeate > cholesteryl caffeate isomers. | (Marinova et al., 1998) |
| Cholesterol in emulsion | Formation of cholesterol oxidation products accelerated by AAPH at 37°C for 0-24 h. | 24-methylenecycloartanyl ferulate > campesteryl ferulate ≥ cycloartenyl ferulate. | (Xu et al., 2001) |
| Linoleic acid | 37°C air flow for 0-200 min, formation of hydroperoxide. | Cycloartenyl ferulate = 24-methylenecycloartanyl ferulate = campesteryl ferulate. | (Xu and Godber, 2001) |
| Soybean oil | Evaluation of oxidative stability index and the viscosity increase of oil at 100°C for 20-25 h and at 90°C for 17.5-18 h. | Sitostanyl ferulate > ORY. | (Wang et al., 2002) |
| Oxidation in multiple different systems | 1) Scavenging effect on DPPH$^{\bullet}$; 2) Inhibitory effect on autoxidation of methyl linoleate in bulk phase; 3) Evaluation of oxidative stability index; 4) Effect in peroxidation of PC liposomes. | 1&2): Cycloartenyl ferulate = 24-methylenecycloartanyl ferulate = ORY 3) Cycloartenyl ferulate = ORY ≥ 24-methylenecycloartanyl ferulate 4) No effect. | (Kikuzaki et al., 2002) |

| | | | |
|---|---|---|---|
| Refrigerated cooked beef | Stability test: oxidation products and flavor. | ORY effectively improved its flavor and oxidative stability. | (Kim et al., 2003) |
| Radical scavenging *in vitro*; rat brain cell homogenate | Protecting effect on phycoerythrin from peroxyl radical damage; assessing protein damage (carbonyl group content) and lipid peroxidation (malondialdehyde content). | Water soluble ORY scavenged peroxyl radical, prevented protein damage, and inhibited lipid peroxidation. | (Parrado et al., 2003) |
| SVEC4-10 mouse lymph endothelial cells | tBHP as oxidizing agent, cell viability determination. | 24-methylenecycloartanyl ferulate > cycloartenyl ferulate, campesteryl ferulate > ORY > α-tocopherol. | (Huang, 2003) |
| Radical scavenging *in vitro*; AMVN initiated lipid peroxidation; vegetable oils | Scavenging effect on DPPH$^\bullet$, O$_2^{\bullet-}$ and $^\bullet$OH; effect on lipoperoxidation; evaluation of oxidative stability of oils. | ORY scavenged DPPH$^\bullet$, but not O$_2^{\bullet-}$ and $^\bullet$OH, prevented the lipoperoxidation, and improved the oxidative stability of oils. | (Juliano et al., 2005) |
| Radical scavenging *in vitro*; methyl linoleate bulk oil and emulsion | 1) Scavenging effect on DPPH$^\bullet$; Inhibition effect in hydroperoxide formation in bulk oil 2) and emulsion 3). | 1): Ferulic acid > SF rye extract > SF wheat extract > cholesteryl ferulate = sitosteryl ferulate; 2): SF rye extract = SF wheat extract > sitosteryl ferulate = cholesteryl ferulate > ORY = cycloartenyl ferulate; 3): SF rye extract = SF wheat extract = sitosteryl ferulate. | (Nyström et al., 2005) |
| High oleic sunflower oil | Evaluation of triacylglycerol dimers and polymers at 100 and 180°C. | Sitosteryl ferulate prevented polymerization of oil. | (Nyström et al., 2007a) |
| Low-density lipoproteins | Effect on inhibition of its oxidation. | Dihydrocholesteryl ferulate showed no inhibition effect. | (Chigorimbo-Murefu et al., 2009) |
| Mouse lymphatic endothelial cells | Cell viability detection after induced oxidative damage. | 24-methylenecycloartanyl ferulate > cycloartenyl ferulate and campesteryl ferulate. | (Huang et al., 2009) |

| NIH 3T3 fibroblast cells | Measurement of intracellular ROS with DCFH-DA assay. | Cycloartenyl ferulate, ethyl ferulate and cycloartenol decreased the ROS level. | (Islam et al., 2009) |
|---|---|---|---|
| Radical scavenging *in vitro*; ferric reducing antioxidant power | Scavenging effect on DPPH$^{\bullet}$; evaluation of ferric reducing potential. | Microemulsion of rice bran oil plus ORY > microemulsion rice bran oil alone. | (Vorarat et al., 2010) |
| Radical scavenging *in vitro*; meat system | 1) Scavenging effect of oxygen radical; 2) Thiobarbituric acid reactive substances values in cooked ground meat system. | 1) SFs > vinyl ferulate = ferulic acid, 2) SFs > free phytosterols = ferulic acid. | (Tan and Shahidi, 2011) |
| Radical scavenging *in vitro*, linoleic acid | Scavenging effect on ABTS$^{\bullet+}$ and O$_2^{\bullet-}$; effect on linoleic acid peroxidation. | ORY scavenged ABTS$^{\bullet+}$ and O$_2^{\bullet-}$; exhibited strong inhibition effect on lipid peroxidation. | (Saenjum et al., 2012) |
| Soybean oil | The rate of polymerized triacylglycerol formation; two-day frying experiments using a miniature frying protocol with potato cubes. | Anti-polymerization: corn SFs > ORY and ferulic acid; corn SFs protected tocopherols; corn SFs was more stable in frying than ORY, but when corn SFs and ORY were combined, corn SFs protected ORY from degradation. | (Winkler-Moser et al., 2011) |
| Soybean oil | Effect on the reduction of polymerized triacylglycerol formation, monitoring double bonds loss from fatty acid at frying temperature 180°C. | Antipolymerization activity: corn SFs = ORY+ tocopherols > ORY; tocopherols had a protective effect on SFs; corn SFs were degraded more quickly during heating than ORY; they are effective antioxidants in frying oils. | (Winkler-Moser et al., 2013) |
| Hydrogen atom transfer and single electron transfer | Oxygen radical absorbance capacity; ferric reducing antioxidant power. | Ferulic acid = α-tocopherol = cholesteryl ferulate. | (Nagy et al., 2013) |
| Bulk oil model; emulsion system; low-density | 1) Evaluation of induction time in stripped corn oil system | 1) Steryl caffeate > sinapate ≥ vanillate and ferulate; | (Tan and Shahidi, 2013) |

| | | | |
|---|---|---|---|
| lipoprotein cholesterol oxidation model | under accelerated oxidative conditions; 2) The ability to decrease the oxidative bleaching of β-carotene in a β-carotene-linoleic acid emulsion; 3) The formation of conjugated dienes during low-density lipoprotein cholesterol oxidation. | phenolic acids ≥ steryl phenolates; 2) Steryl caffeate and sinapate > ferulate > vanillate; Steryl phenolates > phenolic acids (exception: ferulic acid = SF); 3) Ferulic acid > steryl caffeate, sinapate and ferulate and free phytosterol. | |
| Radical scavenging *in vitro*; soybean oil | 1) Scavenging ABTS$^{\bullet+}$; 2) Evaluation of oxidative stability index; 3) Analysis of antioxidant activity during frying. | 1) Ferulic acid > SFs; 2) Low antioxidant effect of ferulic acid and SFs 3) SF with stanol moiety > SF with sterol moiety. | (Winkler-Moser et al., 2015) |
| Radical scavenging *in vitro* | Scavenging effect on DPPH$^{\bullet}$ and ABTS$^{\bullet+}$. | Ferulic acid (*trans & cis*) and methyl caffeate > methyl ferulate (*trans & cis*) > cycloeucalenyl ferulate (*trans & cis*). | (Wang et al., 2015) |

**Abbreviations**: ABTS$^{\bullet+}$: 2,2'-azinobis(3-ethylbenzothiazoline-6-sulfonic acid) cation radical; AMVN: 2,2'-azobis(2,4-dimethylvaleronitrile); DPPH$^{\bullet}$: 2,2'-diphenyl-1-picrylhydrazyl radical; $^{\bullet}$OH: hydroxyl radical; $O_2^{\bullet-}$: superoxide anion radical; ORY: γ-oryzanol; ROS: reactive oxygen species; SF: steryl ferulate.

To date, antioxidant studies have mostly been performed with steryl ferulates mixture, and steryl ferulates have shown antioxidant activity in many oil systems and radical scavenging systems *in vitro*. A few antioxidant studies were performed in cell models *in vitro*, however, there are nearly no related studies *in vivo*. Furthermore, there are some indications that individual steryl ferulates may vary in their antioxidant activity, and therefore, the sterol composition may be an important aspect in defining the activity of steryl ferulates mixture. However, the relationship of structure and activity is not fully understood. Some studies reported that ferulic acid exhibited higher activity than steryl ferulates due to decreased solubility and steric hindrance by the sterol moiety (Nyström et al., 2005; Winkler-Moser et al., 2015), whereas some observations showed that steryl ferulates were better antioxidants than ferulic acid (Tan and Shahidi, 2011).

In some studies, 4-desmethylsteryl ferulates were observed to be better antioxidants than 4,4-dimethylsteryl ferulates (Nyström et al., 2005; Wang et al., 2002; Winkler-Moser et al., 2015), for which it was suggested to be a relic of the negative effects from the dimethyl group at C4 as well the cyclopropyl ring at C9/C19; However, contrary findings were reported by Huang et al. (2009) and Xu et al. (2001). As there are still discrepancies in the data, it is of great interest to evaluate the antioxidant activity of individual SFs more systematically.

## 3.3 Anti-inflammatory effect

Inflammation is caused by a variety of stimuli including physical damage, ultra violet irradiation, microbial invasion and immune reactions. The inflammatory cells create an inflammatory microenvironment and a network of signaling molecules, promoting their proliferation, angiogenesis, invasion and metastasis. Furthermore, chronic inflammation may lead to cancer development. Many studies have demonstrated that many bioactive dietary components have ant-inflammation activity, which are summarized by Gautam and colleagues (2009). Steryl ferulates have been shown to exhibit anti-inflammatory effect in many biological systems (Table 9). The anti-inflammatory studies of steryl ferulates are mostly related to their inhibition effect of NF-κB activity, one of the major transcription factors in regulating pro-inflammatory gene expression. Moreover, some models have been used to investigate the effect of steryl ferulates on other factors in inflammatory microenvironment, *e.g.*, COX-1, COX-2, iNOS mRNA, IL-1b mRNA and TNF-α mRNA.

**Table 9** Studies on anti-inflammatory activity of steryl ferulates

| Model | Method | Effect | Reference |
| --- | --- | --- | --- |
| Female mice | TPC-induced inflammatory ear edema, ear thickness determination after SF treatment. | Inhibitory activity: cycloartenyl and 24-methylenecycloartanyl ferulates < their corresponding free sterols; cycloeucalenyl, 24-methylenecholesteryl, sitosteryl and stigmastanyl ferulates > their corresponding free sterols. | (Akihisa et al., 2000) |

| | | | |
|---|---|---|---|
| Rats | ORY treatment (1-100 mg/kg) in swelling of the hind paw in adjuvant-induced arthritis in rats. | ORY inhibited COX-1 ($IC_{50}$ = 13 μmol) and COX-2 ($IC_{50}$ = 38 μmol); Cycloartenyl ferulate and stigmasteryl ferulate inhibited COX-1 and COX-2 with $IC_{50}$ values of 14-32 μmol. | (Terada and Haruta, 2003) |
| RAW 264.7 cells | Effect of ORY and cycloartenyl ferulate on NF-κB activation by measurement of cellular RNA and protein. | NF-κB, iNOS mRNA, COX-2 mRNA, and IL-1b mRNA expression decreased; no change of TNF-α mRNA expression; cycloartenyl ferulate significantly reduced NO production, inhibited DNA-binding of NF-κB, but upregulated SOD activity. | (Nagasaka et al., 2007) |
| Eight-week-old male C57BL/6J mice | Colitis induced in mice; Oral intake of 50 mg/kg/day ORY or cycloartenyl ferulate; evaluation of disease activity index, tissue myeloperoxidase activity, mRNA expressions, NF-κB activity in colitis tissue. | ORY and cycloartenyl ferulate markedly inhibited inflammatory reactions. | (Islam et al., 2008) |
| LPS-stimulated RAW 264.7 macrophages | Immunohistochemical analysis of NF-κB p65 nuclear translocation, SF treatment. | Cycloartenyl ferulate, 24-methylenecycloartanyl ferulate, β-sitosteryl ferulate, ethyl ferulate and cycloartenol significantly inhibited the NF-κB activity. | (Islam et al., 2009) |
| Eight-week-old, male Sprague-Dawley rats | CAF and ORY were injected intradermally with anti-DNP IgE into the dorsal skin of rats; analysis of cellular RNA, β-hexosaminidase release and light & heavy chains of anti-DNP or anti-TNP IgE. | Attenuated the passive cutaneous anaphylaxis reaction; inhibited the degranulation of DNP-IgE sensitized RBL-2H3 mast cells; cycloartenyl ferulate captured IgE, prevented it from binding to FcεRI, and attenuated mast cell degranulation. | (Oka et al., 2010) |
| Bovine aortic endothelial cells (BAECs), human umbilical vein endothelial cells (HUVECs) | LPS elevated the mRNA expression of VCAM-1, ICAM-1 and E-selectin; incubation with ORY (1-30 μM) for 24 h; measurement of cell viability, cellular RNA and protein. | ORY reduced adhesion molecule protein expression in HUVECs; reduced U937 monocyte adhesion to BAECs; inhibited NF-κ B activation in BAECs without affecting its viability. | (Sakai et al., 2012) |

| | | | |
|---|---|---|---|
| Rats with non-bacterial prostatitis | 1) Evaluation of prostate weight, prostate index, acid phosphatase, density of lecithin corpuscles, white blood cell and prostatic histologic section after SFs treatment<br>2) prostate gene expression profiling<br>3) pathway analysis and gene ontology analysis. | 1) Inhibition effect by SFs;<br>2) SF treatment group contained 238 up-regulated genes and 111 down-regulated genes;<br>3) Significant expression genes were related to the terms of fibrinolysis, inflammatory response, high-density lipoprotein particle, protein–lipid complex, enzyme inhibitor activity, peptidase inhibitor activity; canonical pathway analysis indicated that five pathways (associated with inflammation and tumorgenesis) were regulated. | (Hu et al., 2014) |

**Abbreviations**: DNP: dinitrophenyl; FcεRI: high affinity IgE receptor; ICAM-1: intercellular adhesion molecule-1; IgE: immunoglobulin E; LPS: lipopolysaccharide; ORY: γ-oryzanol; SF: steryl ferulate; TNP: trinitrophenyl; TPC: 12-O-tetradecanoylphorbol-13-acetate. VCAM-1: vascular cell adhesion molecule-1.

## 3.4 Anti-carcinogenic effect

Cancer prevention is now one of the most urgent projects in public health. There are a few studies about the anti-cancer potential of steryl ferulates (Table 10).

**Table 10** Studies on anti-carcinogenic effect of steryl ferulates

| Model | Method | Effect | Reference |
|---|---|---|---|
| Carcinogenesis in mouse skin of female mice | Two-stage model of skin carcinogenesis with injection of DMBA and promotion by TPA, treatment with 2 μmol cycloartenyl ferulate for 20 weeks. | Cycloartenyl ferulate inhibited accumulation of ornithine decarboxylase, and reduced 86% of number of tumors per mouse. | (Yasukawa et al., 1998) |
| Human breast adenocarcinoma MCF-7 cells | Incubation with SF, cell cytotoxicity. | The order of $IC_{50}$ of cytotoxicity:<br>24-diol-cycloarteneyl (24S) ><br>25-diol-cycloarteneyl = cycloartenyl ><br>24-diol-cycloarteneyl (24R) ><br>24-methylenecyoartenyl ferulate. | (Luo et al., 2005) |

| Human colorectal adenocarcinoma SW480 and SW620, Colo-201 Cells | Incubation with cycloartenyl ferulate (0-640 μM); evaluation of cytotoxicity, apoptotic population, mitochondrial membrane potential, regression of tumor xenografts in nude mice. | Cycloartenyl ferulate elicited apoptosis in SW480 and sensitized metastatic SW620 cells to TRAIL-induced apoptosis. | (Kong et al., 2009) |
| --- | --- | --- | --- |
| Pathogen-free female BALB/c mice | Transplantation of CT-26 murine colon cancer cells; determination of tumor growth and tumor related biomarkers: splenic natural killer cell cytolysis, nitric oxide generation, phagocytotic uptake, cellular RNA and protein, cytokines and eicosanoids. | Reduction of the tumor growth by 44% without affecting the weight of other organs; inhibition effect by induction of splenic natural killer activity, activation of macrophages, and inhibition of angiogenesis. | (Kim et al., 2012) |

**Abbreviations**: DMBA: 7,12-dimethylbenz(a)anthracene; ORY: γ-oryzanol; SF: steryl ferulate; TPA: 12-O-tetradecanoylphorbol-13-acetate.

Although there are some data related to anti-carcinogenic effect of steryl ferulate, the mechanism is unclear. Yasukawa and colleagues (1998) suggested that the possible reason to reduce the number of tumors by steryl ferulates might be: (1) improve peripheral blood flow, (2) increase sebaceous gland cell turnover and secretion, (3) exhibit antioxidant and anti-inflammatory effect further to anti-tumor. In the study by Kong and colleagues (2009), steryl ferulate (cycloartenyl ferulate) elevated the death receptors DR4 and DR5 and triggered both of death receptor and mitochondrial apoptosis pathways in SW480 cells. After incubation with steryl ferulate, the anti-apoptotic Bcl-2 was reduced whereas the pro-apoptotic Bak was up-regulated, then the mitochondrial membrane potential dissipated, and cyto c as well as SMAC/DIABLO from mitochondria were released into the cytosol. Additionally, Bid was cleaved by caspase-8, so that the death receptor pathway might be exaggerated by the mitochondrial pathway. Moreover, cycloartenyl ferulate could sensitize the metastatic and resistant colon cancer SW620 to TRAIL-induced apoptosis with the mechanisms involved at least enhance activation of caspase-8 and caspase-3. Recently, Kim and

colleagues (2012) observed that the inhibition effect of tumor growth was associated with regulation of some biomarkers, which might shed light on the mechanism. The treatment of steryl ferulates could increase the activity of splenic natural killer cells. And the partial restoration of nitric oxide production and phagocytosis in peritoneal macrophages promoted the release of pro-inflammatory cytokines TNF-α, IL-1β and IL-6. Additionally, they observed that the number of blood vessels inside the tumor reduced after the treatment. Moreover, pro-angiogenic biomarkers like COX-2 and 5-lipoxygenase were also significantly reduced. The reduced COX-2 and 5-lipoxygenase expression down regulated vascular endothelial growth factor VEGF and further inhibited neoangiogenesis inside the tumors. All of these observations support the anti-cancer effect of steryl ferulates. However, there is still need for more studies to understand the exact mechanism.

## 3.5 Other properties

**Anti-ulcer effect.** Several experiments have been conducted to analyze the anti-ulcer potential of steryl ferulates in 1970s-1980s. Itaya and colleagues suggested that the antiulcerogenic effect of γ-oryzanol was due to the participation of autonomic nervous system (1976), involvement of monoaminergic neuron system (1976) and circadian rhythms (1977). Further, it was assumed that the gastric anti-secretory effect was mediated by the vagus nerve (Mizuta et al., 1978). These findings were confirmed both in gastric ulcer and duodenal ulcer rat models (Itaya and Isikawa, 1978). Moreover, Ichimaru and colleagues (1984) reported that γ-oryzanol had an antiulcerative action on gastric lesions induced by both conditioned emotional stimuli and rapid eye movement sleep deprivations in mice model. γ-oryzanol was also found to improve dyspepsia symptoms in patients with chronic gastritis (Arai, 1982).

**Effect on type 2 diabetes.** Some studies have been conducted to evaluate the potential of steryl ferulate as a therapeutic agent against diabetes mellitus. Ohara and colleagues (2009) found that γ-oryzanol could increase the concentration of serum adiponectin by the inhibition of NF-κB activation, increase the insulin sensitivity, and ameliorate type

2 diabetes in mice. γ-Oryzanol was also reported to ameliorate insulin resistance and hyperlipidemia in rats with streptozotocin/nicotinamide-induced type 2 diabetes (Cheng et al., 2010). Recently, Ghatak and colleagues reported that γ-oryzanol possessed the potential to effectively produce a reduction in blood glucose levels (2012b) and exhibited protective effect on diabetic neuropathy in rat model (2012c).

**Effect on menopausal disorders.** In the 1960s, γ-oryzanol ($3 \times 100$ mg/day for 38 days) was administrated to women with hysterectomy (surgical menopause); most of the women had a significant reduction in menopausal symptoms such as hot flushes (Murase and Lishima, 1963). Furthermore, in another study, women with climacteric disturbances were administered with γ-oryzanol (300 mg/day) for 4-8 weeks. Most of them were observed with a general improvement concerning the reduction of menopausal disorders (Ishihara et al., 1982).

**Effect on serum thyroid stimulation hormone.** Shimomura and colleagues (1980) reported that 300 mg γ-oryzanol reduced significantly the elevated serum thyroid stimulation hormone levels in hypothyroid patients, possibly by a direct action at the hypothalamus.

**Effect on muscle.** A recent study indicated that γ-oryzanol supplementation (600 mg/day) during the 9-week resistance training did not change anthropometric and body measurements, but increased the muscular strength in young healthy males (Eslami et al., 2014). Nevertheless, some evidence showed that γ-oryzanol supplementation (500 mg/day for 9 weeks) did not influence performance or related physiological parameters in moderately weight-trained males (Fry et al., 1997).

**Effect on osteogenesis.** γ-oryzanol from germinated brown rice was found to stimulate osteoblastogenesis by up regulation of bone formation genes, possibly via the activation of $GABA_B$ receptors (Muhammad et al., 2013).

**Antiviral activity.** Galabov and colleagues (1998) reported that cholesteryl ferulate had activity against the poliovirus type 1 (Mahoney). Further, cycloartenyl ferulate and 24-methylenecycloartanyl ferulate were found to have activity against Human Immunodeficiency Virus-1 (HIV-1) by inhibition of HIV-1 reserve transcriptase, with $IC_{50}$ values at 2.2 μM and 1.9 μM, respectively (Akihisa et al., 2001). Moreover, campestanyl, $\Delta^5$ and $\Delta^7$-campesteryl, sitostanyl, $\Delta^5$ and $\Delta^7$-sitosteryl, and 24-methlenecholestanyl ferulates were reported to inhibit Epstein-Barr virus activation (Iwatsuki et al., 2003).

## 3.6 Safety aspects

Some studies have been performed to explore the safety of steryl ferulates regarding their carcinogenic properties. The results showed that γ-oryzanol was not carcinogenic at 2000 mg/kg body weight/day for 78 weeks in B6C3F1 mouse (Tamagawa et al., 1992a) and for 2 years in F344 rat (Tamagawa et al., 1992b). Some studies reported that γ-oryzanol could not initiate the carcinogenesis, but it could enhance the lung carcinogenesis in high dose (1% in diet for 36 weeks) in F344 rat (Hirose et al., 1999; Hirose et al., 1991). Moreover, one study showed that γ-oryzanol stimulated sebaceous gland secretion after topical application in cosmetics, which might be a negative effect (Ueda et al., 1976). Its genotoxicity was also investigated, and it was found to be negative in the bacterial DNA repair, the rat bone marrow chromosome aberration and the Ames test (Ghatak and Panchal, 2011). Furthermore, some adverse effects including nocturia and breast pain have been reported, when γ-oryzanol was administered together with some drugs such as domperidome and pyrixodine hydrochloride (Ghatak and Panchal, 2011).

# 4 Absorption and metabolism

## 4.1 Bioaccessibility

**Liberation from food matrix**. Dietary intake of steryl ferulates usually comes from cereal grains like rice, wheat and corn. Recently, an *in vitro* digestion model was applied to evaluate the availability of steryl ferulates from raw rice, wild rice, corn bran, wheat flour and bread for absorption in the gastrointestinal tract (Mandak and Nyström, 2012; Mandak and Nyström, 2013). The authors found that the liberation of steryl ferulates from these grain matrices was very low (0.03-1.5%). Furthermore, the processing of rice, wild rice or corn did not result in an increased liberation.

**Possible hydrolysis during digestion.** It has been hypothesized that steryl ferulates are cleaved in the gastrointestinal tract by some enzymes and then the products are subsequently absorbed into the systemic circulation (Berger et al., 2005). According to the structure of steryl ferulate, the enzymes, *e.g.*, lipases, cholesterol esterase and ferulic acid esterase, may hydrolyse the ester bond between the sterol and ferulic acid moiety.

Miller and colleagues (2004) found that cholesterol esterase (EC 3.1.1.13) from porcine and bovine pancreas only hydrolysed the 4-desmethylsteryl ferulates (β-sitosteryl ferulate and campesteryl ferulate) in γ-oryzanol in 24 h *in vitro*. The hydrolysis of steryl ferulates by pancreatic cholesterol esterase *in vitro* was also confirmed by Moreau and Hicks (2004) and Nyström and colleagues (2008). However, in the previously described studies, the extent of hydrolysis was only based on the decrease of substrate, not simultaneous increase of hydrolysis products (free sterols and ferulic acid). In another study by Huang (2003), the decrease in γ-oryzanol was not accompanied by the hydrolysis products using an *in vitro* cell model. Furthermore, ferulic acid esterases are also present in the gastrointestinal tract, mostly in the small and large intestine, generated by mammalian mucosa cells or bacteria (Andreasen et al., 2001). Ferulic acid esterases might also have a potential to cleave steryl ferulates, however, there are no related studies available.

Recently, it was found that an *in vitro* digestion led to a decrease in steryl ferulates and an increase in free sterols, which might imply that free sterols were from steryl ferulates by hydrolytic enzymes during digestion. However, when steryl ferulate standards were

incubated with related enzymes, the decrease of steryl ferulates was not accompanied by formation of hydrolysis products (Mandak and Nyström, 2012; Mandak and Nyström, 2013). Moreover, the conditions applied for steryl ferulate hydrolysis in *in vitro* models are not truly representative of that *in vivo*. Therefore, the hydrolysis of steryl ferulate during digestion *in vivo* is still unclear.

## 4.2 Absorption and metabolism

**Animal or cell models**. Fujiwara and colleagues studied the absorption and metabolism of γ-oryzanol *in vivo* with rabbits (1980), dogs (1982) and rats (1983), and they found that the absorption in animal models was very low.

When the rats were fed with ^{14}C-labelled γ-oryzanol (triterpenyl esters of ferulic acid-3-^{14}C) at a dose of 50 mg/kg body weight, 9.8% of radioactivity was detected in the urine within 72 h after oral administration, and about 85% of the radioactive dose was found in the feces, suggesting that the majority of steryl ferulates were not absorbed in the intestine. Furthermore, only a small fraction of radioactivity transferred to blood, with a peak concentration corresponding to 0.06% of the dose at 4 h after administration. Intact steryl ferulates were not detected in the urine. An *in situ* intestinal absorption experiment suggested that more than 80% of the absorbed radioactivity was transferred into the mesenteric vein as an intact form, suggesting that some was metabolized in the small intestine during absorption. Moreover, the authors also suggested that steryl ferulates were absorbed mainly into blood via the portal vein system, not the lymph via the thoracic duct. In urine, ferulic acid, dihydroferulic acid, *m*-hydroxyphenylpropionic acid, *m*-coumaric acid, hippuric acid as well as *m*-hydroxyhippuric acid in free and conjugated forms (glucuronides or sulfates) were identified as urinary metabolites of γ-oryzanol (Fujiwara et al., 1983).

In the study of rabbits with oral administration of ^{14}C-labelled γ-oryzanol at a dose of 40 mg/kg, the absorption of γ-oryzanol was extremely low and the radioactivity in blood reached a maximum at 3 h and no detection at 24 h; but unlike in rats, in rabbits the

absorbed γ-oryzanol was found as the intact form (Fujiwara et al., 1980). Moreover, γ-oryzanol was administered orally to rabbit and dog at the dose of 25, 50, 100 mg/kg in the sesame oil; and ferulic acid was suggested as the main metabolite of γ-oryzanol in plasma, with extremely low concentrations of 5-150 ng/mL (Fujiwara et al., 1982).

Furthermore, there is a study available to investigate the uptake behavior in *in vitro* human intestinal cells C2BBe1 cell model. However, no uptake of γ-oryzanol was found during 2 hours incubation, whereas under the same conditions some cholesterol was taken up by the cells. To conclude, all these models suggest that steryl ferulates are poorly absorbed compounds.

**Clinical studies**. There are very few studies concerning their fate in human. In the study by Umehara and colleagues (2004), after an oral dose of 600 mg, the peak plasma concentration of steryl ferulates in healthy volunteers was 21 to 107 ng/mL (equivalent to 0.01-0.05% of the total administered dose); and after repetitive oral dose of 100 mg three times a day for 10 days, the peak plasma concentration was 112 ng/mL ($< 0.3\%$ of the dose).

Lubinus and colleagues (2013) investigated the metabolic fate of steryl ferulates in human after consumption. Volunteers took a daily dose of 5% γ-oryzanol in skimmed milk yogurt for 3 days, and nearly 80% of intact γ-oryzanol was recovered in the feces. No intact steryl ferulate was reported in the blood sample after consumption, and only cycloartenol, which was thought as the product from cycloartenyl ferulate, was increased significantly by 24 % from day 0 (59 ng/mL) to day 3 (73 ng/mL). After consumption of γ-oryzanol-rich yogurt, the authors also detected coprostanol, 24-methylcoprostanol, 24-ethylcoprostanol, campesterol, campestanol and sitosterol in feces; compounds 24-methylcoprostanol and 24-ethylcoprostanol were suggested as the microbial transformation products of campesterol and sitosterol, respectively. Thus, the free sterols were only from 4-desmethylsteryl ferulates and there was no products from 4,4'-dimethylsteryl ferulates. The hydrolysis ratio of campesteryl, campestanyl and sitosteryl ferulate was reported to be 26%, 12% and 27%, respectively.

**Possible hydrolysis occurs.** Pancreatic cholesterol esterase may hydrolyse steryl ferulate and the possible uptake/transport of ferulic acid and sterol can occur in small intestine. Intestinal microorganisms may also hydrolyse steryl ferulate, however the uptake of its product in the large intestine is unlikely. The intestinal absorption of phytosterols and ferulic acid have been extensively studied.

For healthy humans, the absorption ratio of phytosterols is usually less than 5% of dietary level, which is much lower than that of cholesterol (over 40%). Moreover, there is some evidence that various phytosterols have different absorption ratio, which may be caused by the variation of side chain (campesterol > sitosterol > stigmasterol) and double bond at C5 (sitosterol > sitostanol) (Ling and Jones, 1995). The passage of sterols across intestinal barrier has been studied for a long time. Generally, within the intestinal lumen, the micellar solubilization of sterol moves through the diffusion barrier overlaying the surface of absorptive cells. Phytosterols have a higher affinity to micelles than cholesterol, and they thereby displace cholesterol from these micelles and reduce cholesterol absorption. Sterol influx transporter (Niemann-Pick C1-Like 1) is located at the apical membrane of the enterocyte, which may actively facilitate the uptake of cholesterol and phytosterols by promoting the passage of sterols across the brush border membrane of the enterocyte. In contrast, the 2 adenosine triphosphate (ATP)-binding cassette (ABC) half-transporters ABCG5 and ABCG8 promote active efflux of sterols, especially absorbed phytosterols, from the enterocyte into the intestinal lumen for excretion. Defects of either of these cotransporters lead to the rare inherited disease of phytosterolemia. In enterocyte, sterols are esterified, further incorporated into nascent chylomicrons, and then subsequently secreted into the lymph (von Bergmann et al., 2005; Wang, 2007).

The absorption and metabolism of ferulic acid were summarized by Zhao and Moghadasian (2008). Absorption models *in situ* and *ex vivo* suggest that ferulic acid has high absorption rate in the stomach, jejunum and ileum. Furthermore, $H^+$-driven transport system, $Na^+$-dependent carrier-mediated transport process and monocarboxylic acid transporters have been suggested for ferulic acid across the brush

border membrane, but there are still some discrepancies in this topic. Moreover, ferulic acid can be metabolized *in vivo* into a number of metabolites including ferulic acid (FA)-glucuronide, FA-sulfate, FA-diglucuronide, FA-sulfoglucuronide, *m*-hydroxyphenylpropionic acid, feruloylglycine, dihydroferulic acid, vanillic acid and vanilloylglycine.

In the case of steryl ferulate, after oral intake of γ-oryzanol in rat, ferulic acid, dihydroferulic acid, *m*-hydroxyphenylpropionic acid and *m*-hydroxyhippuric acid were detected in the urine, suggesting that the hydrolysis of steryl ferulate may occur *in vivo* (Fujiwara et al., 1983). Moreover, the hydrolysis *in vivo* might take place by pancreatic cholesterol esterase and intestinal microorganisms, maximum 15% according to the clinical study by Lubinus and colleagues (2013). Additionally, in a recent study, Nagy and colleagues (2013) detected cholesteryl ferulate in human plasma after coffee consumption, and hypothesized that esterification of ferulic acid with cholesterol can occur *in vivo*. This study may provide new thoughts concerning the regulation of enzyme activity by reverse hydrolysis reactions *in vivo*.

To date, there are no studies regarding the passage of steryl ferulates across the intestinal barrier. As the conjugate of sterol and ferulic acid, there is no evidence suggesting the similarity of passage mechanism between intact steryl ferulate and phytosterol or ferulic acid. Previous studies suggest low absorption behavior of steryl ferulates. Nevertheless, none of these studies provide clear evidence regarding their exact behavior of absorption or metabolism, let alone the possible difference from individual steryl ferulates. Therefore, more studies are needed to explore this topic.

## 4.3 Daily intake

Assessment on the daily intake of steryl ferulates has not been published yet. Steryl ferulates are obtained from certain cereal grains and seeds in daily life. Since the bioaccessibility of steryl ferulates from a grain matrix is negligible, the rice bran oil (with 0.4-55 mg/g steryl ferulates), wheat bran oil (2 mg/g), corn oil (3-6 mg/g), and

supplementation may be better sources of steryl ferulates. The dosages of steryl ferulates used are highly variable in their health promoting studies, *e.g.*, low dose of 50 mg or high dose of 300-800 mg daily. As there are no solid benefits associated with steryl ferulate supplementation in the first place, the recommendation dosage is still unsure.

# 5 Applications

Steryl ferulates possess a wide range of health promoting properties. In Japan, γ-oryzanol is approved as food additive. Several food including γ-oryzanol have been patented, *e.g.*, "Food additive for fried food coating comprises gamma-oryzanol" (Kaneya et al., 2010), "Oral or food and drink composition used as anti-fatigue agent comprises sesamin and (gamma)-oryzanol" (Ono et al., 2007) and "Agent e.g. food/beverage product for treating osteoporosis and preventing or improving hyperuricemia, contains gamma-oryzanol as an active ingredient" (Yamada, 2009). However, neither the EFSA nor FDA have yet declared it as a food additive.

Nowadays, γ-oryzanol has been applied in the cosmetic industry as a sunscreen or anti-aging agent, due to its antioxidant potential, such as preventing UV-light induced lipid peroxidation, preventing skin aging and attenuating melanin-related disorders activities. Many products like skin cream, shampoo, cleaning cream or hair products contain γ-oryzanol, which are partially listed in Environmental Working Group's Skin Deep® Cosmetics Database. There are also patents in cosmetic using γ-oryzanol, *e.g.*, "Mascara and eyebrow pencils containing γ-oryzanoland calcium salts" (Petsitis and Riedel, 1999), "Aqueous cosmetic composition containing composite material particles and γ-oryzanol"(Grace et al., 2013), and "Non-chemical sunscreen composition" (Manirazman, 1998).

γ-Oryzanol is also available as a supplement in the market, *e.g.*, the product called "Gamma Oryzanol" with tablet form from nutraceutical company KAL® and Source Naturals®. In the USA, it is widely used as a sport supplement to improve athletic

performance and body building with the claim of increase of testosterone production and stimulation of human growth hormone release. This supplement is recommended by the producer with the other uses, *e.g.*, cholesterol reduction, heart disease prevention, menopausal symptoms treatment, and ulcers protection, with the therapeutic dosage of 500 mg daily. However, there is no daily requirement standard for γ-oryzanol and no solid valid evidence supporting its use for these purposes.

# References

Akihisa, T., Ogihara, J., Kato, J., Yasukawa, K., Ukiya, M., Yamanouchi, S. and Oishi, K., 2001. Inhibitory effects of triterpenoids and sterols on human immunodeficiency virus-1 reverse transcriptase. Lipids, 36(5): 507-512.

Akihisa, T., Yasukawa, K., Yamaura, M., Ukiya, M., Kimura, Y., Shimizu, N. and Arai, K., 2000. Triterpene alcohol and sterol ferulates from rice bran and their anti-inflammatory effects. Journal of Agricultural and Food Chemistry, 48(6): 2313-2319.

Aladedunye, F., Przybylski, R., Rudzinska, M. and Klensporf-Pawlik, D., 2013. γ-Oryzanols of North American wild rice (Zizania palustris). Journal of the American Oil Chemists' Society, 90(8): 1101-1109.

Andreasen, M.F., Kroon, P.A., Williamson, G. and Garcia-Conesa, M.T., 2001. Esterase activity able to hydrolyze dietary antioxidant hydroxycinnamates is distributed along the intestine of mammals. Journal of Agricultural and Food Chemistry, 49(11): 5679-5684.

Anwar, F., Anwer, T. and Mahmood, Z., 2005. Methodical characterization of rice (Oryza sativa) bran oil from Pakistan. Grasas Y Aceites, 56(2): 125-134.

Arai, T., 1982. Effect of gamma-oryzanol on indefinite complaints in the gastrointestinal symptoms in patients with chronic gastritis -- studies on the endocrinological environment. Horumon To Rinsho, 30(3): 271-279.

Arruda Filho, A.C.V., Guedes, M.I.F., Duarte, L.S.F., Lima-neto, A.B.M., Cameron, L.-c., Bassini, A., Vieira, Í.G.P., De Melo, T.S., De Almeida, L.M. and Queiroz, M.G.R., 2014. Gamma-oryzanol has an equivalent efficacy as a lipid lowering agent compared to fibrate and statin in two dyslipidemia mice models International Journal of Pharmacy and Pharmaceutical Sciences, 6(11):61-64.

Benveniste, P., 2002. Sterol Metabolism. The Arabidopsis Book / American Society of Plant Biologists, 1: e0004.

Berger, A., Rein, D., Schafer, A., Monnard, I., Gremaud, G., Lambelet, P. and Bertoli, C., 2005. Similar cholesterol-lowering properties of rice bran oil, with varied gamma-oryzanol, in mildly hypercholesterolemic men. European Journal of Nutrition, 44(3): 163-173.

Bergman, C.J. and Xu, Z., 2003. Genotype and environment effects on tocopherol, tocotrienol, and γ-oryzanol contents of southern U.S. rice. Cereal Chemistry, 80(4): 446-449.

Britz, S.J., Prasad, P.V., Moreau, R.A., Allen, L.H.J., Kremer, D.F. and Boote, K.J., 2007. Influence of growth temperature on the amounts of tocopherols, tocotrienols, and gamma-oryzanol in brown rice. Journal of Agricultural and Food Chemistry, 55(18): 7559-7565.

Buri, R.C., von Reding, W. and Gavin, M.H., 2004. Description and characterization of wheat aleurone. Cereal Foods World, 49(5): 274-282.

Chen, Q., Steinhauer, L., Hammerlindl, J., Keller, W. and Zou, J., 2007. Biosynthesis of phytosterol esters: identification of a sterol o-acyltransferase in Arabidopsis. Plant Physiology, 145(3): 974-984.

Cheng, H.H., Ma, C.Y., Chou, T.W., Chen, Y.Y. and Lai, M.H., 2010. Gamma-oryzanol ameliorates insulin resistance and hyperlipidemia in rats with streptozotocin/nicotinamide-induced type 2 diabetes. International Journal for Vitamin and Nutrition Research. , 80(1): 45-53.

Chigorimbo-Murefu, N.T.L., Riva, S. and Burton, S.G., 2009. Lipase-catalysed synthesis of esters of ferulic acid with natural compounds and evaluation of their antioxidant properties. Journal of Molecular Catalysis B-Enzymatic, 56(4): 277-282.

Cho, J.-Y., Lee, H.J., Kim, G.A., Kim, G.D., Lee, Y.S., Shin, S.C., Park, K.-H. and Moon, J.-H., 2012. Quantitative analyses of individual γ-Oryzanol (steryl ferulates) in conventional and organic brown rice (Oryza sativa L.). Journal of Cereal Science, 55(3): 337-343.

De Smet, E., Mensink, R.P. and Plat, J., 2012. Effects of plant sterols and stanols on intestinal cholesterol metabolism: suggested mechanisms from past to present. Molecular Nutrition & Food Research, 56(7): 1058-1072.

Esche, R., Barnsteiner, A., Scholz, B. and Engel, K.H., 2012. Simultaneous analysis of free phytosterols/phytostanols and intact phytosteryl/phytostanyl fatty acid and phenolic acid esters in cereals. Journal of Agricultural and Food Chemistry, 60(21): 5330-5339.

Esche, R., Scholz, B. and Engel, K.H., 2013a. Analysis of free phytosterols/stanols and their intact fatty acid and phenolic acid esters in various corn cultivars. Journal of Cereal Science, 58(2): 333-340.

Esche, R., Scholz, B. and Engel, K.H., 2013b. Online LC-GC analysis of free sterols/stanols and intact steryl/stanyl esters in cereals. Journal of Agricultural and Food Chemistry, 61(46): 10932-10939.

Eslami, S., Esa, N.M., Marandi, S.M., Ghasemi, G. and Eslami, S., 2014. Effects of gamma oryzanol supplementation on anthropometric measurements & muscular strength in healthy males following chronic resistance training. The Indian Journal of Medical Research, 139(6): 857-863.

European Food Safety Authority 2010. Scientific Opinion on the Substantiation of Health Claims Related to Plant Sterols and Plant Stanols and Maintenance of Normal Blood Cholesterol Concentrations (Id 549, 550, 567, 713, 1234, 1235,1466, 1634, 1984, 2909, 3140), and Maintenance of Normal Prostate Size

and Normal Urination (Id 714, 1467, 1635) Pursuant to Article 13(1) of Regulation (Ec) No 1924/20061. EFSA Journal, 8, 1813-1836.

Fang, N., Yu, S. and Badger, T.M., 2003. Characterization of triterpene alcohol and sterol ferulates in rice bran using LC-MS/MS. Journal of Agricultural and Food Chemistry, 51(11): 3260-3267.

Finocchiaro, F., Ferrari, B., Gianinetti, A., Dall'asta, C., Galaverna, G., Scazzina, F. and Pellegrini, N., 2007. Characterization of antioxidant compounds of red and white rice and changes in total antioxidant capacity during processing. Molecular Nutrition & Food Research, 51(8): 1006-1019.

Fujiwara, S., Noumi, K., Sugimoto, I. and Awata, N., 1982. Mass fragmentographic determination of ferulic acid in plasma after oral administration of gamma-oryzanol. Chemical & pharmaceutical bulletin, 30(3): 973-979.

Fujiwara, S., Sakurai, S., Noumi, K., Sugimoto, I. and Awata, N., 1980. Metabolism of gamma-oryzanol in rabbit. Yakugaku zasshi, 100(10): 1011-1018.

Fujiwara, S., Sakurai, S., Sugimoto, I. and Awata, N., 1983. Absorption and metabolism of gamma-oryzanol in rats. Chemical & pharmaceutical bulletin, 31(2): 645-652.

Galabov, A.S., Nikolaeva, L., Todorova, D. and Milkova, T., 1998. Antiviral activity of cholesteryl esters of cinnamic acid derivatives. Zeitschrift fur Naturforschung C, 53(9-10): 883-887.

Gautam, R. and Jachak, S.M., 2009. Recent developments in anti-inflammatory natural products. Medicinal Research Reviews, 29(5): 767-820.

Ghatak, S.B. and Panchal, S.J., 2011. Gamma-oryzanol-A multi-purpose steryl ferulate. Current Nutrition and Food Science, 7(1): 10-20.

Ghatak, S.B. and Panchal, S.J., 2012a. Anti-hyperlipidemic activity of oryzanol, isolated from crude rice bran oil, on Triton WR-1339-induced acute hyperlipidemia in rats. Revista Brasileira De Farmacognosia-Brazilian Journal of Pharmacognosy, 22(3): 642-648.

Ghatak, S.B. and Panchal, S.S., 2012b. Anti-diabetic activity of oryzanol and its relationship with the anti-oxidant property. International Journal of Diabetes in Developing Countries, 32(4): 185-192.

Ghatak, S.B. and Panchal, S.S., 2012c. Protective effect of oryzanol isolated from crude rice bran oil in experimental model of diabetic neuropathy. Revista Brasileira De Farmacognosia-Brazilian Journal of Pharmacognosy, 22(5): 1092-1103.

Grace, C., Marion, C. and Philippon, C., 2013. Aqueous cosmetic composition containing composite material particles and gamma-oryzanol. WO 2012110303 A3, France.

Graf, E., 1992. Antioxidant potential of ferulic acid. Free Radical Biology and Medicine, 13(4): 435-448.

Gylling, H., Plat, J., Turley, S., Ginsberg, H.N., Ellegard, L., Jessup, W., Jones, P.J., Lutjohann, D., Maerz, W., Masana, L., Silbernagel, G., Staels, B., Boren, J., Catapano, A.L., De Backer, G., Deanfield, J., Descamps, O.S., Kovanen, P.T., Riccardi, G., Tokgozoglu, L., Chapman, M.J. and European Atherosclerosis Society Consensus Panel on, P., 2014. Plant sterols and plant stanols in the management of dyslipidaemia and prevention of cardiovascular disease. Atherosclerosis, 232(2): 346-360.

Hakala, P., Lampi, A.M., Ollilainen, V., Werner, U., Murkovic, M., Wahala, K., Karkola, S. and Piironen, V., 2002. Steryl phenolic acid esters in cereals and their milling fractions. Journal of Agricultural and Food Chemistry, 50(19): 5300-5307.

Hirose, M., Fukushima, S., Imaida, K., Ito, N. and Shirai, T., 1999. Modifying effects of phytic acid and gamma-oryzanol on the promotion stage of rat carcinogenesis. Anticancer Research, 19(5A): 3665-3670.

Hirose, M., Ozaki, K., Takaba, K., Fukushima, S., Shirai, T. and Ito, N., 1991. Modifying effects of the naturally occurring antioxidants gamma-oryzanol, phytic acid, tannic acid and n-tritriacontane-16, 18-dione in a rat wide-spectrum organ carcinogenesis model. Carcinogenesis, 12(10): 1917-1921.

Hu, Y.Z., Xiong, L.N., Huang, W.S., Cai, H.F., Luo, Y.X., Zhang, Y. and Lu, B.Y., 2014. Anti-inflammatory effect and prostate gene expression profiling of steryl ferulate on experimental rats with non-bacterial prostatitis. Food & Function, 5(6): 1150-1159.

Huang, C.J., 2003. Potential functionality and digestibility of oryzanol as determined using in vitro cell culture models. PhD Thesis Thesis, Louisiana State University.

Huang, C.J., Xu, Z. and Godber, J.S., 2009. Potential antioxidant activity of gammaoryzanol in rice bran as determined using an in vitro-mouse lymph axilliary endothelial model. Cereal Chemistry, (86): 679-684.

Huang, S.H. and Ng, L.T., 2011. Quantification of tocopherols, tocotrienols, and γ-oryzanol contents and their distribution in some commercial rice varieties in Taiwan. Journal of Agricultural and Food Chemistry, 59(20): 11150-11159.

Ichimaru, Y., Moriyama, M., Ichimaru, M. and Gomita, Y., 1984. Effects of gamma-oryzanol on gastric lesions and small intestinal propulsive activity in mice. Nihon Yakurigaku Zasshi, 84(6): 537-542.

Imsanguan, P., Roaysubtawee, A., Borirak, R., Pongamphai, S., Douglas, S. and Douglas, P.L., 2008. Extraction of α-tocopherol and γ-oryzanol from rice bran. LWT - Food Science and Technology, 41(8): 1417-1424.

Ishihara, M., Ito, Y., Nakakita, T., Maehama, T., Hieda, S., Yamamoto, K. and Ueno, N., 1982. Clinical effect of gamma-oryzanol on climacteric disturbance -on serum lipid peroxides. Nihon Sanka Fujinka Gakkai Zasshi, 34(2): 243-251.

Islam, M.S., Murata, T., Fujisawa, M., Nagasaka, R., Ushio, H., Bari, A.M., Hori, M. and Ozaki, H., 2008. Anti-inflammatory effects of phytosteryl ferulates in colitis induced by dextran sulphate sodium in mice. British Journal of Pharmacology, 154(4): 812-824.

Islam, M.S., Yoshida, H., Matsuki, N., Ono, K., Nagasaka, R., Ushio, H., Guo, Y., Hiramatsu, T., Hosoya, T., Murata, T., Hori, M. and Ozaki, H., 2009. Antioxidant, free radical-scavenging, and NF-kappaB-inhibitory activities of phytosteryl ferulates: structure-activity studies. Journal of Pharmacological Sciences, 111(4): 328-337.

Itaya, K. and Isikawa, M., 1978. Effect of γ-oryzanol on experimental gastric ulcer and duodenal ulcer in rat. Pharmacometrics, 16(3): 493-501.

Itaya, K., Kitonaga, J. and Ishikawa, M., 1976. Studies of gamma-oryzanol (2). The antiulcerogenic action. Nihon Yakurigaku Zasshi, 72(8): 1001-1011.

Itaya, K. and Kiyonaga, J., 1976. Studies of gamma-oryzanol (1). Effects on stress-induced ulcer. Nihon Yakurigaku Zasshi, 72(4): 475-481.

Itaya, K., Kiyonaga, J., Ishikawa, M. and Mizuta, K., 1977. Studies on gamma-oryzanol (3). Influence of gamma-oryzanol on circadian rhythms of serum gastrin, 11-OHCS and gastric secretion in rats. Nihon Yakurigaku Zasshi, 73(4): 457-463.

Iwatsuki, K., Akihisa, T., Tokuda, H., Ukiya, M., Higashihara, H., Mukainaka, T., Iizuka, M., Hayashi, Y., Kimura, Y. and Nishino, H., 2003. Sterol ferulates, sterols, and 5-alk(en)ylresorcinols from wheat, rye, and corn bran oils and their inhibitory effects on Epstein-Barr virus activation. Journal of Agricultural and Food Chemistry, 51(23): 6683-6688.

Jain, D., Ebine, N., Jia, X., Kassis, A., Marinangeli, C., Fortin, M., Beech, R., Hicks, K.B., Moreau, R.A., Kubow, S. and Jones, P.J., 2008. Corn fiber oil and sitostanol decrease cholesterol absorption independently of intestinal sterol transporters in hamsters. The Journal of Nutritional Biochemistry, 19(4): 229-236.

Jiang, Y.Z. and Wang, T., 2005. Phytosterols in cereal by-products. Journal of the American Oil Chemists Society, 82(6): 439-444.

Juliano, C., Cossu, M., Alamanni, M.C. and Piu, L., 2005. Antioxidant activity of gamma-oryzanol: mechanism of action and its effect on oxidative stability of pharmaceutical oils. International Journal of Pharmaceutics, 299(1-2): 146-154.

Kaneko, R. and Tsuchiya, T., 1954. New compound in rice bran and germ oils. Journal of Chemical Society of Japan, 57: 526-529.

Kaneya, Y., Tsuno, T. and Yamamoto, S., 2010. Food additive for fried food coating comprises gamma-oryzanol. JP2010042028-A, Japan.

Kikuzaki, H., Hisamoto, M., Hirose, K., Akiyama, K. and Taniguchi, H., 2002. Antioxidant properties of ferulic acid and its related compounds. Journal of Agricultural and Food Chemistry, 50(7): 2161-2168.

Kim, J.S., Suh, M.H., Yang, C.B. and Lee, H.G., 2003. Effect of γ-oryzanol on the flavor and oxidative stability of refrigerated cooked beef. Journal of Food Science, 68(8): 2423-2429.

Kim, S.P., Kang, M.Y., Nam, S.H. and Friedman, M., 2012. Dietary rice bran component gamma-oryzanol inhibits tumor growth in tumor-bearing mice. Molecular Nutrition & Food Research, 56(6): 935-944.

Kochhar, S.P., 2000. Stabilisation of frying oils with natural antioxidative components. European Journal of Lipid Science and Technology, 102(8-9): 552-559.

Kong, C.K., Lam, W.S., Chiu, L.C., Ooi, V.E., Sun, S.S. and Wong, Y.S., 2009. A rice bran polyphenol, cycloartenyl ferulate, elicits apoptosis in human colorectal adenocarcinoma SW480 and sensitizes metastatic SW620 cells to TRAIL-induced apoptosis. Biochemical Pharmacology, 77(9): 1487-1496.

Krishna, A.G.G., Hemakumar, K.H. and Khatoon, S., 2006. Study on the composition of rice bran oil and its higher free fatty acids value. Journal of the American Oil Chemists Society, 83(2): 117-120.

Kumar, M.S., Dahuja, A., Rai, R.D., Walia, S. and Tyagi, A., 2014. Role of gamma-oryzanol in drought-tolerant and susceptible cultivars of rice (Oryza sativa L.). Indian Journal of Biochemistry & Biophysics, 51(1): 75-80.

Li, L., Shewry, P.R. and Ward, J.L., 2008. Phenolic acids in wheat varieties in the HEALTHGRAIN Diversity Screen. Journal of Agricultural and Food Chemistry, 56(21): 9732-9739.

Ling, W.H. and Jones, P.J., 1995. Dietary phytosterols: a review of metabolism, benefits and side effects. Life Sciences, 57(3): 195-206.

Lloyd, B.J., Siebenmorgan, T.J. and Beers, K.W., 2000. Effects of commercial processing on antioxidants in rice bran. Cereal Chemistry, 77(5): 551-555.

Lubinus, T., Barnsteiner, A., Skurk, T., Hauner, H. and Engel, K.H., 2013. Fate of dietary phytosteryl/-stanyl esters: analysis of individual intact esters in human feces. European Journal of Nutrition, 52(3): 997-1013.

Luo, H.F., Li, Q., Yu, S., Badger, T.M. and Fang, N., 2005. Cytotoxic hydroxylated triterpene alcohol ferulates from rice bran. Journal of Natural Products, 68(1): 94-97.

Mäkynen, K., Chitchumroonchokchai, C., Adisakwattana, S., Failla, M. and Ariyapitipun, T., 2012. Effect of gamma-oryzanol on the bioaccessibility and synthesis of cholesterol. European Review for Medical and Pharmacological Sciences, 16(1): 49-56.

Mandak, E. and Nyström, L., 2012. The effect of in vitro digestion on steryl ferulates from rice (Oryza sativa L.) and other grains. Journal of Agricultural and Food Chemistry, 60(24): 6123-6130.

Mandak, E. and Nyström, L., 2013. Influence of baking and in vitro digestion on steryl ferulates from wheat. Journal of Cereal Science, 57(3): 356-361.

Manirazman, A.M., 1998. Non-chemical sunscreen composition. US5817299, USA.

Marinova, E.M., Yanishlieva, N.V., Raneva, V.G. and Todorova, D.I., 1998. Antioxidative action of the cholesteryl esters of ferulic and caffeic acids and their isomers. La Rivista Italiana Delle Sostanze Grasse, (75): 11-14.

Meijer, G.W., Bressers, M.A., de Groot, W.A. and Rudrum, M., 2003. Effect of structure and form on the ability of plant sterols to inhibit cholesterol absorption in hamsters. Lipids, 38(7): 713-721.

Miller, A. and Engel, K.H., 2006. Content of $\gamma$-oryzanol and composition of steryl ferulates in brown rice (Oryza sativa L.) of European origin. Journal of Agricultural and Food Chemistry, 54(21): 8127-8133.

Miller, A., Majauskaite, L. and Engel, K.H., 2004. Enzyme-catalyzed hydrolysis of $\gamma$-oryzanol. European Food Research and Technology, 218(4): 349-354.

Mizuta, K., Kaneta, H. and Itaya, K., 1978. Effects of gamma-oryzanol on gastric secretions in rats. Nihon Yakurigaku Zasshi, 74(2): 285-295.

Moongngarm, A. and Saetung, N., 2010. Comparison of chemical compositions and bioactive compounds of germinated rough rice and brown rice. Food Chemistry, 122(3): 782-788.

Moreau, R.A. and Hicks, K.B., 2004. The in vitro hydrolysis of phytosterol conjugates in food matrices by mammalian digestive enzymes. Lipids, 39(8): 769-776.

Moreau, R.A., Powell, M.J. and Hicks, K.B., 1996. Extraction and quantitative analysis of oil from commercial corn fiber. Journal of Agricultural and Food Chemistry, 44(8): 2149-2154.

Moreau, R.A., Powell, M.J., Hicks, K.B. and Norton, R.A., 1998. A comparaison of the levels of ferulate-phytosterol esters in corn and other seeds. In: J. Sanchez, E. Cerda-Olmedo and E. Martinez-Force (Editors), Advances in Plant Lipid Research. Universidad de Sevilla, Spain, pp. 472-474.

Muhammad, S.I., Maznah, I., Mahmud, R., Zuki, A.B.Z. and Imam, M.U., 2013. Upregulation of genes related to bone formation by $\gamma$-amino butyric acid and

γ-oryzanol in germinated brown rice is via the activation of GABA(B)-receptors and reduction of serum IL-6 in rats. Clinical Interventions in Aging, 8: 1259-1271.

Murase, Y. and Lishima, H., 1963. Clinical studies of oral administration of γ-oryzanol on climacteric complaints and its syndrome. Obstetrics and Gynecology Practice, 12: 147-149.

Nagasaka, R., Chotimarkorn, C., Shafiqul, I.M., Hori, M., Ozaki, H. and Ushio, H., 2007. Anti-inflammatory effects of hydroxycinnamic acid derivatives. Biochemical and Biophysical Research Communications, 358(2): 615-619.

Nagy, K., Actis-Goretta, L., Redeuil, K., Barron, D., Fumeaux, R., Giuffrida, F., Cruz-Hernandez, C. and Destaillats, F., 2013. Identification of cholesteryl ester of ferulic acid in human plasma by mass spectrometry. Journal of Chromatography A, 1301: 162-168.

Nakamura, H., 1966. Effect of gamma-oryzanol on hepatic cholesterol biosynthesis and faecal excretion of cholesterol metabolites. Radioisotopes, 15: 371-274.

Nakayama, S., Manabe, A., Suzuki, J., Sakamoto, K. and Inagaki, T., 1987. Comparative effects of two forms of gamma-oryzanol in different sterol compositions on hyperlipidemia induced by cholesterol diet in rats. Japanese Journal of Pharmacology, 44(2): 135-143.

Nantiyakul, N., Furse, S., Fisk, I., Foster, T., Tucker, G. and Gray, D., 2012. Phytochemical composition of Oryza sativa (rice) bran oil bodies in crude and purified Isolates. Journal of the American Oil Chemists' Society, 89(10): 1867-1872.

Nes, W.D., Song, Z., Dennis, A.L., Zhou, W., Nam, J. and Miller, M.B., 2003. Biosynthesis of phytosterols. Kinetic mechanism for the enzymatic C-methylation of sterols. The Journal of Biological Chemistry, 278(36): 34505-34516.

Ng, L.T., Huang, S.H., Chen, Y.T. and Su, C.H., 2013. Changes of tocopherols, tocotrienols, gamma-oryzanol, and gamma-aminobutyric acid levels in the germinated brown rice of pigmented and nonpigmented cultivars. Journal of Agricultural and Food Chemistry, 61(51): 12604-12611.

Norton, R.A., 1994. Isolation and identification of steryl cinnamic acid derivatives from corn bran. Cereal Chemistry Journal, 71(2): 111-117.

Norton, R.A., 1995. Quantitation of steryl ferulate and p-coumarate esters from corn and rice. Lipids, 30(3): 269-274.

Nurmi, T., Lampi, A.M., Nyström, L., Hemery, Y., Rouau, X. and Piironen, V., 2012. Distribution and composition of phytosterols and steryl ferulates in wheat grain and bran fractions. Journal of Cereal Science, 56(2): 379-388.

Nurmi, T., Lampi, A.M., Nyström, L., Turunen, M. and Piironen, V., 2010. Effects of genotype and environment on steryl ferulates in wheat and rye in the HEALTHGRAIN diversity screen. Journal of Agricultural and Food Chemistry, 58(17): 9332-9340.

Nyström, L., 2012. Analysis methods of phytosterols. In: Z. Xu and L.R. Howard (Editors), Analysis of Antioxidant-Rich Phytochemicals. Wiley-Blackwell, Oxford, UK, pp. 313-351.

Nyström, L., Achrenius, T., Lampi, A.M., Moreau, R.A. and Piironen, V., 2007a. A comparison of the antioxidant properties of steryl ferulates with tocopherol at high temperatures. Food Chemistry, 101(3): 947-954.

Nyström, L., Mäkinen, M., Lampi, A.M. and Piironen, V., 2005. Antioxidant activity of steryl ferulate extracts from rye and wheat bran. Journal of Agricultural and Food Chemistry, 53(7): 2503-2510.

Nyström, L., Moreau, R.A., Lampi, A.M., Hicks, K.B. and Piironen, V., 2008. Enzymatic hydrolysis of steryl ferulates and steryl glycosides. European Food Research and Technology, 227(3): 727-733.

Nyström, L., Paasonen, A., Lampi, A.M. and Piironen, V., 2007b. Total plant sterols, steryl ferulates and steryl glycosides in milling fractions of wheat and rye. Journal of Cereal Science, 45(1): 106-115.

Ohara, K., Uchida, A., Nagasaka, R., Ushio, H. and Ohshima, T., 2009. The effects of hydroxycinnamic acid derivatives on adiponectin secretion. Phytomedicine, 16(2-3): 130-137.

Oka, T., Fujimoto, M., Nagasaka, R., Ushio, H., Hori, M. and Ozaki, H., 2010. Cycloartenyl ferulate, a component of rice bran oil-derived gamma-oryzanol, attenuates mast cell degranulation. Phytomedicine, 17(2): 152-156.

Ono, K., Takemoto, D. and Yasutake, Y., 2007. Oral or food and drink composition used as anti-fatigue agent comprises sesamin and (gamma)-oryzanol. JP2009073749-A, Japan.

Parrado, J., Miramontes, E., Jover, M., Marquez, J.C., Angeles Mejias, M., Collantes De Teran, L., Absi, E. and Bautista, J., 2003. Prevention of brain protein and lipid oxidation elicited by a water-soluble oryzanol enzymatic extract derived from rice bran. European Journal of Nutrition, 42(6): 307-314.

Pascual, C.d.S.C.I., Massaretto, I.L., Kawassaki, F., Barros, R.M.C., Noldin, J.A. and Marquez, U.M.L., 2013. Effects of parboiling, storage and cooking on the levels of tocopherols, tocotrienols and γ-oryzanol in brown rice (Oryza sativa L.). Food Research International, 50(2): 676-681.

Pereira-Caro, G., Watanabe, S., Crozier, A., Fujimura, T., Yokota, T. and Ashihara, H., 2013. Phytochemical profile of a Japanese black-purple rice. Food Chemistry, 141(3): 2821-2827.

Petsitis, X. and Riedel, J.H., 1999. Mascara and eyebrowpencils containing gamma-oryzanol and calcium salts. Eur Patent 0945120 A1, Germany.

Piironen, V., Lindsay, D.G., Miettinen, T.A., Toivo, J. and Lampi, A.M., 2000. Plant sterols: biosynthesis, biological function and their importance to human nutrition. Journal of the Science of Food and Agriculture, 80(7): 939-966.

Rohrer, C.A. and Siebenmorgen, T.J., 2004. Nutraceutical concentrations within the bran of various rice kernel thickness fractions. Biosystems Engineering, 88(4): 453-460.

Rong, N., Ausman, L.M. and Nicolosi, R.J., 1997. Oryzanol decreases cholesterol absorption and aortic fatty streaks in hamsters. Lipids, 32(3): 303-309.

Rosazza, J.P., Huang, Z., Dostal, L., Volm, T. and Rousseau, B., 1995. Review: biocatalytic transformations of ferulic acid: an abundant aromatic natural product. Journal of Industrial Microbiology, 15(6): 457-471.

Saenjum, C., Chaiyasut, C., Chansakaow, S., Suttajit, M. and Sirithunyalug, B., 2012. Antioxidant and anti-inflammatory activities of gamma-oryzanol rich extracts from Thai purple rice bran. Journal of Medicinal Plants Research, 6: 1070-1077.

Sakai, S., Murata, T., Tsubosaka, Y., Ushio, H., Hori, M. and Ozaki, H., 2012. gamma-Oryzanol reduces adhesion molecule expression in vascular endothelial cells via suppression of nuclear factor-kappaB activation. Journal of Agricultural and Food Chemistry, 60(13): 3367-3372.

Sakamoto, K., Tabata, T., Shirasaki, K., Inagaki, T. and Nakayama, S., 1987. Effects of gamma-oryzanol and cycloartenol ferulic acid ester on cholesterol diet induced hyperlipidemia in rats. Japanese Journal of Pharmacology, 45(4): 559-565.

Sasaki, J., Takada, Y., Handa, K., Kusuda, M., Tanabe, Y., Matsunaga, A. and Arakawa, K., 1990. Effects of gamma-oryzanol on serum lipids and apolipoproteins in dyslipidemic schizophrenics receiving major tranquilizers. Clinical Therapeutics, 12(3): 263-268.

Saulnier, L., Guillon, F. and Chateigner-Boutin, A.L., 2012. Cell wall deposition and metabolism in wheat grain. Journal of Cereal Science, 56(1): 91-108.

Schaller, H., 2003. The role of sterols in plant growth and development. Progress in Lipid Research, 42(3): 163-175.

Seetharamaiah, G.S. and Chandrasekhara, N., 1988. Hypocholesterolemic activity of oryzanol in rats. Nutrition Reports International, 38(5): 927-935.

Seitz, L.M., 1989. Stanol and sterol esters of ferulic and p-coumaric acids in wheat, corn, rye, and triticale. Journal of Agricultural and Food Chemistry, 37(3): 662-667.

Shimomura, Y., Kobayashi, I., Maruto, S., Ohshima, K., Mori, M., Kamio, N. and Fukuda, H., 1980. Effect of gamma-oryzanol on serum TSH concentrations in primary hypothyroidism. Endocrinologia Japonica, 27(1): 83-86.

Shin, T.S. and Godber, J.S., 1996. Changes of Endogenous Antioxidants and Fatty Acid Composition in Irradiated Rice Bran during Storage. Journal of Agricultural and Food Chemistry, 44(2): 567-573.

Singh, V., Moreau, R.A. and Cooke, P.H., 2001. Effect of corn milling practices on aleurone layer cells and their unique phytosterols. Cereal Chemistry Journal, 78(4): 436-441.

Singh, V., Moreau, R.A., Haken, A.E., Eckhoff, S.R. and Hicks, K.B., 2000. Hybrid variability and effect of growth location on corn fiber yields and corn fiber oil composition. Cereal Chemistry Journal, 77(5): 692-695.

Sirikul, A., Moongngarm, A. and Khaengkhan, P., 2009. Comparison of proximate composition, bioactive compounds and antioxidant activity of rice bran and defatted rice bran from organic rice and conventional rice. Asian Journal of Food and Agro-Industry, (2): 731-743.

Suzuki, M. and Muranaka, T., 2007. Molecular genetics of plant sterol backbone synthesis. Lipids, 42(1): 47-54.

Suzuki, S. and Oshima, S., 1970. Influence of blending of edible fats and oils on human serum cholesterol level (part1) blending of rice bran oil and safflower oil. The Japanese Journal of Nutrition and Dietetics, 28(1): 3-6.

Tajima, K., Sakamoto, M., Okada, K., Mukai, K., Ishizu, K., Sakurai, H. and Mori, H., 1983. Reaction of biological phenolic antioxidants with superoxide generated by cytochrome P-450 model system. Biochemical and Biophysical Research Communications, 115(3): 1002-1008.

Tamagawa, M., Otaki, Y., Takahashi, T., Otaka, T., Kimura, S. and Miwa, T., 1992a. Carcinogenicity study of gamma-oryzanol in B6C3F1 mice. Food and Chemical Toxicology, 30(1): 49-56.

Tamagawa, M., Shimizu, Y., Takahashi, T., Otaka, T., Kimura, S., Kadowaki, H., Uda, F. and Miwa, T., 1992b. Carcinogenicity study of gamma-oryzanol in F344 rats. Food and Chemical Toxicology, 30(1): 41-48.

Tan, Z. and Shahidi, F., 2011. Chemoenzymatic synthesis of phytosteryl ferulates and evaluation of their antioxidant activity. Journal of Agricultural and Food Chemistry, 59(23): 12375-12383.

Tan, Z. and Shahidi, F., 2013. Antioxidant activity of phytosteryl phenolates in different model systems. Food Chemistry, 138(2-3): 1220-1224.

Terada, S. and Haruta, K., 2003. Anti-inflammatory effects of gamma-oryzanol. Nature Medicine, 57(3): 95-99.

Ueda, H., Hayakawa, R., Hoshino, S. and Kobayashi, M., 1976. The effect of topically applied gamma-Oryzanol on sebaceous glands. The Journal of Dermatology, 3(1): 19-24.

Umehara, K., Shimokawa, Y. and Miyamoto, G., 2004. Effect of gamma-oryzanol on cytochrome P450 activities in human liver microsomes. Biological & Pharmaceutical Bulletin, 27(7): 1151-1153.

von Bergmann, K., Sudhop, T. and Lutjohann, D., 2005. Cholesterol and plant sterol absorption: recent insights. The American Journal of Cardiology, 96(1A): 10D-14D.

Vorarat, S., Managit, C., Iamthanakul, L., Soparat, W. and Kamkaen, N., 2010. Examination of antioxidant activity and development of rice bran oil and gamma-oryzanol microemulsion. Journal of Health Research, 24(2): 67-72.

Wang, D.Q., 2007. Regulation of intestinal cholesterol absorption. Annual Review of Physiology, 69: 221-248.

Wang, T., Hicks, K. and Moreau, R., 2002. Antioxidant activity of phytosterols, oryzanol, and other phytosterol conjugates. Journal of the American Oil Chemists' Society, 79(12): 1201-1206.

Wang, W., Guo, J., Zhang, J., Peng, J., Liu, T. and Xin, Z., 2015. Isolation, identification and antioxidant activity of bound phenolic compounds present in rice bran. Food Chemistry, 171: 40-49.

Wilson, T.A., Nicolosi, R.J., Woolfrey, B. and Kritchevsky, D., 2007. Rice bran oil and oryzanol reduce plasma lipid and lipoprotein cholesterol concentrations and aortic cholesterol ester accumulation to a greater extent than ferulic acid in hypercholesterolemic hamsters. The Journal of Nutritional Biochemistry, 18(2): 105-112.

Winkler-Moser, J.K., Hwang, H.S., Bakota, E.L. and Palmquist, D.A., 2015. Synthesis of steryl ferulates with various sterol structures and comparison of their antioxidant activity. Food Chemistry, 169(0): 92-101.

Winkler-Moser, J.K., Rennick, K.A., Hwang, H.S., Berhow, M.A. and Vaughn, S.F., 2013. Effect of tocopherols on the anti-polymerization activity of oryzanol and corn steryl ferulates in soybean oil. Journal of the American Oil Chemists' Society, 90(9): 1351-1358.

Winkler-Moser, J.K., Rennick, K.A., Palmquist, D.A., Berhow, M.A. and Vaughn, S.F., 2012. Comparison of the impact of gamma-oryzanol and corn steryl ferulates on the polymerization of soybean oil during frying. Journal of the American Oil Chemists' Society, 89(2): 243-252.

Xu, Z. and Godber, J.S., 1999. Purification and identification of components of gamma-oryzanol in rice bran Oil. Journal of Agricultural and Food Chemistry, 47(7): 2724-2728.

Xu, Z. and Godber, J.S., 2001. Antioxidant activities of major components of γ-oryzanol from rice bran using a linoleic acid model. Journal of the American Oil Chemists' Society, 78(6): 645-649.

Xu, Z., Hua, N. and Godber, J.S., 2001. Antioxidant activity of tocopherols, tocotrienols, and γ-oryzanol components from rice bran against cholesterol oxidation accelerated by 2,2'-azobis(2-methylpropionamidine) dihydrochloride. Journal of Agricultural and Food Chemistry, 49(4): 2077-2081.

Yagi, K. and Ohishi, N., 1979. Action of ferulic acid and Its derivatives as antioxidants. Journal of Nutritional Science and Vitaminology, 25(2): 127-130.

Yamada, S., 2009. Agent e.g. food/beverage product for treating osteoporosis and preventing or improving hyperuricemia, contains gamma-oryzanol as active ingredient. JP2009143943-A, Japan.

Yasukawa, K., Akihisa, T., Kimura, Y., Tamura, T. and Takido, M., 1998. Inhibitory effect of cycloartenol ferulate, a component of rice bran, on tumor promotion in two-stage carcinogenesis in mouse skin. Biological & Pharmaceutical Bulletin, 21(10): 1072-1076.

Yokoyama, W.H., 2004. Plasma LDL cholesterol lowering by plant phytosterols in a hamster model. Trends in Food Science & Technology, 15(11): 528-531.

Yoshino, G., Kazumi, T., Amano, M., Tateiwa, M., Yamasaki, T., Takashima, S., Iwai, M., Hatanaka, H. and Baba, S., 1989. Effects of gamma-oryzanol on hyperlipidemic subjects. Current Therapeutic Research, 45(4): 543-552.

Zhao, Z.H. and Moghadasian, M.H., 2008. Chemistry, natural sources, dietary intake and pharmacokinetic properties of ferulic acid: A review. Food Chemistry, 109(4): 691-702.

# PART 2 - Research Papers

Dan Zhu and Laura Nyström (2015). Differentiation of rice varieties using small bioactive lipids as markers. European Journal of Lipid Science and Technology. (doi: 10.1002/ejlt.201500089).

Dan Zhu, Antoni Sánchez-Ferrer, Laura Nyström. Antioxidant activity of individual steryl ferulates from various cereal grain sources. *Submitted manuscript* (November 2014).

Dan Zhu, Eleni Dimitriadou, Laura Nyström. Effect of steryl ferulates on the kinetics of methyl linoleate autoxidation. *To be published after additional studies*.

Dan Zhu, Davide Brambilla, Jean-Christophe Leroux, Laura Nyström (2015). Permeation of steryl ferulates through an in vitro intestinal barrier model. Molecular Nutrition and Food Research. (doi: 10.1002/mnfr.201400862).

# Differentiation of Rice Varieties Using Small Bioactive Lipids as Markers

## Abstract

Steryl ferulates (γ-oryzanol) are a group of important lipid antioxidants found in rice. This study uses OMIC-technologies to differentiate between rice varieties based on these minor bioactive lipids. The γ-oryzanol rich-lipid fractions were first extracted from six types of common cargo rice and two types of wild rice, which were subsequently analyzed using ultra performance liquid chromatography with high-resolution quadrupole time-of-flight mass spectrometric detection (UPLC-HR-Q-TOF-MS). Unique spectral profiles were produced for each rice variety, and the MS data was further converted into markers. Multivariate statistical analysis including principal component analysis (PCA) and the observed partial least squares-discriminant analysis (OPLS-DA) was utilized to find the characteristic markers, enabling us to differentiate between various rice varieties based on their steryl ferulate profiles and other small lipids.

**Practical applications:** This study provides a targeted method to distinguish between various common rice varieties as well as wild rice from different geographic regions, which could be a new approach for rice authentication. Additionally, this sensitive analytical technique may reveal several new compounds of bioactive lipids in rice. Furthermore, the OMIC approach to rice differentiation also has the potential to lead to the selection of rice varieties with optimal profiles of bioactive lipids for food use.

## Keywords

Differentiation / γ-oryzanol / Rice / Steryl ferulates / UPLC-MS

## Abbreviations

CM, characteristic marker; ESI, electrospray ionization; m/z, mass to charge ratio; OPLS-DA, observed partial least squares-discriminant analysis; PCA, principal component analysis; RT, retention time; UPLC-HR-Q-TOF-MS, ultra performance liquid chromatography with high-resolution quadrupole time-of-flight mass spectrometric detection.

## 1 Introduction

Rice (*Oryza sativa L.*) is one of the most important grains in the world, with more than half of the population consuming rice as their main caloric intake [1]. Due to the differences in quality, quantity, variety, and processing, its price is not homogeneous in the international rice market. Owing to the tremendous increase of the global trade, the authenticity of rice is an increasing concern. Traditionally, morphological characteristics, shape, size and height, and physiological factors, starch, protein and lipid contents, are often used in rice identification and differentiation [2]. While morphological classification cannot be applied to rice flour, some authors [3] have suggested that both morphological and physiological methods are unreliable and that better methods for rice authentication are necessary.

The brown rice, also known as cargo rice, is a rich source of many bioactive lipids, including γ-oryzanol, phytosterols, tocopherols, tocotrienols, squalene, linoleic acid and carotenoids [1]. γ-Oryzanol, a mixture of steryl ferulates (esters of plant sterols with ferulic acid), has gained great interest due to its bioactive properties. In various studies, γ-oryzanol has been reported with cholesterol lowering [4], antioxidant [5], anti-

inflammatory [6] and anti-carcinogenic effects [7], which are responsible for the health benefits of the whole rice grain. The varying profiles in bioactive lipids within rice may suggest different health benefits of rice. Literature demonstrates that rice varieties may differ in the total amount of steryl ferulates, nevertheless they are composed of the same steryl ferulate components [8, 9]. For instance, Miller and co-workers [9] found that the γ-oryzanol content ranged from 26 to 62 mg/100g (dry matter basis) in 12 types of cultivars of cargo rice, and the composition of steryl ferulates also varied, e.g., cycloartenyl ferulate (32-51% of γ-oryzanol), 24-methylenecycloartanyl ferulate (23-37%), campesteryl ferulate (5-18%), sitosteryl ferulate (5-10%) and campestanyl ferulate (3-14%). Yet the main compounds in all varieties are the same and present in all the different rice types, and would therefore not be different enough to discriminate the varieties from one another.

The ultra performance liquid chromatography with high-resolution quadrupole time-of-flight mass spectrometric detection (UPLC-HR-Q-TOF-MS) is known for its powerful capability of measurement with high resolution, selectivity and mass accuracy. It can provide a large amount of information more rapidly and efficiently than traditional analytical techniques, and to together with OMIC informatics analysis, be used for characterization of complex samples, such as food. Recently, OMIC approach, profiling a large number of variables in samples together with statistical analysis, has been studied in the food authentication and classification, e.g., in tomato [10], broccoli [11] and potatoes [12].

The aim of this study was to differentiate various rice varieties based on the profile of minor bioactive lipids of interest in rice with OMIC-technologies. The γ-oryzanol rich-lipid fractions were first extracted from six types of cargo rice. After UPLC separation and MS detection, unique spectral profiles were produced for each rice variety, and the MS data was further converted into markers. After multivariate statistical analysis, potential compounds including the individual steryl ferulates were successfully identified and used to differentiate between rice varieties. For comparison, two types of wild rice (*Zizania palustris L.*), which have similar appearance to common rice and

contain various steryl ferulates, were also investigated in this study. To the best of our knowledge, this study is the first to provide a differentiation method of rice using individual steryl ferulates and other potential small lipids as markers with OMIC tool.

# 2 Materials and methods

## 2.1 Materials

Acetone, ammonium hydroxide solution ($NH_4OH$), hexane, isopropanol (HPLC grade) were purchased from Sigma Aldrich (Buchs, Switzerland). $H_2O$, acetonitrile and isopropanol (MS grade) were purchased from Biosolve (Dieuze, France). γ-Oryzanol standard (≥95% purity) was obtained from CTC Organics (Atlanta, GA). Cargo rice (*Oryza sativa L.*) and wild rice (*Zizania palustris L.*) samples were obtained from La Riseria (Taverne, Switzerland). Six types of cargo rice cultivars were Camargue (France), S. Andrea (Italy), Baldo (Italy), Perfume (Thailand), Basmati (India) and Jasmine (Thailand). Two types of wild rice were from Canada and USA.

## 2.2 Preparation of rice samples

All rice samples were milled to below 0.5 mm (pore size of sieve: 0.5 mm, 10 000 rpm; Retsch ZM 200, Haan, Germany) and stored at -20 °C before use. Accelerated solvent extractor (ASE 350 Dionex, Sunnyvale, CA) was used to extract the total rice lipids. A total of 2 g sample was loaded within each cell, and acetone was used as extraction solvent. The parameters of ASE were set as: pressure 1500 psi, temperature 100 °C, static time 10 min, the purge 60 s and the flush 60%. Each extraction consisted in three runs. The extract was evaporated to dryness under vacuum at 50 °C and then the residue was dissolved in 2.5 mL hexane [13].

To separate steryl ferulate-rich lipids from other sterols and neutral lipids, a fractionation by solid phase extraction (SPE) was performed. First, the Diol SPE-cartridge (InertSep 500 mg, 3 mL; GL Science, Tokyo, Japan) was activated with 5 mL

of heptane. Then 2.5 mL sample was loaded to the cartridge. After washing the column with 5 mL of heptane, the steryl ferulate-rich lipid fraction was eluted with 5 mL of mix of heptane and isopropanol (97:3). The solvents were evaporated under nitrogen at 50°C. Then the residue was dissolved in 6 mL of acetonitrile and further passed through with a 0.2-µm PTFE syringe filter (BGB-Analytik, Adliswil, Switzerland).

## 2.3 UPLC-MS analysis

### 2.3.1 Instrument conditions

The analysis was performed on a Waters ACQUITY UPLC system (Waters Corp., Milford, MA) connected to a MS system (Synapt G2) equipped with an electrospray ionization source (ESI) and a Q-TOF analyzer.

Sample separation was carried out with an ACQUITY UPLC BEH C18 column (50 mm × 2.1 mm, 1.7 µm particle size; Waters). The mobile phase was composed of A ($H_2O$ with 10 mM $NH_4OH$) and B (acetonitrile: isopropanol 90:10), with a gradient from 20% A to 7% A in the first 1 min, followed by gradient from 7% A to 10% A till 7.2 min, then in the last 1.8 min back to 20% A. The total run time was 10 min. The column temperature was maintained at 50 ℃ with a flow rate of 0.5 mL/min. A total of 2 µL of the sample was injected for each run.

The MS was operated in ESI negative ionization mode. The voltages of capillary, sampling cone and extraction cone were 2.5 kV, 35 V and 4 V, respectively. The temperature for source and desolvation were 120 ℃ and 250 ℃, respectively. Nitrogen was used as the desolvation gas. The desolvation gas flow rate was 800 L/h, and the cone gas flow was 20 L/h. Mass spectra were acquired from $m/z$ 50-1200 at a scan rate of 0.5 s in centroid mode. In order to decrease the influence from unexpected and relatively polar lipids, the first 0.8 min eluent from UPLC system went to the waste instead of MS system. Leucine enkephalin (2 µg/mL, Waters) was infused intermittently every 20 s and applied as a lock mass for accurate on-line mass calibration

(MS mode with all the settings above). To get more structural information, a trap collision energy ramp from 40 to 60 V ($MS^E$ mode) was added for each type of sample.

## 2.3.2 Sample sequence

Equal aliquots from every rice sample were combined in a representative pool sample. The pool sample was used as quality control sample, which was analyzed at the beginning, end and randomly through the analytical sequence. All the rice samples were also randomly arranged in the sample list, carried out in MS mode and $MS^E$ mode. Also, blank sample (acetonitrile alone) and system suitability sample (TestMix, 2 µg/mL, containing acetaminophen, caffeine, sulfadimethoxine, terfenadine, reserpine; Waters) were analyzed repeatedly randomly through the whole analytical sequence.

## 2.4 Data collection and analysis

Data was acquired using MassLynx 4.1 software (Waters). For extracting relevant marker information, the mass spectral information was then processed within Markerlynx XS software (Waters). The chromatographic peak detection was performed from 0.8 to 8.5 min, and the mass range of interest was set from 130 to 750 *m/z* with mass accuracy (tolerance) of 0.05 Da. ApexPeakTrack algorithm was applied to automatically determine the peak width (peak width at 5% height) and the peak-to-peak baseline noise. For the spectral peak collection, the minimum level (counts) was set as 1200, the mass window was 0.05 Da, and the retention time window was 0.5 min. Data was deisotoped to prevent the assignment of isotope peaks as markers. The noise elimination level was set as 6. Then the MS data were integrated and converted in to the pairs of retention time and mass to charge ratio of $[M-H]^-$ (RT_*m/z*). The generated dataset table was a matrix of detected markers (rows of RT_*m/z*) by rice samples (columns) with the intensity of markers filling the matrix.

These markers were "fingerprint" for each sample, and further were subjected to multivariate statistical analysis by EZ info 2.0 software (Umetrics, Umea, Sweden). For

detecting the dominant patterns and grouping, principal component analysis (PCA) with Pareto scaling algorithm was applied to these markers from the common rice and wild rice samples. Furthermore, S-plot from the observed partial least squares-discriminant analysis (OPLS-DA) model was used to further indicate the most important differentiating features that separated the groups by PCA.

## 2.5 Tentative identification of markers

Markers (RT_*m/z*) extracted by Markerlynx XS were tentatively identified, by clustering of fragmentation patterns using $MS^E$ mode for structural elucidation. The elemental composition tool in the software platform was applied to assist in prediction (mass tolerance 10 ppm), and MassFragment tool was used to predict possible chemical structures. The identification of markers of individual steryl ferulates was confirmed by γ-oryzanol standard (containing 32% cycloartenyl ferulate, 40% 24-methylenecycloartanyl ferulate, 14% campesteryl ferulate, 5% sitosteryl ferulate, 3% campestanyl ferulate, 1% sitostanyl ferulate). For the other markers, the accurate masses obtained by HR-MS were used for molecular formula prediction.

# 3 Results and discussion

## 3.1 Multivariate analysis of markers

UPLC-HR-Q-TOF-MS was used to collect the spectrometric information of steryl ferulate-rich lipid fractions. First, the separation conditions and ionization parameters were optimized for individual steryl ferulates with γ-oryzanol standard. The same methodology was then applied to the extracts from different common rice and wild rice samples. Their MS data were converted in to markers with RT_*m/z* pair by Markerlynx XS software. In total, 156 markers were extracted (listed in supporting information).

PCA was used to better visualize the 156 markers from common rice and wild rice (Fig. 1). Projecting the markers into the space, it is possible to visualize the differences

amongst the various rice samples. Six principal components, obtained by PCA, account for 85% of the total variance. Figure 1 displays both the score values of the observations (rice varieties) and the weights of the X variables (markers). From PC1 versus PC2 (Fig. 1A), clear separation of common rice and wild rice samples is observed, indicating the profiles of targeted extracts are very distinctive between common rice and wild rice. The pool samples, containing the information of all samples and markers, are located in the center of the plot. Baldo and Camargue rice behave similarly, and seem to be closely related each other in the plot, indicating that their extract profiles are similar. Similar observation can also be made for Basmati and Perfume rice. The two types of wild rice can be separated, but their distance in the plot is small. In addition to these, other types of rice are well separated under PC1 and PC2. PCA also can provide multidimensional visualization. From these, Baldo and Camargue, which are partially overlapping in PC1 versus PC2, can be fully resolved in PC2 versus PC3 (Fig. 1B). On the other hand, Basmati and Perfume rice, as well as wild rice from the USA and Canada have a better separation in PC2 versus PC4 (Fig. 1C). The spatial distribution of the markers from the loading plot correlates to the distribution of the rice samples on the scores plot. These bi-plots from different components demonstrate these markers can contribute to the separation of various common rice as well as wild rice.

In order to indicate the most important differentiating markers for any two types of rice within PCA, S-plots from OPLS-DA model were applied. In the S-plot each point represents a marker, and the S-plot demonstrates which are the markers that can be used to discriminate the two samples in question. In the case of Baldo and S.Andrea (Fig. 2A), the x-axis shows the variable contributions; the further away a data point of the marker is from zero, the more it contributes to the variance of the sample. The y-axis shows the sample correlations within the same sample group; the further away a marker is from zero, the stronger correlation it has with the sample. The highlighted markers in the S-plot demonstrate a statistical confidence of $\geq 90\%$. Furthermore, the markers on both ends of the S-plot curve (marked with mass-to-charge ratios) represent the ions with strongest contribution for each sample allowing one to distinguish between rice

(A)
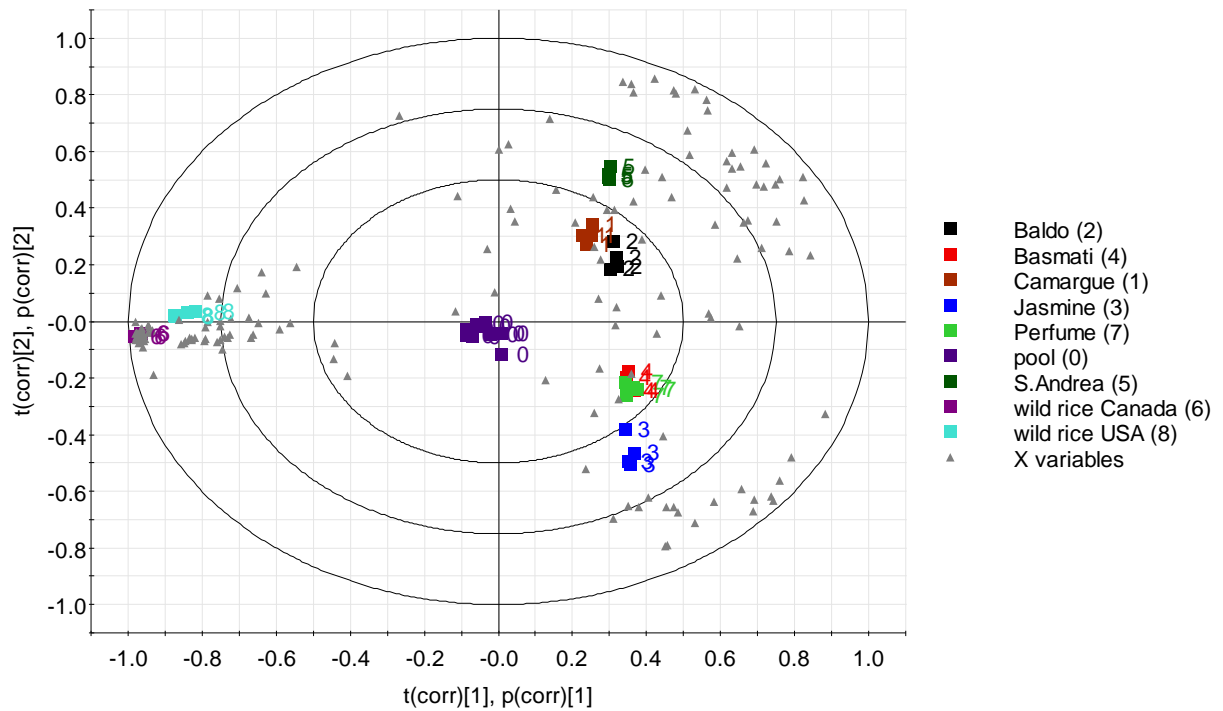


(B)
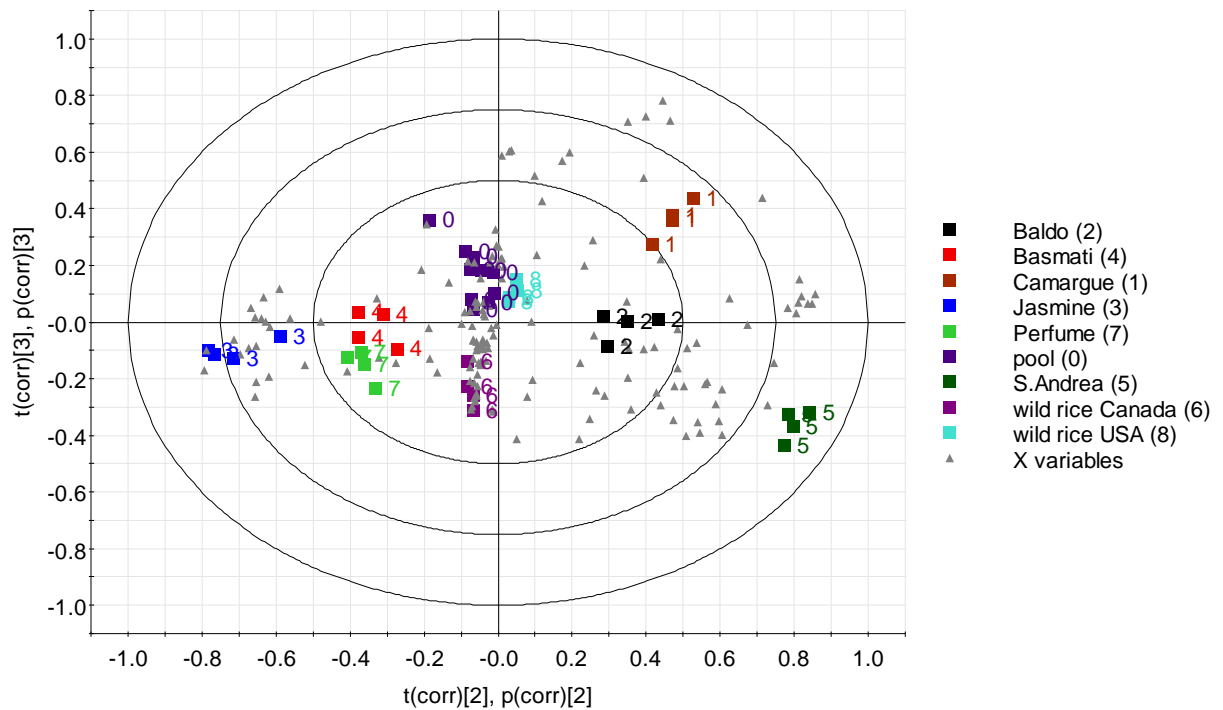
(C)
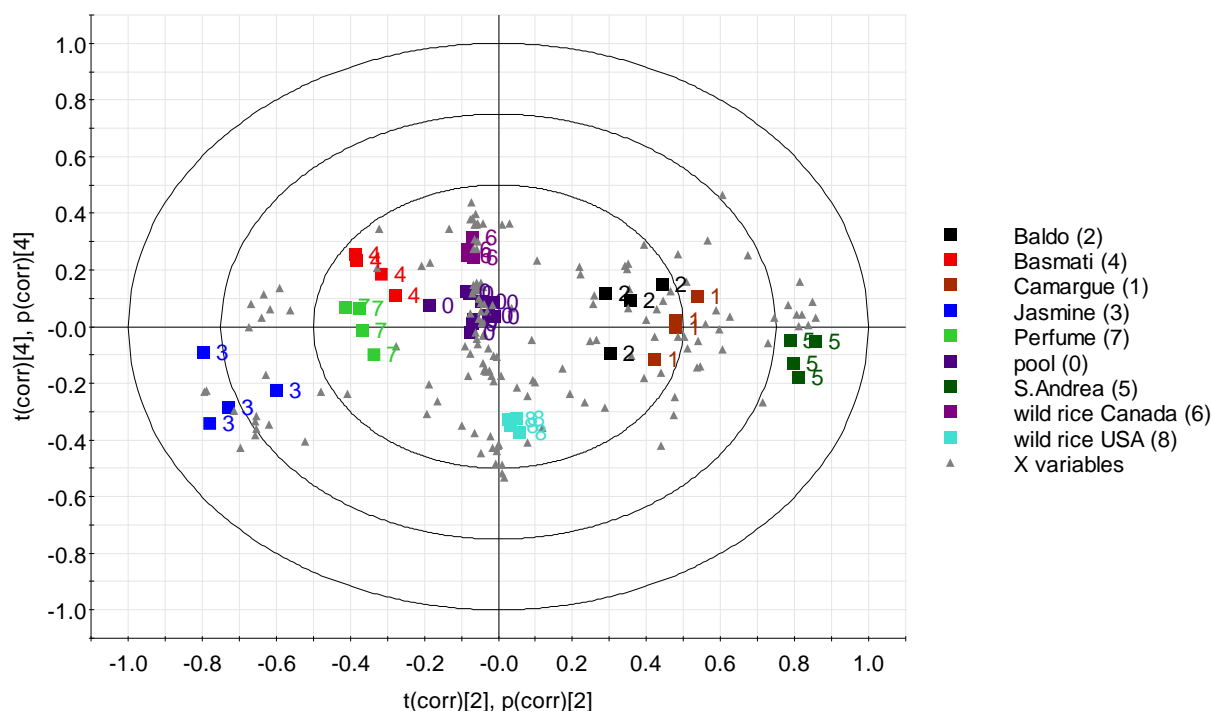


**Figure 1.** PCA bi-plot (scores and loadings) of six types of rice (*Oryza sativa L.*) and two types of wild rice (*Zizania palustris L.*) with 156 markers. (A) PC1 versus PC2; (B) PC2 versus PC3; (C) PC2 versus PC4. The circles on the plot indicate different levels of correlation, from 1.0 (100%), 0.75 (75%), 0.5 (50%) to 0 (0%) in the center of the plot. The six types of rice are Baldo (2), Basmati (4), Camargue (1), Jasmine (3), Perfume (7) and S.Andrea (5). The two types of wild rice are wild rice from Canada (6) and wild rice from USA (8).

varieties with the highest confidence, and considered as the characteristic markers (CM). The intensity of these markers from Baldo and S.Andrea are shown in Fig. 2B. The markers *m/z* 601.4253 and 615.4408 are very strong in S.Andrea but weak in Baldo, whereas the *m/z* 559.4724, 557.4563, 633.4150, 561.4877, and 533.4567 ions are much higher in Baldo than S.Andrea. S-plots have shown to be a useful tool for identifying CM within various rice varieties.

(A)



(B)



**Figure 2**. (A) S-plot from OPLS-DA model of two types of rice (Baldo = -1, S.Andrea =1). The variables marked with box refer to variables of above 90% significance; the variables marked with $m/z$ of [M-H]$^-$ were chosen as the characteristic markers (CM) to separate Baldo and S.Andrea rice. (B) Comparison of intensity of CM from S-plot of Baldo and S.Andrea rice; marker is expressed as "RT_ $m/z$ of [M-H]$^-$ ".

## 3.2 Characteristic markers (CM) for separating different varieties of rice
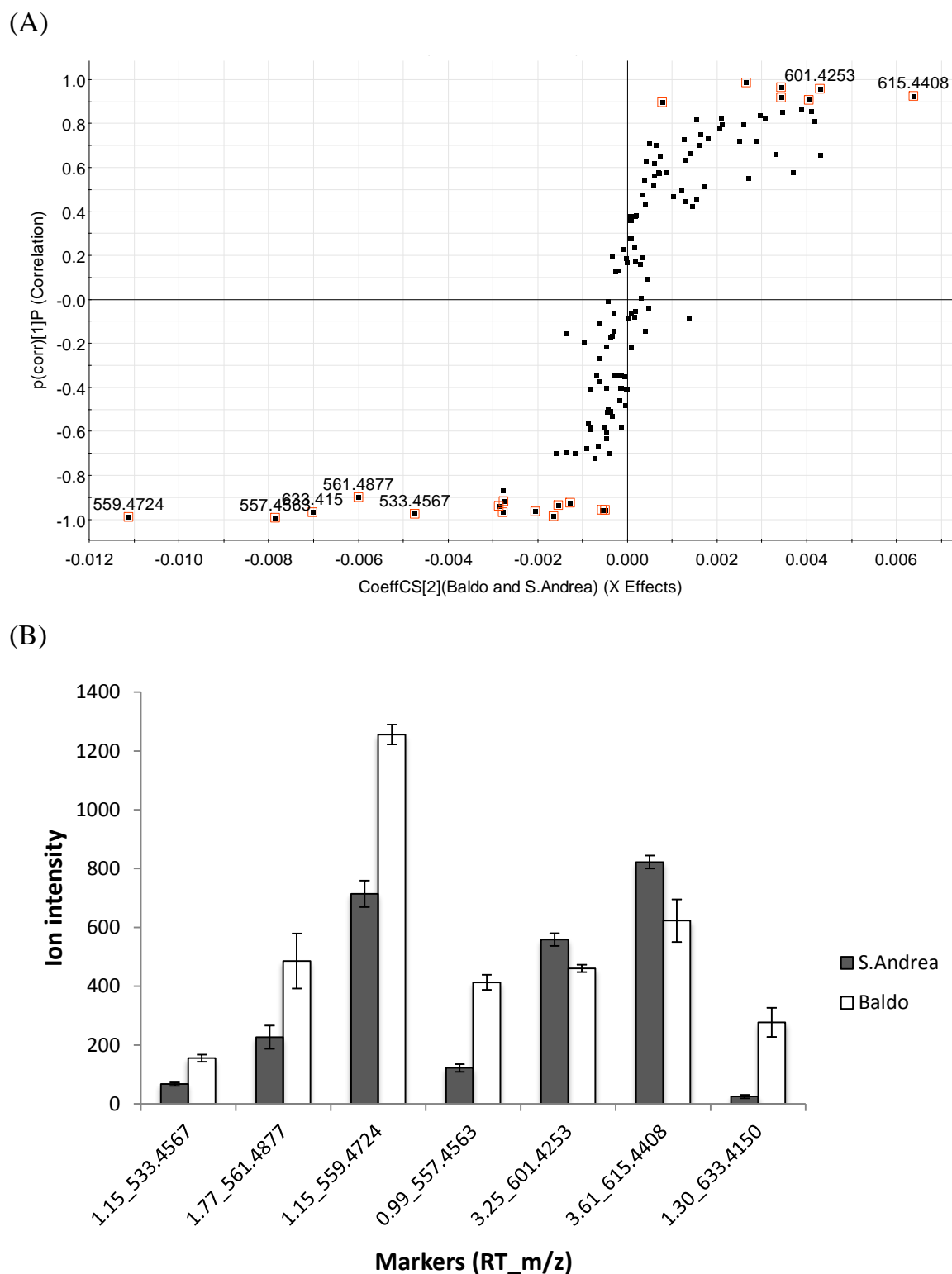
γ-Oryzanol rich-lipid fractions successfully separated rice varieties based on small lipids as markers. The CM extracted from S-plots with OPLS-DA models were used to separate any two types of common rice, this was done for all rice varieties (Table 1). In the case of Baldo and Basmati, markers 105, 120, 126, 128, 136, and 146 are more abundant in Baldo than in Basmati, whereas markers 80, 98, 97, and 118 are more abundant in Basmati than in Baldo. The two sets of markers combine can successfully separate Baldo and Basmati rice. The presence and absence (or presence with very low amount) of certain markers are characteristic for separation of each pair of rice varieties.

### 3.2.1 Diagnostic markers of specific rice varieties

Furthermore, the CM selected from Table 1, which are highly abundant in a certain rice variety, help to distinguish this type of rice from the other varieties, one can consider these markers diagnostic to these rice varieties. Whereas some rice varieties contain as few as one of these diagnostic markers: Jasmine (marker 118) and Perfume (marker 97), others contain multiple markers: Baldo (markers 136 and 146), Basmati (markers 97 and 106), Camargue (markers 128 and 136) and S.Andrea (markers 120, 128, 134, and 146), facilitating their differentiation.

### 3.2.2 Characterization of steryl ferulates as CM by UPLC-MS

As expected, some of the CM used to separate different rice varieties were identified as steryl ferulates (Fig. 3). The most common steryl ferulates species were confirmed by γ-oryzanol standard (Table 2). Under the applied UPLC-MS conditions, the deprotonated molecular ions [M-H]⁻ are the most abundant species for all individual steryl ferulates. Their characteristic fragment ions are detected as [M-H-Me]⁻ and related ferulic acid ions at *m/z* 193, 177, 175, 133, well in agreement with the previous studies [8,14-16]. Moreover, two additional CM, markers 106 and 136, are also tentatively identified by their molecular ion and fragmentation pattern as steryl

ferulates, 24-methylenecholesteryl ferulate and 25-hydroxy-24-methylcycloartanyl ferulate, respectively. From literature, 24-methylenecholesteryl ferulate and 25-hydroxy-24-methylcycloartanyl ferulate have also been detected in rice [14, 16].

Evidence toward the identity of some CM suggests that they are sterol esters of other phenolic acids, like cycloartenyl *p*-coumarate (marker 105), 24-methylenecycloartanyl *p*-coumarate (marker 120) and 24-methylenecholesteryl sinapate (marker 129) (Fig. 3 and Table 2). The structural elucidation was based on the deprotonated molecular ions [M-H]⁻, related fragments from *p*-coumaric acid at *m/z* 163, 162, 145, and sinapic acid at *m/z* 223. Literature suggests that steryl *p*-coumarate is only present within corn, wheat and rye [17-19], and has yet to be reported in rice, as has been found in the present study. In plants, the enzymes involved in the biosynthesis of steryl ferulates are also suggested to accept other phenolic acids similar to ferulic acid as substrates, thus explaining the presence of other steryl phenolates observed [20].

### 3.2.3 Steryl ferulates role in the differentiation of rice

Generally, steryl ferulates play an important role in the separation of different rice varieties (Table 2). 24-methylenecholesteryl ferulate can distinguish Basmati from other types of rice. Moreover, campesteryl ferulate, as well as its saturated form campestanyl ferulate, contribute to the separation of Basmati and S.Andrea with various other rice varieties. Sitosteryl ferulate's content is higher in Basmati than in Jasmine; whereas its saturated form, sitostanyl ferulate, is relatively high in Baldo, Camargue and S.Andrea. Furthermore, also cycloartenyl ferulate is very important for distinguishing many pairs of rice separation (Table 2). 24-methylenecycloartanyl ferulate is abundant in S.Andrea and distinguishes S.Andrea from the other rice varieties, such as Baldo and Basmati rice. Another identified trace steryl ferulate, 25-hydroxy-24-methylcycloartanyl ferulate, is also a CM in the separation of Baldo or Camargue from other rice varieties. The newly identified steryl coumarates, cycloartenyl *p*-coumarate and 24-methylenecycloartanyl *p*-coumarate, also play

**Table 1.** Characteristic markers (CM) from OPLS-DA model for separating rice varieties (*Oryza sativa L.*). Marker is expressed as "RT_ *m/z* of [M-H]$^-$ (the number of marker)".

| Rice | Baldo (+) | Basmati (+) | Camargue (+) | Jasmine (+) | Perfume (+) | S.Andrea (+) |
|---|---|---|---|---|---|---|
| Baldo (−) | | 1.62_535.4722 (80) | 1.31_407.3165 (33) | 1.62_535.4722 (80) | 1.62_535.4722 (80) | 3.25_601.4253 (128) |
| | | 1.15_559.4724 (97) | 3.25_601.4253 (128) | 0.86_553.4826 (89) | 0.86_553.4826 (89) | 3.61_615.4408 (134) |
| | | 1.77_561.4877 (98) | | 0.99_557.4563 (93) | 1.15_559.4724 (97) | |
| | | 0.91_579.4983 (118) | | 1.77_561.4877 (98) | 1.77_561.4877 (98) | |
| | | | | 0.91_579.4983 (118) | 0.91_579.4983 (118) | |
| Basmati (−) | 3.17_571.4143 (105) | | 0.97_367.3575 (28) | 0.97_295.2277 (25) | 0.96_575.4670 (111) | 3.17_571.4143 (105) |
| | 3.53_585.4301 (120) | | 3.17_571.4143 (105) | 2.09_535.4724 (81) | 3.61_615.4408 (134) | 4.47_577.4252 (113) |
| | 5.16_591.4410 (126) | | 4.47_577.4252 (113) | 0.86_553.4826 (89) | | 3.53_585.4301 (120) |
| | 3.25_601.4253 (128) | | 5.16_591.4410 (126) | 0.96_575.4670 (111) | | 5.16_591.4410 (126) |
| | 1.30_633.4150 (136) | | 3.25_601.4253 (128) | 0.91_579.4983 (118) | | 3.25_601.4253 (128) |
| | 4.53_663.5191 (146) | | 1.26_603.4050 (129) | | | 3.61_615.4408 (134) |
| | | | 1.30_633.4150 (136) | | | 4.53_663.5191 (146) |
| Camargue (−) | 0.99_557.4563 (93) | 1.15_533.4567 (79) | | 0.99_557.4563 (93) | 1.15_533.4567 (79) | 3.53_585.4301 (120) |
| | 4.53_663.5191 (146) | 1.62_535.4722 (80) | | 1.77_561.4877 (98) | 1.62_535.4722 (80) | 3.61_615.4408 (134) |
| | | 0.86_553.4826 (89) | | 0.96_575.4670 (111) | 0.86_553.4826 (89) | 4.53_663.5191 (146) |
| | | 0.99_557.4563 (93) | | 0.91_579.4983 (118) | 0.99_557.4563 (93) | |
| | | 1.15_559.4724 (97) | | | 1.15_559.4724 (97) | |
| | | 1.77_561.4877 (98) | | | 1.77_561.4877 (98) | |
| | | 2.80_573.3938 (106) | | | 0.91_579.4983 (118) | |
| | | 0.91_579.4983 (118) | | | | |
| Jasmine (−) | 3.17_571.4143 (105) | 1.15_559.4724 (97) | 0.86_280.2639 (89) | | 1.15_559.4724 (97) | 3.17_571.4143 (105) |
| | 3.53_585.4301 (120) | 3.17_571.4143 (105) | 3.17_571.4143 (105) | | 3.61_615.4408 (134) | 3.84_575.4097 (109) |
| | 3.25_601.4253 (128) | 2.80_573.3938 (106) | 3.25_601.4253 (128) | | | 4.47_577.4252 (113) |
| | 1.30_633.4150 (136) | 3.84_575.4097 (109) | 1.30_633.4150 (136) | | | 3.53_585.4301 (120) |
| | 6.82_665.5344 (147) | 4.43_589.4253 (125) | | | | 5.16_591.4410 (126) |
| | 4.53_663.5191 (146) | 3.25_601.4253 (128) | | | | 3.25_601.4253 (128) |
| | | 6.82_665.5344 (147) | | | | 3.61_615.4408 (134) |
| | | | | | | 4.53_663.5191 (146) |

| Variety | | | | | |
|---|---|---|---|---|---|
| Perfume (−) | 3.17_571.4143 (105)<br>3.53_585.4301 (120)<br>3.25_601.4253 (128)<br>1.30_633.4150 (136)<br>4.53_663.5191 (146) | 2.80_573.3938 (106)<br>3.84_575.4097 (109)<br>3.25_601.4253 (128) | 0.97_367.3575 (28)<br>3.17_571.4143 (105)<br>3.25_601.4253 (128)<br>1.30_633.4150 (136) | 0.97_295.2277 (25)<br>0.86_553.4826 (89)<br>0.99_557.4563 (93)<br>0.91_579.4983 (118) | 3.17_571.4143 (105)<br>3.84_575.4097 (109)<br>4.47_577.4252 (113)<br>3.53_585.4301 (120)<br>5.16_591.4410 (126)<br>3.25_601.4253 (128)<br>3.61_615.4408 (134)<br>4.53_663.5191 (146) |
| S.Andrea (−) | 1.15_533.4567 (79)<br>0.99_557.4563 (93)<br>1.15_559.4724 (97)<br>1.77_561.4877 (98)<br>1.30_633.4150 (136) | 1.15_533.4567 (79)<br>1.62_535.4722 (80)<br>0.86_553.4826 (89)<br>0.99_557.4563 (93)<br>1.15_559.4724 (97)<br>1.77_561.4877 (98)<br>2.77_563.5028 (100)<br>2.80_573.3938 (106)<br>0.91_579.4983 (118) | 1.15_559.4724 (97)<br>1.77_561.4877 (98)<br>1.30_633.4150 (136) | 1.62_535.4722 (80)<br>0.99_557.4563 (93)<br>1.15_559.4724 (97)<br>1.77_561.4877 (98)<br>0.96_575.4670 (111)<br>0.91_579.4983 (118) | 1.15_533.4567 (79)<br>1.62_535.4722 (80)<br>0.99_557.4563 (94)<br>1.15_559.4724 (97)<br>1.77_561.4877 (98) |

The markers are listed for separation of any two types of rice. Ion intensity of markers in rice (+) is significantly higher than that in rice (−). For example, the two sets of markers both in Baldo (+) *vs.* Basmati (−) and Baldo (−) *vs.* Basmati (+) combined can separate Baldo and Basmati; the ion intensity of markers 80, 98, 97, and 118 are high in Basmati (+) and low in Baldo (−); whereas the ion intensity of markers 105, 120, 126, 128, 136, and 146 are high in Baldo (+) and low in Basmati (−). The markers are selected from the S-plots of pair of rice varieties.
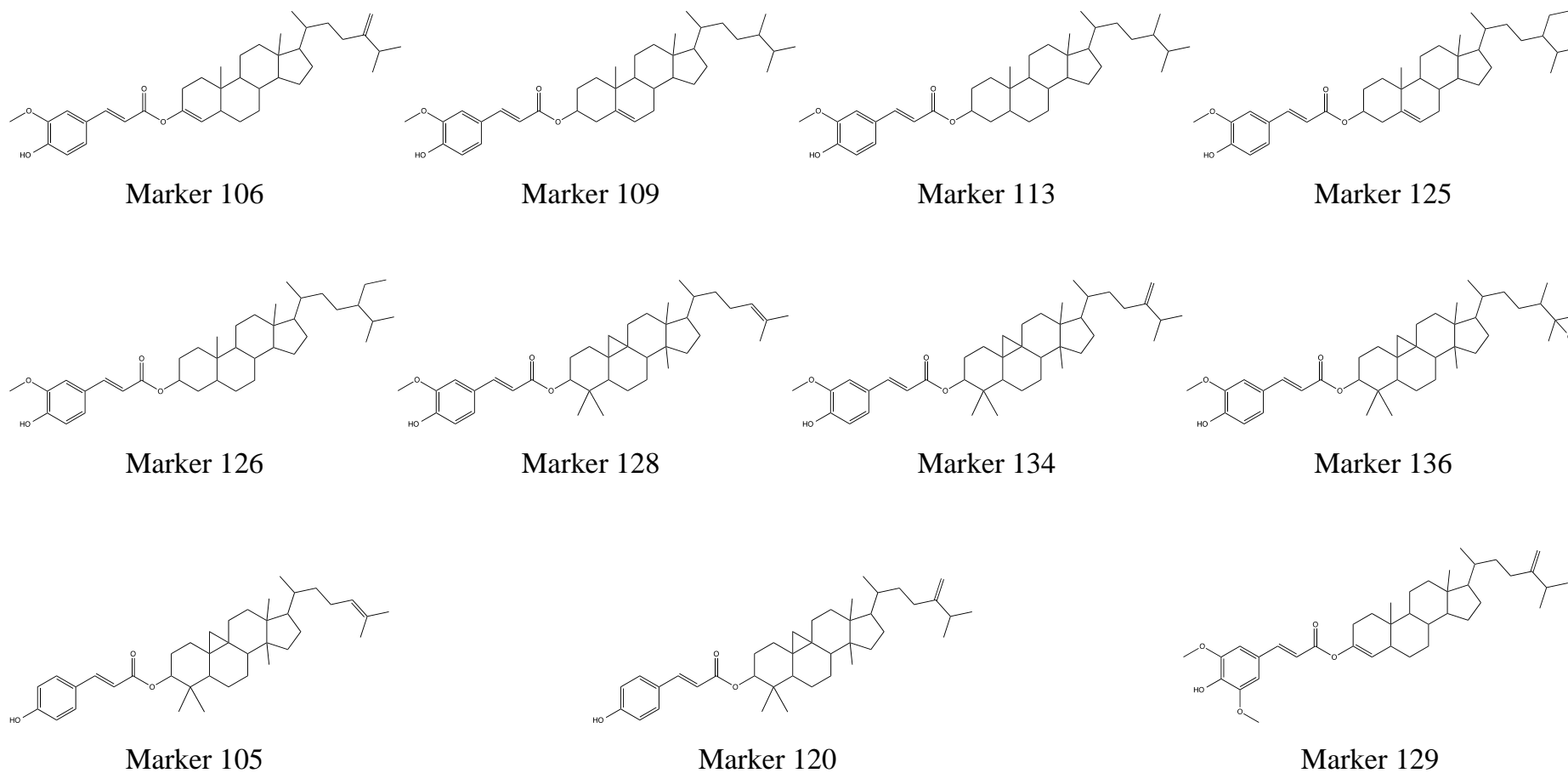
**Figure 3.** Structures of steryl ferulates and other steryl phenolates: 24-methylenecholesteryl ferulate (marker 106); campesteryl ferulate (marker 109); sitosteryl ferulate (marker 125); sitostanyl ferulate (marker 126); cycloartenyl ferulate (marker 128); 24-methylenecycloartanyl ferulate (marker 134); 25-hydroxy-24-methylcycloartanyl ferulate (marker 136); cycloartenyl *p*-coumarate (marker 105); 24-methylenecycloartanyl *p*-coumarate (marker 120); 24-methylenecholesteryl sinapate (marker 129).

**Table 2.** Steryl ferulates and steryl phenolates – characteristic markers (CM) for separating different types of rice (*Oryza sativa L.*).

| | RT (min) | [M-H]⁻ (*m/z*) | Mass | Fragment ions (*m/z*) | Tentatively Elemental composition | Tentative identification | Differentiation between rice varieties (high ion intensity versus low ion intensity) |
|---|---|---|---|---|---|---|---|
| **Steryl ferulates** | | | | | | | |
| Marker 106 | 2.80 | 573.3938 | 574.4016 | 573, 558, 193, 175, 133 | $C_{38}H_{54}O_4$ | 24-Methylenecholesteryl ferulate | Basmati versus Camargue; Jasmine; Perfume; S.Andrea. |
| Marker 109 [a] | 3.84 | 575.4097 | 576.4175 | 575, 560, 193, 177, 175, 133 | $C_{38}H_{56}O_4$ | Campesteryl ferulate | Basmati versus Jasmine; Perfume. S.Andrea versus Jasmine; Perfume. |
| Marker 113 [a] | 4.47 | 577.4252 | 578.4330 | 577, 562, 193, 177, 175, 133 | $C_{38}H_{58}O_4$ | Campestanyl ferulate | Camargue versus Basmati. S.Andrea versus Basmati; Jasmine; Perfume. |
| Marker 125 [a] | 4.43 | 589.4253 | 590.4331 | 589, 574, 193, 177, 175, 133 | $C_{39}H_{58}O_4$ | Sitosteryl ferulate | Basmati versus Jasmine. |
| Marker 126 [a] | 5.16 | 591.4410 | 592.4488 | 591, 576, 177, 175, 133 | $C_{39}H_{60}O_4$ | Sitostanyl ferulate | Baldo versus Basmati. Camargue versus Basmati. S.Andrea versus Basmati; Jasmine; Perfume. |
| Marker 128 [a] | 3.25 | 601.4253 | 602.4331 | 601, 586, 177, 175, 133 | $C_{40}H_{58}O_4$ | Cycloartenyl ferulate | Baldo versus Basmati; Jasmine; Perfume. Basmati versus Jasmine; Perfume. |

| | | | | | | | |
|---|---|---|---|---|---|---|---|
| | | | | | | | Camargue versus Baldo; Basmati; Jasmine; Perfume. S.Andrea versus Baldo; Basmati; Jasmine; Perfume. |
| Marker 134 [a] | 3.61 | 615.4408 | 616.4486 | 615, 600, 177, 175, 133 | $C_{41}H_{60}O_4$ | 24-Methylenecycloartanyl ferulate | S.Andrea versus Baldo; Basmati; Camargue; Jasmine; Perfume. |
| Marker 136 | 1.30 | 633.4150 | 634.4228 | 633, 175,133 | $C_{40}H_{58}O_6$ | 25-Hydroxy-24-methylcycloartanyl ferulate | Baldo versus Basmati; Jasmine; Perfume; S.Andrea. Camargue versus Basmati; Jasmine; Perfume; S.Andrea. |
| **Other steryl phenolates** | | | | | | | |
| Marker 105 | 3.17 | 571.4143 | 572.4221 | 571, 162, 145 | $C_{39}H_{56}O_3$ | Cycloartenyl *p*-coumarate | Baldo versus Basmati; Jasmine; Perfume. Basmati versus Jasmine. Camargue versus Basmati; Jasmine; Perfume. S.Andrea versus Basmati; Jasmine; Perfume. |
| Marker 120 | 3.53 | 585.4301 | 586.4379 | 585, 570, 163, 162, 145 | $C_{40}H_{58}O_3$ | 24-Methylenecycloartanyl *p*-coumarate | Baldo versus Basmati; Jasmine; Perfume. S.Andrea versus Basmati; Camargue; Jasmine; Perfume. |
| Marker 129 | 1.26 | 603.4050 | 604.4128 | 603, 588, 223 | $C_{39}H_{56}O_5$ | 24-Methylenecholesteryl sinapate | Basmati versus Camargue. |

[a] Confirmed by γ-oryzanol standard.

76

important roles in separation of the rice varieties, such as Baldo *vs.* Basmati. Furthermore, the tentatively identified steryl sinapate, 24-methylenecholesteryl sinapate also contributes to the differentiation between Basmati and Camargue.

In addition to the above-mentioned steryl phenolate markers, the possible elemental composition of other CM found in Table 1 are also suggested (in the supporting information). This OMIC approach provides effective information for the differentiation and characterization of various rice varieties. Furthermore, adopting such an analytical approach contains the potential of revealing novel bioactive compounds.

## 3.3 Markers for wild rice

### 3.3.1 Markers for separating wild rice and common rice

Common rice and wild rice samples are clearly separated within the PCA plot (PC1 versus PC2), indicating that their lipid profiles are different. 16 markers that are present at much higher intensity in wide rice than common rice samples and therefore can be used to separate common rice from wild rice varieties (Table 3). Wild rice was reported with 0.7-1.1% lipids, including fatty acids, phytosterols and γ-oryzanol [21]. In our study, the selected 16 markers are characteristic in wild rice with the masses ranging from 390 to 570. However, steryl ferulates are not within the markers capable of distinguishing common rice and wild rice varieties.

### 3.3.2 Characteristic markers (CM) for separating two types of wild rice

Wild rice from USA and Canada were compared using an S-plot with OPLS-DA model and CM to differentiate between the two types of wild rice were successfully extracted (Table 3). Markers 28 and 63 have high ion intensity in wild rice from USA, whereas the markers 55, 61, 73, 84, 90, and 125 are found to be specific for the wild rice from Canada. In our study, sitosteryl ferulate (marker 125) is also a prominent marker for

**Table 3.** Markers for (1) separating rice (*Oryza sativa L.*) and wild rice (*Zizania palustris L.*) from PCA plot (PC1 versus PC2), (2) separating wild rice USA and wild rice Canada from OPLS-DA model.

| | RT (min) | [M-H]⁻ (m/z) | Mass | Possible elemental composition |
|---|---|---|---|---|
| **Wild rice versus common rice** | | | | |
| Marker 31 | 0.95 | 393.3729 | 394.3807 | $C_{28}H_{42}O$ |
| Marker 38 | 1.57 | 421.4048 | 422.4126 | $C_{28}H_{54}O_2$ |
| Marker 45 | 2.79 | 449.4357 | 450.4435 | $C_{30}H_{58}O_2$ |
| Marker 55 | 4.37 | 477.4671 | 478.4749 | $C_{32}H_{62}O_2$ |
| Marker 61 | 2.49 | 499.3789 | 500.3867 | $C_{32}H_{52}O_4$ |
| Marker 63 | 3.37 | 501.3944 | 502.4022 | $C_{32}H_{54}O_4$ |
| Marker 64 | 6.57 | 505.4982 | 506.5060 | $C_{34}H_{66}O_2$ |
| Marker 67 | 1.25 | 513.3579 | 514.3657 | $C_{32}H_{50}O_5$ |
| Marker 71 | 2.52 | 525.3938 | 526.4016 | $C_{34}H_{54}O_4$ |
| Marker 73 | 3.31 | 527.4097 | 528.4175 | $C_{34}H_{56}O_4$ |
| Marker 75 | 4.76 | 529.4292 | 530.4370 | $C_{34}H_{58}O_4$ |
| Marker 77 | 1.25 | 531.3680 | 532.3758 | $C_{32}H_{52}O_6$ |
| Marker 84 | 5.09 | 541.4614 | 542.4692 | $C_{36}H_{62}O_3$ |
| Marker 90 | 4.66 | 555.4406 | 556.4484 | $C_{36}H_{60}O_4$ |
| Marker 95 | 1.50 | 559.3997 | 560.4075 | $C_{34}H_{56}O_6$ |
| Marker 103 | 1.28 | 569.4565 | 570.4643 | $C_{37}H_{62}O_4$ |
| **Wild rice USA versus wild rice Canada** | | | | |
| High ion intensity in wild rice USA | | | | |
| Marker 28 | 0.97 | 367.3575 | 368.3653 | $C_{24}H_{48}O_2$ |
| Marker 63 | 3.37 | 501.3944 | 502.4022 | $C_{32}H_{54}O_4$ |
| High ion intensity in wild rice Canada | | | | |
| Marker 55 | 4.37 | 477.4671 | 478.4749 | $C_{32}H_{62}O_2$ |
| Marker 61 | 2.49 | 499.3789 | 500.3867 | $C_{32}H_{52}O_4$ |
| Marker 73 | 3.31 | 527.4097 | 528.4175 | $C_{34}H_{56}O_4$ |
| Marker 84 | 5.09 | 541.4614 | 542.4692 | $C_{36}H_{62}O_3$ |
| Marker 90 | 4.66 | 555.4406 | 556.4484 | $C_{36}H_{60}O_4$ |
| Marker 125 | 4.43 | 589.4253 | 590.4331 | $C_{39}H_{58}O_4$ |

wild rice, which is observed as having a higher intensity in wild rice coming from Canada than originating from USA. In the literature, profiles of individual steryl ferulates including sitosteryl ferulate in wild rice have been reported to be location dependent [22]. The approach applied in this study can also distinguish different types of wild rice from different origins mainly based on compounds other than steryl ferulates.

# 4 Conclusions

This study provides a novel and targeted method to distinguish between various common rice varieties as well as geographic regions wild rice using UPLC-HR-Q-TOF-MS with OMIC technique. We were able to find CM that can classify different rice types based on their steryl ferulate profiles and other potential small lipids. This sensitive analytical technique may reveal several new compounds of bioactive lipids in rice, but these small lipids need further elucidation. While OMIC techniques demonstrate great analytic potential, a large library of samples is often necessary to increase the reliability of the method. Furthermore, these results also can be applied for the selection of rice varieties with optimal profiles of bioactive lipids for food use.

# Acknowledgements

# References

[1]     Ryan, E. P., Bioactive food components and health properties of rice bran. J. Am. Vet. Med. Assoc. 2011, 238, 593-600.

[2]     Vlachos, A., Arvanitoyannis, I. S., A review of rice authenticity/adulteration methods and results. Crit. Rev. Food. Sci. Nutr. 2008, 48, 553-598.

[3]     Chuang, H. Y., Lur, H. S., Hwu, K. K., Chang, M. C., Authentication of domestic Taiwan rice varieties based on fingerprinting analysis of microsatellite DNA markers. Bot. Stud. 2011, 52, 393-405.

[4]     Arruda Filho, A. C. V., Guedes, M. I. F., Duarte, L. S. F., Lima-neto, A. B. M., Cameron, L.C., Bassini, A., Vieira, Í. G. P., De Melo, T. S., De Almeida, L. M., Queiroz, M. G. R., Gamma-oryzanol has an equivalent efficacy as a lipid lowering agent compared to fibrate and statin in two dyslipidemia mice models. Int. J. Pharm. Pharm. Sci. 2014, 6, 61-64.

[5]     Nyström, L., Mäkinen, M., Lampi, A. M., Piironen, V., Antioxidant activity of steryl ferulate extracts from rye and wheat bran. J. Agric. Food. Chem. 2005, 53, 2503-2510.

[6]     Hu, Y. Z., Xiong, L. N., Huang, W. S., Cai, H. F., Luo, Y. X., Zhang, Y., Lu, B. Y., Anti-inflammatory effect and prostate gene expression profiling of steryl ferulate on experimental rats with non-bacterial prostatitis. Food. Funct. 2014, 5, 1150-1159.

[7]     Kong, C. K., Lam, W. S., Chiu, L. C., Ooi, V. E., Sun, S. S., Wong, Y. S., A rice bran polyphenol, cycloartenyl ferulate, elicits apoptosis in human colorectal adenocarcinoma SW480 and sensitizes metastatic SW620 cells to TRAIL-induced apoptosis. Biochem. Pharmacol. 2009, 77, 1487-1496.

[8]     Mandak, E., Nyström, L., The effect of in vitro digestion on steryl ferulates from rice (Oryza sativa L.) and other grains. J. Agric. Food. Chem. 2012, 60, 6123-6130.

[9]     Miller, A., Engel, K.H., Content of γ-oryzanol and composition of steryl ferulates in brown rice (Oryza sativa L.) of European origin. J. Agric. Food. Chem. 2006, 54, 8127-8133.

[10]    Moco, S., Forshed, J., De Vos, R. C. H., Bino, R. J., Vervoort, J., Intra- and inter-metabolite correlation spectroscopy of tomato metabolomics data obtained by liquid chromatography-mass spectrometry and nuclear magnetic resonance. Metabolomics. 2008, 4, 202-215.

[11]    Luthria, D. L., Lin, L. Z., Robbins, R. J., Finley, J. W., Banuelos, G. S., Harnly, J. M., Discriminating between cultivars and treatments of broccoli using mass

spectral fingerprinting and analysis of variance-principal component analysis. J. Agric. Food. Chem. 2008, 56, 9819-9827.

[12]   Dobson, G., Shepherd, T., Verrall, S. R., Conner, S., McNicol, J. W., Ramsay, G., Shepherd, L. V. T., Davies, H. V., Stewart, D., Phytochemical diversity in tubers of potato cultivars and landraces using a GC-MS metabolomics approach. J. Agric. Food. Chem. 2008, 56, 10280-10291.

[13]   Mandak, E., Nyström, L., Influence of baking and in vitro digestion on steryl ferulates from wheat. J. Cereal. Sci. 2013, 57, 356-361.

[14]   Angelis, A., Urban, A., Halabalaki, M., Aligiannis, N., Skaltsounis, A. L., One-step isolation of gamma-oryzanol from rice bran oil by non-aqueous hydrostatic countercurrent chromatography. J. Sep. Sci. 2011, 34, 2528-2537.

[15]   Cho, J.Y., Lee, H. J., Kim, G. A., Kim, G. D., Lee, Y. S., Shin, S. C., Park, K.H., Moon, J.H., Quantitative analyses of individual γ-oryzanol (steryl ferulates) in conventional and organic brown rice (Oryza sativa L.). J. Cereal. Sci. 2012, 55, 337-343.

[16]   Fang, N., Yu, S., Badger, T. M., Characterization of triterpene alcohol and sterol ferulates in rice bran using LC-MS/MS. J. Agric. Food. Chem. 2003, 51, 3260-3267.

[17]   Esche, R., Barnsteiner, A., Scholz, B., Engel, K. H., Simultaneous analysis of free phytosterols/phytostanols and intact phytosteryl/phytostanyl fatty acid and phenolic acid esters in cereals. J. Agric. Food. Chem. 2012, 60, 5330-5339.

[18]   Norton, R. A., Quantitation of steryl ferulate and p-coumarate esters from corn and rice. Lipids. 1995, 30, 269-274.

[19]   Seitz, L. M., Stanol and sterol esters of ferulic and p-coumaric acids in wheat, corn, rye, and triticale. J. Agric. Food. Chem. 1989, 37, 662-667.

[20]   C. Lemus, A. Angelis, M. Halabalaki, A. Leandros: γ-Oryzanol: an attractive bioactive component from rice bran. In: Wheat and Rice in Disease Prevention and Health: Benefits, risks and mechanisms of whole grains in health promotion. Eds. R. R. Watson, V. R. Preedy, S. Zibadi, Academic Press, London, UK 2014, pp. 409-430.

[21]   Przybylski, R., Klensporf-Pawlik, D., Anwar, F., Rudzinska, M., Lipid components of North American wild rice (Zizania palustris). J. Am. Oil. Chem. Soc. 2009, 86, 553-559.

[22]   Aladedunye, F., Przybylski, R., Rudzinska, M., Klensporf-Pawlik, D., γ-Oryzanols of North American wild rice (Zizania palustris). J. Am. Oil. Chem. Soc. 2013, 90, 1101-1109.

# Supporting information

**Table S1.** 156 markers in different common rice varieties and wild rice

|  | Retention Time (min) | [M-H]⁻ (m/z) | Mass | Possible elemental composition |
|---|---|---|---|---|
| Marker 1 | 0.82 | 146.9661 | 147.9739 | C8H4O3 |
| Marker 2 | 0.82 | 188.9387 | 189.9465 | n.s. |
| Marker 3 | 0.90 | 200.8924 | 201.9002 | n.s. |
| Marker 4 | 0.83 | 213.0555 | 214.0633 | C13H10O3 |
| Marker 5 | 0.83 | 254.2486 | 255.2564 | C16H33NO |
| Marker 6 | 6.83 | 255.2325 | 256.2403 | C16H32O2 |
| Marker 7 | 1.99 | 255.2327 | 256.2405 | C16H32O2 |
| Marker 8 | 6.24 | 255.2327 | 256.2405 | C16H32O2 |
| Marker 9 | 4.44 | 255.2328 | 256.2406 | C16H32O2 |
| Marker 10 | 0.94 | 255.2329 | 256.2407 | C16H32O2 |
| Marker 11 | 1.06 | 275.2019 | 276.2097 | C18H28O2 |
| Marker 12 | 2.69 | 277.2174 | 278.2252 | C18H30O2 |
| Marker 13 | 4.52 | 279.2328 | 280.2406 | C18H32O2 |
| Marker 14 | 3.40 | 279.2328 | 280.2406 | C18H32O2 |
| Marker 15 | 1.69 | 279.233 | 280.2408 | C18H32O2 |
| Marker 16 | 0.97 | 279.2331 | 280.2409 | C18H32O2 |
| Marker 17 | 0.86 | 280.2639 | 281.2717 | C18H35NO |
| Marker 18 | 2.06 | 281.2483 | 282.2561 | C18H34O2 |
| Marker 19 | 6.30 | 281.2484 | 282.2562 | C18H34O2 |
| Marker 20 | 6.83 | 281.2487 | 282.2565 | C18H34O2 |
| Marker 21 | 1.77 | 291.1965 | 292.2043 | C18H28O3 |
| Marker 22 | 1.89 | 293.2119 | 294.2197 | C18H30O3 |
| Marker 23 | 1.01 | 293.2123 | 294.2201 | C18H30O3 |
| Marker 24 | 0.82 | 294.9037 | 295.9115 | n.s. |

| Marker 25 | 0.97 | 295.2277 | 296.2355 | C18H32O3 |
| Marker 26 | 0.83 | 305.0817 | 306.0895 | C19H14O4 |
| Marker 27 | 0.84 | 353.3408 | 354.3486 | C23H46O2 |
| Marker 28 | 0.97 | 367.3575 | 368.3653 | C24H48O2 |
| Marker 29 | 0.84 | 379.3578 | 380.3656 | C25H48O2 |
| Marker 30 | 1.21 | 381.3734 | 382.3812 | C27H42O |
| Marker 31 | 0.95 | 393.3729 | 394.3807 | C28H42O |
| Marker 32 | 1.60 | 395.3891 | 396.3969 | C28H44O |
| Marker 33 | 1.31 | 407.3165 | 408.3243 | C24H40O5 |
| Marker 34 | 1.43 | 409.3108 | 410.3186 | C28H42O2 |
| Marker 35 | 0.95 | 409.3480 | 410.3558 | C30H50 |
| Marker 36 | 1.17 | 413.3059 | 414.3137 | C27H42O3 |
| Marker 37 | 2.25 | 415.3571 | 416.3649 | C27H44O3 |
| Marker 38 | 1.57 | 421.4048 | 422.4126 | C28H54O2 |
| Marker 39 | 5.08 | 421.4059 | 422.4137 | C28H54O2 |
| Marker 40 | 2.85 | 423.4204 | 424.4282 | C28H56O2 |
| Marker 41 | 1.96 | 429.3731 | 430.3809 | C29H50O2 |
| Marker 42 | 0.96 | 439.3559 | 440.3637 | C30H48O2 |
| Marker 43 | 1.17 | 441.3001 | 442.3079 | C28H42O4 |
| Marker 44 | 1.42 | 443.2464 | 444.2542 | C31H40O2 |
| Marker 45 | 2.79 | 449.4357 | 450.4435 | C30H58O2 |
| Marker 46 | 4.42 | 451.4509 | 452.4587 | C30H60O2 |
| Marker 47 | 1.55 | 461.3629 | 462.3707 | C29H50O4 |
| Marker 48 | 0.95 | 463.3591 | 464.3669 | C32H48O2 |
| Marker 49 | 0.89 | 467.4103 | 468.4181 | C29H56O4 |
| Marker 50 | 2.43 | 469.3677 | 470.3755 | C31H50O3 |
| Marker 51 | 3.28 | 471.3845 | 472.3923 | C31H52O3 |
| Marker 52 | 2.55 | 473.3697 | 474.3775 | C30H50O4 |
| Marker 53 | 2.68 | 473.4003 | 474.4081 | C31H54O3 |
| Marker 54 | 1.02 | 477.3752 | 478.3830 | C33H50O2 |

| | | | | |
|---|---|---|---|---|
| Marker 55 | 4.37 | 477.4671 | 478.4749 | C32H62O2 |
| Marker 56 | 2.96 | 479.3871 | 480.3949 | C27H44O7 |
| Marker 57 | 2.89 | 487.3786 | 488.3864 | C31H52O4 |
| Marker 58 | 0.91 | 491.4468 | 492.4546 | C32H60O3 |
| Marker 59 | 1.99 | 497.3631 | 498.3709 | C32H50O4 |
| Marker 60 | 3.23 | 497.3992 | 498.4070 | C33H54O3 |
| Marker 61 | 2.49 | 499.3789 | 500.3867 | C32H52O4 |
| Marker 62 | 4.64 | 499.4153 | 500.4231 | C33H56O3 |
| Marker 63 | 3.37 | 501.3944 | 502.4022 | C32H54O4 |
| Marker 64 | 6.57 | 505.4982 | 506.5060 | C34H66O2 |
| Marker 65 | 1.03 | 507.4406 | 508.4484 | C32H60O4 |
| Marker 66 | 1.42 | 509.4571 | 510.4649 | C32H62O4 |
| Marker 67 | 1.25 | 513.3579 | 514.3657 | C32H50O5 |
| Marker 68 | 3.54 | 513.4302 | 514.4380 | C34H58O3 |
| Marker 69 | 5.21 | 515.4463 | 516.4541 | C34H60O3 |
| Marker 70 | 2.07 | 523.3776 | 524.3854 | C34H52O4 |
| Marker 71 | 2.52 | 525.3938 | 526.4016 | C34H54O4 |
| Marker 72 | 4.53 | 525.4305 | 526.4383 | C35H58O3 |
| Marker 73 | 3.31 | 527.4097 | 528.4175 | C34H56O4 |
| Marker 74 | 5.19 | 527.4456 | 528.4534 | C35H60O3 |
| Marker 75 | 4.76 | 529.4292 | 530.4370 | C34H58O4 |
| Marker 76 | 3.24 | 529.4621 | 530.4699 | C35H62O3 |
| Marker 77 | 1.25 | 531.3680 | 532.3758 | C32H52O6 |
| Marker 78 | 0.86 | 531.4402 | 532.4480 | C34H60O4 |
| Marker 79 | 1.15 | 533.4567 | 534.4645 | C34H62O4 |
| Marker 80 | 1.62 | 535.4722 | 536.4800 | C40H56 |
| Marker 81 | 2.09 | 535.4724 | 536.4802 | C40H56 |
| Marker 82 | 3.61 | 539.4455 | 540.4533 | C36H60O3 |
| Marker 83 | 1.50 | 541.3893 | 542.3971 | C34H54O5 |
| Marker 84 | 5.09 | 541.4614 | 542.4692 | C36H62O3 |

| Marker 85 | 3.74 | 545.3986 | 546.4064 | C37H54O3 |
| Marker 86 | 4.30 | 547.4139 | 548.4217 | C37H56O3 |
| Marker 87 | 0.89 | 549.4504 | 550.4582 | C34H62O5 |
| Marker 88 | 3.36 | 553.4251 | 554.4329 | C36H58O4 |
| Marker 89 | 0.86 | 553.4826 | 554.4904 | C34H66O5 |
| Marker 90 | 4.66 | 555.4406 | 556.4484 | C36H60O4 |
| Marker 91 | 0.84 | 555.4407 | 556.4485 | C36H60O5 |
| Marker 92 | 7.39 | 557.4563 | 558.4641 | C36H62O4 |
| Marker 93 | 0.99 | 557.4563 | 558.4641 | C36H62O4 |
| Marker 94 | 0.89 | 558.4602 | 559.468 | C36H63O4 |
| Marker 95 | 1.50 | 559.3997 | 560.4075 | C34H56O6 |
| Marker 96 | 4.27 | 559.4145 | 560.4223 | C38H56O3 |
| Marker 97 | 1.15 | 559.4724 | 560.4802 | C36H64O4 |
| Marker 98 | 1.77 | 561.4877 | 562.4955 | C37H54O4 |
| Marker 99 | 5.00 | 561.4303 | 562.4381 | C38H58O3 |
| Marker 100 | 2.77 | 563.5028 | 564.5106 | C36H68O4 |
| Marker 101 | 3.84 | 565.4621 | 566.4699 | C38H62O3 |
| Marker 102 | 5.21 | 567.4761 | 568.4839 | C38H64O3 |
| Marker 103 | 1.28 | 569.4565 | 570.4643 | C37H62O4 |
| Marker 104 | 8.00 | 569.4925 | 570.5003 | C38H66O3 |
| Marker 105 | 3.17 | 571.4143 | 572.4221 | C39H56O3 |
| Marker 106 | 2.80 | 573.3938 | 574.4016 | C38H54O4 |
| Marker 107 | 1.87 | 573.4502 | 574.4580 | C36H62O4 |
| Marker 108 | 0.92 | 573.4513 | 574.4591 | C36H62O5 |
| Marker 109 | 3.84 | 575.4097 | 576.4175 | C38H56O4 |
| Marker 110 | 3.15 | 575.4097 | 576.4175 | C38H56O4 |
| Marker 111 | 0.96 | 575.4670 | 576.4748 | C36H64O5 |
| Marker 112 | 3.16 | 576.4130 | 577.4208 | C38H57O4 |
| Marker 113 | 4.47 | 577.4252 | 578.4330 | C38H58O4 |
| Marker 114 | 0.84 | 577.4822 | 578.4900 | C36H66O5 |

| Marker 115 | 0.91 | 579.4983 | 580.5061 | C36H68O5 |
| Marker 116 | 1.14 | 581.4622 | 582.4700 | C38H62O4 |
| Marker 117 | 7.14 | 583.4714 | 584.4792 | C38H64O4 |
| Marker 118 | 1.96 | 583.4723 | 584.4801 | C38H63O4 |
| Marker 119 | 2.58 | 585.3277 | 586.3355 | C30H52O7P2 |
| Marker 120 | 3.53 | 585.4301 | 586.4379 | C40H58O3 |
| Marker 121 | 1.79 | 587.4309 | 588.4387 | C39H56O4 |
| Marker 122 | 2.99 | 587.4095 | 588.4173 | C39H56O4 |
| Marker 123 | 5.08 | 587.4673 | 588.4751 | C37H64O5 |
| Marker 124 | 3.94 | 587.4098 | 588.4176 | C39H56O4 |
| Marker 125 | 4.43 | 589.4253 | 590.4331 | C39H58O4 |
| Marker 126 | 5.16 | 591.4410 | 592.4488 | C39H60O4 |
| Marker 127 | 1.27 | 595.4728 | 596.4806 | C39H64O4 |
| Marker 128 | 3.25 | 601.4253 | 602.4331 | C40H58O4 |
| Marker 129 | 1.26 | 603.4050 | 604.4128 | C39H56O5 |
| Marker 130 | 4.55 | 603.4414 | 604.4492 | C40H60O4 |
| Marker 131 | 3.25 | 607.4569 | 608.4647 | C39H60O5 |
| Marker 132 | 1.55 | 609.4878 | 610.4956 | C40H66O4 |
| Marker 133 | 1.50 | 615.4043 | 616.4121 | C41H60O4 |
| Marker 134 | 3.61 | 615.4408 | 616.4486 | C41H60O4 |
| Marker 135 | 1.38 | 619.3998 | 620.4076 | C39H56O6 |
| Marker 136 | 1.30 | 633.4150 | 634.4228 | C40H58O6 |
| Marker 137 | 3.42 | 635.5034 | 636.5112 | C44H76O2 |
| Marker 138 | 4.50 | 637.5067 | 638.5145 | C42H70O4 |
| Marker 139 | 6.26 | 639.5208 | 640.5286 | C44H80O2 |
| Marker 140 | 6.82 | 639.5231 | 640.5309 | C44H80O2 |
| Marker 141 | 2.69 | 649.4578 | 650.4656 | C44H58O4 |
| Marker 142 | 3.40 | 651.4737 | 652.4815 | C44H60O4 |
| Marker 143 | 1.76 | 657.4451 | 658.4529 | C43H62O5 |
| Marker 144 | 1.95 | 659.4648 | 660.4726 | C43H64O5 |

| | | | | |
|---|---|---|---|---|
| Marker 145 | 3.38 | 661.5026 | 662.5104 | C46H78O2 |
| Marker 146 | 4.53 | 663.5191 | 664.5269 | C46H80O2 |
| Marker 147 | 6.82 | 665.5344 | 666.5422 | C44H74O3 |
| Marker 148 | 6.29 | 665.5345 | 666.5423 | C44H74O4 |
| Marker 149 | 1.77 | 667.4773 | 668.4851 | C45H64O4 |
| Marker 150 | 1.97 | 669.493 | 670.5008 | C45H66O4 |
| Marker 151 | 2.33 | 671.5097 | 672.5175 | C47H76O2 |
| Marker 152 | 3.42 | 681.5073 | 682.5151 | C43H70O6 |
| Marker 153 | 1.68 | 683.4642 | 684.4720 | C45H64O5 |
| Marker 154 | 1.67 | 693.4939 | 694.5017 | C48H86O2 |
| Marker 155 | 1.98 | 695.5087 | 696.5165 | C48H88O2 |
| Marker 156 | 3.93 | 737.5917 | 738.5995 | C44H81O8 |

n.s.: No suggestion.

# Antioxidant Activity of Individual Steryl Ferulates from Various Cereal Grain Sources

Dan Zhu, Antoni Sánchez-Ferrer, Laura Nyström. *Submitted manuscript* (November 2014).

## Abstract

Steryl ferulates (SFs) are a subclass of bioactive lipids contributing to the health promoting effects of whole grains. There is little evidence that individual SFs may vary in their bioactivity. The aim of this study was to evaluate the antioxidant activity of eight individual SFs by determining their radical scavenging capacity. Additional molecular properties of the individual SFs were determined by molecular simulation in order to identify correlations with their antioxidant activities. Our study demonstrates that individual SFs exhibit DPPH radical, hydroxyl radical, and superoxide anion radical scavenging abilities with subtle differences that were highly dependent on the kind of reaction taking place. The grouping of SFs by principle component analysis was mainly attributed to molecular properties, not antioxidant activities. Solvation energy was significantly correlated with some experimental observations. Results of this work will provide better insight to the antioxidant activity of SFs and the health benefits of whole grains.

## Keywords

Cereal grain / γ-oryzanol / Radical scavenging / Steryl ferulate / Simulation

## Abbreviations

ACN, acetonitrile; DPPH$^\bullet$, DPPH radical; $^\bullet$OH, hydroxyl radical; HPX, hypoxanthine; NBT, nitrotetrazolium blue chloride; ORY, γ-oryzanol; PCA, principle component

analysis; SF, steryl ferulate; WB, steryl ferulate mixtures from wheat bran; $O_2^{\bullet-}$, superoxide anion radical; TEMPO, 2,2,6,6-tetramethyl-1-piperidinyloxy; XOD, xanthine oxidase.

## Introduction

Steryl ferulates (SFs) are the esters of phytosterols and ferulic acid, which are present in the bran of some grains such as rice, wheat, corn, rye, barley, and triticale [1]. They are bioactive lipids shown to possess health benefits such as lowering cholesterol, and exhibiting antioxidant and anti-inflammatory activities. These activities have recently been compiled and summarized by Ghatak and Panchal [2]. The different SFs investigated in this study varied only in the type of sterol moiety, as shown in Figure 1. Their total content, as well as the composition of individual SFs, varied depending on the grain source, genotype, and environmental factors [3]. In rice bran (total SFs, commonly known as γ-oryzanol (ORY), 1550-8400 $\mu g \cdot g^{-1}$ dry weight) the ratio of 4,4-dimethylsteryl ferulates (SFs **1** and **2**), and 4-desmethylsteryl ferulates (SFs **3** - **7**) is around 65:35 [4]. However, only 4-desmethylsteryl ferulates are found in wheat bran (SFs **3** - **6**, total 297-584 $\mu g \cdot g^{-1}$) and corn bran (SFs **3** - **7**, total 200-250 $\mu g \cdot g^{-1}$) [5, 6]. SF **3** accounts for approximate 60% of SFs in wheat; while in corn, the most abundant is SF **4**, representing approximately 70% of total SFs [1].

SFs have been shown to prevent oxidation in various biological systems. The mechanism of their antioxidant activity results from the phenolic proton in the ferulic acid moiety, which can be abstracted by any radical present in the media, and the resulting SF radical is stabilized by resonance along the π-electron system constituted by the aromatic ring and the carboxylate in *para* position to the phenol group [5, 7]. Some researchers have also suggested that the SF radical might still influence oxidation, for example, by interfering with the chain reaction of lipid oxidation as alkyl radicals [8]. To date, bioactivity studies of SFs have mostly been performed with ORY due to the lack of individual SFs on the market. For instance, Kim *et al.* proved that ORY effectively improved flavour and oxidative stability of refrigerated cooked beef [9]. Juliano *et al.*
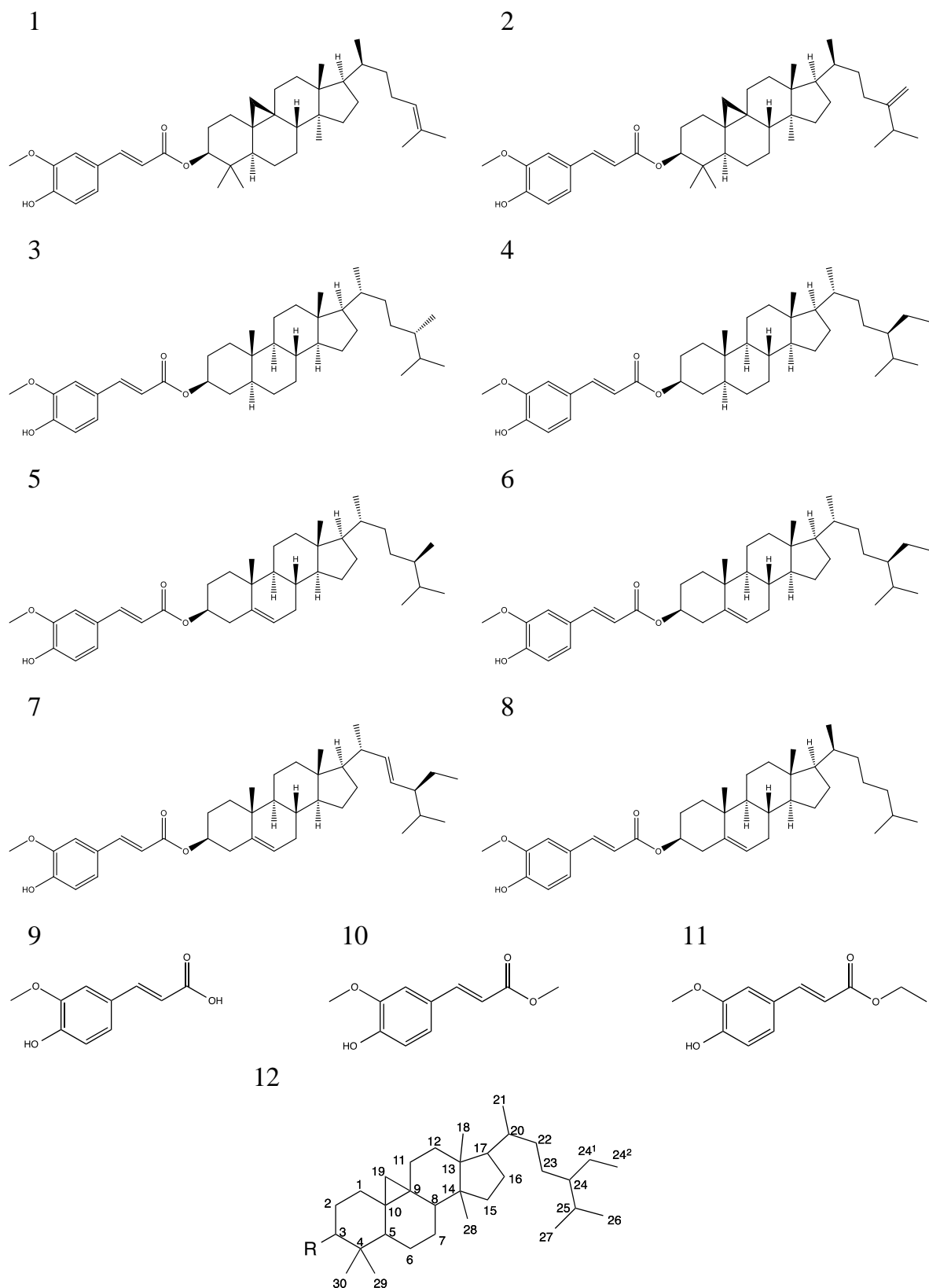
**Figure 1**. Molecular structures of (**1**) cycloartenyl ferulate, (**2**) 24-methylenecycloartanyl ferulate, (**3**) campestanyl ferulate, (**4**) sitostanyl ferulate, (**5**) campesteryl ferulate, (**6**) sitosteryl ferulate, (**7**) stigmasteryl ferulate, (**8**) cholesteryl ferulate, (**9**) ferulic acid, (**10**) methyl ferulate, (**11**) ethyl ferulate, (**12**) a general sterol skeleton based on IUPAC-IUB 1989.

demonstrated that ORY prevented AMVN-triggered lipoperoxidation and improved the oxidative stability of oils [10]. Recently, ORY was also determined to exhibit 2,2'-azinobis(3-ethylbenzothiazoline-6-sulfonic acid) cation radical (ABTS$^{•+}$) and superoxide anion radical (O$_2^{•−}$) scavenging activity, as well as a strong inhibition effect on linoleic acid peroxidation [11].

Furthermore, there are indications that individual SFs may vary in their antioxidant activity, and therefore, the sterol composition may be an important aspect in defining the activity of SF mixtures. However, there is limited data available on these differences in antioxidant effects. Xu *et al.* reported that SFs **2** > **5** = **1** in preventing cholesterol oxidation [12]. Furthermore, in terms of preventing hydroperoxide formation in methyl linoleate bulk oil systems, SFs mixture from wheat and rye > SFs **6** and **8** > ORY and **1** [13]. Huang demonstrated that the antioxidant activity of SFs **2** > **1**, and SFs **5** > ORY in an SVEC-10 mouse lymph endothelial cell model, using tBHP as an oxidizing agent [14]. Since their antioxidant capacities differ considerably from one to another, it is of great interest to evaluate the activities of individual SFs more systematically.

The aim of this study was to evaluate the antioxidant activity of eight individual SFs. SFs (**2** - **6**) were purified from ORY and wheat bran. SF **7** and SF **8**, which occur only in trace amounts in nature, were synthesized. SFs were divided into groups according to structure similarity: SFs **1** and **2** (with methyl groups at C4 and C14, cyclopropyl ring at C9/C10); SFs **3** and **4** (with saturated sterol, no double bond at C5 and C6); and SFs **5**, **6**, **7**, and **8** (with unsaturated sterol, double bond at C5 and C6). Additionally, antioxidant effects of ferulic acid (**9**), methyl ferulate (**10**), ethyl ferulate (**11**), ORY, and the SF mixtures from wheat bran (WB) were evaluated. Antioxidant activity was determined by evaluating the scavenging capacity of DPPH radicals (DPPH$^•$) in methanol, hydroxyl radical ($^•$OH) and superoxide anion radical (O$_2^{•−}$) in an *in vitro* water environment. Additional molecular properties of individual SFs were determined by molecular simulation, in order to correlate them with their antioxidant activities. As far as we know, this study is the first to provide a comprehensive comparison of the antioxidant activity of individual SFs.

# Materials and methods

## Materials and apparatus

Acetic acid (Ph Eur) and 1-butanol (Ph Eur) were purchased from Merck, Darmstadt, Germany. Acetone ($\geq$99.9%), acetonitrile (ACN; $\geq$99.9%), cholesterol (99%), 3,4-dihydro-2H-pyran (97%), 5,5-dimethyl-1-pyrroline $N$-oxide (DMPO; $\geq$99%), 2,2-diphenyl-1-picrylhydrazyl (DPPH), ethylenediaminetetraacetic acid dipotassium salt dihydrate (EDTA; $\geq$99.0%), hydrochloric acid (37%), hydrogen peroxide solution ($H_2O_2$; $\geq$35%), hypoxanthine (HPX; $\geq$99%), iron (II) sulfate heptahydrate ($FeSO_4 \cdot 7H_2O$; $\geq$99%), methanol ($\geq$99.9%), nitrotetrazolium blue chloride (NBT; 98%), pyrogallol ($\geq$99%), 2,2,6,6-tetramethyl-1-piperidinyloxy (TEMPO; $\geq$99%), $p$-toluenesulfonic acid monohydrate ($\geq$98%), $trans$-ferulic acid ($\geq$99%), and xanthine oxidase (XOD) from bovine milk (Grade IV) were obtained from Sigma-Aldrich, St. Louis, MO, USA. Stigmasterol was bought from Research Plus, Bayonne, NJ, USA. Cycloartenyl ferulate ($\geq$99%; SF **1**) was purchased from Wako, Osaka, Japan. γ-Oryzanol (ORY) was obtained from CTC Organics, Atlanta, GA, USA. Methyl ferulate (99%) and ethyl ferulate (99%) were from Alfa Aesar, Ward Hill, MA, USA. Wheat bran was from Swissmill, Switzerland.

Preparative HPLC (Merck-Hitachi, Japan) with an XBridge Prep Shield RP C18 column (5.0 μm, 10 × 250 mm, Waters, Ireland), analytical HPLC (Agilent 1100, Germany) with an XBridge Shield C18 column (3.5 μm, 3 × 150 mm, Waters, Ireland), UV/VIS spectrophotometer U-2800 (Hitachi, Japan) and Benchtop electron spin resonance spectrometer (ESR) MiniScope MS300 (Magnettech, Berlin, Germany) were used for analyses. ^{1}H NMR experiments were carried out on a Bruker Avance Spectrometer (Bruker BioSpin GmbH, Rheinstetten, Germany) operating at 400 MHz (^{1}H) and using $CDCl_3$ as solvent and as internal standard.

## Sample synthesis and extraction

*Synthesis of SF 7 and SF 8.* A new two-step synthetic approach was designed for the synthesis of high purity SFs **7** and **8**. The first step was Steglich esterification using the protected tetrahydropyranyl ferulic acid and stigmasterol or cholesterol. The molecules obtained were the corresponding protected SF **7** and **8** derivatives, for which good yields (85%) were isolated. The second and final step was cleavage of the previous protected molecules, carried out in the presence of methanol and catalytic amounts of *p*-toluenesulfonic acid, yielding the target molecules with very good yields (>99%). Both molecules were analyzed by NMR and HPLC-MS to confirm high purity of the compounds synthesized according to the starting stigmasterol and cholesterol.

SF **7**: $^1$H NMR (400 Hz, CDCl$_3$, δ): 7.59 (1H, d, ArCH=, $J$ = 15.0 Hz), 7.05 (2H, m, Ar), 6.90 (1H, d, Ar, $J$ = 7.8 Hz), 6.27 (1H, d, OCOCH=, $J$ = 15.0 Hz), 5.83 (1H, s, OH), 5.40 (1H, t, CH=, $J$ = 6.3 Hz), 5.15 (1H, dd, CH=, $J$ = 15.2 Hz, $J$ = 8.5 Hz), 5.01 (1H, dd, CH=, $J$ = 15.1 Hz, $J$ = 8.5 Hz), 4.74 (1H, m, CHOCO), 3.92 (3H, s, OCH$_3$), 2.39 (2H, d, OCHCH2C=, $J$ = 3.1 Hz), 2.1-0.8 (38H, stigmasterol), 0.70 (3H, s, CH$_3$) ppm.

SF **8**: $^1$H NMR (400 Hz, CDCl$_3$, δ): 7.59 (1H, d, ArCH=, $J$ = 15.0 Hz), 7.05 (2H, m, Ar), 6.90 (1H, d, Ar, $J$ = 7.8 Hz), 6.27 (1H, d, OCOCH=, $J$ = 15.0 Hz), 5.85 (1H, s, OH), 5.40 (1H, t, CH=, $J$ = 6.3 Hz), 4.74 (1H, m, CHOCO), 3.92 (3H, s, OCH3), 2.39 (2H, d, OCHCH2C=, $J$ = 3.1 Hz), 2.1-0.8 (38H, cholesterol), 0.68 (3H, s, CH$_3$) ppm.

*Extraction and purification of SFs 2 - 6.* Extraction and purification of SFs **2-6** from ORY and wheat bran was performed by the method we previously designed and reported [15]. First, total lipids from wheat bran were extracted at 50 °C with acetone, then subjected to base-acid cleanup in order to eliminate neutral lipids. Subsequently, the residues from wheat bran and ORY were purified by preparative HPLC using a UV detector at 325 nm, and ACN-H$_2$O-butanol-acetic acid (88:6:4:2, v/v/v/v) as eluent, with a 6.6 mL·min$^{-1}$ flow rate at 25 °C. SF **2** was only collected from ORY. WB, SFs **3** and **4** were collected from the wheat bran. SFs **5** and **6** were collected from both ORY and wheat bran. Purity and quantification of SFs were also carried out with analytical

HPLC using a UV detector at 325 nm and an eluent mixture of ACN-$H_2O$-butanol-acetic acid (88:6:4:2, v/v/v/v); however the flow rate was 1 mL·min$^{-1}$ at 25°C. For quantification, SF **1**, the only commercially available SF standard, was used as an external standard.

Eight SFs in total were used in this study: SFs **1**, **2**, **3**, **4**, **5**, **6**, **7**, and **8**. The respective purities, reported as area percentage from the HPLC analysis were 99, 96, 95, 98, 98, 96, 99, and 97%, and the purity of the WB and ORY were 99 and 95%, respectively.

## DPPH radical scavenging activity measurement

The DPPH$^•$ scavenging activity method used in this study was modified from Nyström *et al.* [13]. The DPPH solution was freshly prepared in methanol and was brought to a concentration of 112 μM in the reaction system. The compounds **1-11**, ORY, and WB were also dissolved in methanol with final concentrations of 1.7, 16.7 and 60.0 μM, respectively, in the reaction system. Pyrogallol in methanol (final concentration 66 μM) was used as the positive control. After mixing the antioxidant and DPPH for 10 s, the absorbance at 517 nm was recorded immediately, and subsequently every 15 s for 5 min. Reaction kinetics were analyzed by fitting the absorbance *vs.* time curves with Origin 9.0.

## Hydroxyl radical scavenging activity measurement

The $^•$OH scavenging activity method used in this study was a modified version of the methods reported by Cheng *et al.* [16] and Faure *et al.*[17]. The $^•$OH radical was generated by the Fenton reaction and measured with the spin trapping technique by ESR. The solutions were added in the following order: 30 μL of 250 mM spin trap DMPO, 30 μL of 1.0 mM $H_2O_2$, 30 μL of 1.0 mM EDTA, 22.5 μL of $H_2O$, 7.5 μL antioxidants in ACN at various concentrations or ACN alone as control, and 30 μL of 1.0 mM $FeSO_4$ to initial the reaction. The solutions of DMPO, $H_2O_2$, EDTA, and $FeSO_4$ were prepared in Milli-Q water. The compounds **1-11**, ORY, and WB were each dissolved in ACN at

four concentrations - 0.03, 0.05, 0.1, and 0.3 mM -, thus leading to final concentrations of 1.5, 2.5, 5.0, and 15.0 μM in the respective reaction systems. An aliquot of the reaction mixture was loaded in a 50 μL micropipette and the ESR spectra were recorded. The ESR parameters were as follows: B0-field, 3350G; sweep width, 100 G; steps, 4096; sweep time, 30 s; number of passes; 2, modulation frequency, 1000 mG; microwave attenuation, 10 dB; and receiver gain, 900. TEMPO in $H_2O$ (2 μM) was used as a daily reference standard for the EPR instrument. The relative ESR signal was obtained by calculating the ratio of the peak-to-peak-amplitude of the second singlet in the ESR signal of DMPO adduct and the peak-to-peak-amplitude of the first singlet in the ESR signal of the TEMPO. The preparation and measurement were operated at room temperature. The percentage of radical scavenging activity was calculated by: $RSA\% = (h_0 - h_x)/h_0 \times 100$, where $h_0$ is the ESR signal in the control and $h_x$ is the relative ESR signal of the antioxidants.

## Superoxide anion radical scavenging activity measurement

The $O_2^{\bullet-}$ scavenging activity method applied was modified from Saint-Cricq de Gaulejac et al. [18] and Zhou et al. [19]. The $O_2^{\bullet-}$ was generated by the enzymatic hypoxanthine-xanthine oxidase (HPX-XOD) system. The molecular probe NBT reacted with $O_2^{\bullet-}$, forming formazan (NBTH$_2$), which could be detected at 560 nm. This method measures the ability of antioxidants to compete with NBT in scavenging $O_2^{\bullet-}$. In this method, 2 mM HPX, 0.56 U·mL$^{-1}$ XOD, and 0.34 mM NBT were prepared in 50 mM phosphate buffer (PBS) at pH 7.4. The blank solution contained 300 μL PBS, 200 μL NBT, and 500 μL HPX. The solutions required for the reaction were added in the following order: 200 μL NBT, 500 μL HPX, 50 μL PBS, 50 μL antioxidants in DMSO or DMSO alone for control, and 200 μL XOD to initiate the reaction. The compounds **1**-**11**, ORY, and WB were each dissolved in DMSO at concentrations of 0.8, 1.6, 3.2 mM, leading to 40, 80, 160 μM in the final systems, respectively. The absorbance at 560 nm was recorded every minute once the reaction started for a total of 7 min. Reaction kinetics were analyzed by fitting the absorbance vs. time curves with Origin 9.0.

## Simulation

Structures were drawn using HyperChem 8.0.3 software, and the semi-empirical quantum mechanics method Austin Model 1 (AM1), together with the Polak-Ribiere conjugate gradient algorithm with a root-mean-square (RMS) gradient of 0.05 kcal·$Å^{-1}$·$mol^{-1}$, was used for the geometrical optimization of the molecules. The spin pairing Restricted Hartree-Fock (RHF) operators were used for neutral species, while Unrestricted Hartree-Fock (UHF) operators were employed for radicals. The self-consistent field (SCF) convergence limit was set at $10^{-5}$, and the accelerate convergence procedure was used. The dipole moment and some quantitative structure-activity relationship (QSAR) parameters were obtained from the quantum mechanics simulations.

## Data analysis

Principle component analysis (PCA) was conducted with the Unscrambler X 10.1 (Oslo, Norway) to obtain a complete view of comparisons of individual SFs with their antioxidant activities, as well as molecular properties. The relationships of variables were also measured using Pearson's correlation coefficients with IBM SPSS Statistics 19.0 (Armonk, NY, USA).

# Results and discussion

## Scavenging effect on DPPH radical

DPPH$^\bullet$ scavenging measurement was carried out with antioxidants at concentrations of 1.67, 16.7, and 60.0 μM. The irreversible reaction is presented by equation (1). The decrease of the concentration of DPPH$^\bullet$ ([$DPPH^\bullet$]) over time can be written as shown in equation (2), following global second-order kinetics. In the reaction system, the concentrations of DPPH$^\bullet$ and product $DPPH_2$ can be determined from equations (3) and

(4) with a rate constant $k$, as well as initial concentrations of DPPH$^\bullet$ ($[DPPH^\bullet]_0$) and SF ($[SF]_0$). The kinetics parameters, $k$ value and plateau value (the absorption when $t \rightarrow \infty$), were obtained from curve-fitting of the absorbance *vs.* time plots (Table 1).

$$DPPH^\bullet + SF \xrightarrow{\ k\ } DPPH_2 + SF^\bullet \qquad (1)$$

$$-\frac{d[DPPH^\bullet]}{dt} = k[DPPH^\bullet][SF] \qquad (2)$$

$$[DPPH^\bullet] = [DPPH^\bullet]_0 \left( 1 - \frac{1 - e^{\left([DPPH^\bullet]_0 - [SF]_0\right)kt}}{1 - \dfrac{[DPPH^\bullet]_0}{[SF]_0} e^{\left([DPPH^\bullet]_0 - [SF]_0\right)kt}} \right) \qquad (3)$$

$$[DPPH_2] = [DPPH^\bullet]_0 \left( \frac{1 - e^{\left([DPPH^\bullet]_0 - [SF]_0\right)kt}}{1 - \dfrac{[DPPH^\bullet]_0}{[SF]_0} e^{\left([DPPH^\bullet]_0 - [SF]_0\right)kt}} \right) \qquad (4)$$

All of these antioxidants showed DPPH$^\bullet$ scavenging effect. Each antioxidant showed the same rate constant at different concentrations, confirming the kinetic order of the scavenging process. Rate constants of individual SFs decreased in the following order: SFs **3** and **4** $\geq$ SFs **5**, **6**, **7** and **8** $\geq$ SFs **1** and **2**. ORY, which contains mainly SFs **1** and **2**, had a low rate constant, but with high experimental error. Additionally, WB was found to show a higher rate constant than ORY, which was in agreement with the behavior of individual SFs. Furthermore, ferulates **10** and **11** had moderate and similar kinetics. However, compound **9**, the smallest molecule in this study, did not exhibit any advantage in the scavenging process. Moreover, the positive control molecule, pyrogallol, was observed to have a kinetic constant nearly 10-fold of that of the ferulates and compound **9**. Nevertheless, the differences in rate constants among ferulates and compound **9** in this reaction were very small.

**Table 1**. Kinetic parameters for the DPPH radical reaction.

| Compounds | $k$ ($\mu M^{-1} \cdot s^{-1}$) | Absorbance ($t \to \infty$) | | |
|:---:|:---:|:---:|:---:|:---:|
| | | 1.67 µM | 16.7 µM | 60 µM |
| 1 | 0.010 ± 0.004 | 1.301 ± 0.001 | 1.109 ± 0.003 | 0.72 ± 0.01 |
| 2 | 0.011 ± 0.002 | 1.283 ± 0.001 | 1.030 ± 0.004 | 0.82 ± 0.01 |
| 3 | 0.018 ± 0.004 | 1.198 ± 0.001 | 1.091 ± 0.005 | 0.79 ± 0.03 |
| 4 | 0.015 ± 0.002 | 1.156 ± 0.001 | 0.991 ± 0.004 | 0.64 ± 0.01 |
| 5 | 0.013 ± 0.002 | 1.273 ± 0.001 | 1.045 ± 0.004 | 0.70 ± 0.01 |
| 6 | 0.013 ± 0.001 | 1.298 ± 0.001 | 0.944 ± 0.004 | 0.64 ± 0.01 |
| 7 | 0.012 ± 0.002 | 1.144 ± 0.001 | 1.010 ± 0.004 | 0.72 ± 0.01 |
| 8 | 0.012 ± 0.002 | 1.245 ± 0.001 | 0.979 ± 0.005 | 0.74 ± 0.01 |
| 9 | 0.012 ± 0.001 | 1.232 ± 0.001 | 0.913 ± 0.005 | 0.53 ± 0.01 |
| 10 | 0.014 ± 0.002 | 1.008 ± 0.001 | 0.896 ± 0.005 | 0.57 ± 0.01 |
| 11 | 0.013 ± 0.002 | 0.992 ± 0.001 | 0.851 ± 0.003 | 0.58 ± 0.01 |
| ORY | 0.011 ± 0.006 | 1.246 ± 0.001 | 0.981 ± 0.003 | 0.69 ± 0.01 |
| WB | 0.014 ± 0.002 | 1.245 ± 0.001 | 0.992 ± 0.006 | 0.65 ± 0.01 |
| Pyrogallol | 0.12 ± 0.01 | | | |

Note: Data are expressed as mean ± experimental error (n=3-9).

The absorbance in the final state or plateau ($t \to \infty$; $A_\infty$) was also obtained from the curve-fitting. Moreover, the efficiency ($\varepsilon$) of each antioxidant on DPPH$^\bullet$ scavenging can be determined from:

$$\varepsilon_{DPPH} = \frac{A_{0(DPPH)} - A_{\infty(DPPH)}}{A_{0(DPPH)}[SF]_0}$$

(5)

where $A_{0(DPPH)}$ is the absorbance of DPPH$^\bullet$ solution without any antioxidant, $A_{\infty(DPPH)}$ is the absorbance in the presence of an antioxidant when the reaction is finished ($t \to \infty$). Generally, the efficiencies of ferulates, as well as compound **9**, decreased with increasing concentrations (Figure 2). This could be explained by the lower relative amount of DPPH$^\bullet$ per unit of antioxidant in treatments with higher concentrations of

antioxidant, based on the constant concentration of DPPH$^\bullet$. At the lowest antioxidant concentration of 1.67 µM, the differences in DPPH$^\bullet$ scavenging efficiency among these compounds were very clear. Ferulates **10** and **11** were observed to have the highest efficiency. This may be partially explained by the fast diffusion of such small molecules compared to the SFs, ($D = k_B T/6\pi\eta R$, where $k_B$ is the Boltzman constant, $T$ is the absolute temperature, $\eta$ is the viscosity of the medium, and $R$ is the radius of the solute molecule). Ferulates **10** and **11** have much smaller radii than SF molecules; hence they had higher diffusion coefficients ($D$) and exhibited higher reaction efficiencies. However, compound **9**, which also has the smallest radius of molecules studied, showed only a moderate efficiency, which could be explained by the strong solvent interaction between the polar protic solvent (methanol) and the carboxylic group of compound **9**, especially when compound **9** was at very low concentrations. Additionally, compound **9** tended to form non-covalent intermolecular interactions and dimerize via O−H$^{..}$O hydrogen bonds between carboxylic groups, which may further restrict its diffusion compared to the small ferulates. High efficiencies were demonstrated by SFs **7**, **3,** and **4,** as compared with other SFs; however, according to the results of the simulation studies, SFs **7**, **3,** and **4** did not have the smallest radii. We therefore infer that other factors in the reaction may contribute to this observation, for example inner or inter molecular interactions, or solvent iteration. When the concentration of antioxidant was increased to 16.7 and 60 µM, the differences in efficiencies among ferulates and compound **9** were less notable. Ferulates **10** and **11**, and compound **9**, showed slightly higher efficiencies than the SFs at 16.7 µM; nevertheless, all the compounds had the similar efficiencies at 60 µM. This suggests that when the concentration of antioxidant was very low, the number of effective collisions was greatly influenced by the solvent effect; meanwhile with higher concentrations of antioxidant, the effective collisions could mostly result from its high relative concentration.
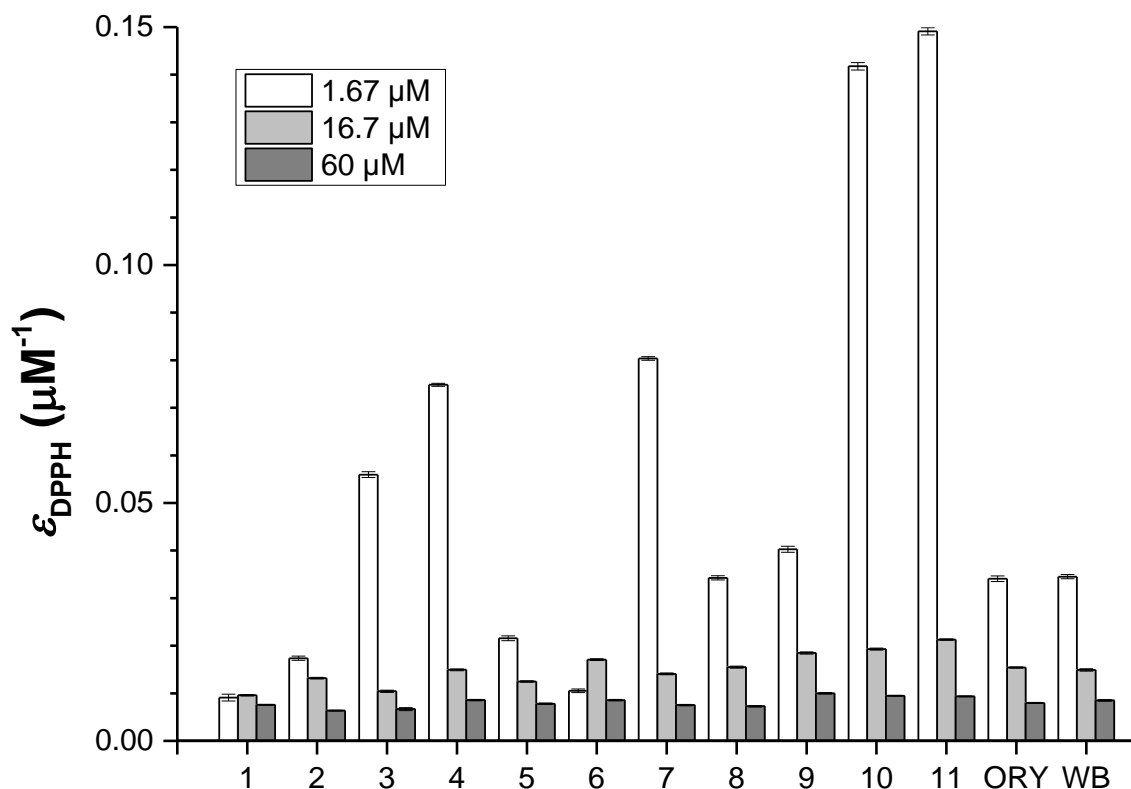
**Figure 2**. Efficiency of DPPH radical scavenging

The DPPH[•] scavenging activities of SFs have also been reported in previous studies. Akiyama *et al.* reported similar DPPH[•] scavenging activity for SFs **1**, **2**, **5**, **6,** and compound **9** (> 100 μM) [20]. Islam *et al.,* who used a comparable reaction system as ours, also found SFs **1**, **2**, **6,** and compound **9** had similar DPPH[•] scavenging activities [21]. In another study, Kikuzaki *et al.* reported that SF **1**, SF **2,** and ORY (20 μM) had the same DPPH[•] scavenging capacity, while compound **9** was slightly better than the SFs [22]. Moreover, compound **9** has also been reported to be a better DPPH[•] scavenger than SFs **6** and **8**, as well as the SF mixture from rye and wheat (17 μM) [13]. However, all of these studies only compared scavenging capacities after the reaction. As far as we know, ours is the first study to investigate reaction kinetics with DPPH[•], which provide more information of individual SFs as DPPH[•] scavengers.

**Scavenging of hydroxyl radical**

In our study, ˙OH scavenging capacity was determined using ESR with spin trap DMPO method. The ˙OH is very short-lived, and DMPO is commonly used to trap ˙OH as the DMPO-OH adduct has a half-life time of 12-156 min in neutral solutions [17]. Due to the limitation of solubility, the highest concentration of SF studied was 15.0 μM. Generally, all the compounds in this study scavenged the ˙OH dose-dependently (Table 2). At 1.5 μM, similar ˙OH scavenging capacities (19-25%) were observed among the antioxidants tested. At 2.5 μM, ferulate **10** (29%) was only slightly more effective than SF **1** and WB (21 and 22%, respectively), and other compounds did not differ from each other. While using a higher concentration of 5 μM, ferulates **10** and **11,** as well as SF **2** exhibited higher scavenging capacities (around 36%) than SF **1** (27%). Nevertheless, at the highest concentration of 15.0 μM, all the ferulates, as well as compound **9**, showed very similar activities (39-44%). In this study, compound **9**, which has a higher solubility than the ferulates, did not show any advantage in scavenging ˙OH. In this water environment (pH around 7.4), the carboxyl group of compound **9** could be deprotonated, leaving only the proton from the phenolic hydroxyl group available for ˙OH scavenging, which could explain why the stable, deprotonated form (carboxylate) may exhibit similar behaviour as other ferulates in this reaction system.

Islam *et al.* also reported SFs **1, 2,** and **6** (concentration of 40 μM, with 0.1% supporting solvent ethanol: DMSO 9:1) had similar ˙OH scavenging capacities, while compound **9** showed significantly higher activity than the SFs [21]. However, Juliano *et al.* reported that ORY (concentrations of 1.65 and 16.5 μM, with 1% ethanol) had no ˙OH scavenging activity, when measured by its inhibition of *p*-nitrosodimethylaniline-trapping of ˙OH [10]. Given the differences in the reaction systems, our data are not directly comparable with their findings. Generally, all the antioxidants in our study were found to have similar ˙OH scavenging abilities.

**Table 2**. Hydroxyl radical scavenging activity (*RSA*).

| Compounds | RSA (%) 1.5 μM | 2.5 μM | 5.0 μM | 15.0 μM |
|:---:|:---:|:---:|:---:|:---:|
| 1 | $23 \pm 2$ | $21 \pm 2$ | $27 \pm 5$ | $43 \pm 3$ |
| 2 | $19 \pm 3$ | $24 \pm 1$ | $36 \pm 3$ | $45 \pm 4$ |
| 3 | $23 \pm 2$ | $27 \pm 2$ | $34 \pm 2$ | $43 \pm 2$ |
| 4 | $22 \pm 3$ | $25 \pm 4$ | $28 \pm 2$ | $40 \pm 2$ |
| 5 | $21 \pm 3$ | $25 \pm 3$ | $29 \pm 2$ | $39 \pm 3$ |
| 6 | $20 \pm 3$ | $24 \pm 3$ | $31 \pm 2$ | $43 \pm 1$ |
| 7 | $23 \pm 4$ | $26 \pm 4$ | $30 \pm 1$ | $44 \pm 2$ |
| 8 | $24 \pm 3$ | $24 \pm 3$ | $30 \pm 3$ | $40 \pm 3$ |
| 9 | $23 \pm 3$ | $26 \pm 1$ | $33 \pm 3$ | $40 \pm 3$ |
| 10 | $19 \pm 5$ | $31 \pm 2$ | $36 \pm 1$ | $43 \pm 3$ |
| 11 | $19 \pm 6$ | $29 \pm 4$ | $36 \pm 3$ | $42 \pm 3$ |
| ORY | $25 \pm 1$ | $25 \pm 4$ | $31 \pm 3$ | $42 \pm 3$ |
| WB | $23 \pm 2$ | $22 \pm 1$ | $33 \pm 3$ | $43 \pm 1$ |

Note: Data are expressed as mean ± SD (n=3).

## Scavenging of superoxide anion radical

Scavenging of $O_2^{\bullet-}$ was investigated with antioxidants at 40, 80, and 160 μM. This method examined the ability of antioxidants to compete with the probe NBT in scavenging $O_2^{\bullet-}$. The irreversible reaction of NBT with $O_2^{\bullet-}$ in the system is described by equation (6). At the onset of the reaction, the concentration of $O_2^{\bullet-}$ ($[O_2^{\bullet-}]_0$) is much higher than that of NBT ($[NBT]_0$), then the decrease in the concentration of NBT ($[NBT]$) over time can be written, as shown in equation (7), as a pseudo-first-order kinetic process. Furthermore, the concentration of NBT and the corresponding product $NBTH_2$ can be determined from equations (8) and (9) with rate constant $k_1$ and $[NBT]_0$ as parameters. The reaction of SF with $O_2^{\bullet-}$ in the system has the same kinetics as NBT,

as shown in equations (10) through (13). The kinetic parameter, $k_1$ of reaction (equation 6) and the absorbance of $NBTH_2$ when the reaction is finished ($t \rightarrow \infty$; $A_\infty$), were also obtained from the curve-fitting experimental measurements (Table 3). The differences in $k_1$ and $A_\infty$ reflect the competitive ability of SFs in reacting $O_2^{\bullet-}$ with NBT.

$$2O_2^{\bullet-} + NBT \xrightarrow{\ k_1\ } 2O_2 + NBTH_2 \tag{6}$$
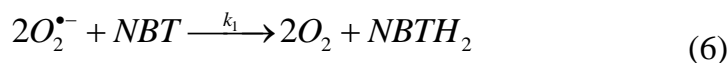
$$-\frac{d[NBT]}{dt} = k_1[O_2^{\bullet-}]^2[NBT] \approx k_1[NBT] \tag{7}$$

$$[NBT] = [NBT]_0 e^{-k_1 t} \tag{8}$$

$$[NBTH_2] = [NBT]_0 \left(1 - e^{-k_1 t}\right) \tag{9}$$
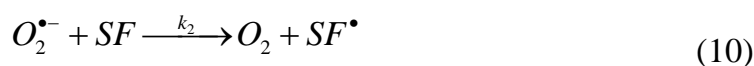
$$O_2^{\bullet-} + SF \xrightarrow{\ k_2\ } O_2 + SF^{\bullet} \tag{10}$$

$$-\frac{d[SF]}{dt} = k_2[O_2^{\bullet-}][SF] \approx k_2[SF] \tag{11}$$

$$[SF] = [SF]_0 e^{-k_2 t} \tag{12}$$

$$[SF^{\bullet}] = [SF]_0 \left(1 - e^{-k_2 t}\right) \tag{13}$$

As shown in Table 3, some of the rate constants of NBT were lower with higher concentrations of antioxidant (SFs **2**, **5**, **6**, **7**, **8**), suggesting these compounds interfere with NBT dose-dependently. The rate constant was dramatically lower (40%) in the presence of SFs **7** and **8** at concentrations of 80 and 160 μM. Meanwhile, for SFs **5** and **6**, significantly lower rate constants (30%) were only observed with the high concentration of 160 μM. Moreover, for SF **2**, the effect was gradual: 0, 30, and 45%, for the concentrations of 40, 80, and 160 μM, respectively. In the case of SF **1**, which has a similar structure as SF **2**, the rate was consistently low (30%) compared to the NBT reaction at all three concentrations. Furthermore, SFs **3** and **4** only demonstrated interference with the NBT reaction (by approximately 30%) at concentrations of 40 and 160 μM. On the other hand, for the SF mixtures, WB and ORY were only able to

**Table 3**. Kinetic parameters for superoxide anion radical reaction

| Compounds | $k_1$ (min$^{-1}$) | | | Absorbance ($t \to \infty$) | | |
|---|---|---|---|---|---|---|
| | 40 μM | 80 μM | 160 μM | 40 μM | 80 μM | 160 μM |
| 1 | 0.12 ± 0.01 | 0.14 ± 0.01 | 0.15 ± 0.01 | 1.8 ± 0.1 | 1.57 ± 0.06 | 1.48 ± 0.06 |
| 2 | 0.18 ± 0.01 | 0.13 ± 0.01 | 0.10 ± 0.01 | 1.68 ± 0.05 | 1.79 ± 0.09 | 1.80 ± 0.06 |
| 3 | 0.13 ± 0.03 | 0.19 ± 0.01 | 0.13 ± 0.01 | 1.89 ± 0.01 | 1.47 ± 0.03 | 1.57 ± 0.08 |
| 4 | 0.14 ± 0.02 | 0.21 ± 0.01 | 0.14 ± 0.01 | 1.85 ± 0.05 | 1.35 ± 0.02 | 1.47 ± 0.05 |
| 5 | 0.17 ± 0.01 | 0.18 ± 0.01 | 0.13 ± 0.01 | 1.65 ± 0.04 | 1.40 ± 0.03 | 1.19 ± 0.05 |
| 6 | 0.19 ± 0.01 | 0.19 ± 0.01 | 0.13 ± 0.01 | 1.64 ± 0.06 | 1.38 ± 0.04 | 1.16 ± 0.03 |
| 7 | 0.18 ± 0.01 | 0.11 ± 0.01 | 0.11 ± 0.01 | 1.68 ± 0.05 | 1.76 ± 0.07 | 1.78 ± 0.06 |
| 8 | 0.17 ± 0.01 | 0.11 ± 0.01 | 0.11 ± 0.01 | 1.76 ± 0.04 | 1.71 ± 0.08 | 1.82 ± 0.08 |
| 9 | 0.20 ± 0.01 | 0.14 ± 0.03 | 0.19 ± 0.02 | 1.27 ± 0.07 | 1.4 ± 0.2 | 1.03 ± 0.08 |
| 10 | 0.15 ± 0.01 | 0.15 ± 0.01 | 0.14 ± 0.02 | 1.90 ± 0.01 | 1.72 ± 0.06 | 1.6 ± 0.2 |
| 11 | 0.14 ± 0.01 | 0.16 ± 0.03 | 0.13 ± 0.02 | 1.90 ± 0.01 | 1.7 ± 0.1 | 1.6 ± 0.2 |
| ORY | 0.17 ± 0.01 | 0.15 ± 0.04 | 0.18 ± 0.01 | 1.60 ± 0.04 | 1.4 ± 0.2 | 1.33 ± 0.07 |
| WB | 0.21 ± 0.01 | 0.10 ± 0.01 | 0.20 ± 0.01 | 1.52 ± 0.03 | 1.75 ± 0.09 | 1.19 ± 0.02 |
| NBT alone | 0.188 ± 0.001 | | | 1.90 ± 0.01 | | |

Note: Data are expressed as mean ± experimental error (n=3).

interfere with NBT at a concentration of 80 μM, with approximately 45% reduction in the rate constant for WB, and 20% for ORY. Additionally, both ferulates **10** and **11** exhibited a 20% difference in rate constants from the NBT reaction for all tested concentrations. However, compound **9** only slightly interfered with the NBT reaction at 80 μM. Nevertheless, SFs were able to effectively compete with NBT-trapping of $O_2^{\bullet-}$. SFs **2**, **7,** and **8** appeared to have slightly higher competitive abilities than the other individual SFs, especially at the highest concentrations.

The absorbance of NBTH$_2$ when the reaction was completed ($t \rightarrow \infty$; $A_\infty$) was also obtained from curve-fitting (Table 3), to determine the amount of $O_2^{\bullet-}$ in the system. The efficiency ($\varepsilon$) of each antioxidant in reducing $O_2^{\bullet-}$ can be determined from equation (14):

$$\varepsilon_{O_2^{\bullet-}} = \frac{A_{0(NBTH_2)} - A_{\infty(NBTH_2)}}{A_{0(NBTH_2)}[SF]_0}$$

(14)

where $A_{0(NBTH2)}$ is the initial absorbance of NBTH$_2$ without the presence of antioxidant, and $A_{\infty(NBTH2)}$ is the absorbance of NBTH$_2$ after complete reaction with the antioxidant. The efficiencies of most of the antioxidants in this study were lower with higher concentrations (Figure 3). At 40 μM level, the differences in efficiency were very clear among these compounds. Compound **9**, which is the most water-soluble antioxidant at pH 7.4, was found to have the highest efficiency. Among the SFs, the SF mixture WB was the most effective, followed by ORY. SFs **2**, **5**, **6**, and **7** showed the similar efficiency and were slightly more effective than SF **1** and **8**. Furthermore, the weakest SFs were found to be SFs **3** and **4**. However, ferulates **10** and **11**, which consistently decreased the rate constant of NBT by 20%, cannot scavenge the $O_2^{\bullet-}$ at this concentration. From this, we deduce that ferulates could be considered as amphiphile molecules due to the hydrophilic (phenolic hydroxyl group) and lipophilic (methyl, ethyl or sterol moiety) characteristics, and therefore self-assembly may occur in this environment. Their different potentials to aggregate in the water/solvent mixture may induce their different efficiencies on radical scavenging. When applying a higher concentration of 80 μM, all the antioxidants showed $O_2^{\bullet-}$ scavenging activity.

Compound **9**, ORY, and SFs **3 - 6**, were observed to have similar efficiency, and were slightly more effective than the other compounds. Moreover, ferulates **10** and **11** showed relatively low efficiency at scavenging $O_2^{\bullet-}$. At the concentration of 160 μM, the highest efficiency was still obtained with Compound **9**, followed by SFs **5** and **6**, ORY, and WB. Overall, among all individual SFs, SFs **5** and **6** generally showed the highest efficiency to scavenge $O_2^{\bullet-}$ at all tested concentrations.
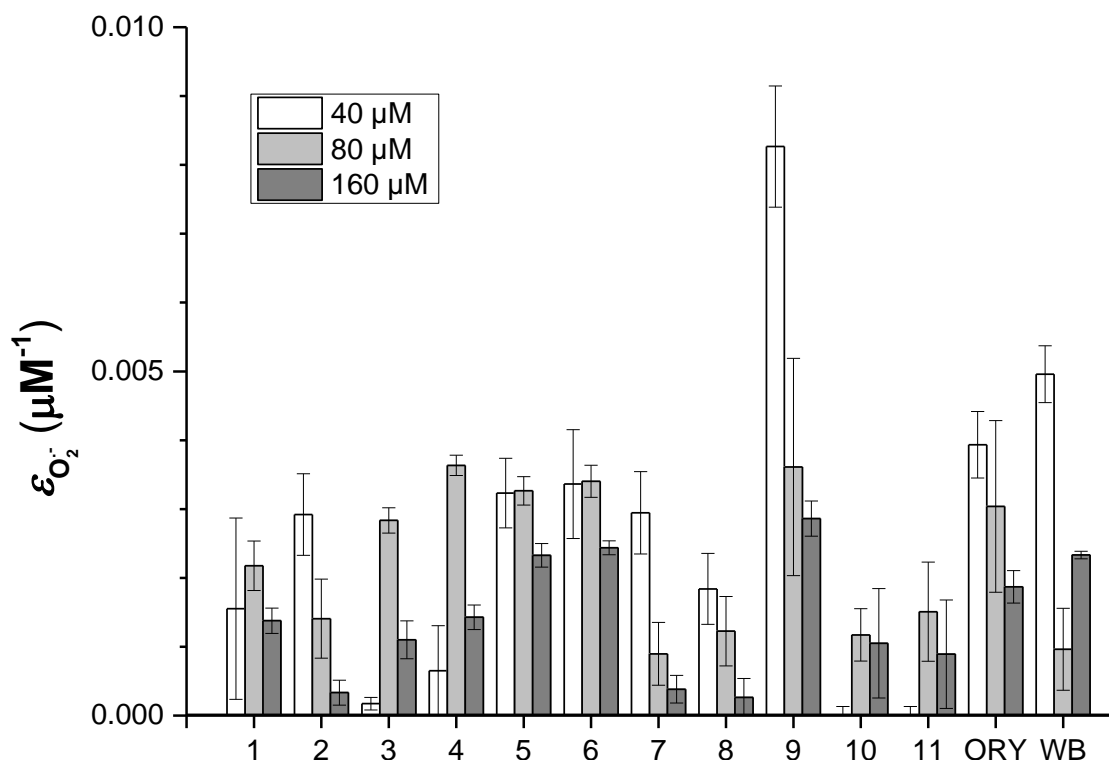


**Figure 3**. Efficiency of superoxide anion radical scavenging

However, the $O_2^{\bullet-}$ scavenging effect of SFs was not observed by Juliano *et al.* [10]. They reported that ORY at the concentration of 10 μM had no scavenging activity in a system where $O_2^{\bullet-}$ was produced by spontaneous autoxidation of $FeCl_2$ in morpholinepropanesulphonic acid buffer. Recently, Saenjum *et al.* reported that ORY showed $O_2^{\bullet-}$ scavenging effect ($IC_{50}$ 30 μM) in a phenazine methosulfate-β-nicotinamide adenine dinucleotide system [11]. Due to the different radical-generating systems and concentrations of antioxidants employed, our data are not directly

comparable with their findings. To the best of our knowledge, this is the first study to investigate and compare the $O_2^{\bullet-}$ scavenging activity of individual SFs.

## Simulation and correlation analysis

We performed molecular simulations to explain the differences in antioxidant activity from the point of view of the SF's molecular properties. The dipole moment and quantitative structure-activity relationship parameters, *i.e.*, log*P*, surface area, volume, solvation energy, were obtained from the quantum mechanics simulations (Table 4). Among the individual SFs, SF **8** was found to have the smallest volume, as well as for the log*P* value; while SF **2** had the highest dipole moment and solvation energy. Generally, the differences between SFs with respect to these parameters were very small.

The grouping of SFs was performed by PCA with variables of their antioxidant activities and molecular properties (Figure 4). The overview of SFs **1**-**8**, as well as all the variables, is presented in a Bi-plot (Figure 4A). PC1 and PC2 explained 94% and 4% (in total 98%) of the variance. Considering the PCA scores (Figure 4B), three groups could be proposed, namely, SFs **1** and **2**, SFs **4**, **6** and **7**, SFs **3** and **5,** and SF **8**. Correlation loadings (Figure 4C) showed that the molecular properties, except for solvation energy, had a position at the right side of PC1, close to the 100% explained variance circle, indicating that these variables greatly contribute to the SF groupings. However, the variables related to the SF's antioxidant activities were located near the inner ellipse (less than 50% of explained variance), indicating these variables had little influence. Nevertheless, the variable of solvation energy was very close to the position of antioxidant activity, suggesting they are somehow correlated.

**Table 4.** Molecular properties from molecular simulations

| Compounds | Connolly surface area ($\text{Å}^2$) | Connolly volume ($\text{Å}^3$) | Solvation energy ($\text{kcal·mol}^{-1}$) | log$P$ | Polarizability ($\text{Å}^3$) | Dipole Moment (D) | Molar Mass (Da) |
|---|---|---|---|---|---|---|---|
| 1 | 928 | 1734 | -4.31 | 7.72 | 71 | 3.55 | 602.9 |
| 2 | 943 | 1776 | -4.60 | 8.09 | 72 | 3.72 | 616.9 |
| 3 | 914 | 1705 | -3.92 | 7.61 | 68 | 3.55 | 578.9 |
| 4 | 939 | 1754 | -3.72 | 8.01 | 70 | 3.52 | 592.9 |
| 5 | 924 | 1706 | -4.15 | 7.17 | 68 | 3.51 | 576.9 |
| 6 | 945 | 1748 | -3.98 | 7.57 | 70 | 3.49 | 590.9 |
| 7 | 942 | 1745 | -4.35 | 7.31 | 69 | 3.45 | 588.9 |
| 8 | 919 | 1672 | -4.28 | 6.84 | 66 | 3.49 | 562.8 |
| 9 | 379 | 591 | -14.1 | -0.63 | 20 | 4.07 | 194.2 |
| 10 | 414 | 652 | -8.77 | -0.60 | 21 | 3.74 | 208.2 |
| 11 | 450 | 709 | -8.03 | -0.25 | 23 | 3.73 | 222.2 |

(A)

### Bi-plot



(B)
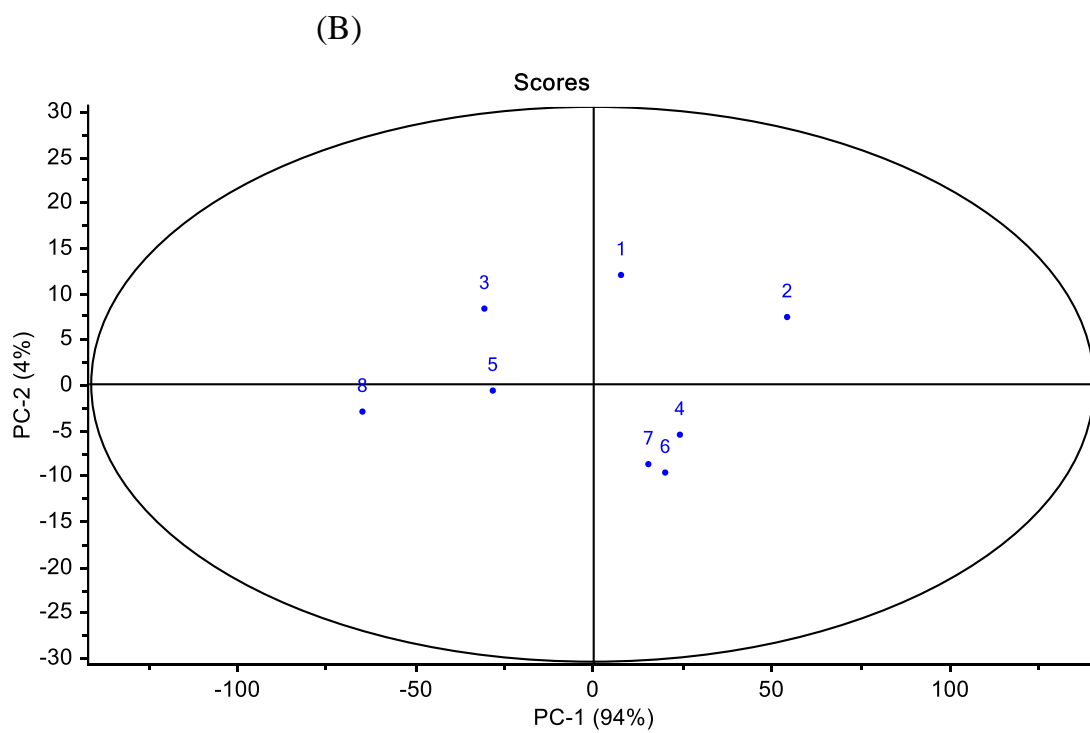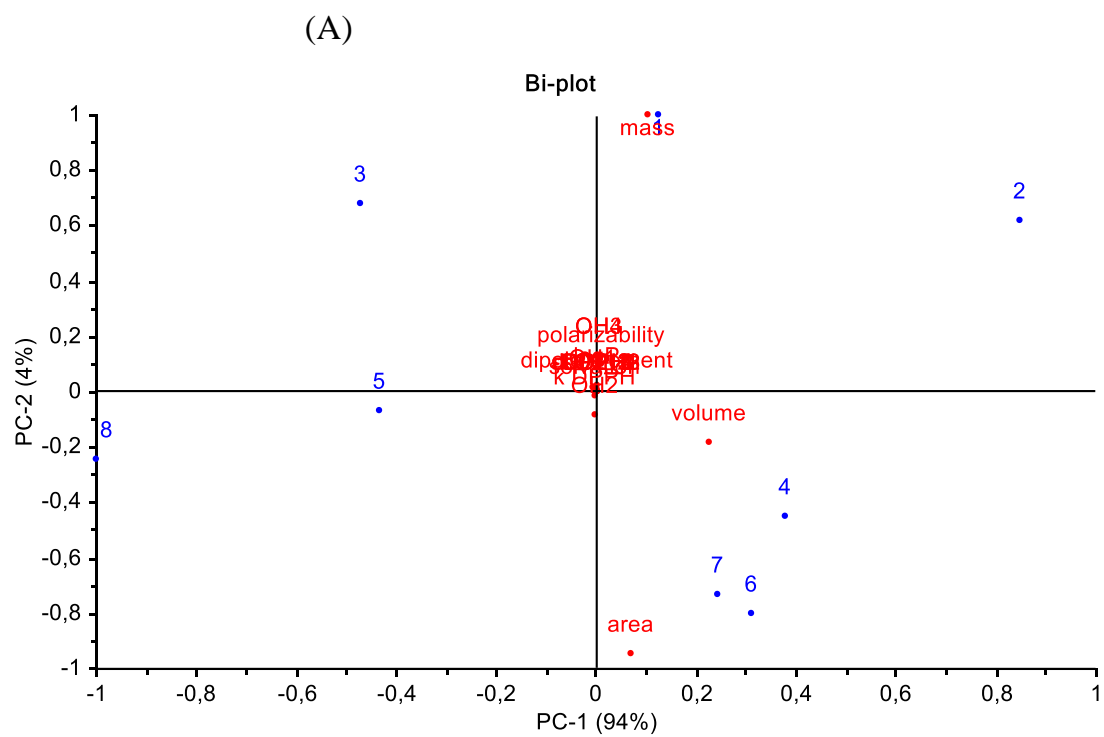
### Scores

(C)
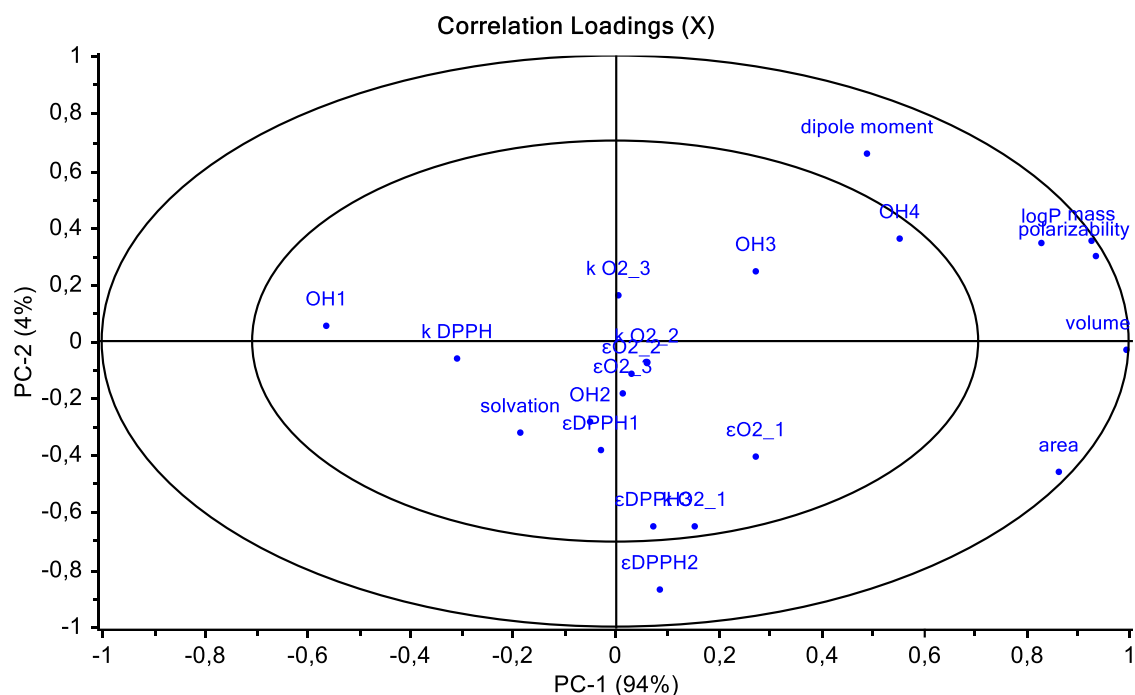


**Figure 4**. Principal component analysis (PCA) of antioxidant activity and molecular properties for the individual SFs (**1**-**8**). (A) Bi-plot. (B) Scores plot of SFs with Hotelling $T^2$ ellipse at 5 % of confidence. (C) Loadings plot of the variables: (a) antioxidant properties: $k_{DPPH}$; $\varepsilon_{DPPH}$ at 1.67, 16.7, and 60 μM (εDPPH1, εDPPH2, and εDPPH3, respectively); $k_{O2\cdot-}$ at 40, 80, and 160 μM (k O2_1, k O2_2, and k O2_3, respectively); $\varepsilon_{O2\cdot-}$ at 40, 80, and 160 μM (εO2_1, εO2_2, and εO2_3, respectively); ˙OH scavenging activity at 1.5, 2.5, 5.0, and 15.0 μM (OH1, OH2, OH3, and OH4, respectively); (b) molecular properties: area, volume, polarizability, dipole moment, solvation, log$P$, and molar mass).

Pearson's correlation was performed to support the correlation loadings of PCA. Examining all the correlations between antioxidant activities and molecular properties of the eight SFs, led us to propose that solvation energy was more likely to influence antioxidant activity (Figure 5); and the trend was that the higher the solvation energy, the better the antioxidant activity. Higher solvation energy led to less solvated SF (with two O−H··O hydrogen bonds between the phenolic hydroxyl group of SF and two water/methanol molecules). Furthermore, SF species  were available to react with

111
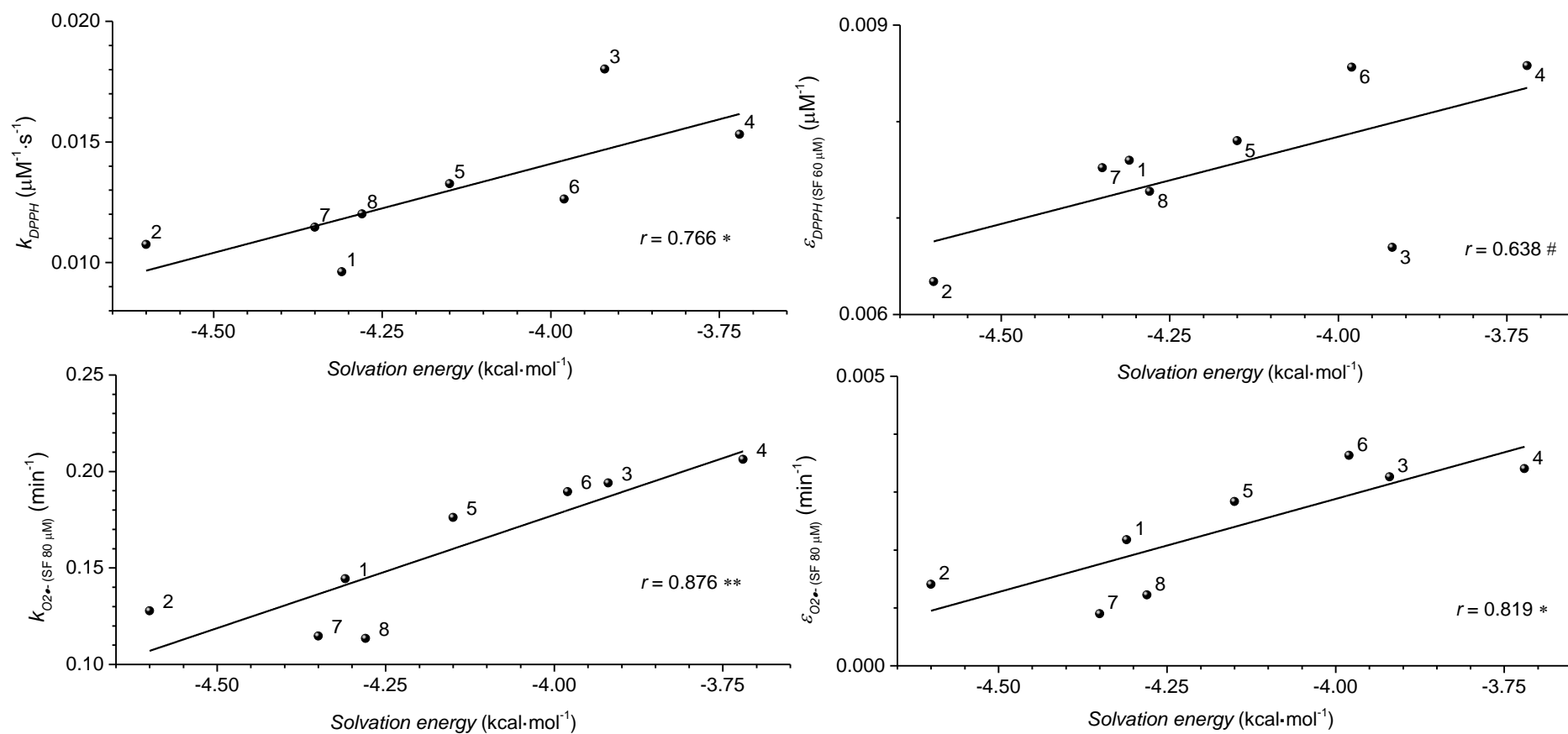
**Figure 5**. The linear correlation among antioxidant activities (*y*-axis) and solvation energy (*x*-axis) of individual SFs (**1-8**) based on Pearson's correlation coefficients (*r*). The symbol *: The correlation is significant at the 0.05 level (2-tailed); **: significant at the 0.01 level (2-tailed); #: significant at the 0.05 level (1-tailed).

radicals in the system. With respect to molecular properties, solvation energy was only identified as a significantly correlated parameter to the scavenging properties in some observations.

Previous studies also reported that different SFs, as well as compound **9**, vary in antioxidant activity. SFs were observed to show less antioxidant activity than compound **9** in some models, *e.g.*, scavenging DPPH$^\bullet$ [13, 22] or ABTS$^{\bullet+}$ [23], which was primarily explained by solubility or steric hindrance. However, SFs were also found to be better antioxidants than compound **9** in scavenging oxygen radical and in cooked meat systems [24]. In some studies, 4-desmethylsteryl ferulates were observed to be better antioxidants than 4,4-dimethylsteryl ferulates in DPPH$^\bullet$ [13] and oil models [13, 23, 25], for which it was suggested to be a relic of the negative effects from the dimethyl groups at C4 as well the cyclopropyl ring as the C9/C19. Moreover, saturated 4-desmethylsteryl ferulates were observed to have slightly higher antioxidant activity during frying than those with a double bond at C5/C6 [23]. Nevertheless, some observations also showed similar antioxidant activity for individual SFs in DPPH [20, 21]. In this study, generally, the difference in antioxidant activity of individual SFs was very small and depended greatly on the reaction models. In addition to the inner-molecular variations, the intermolecular interactions, as well as interactions with the solvent (environment), should also be considered. Thus, the same SF compound might show different scavenging properties depending on the substrate studied, as well as the kind of radical scavenging process taking place. Therefore, the antioxidant activity of SFs should be reconsidered based on the reaction occurring, and with respect to the food product to be studied, along with other synergistic processes that might happen in natural settings.

## Acknowledgement

# References

1.      Seitz, L. M. Stanol and sterol esters of ferulic and p-coumaric acids in wheat, corn, rye, and triticale. *J. Agric. Food Chem.* **1989**, *37*, 662-667.

2.      Ghatak, S. B.; Panchal, S. J. Gamma-oryzanol-A multi-purpose steryl ferulate. *Curr. Nutr. Food Sci.* **2011**, *7*, 10-20.

3.      Bergman, C. J.; Xu, Z. Genotype and environment effects on tocopherol, tocotrienol, and γ-oryzanol contents of southern U.S. rice. *Cereal Chem.* **2003**, *80*, 446-449.

4.      Mandak, E.; Nyström, L. The effect of in vitro digestion on steryl ferulates from rice (Oryza sativa L.) and other grains. *J. Agric. Food Chem.* **2012**, *60*, 6123-6130.

5.      Nyström, L. Analysis Methods of Phytosterols. In *Analysis of Antioxidant-Rich Phytochemicals*, edition no. 1; Xu, Z.; Howard, L. R., Eds.; Wiley-Blackwell: Oxford, UK, 2012; pp 313-351.

6.      Norton, R. A. Isolation and identification of steryl cinnamic acid derivatives from corn bran. *Cereal Chem.* **1994**, *71*, 111-117.

7.      Graf, E. Antioxidant potential of ferulic acid. *Free Radic. Biol. Med.* **1992**, *13*, 435-448.

8.      Kochhar, S. P. Stabilisation of frying oils with natural antioxidative components. *Eur. J. Lipid Sci. Technol.* **2000**, *102*, 552-559.

9.      Kim, J. S.; Suh, M. H.; Yang, C. B.; Lee, H. G. Effect of γ-oryzanol on the flavor and oxidative stability of refrigerated cooked beef. *J. Food Sci.* **2003**, *68*, 2423-2429.

10.     Juliano, C.; Cossu, M.; Alamanni, M. C.; Piu, L. Antioxidant activity of gamma-oryzanol: mechanism of action and its effect on oxidative stability of pharmaceutical oils. *Int. J. Pharm.* **2005**, *299*, 146-154.

11.     Saenjum, C.; Chaiyasut, C.; Chansakaow, S.; Suttajit, M.; Sirithunyalug, B. Antioxidant and anti-inflammatory activities of gamma-oryzanol rich extracts from Thai purple rice bran. *J. Med. Plants Res.* **2012**, *6*, 1070-1077.

12.     Xu, Z.; Hua, N.; Godber, J. S. Antioxidant activity of tocopherols, tocotrienols, and γ-oryzanol components from rice bran against cholesterol oxidation accelerated by 2,2'-azobis(2-methylpropionamidine) dihydrochloride. *J. Agric. Food Chem.* **2001**, *49*, 2077-2081.

13.     Nyström, L.; Mäkinen, M.; Lampi, A. M.; Piironen, V. Antioxidant activity of steryl ferulate extracts from rye and wheat bran. *J. Agric. Food Chem.* **2005**, *53*, 2503-2510.

14.     Huang, C.J. Potential functionality and digestibility of oryzanol as determined using in vitro cell culture models. PhD Thesis, Louisiana State University, 2003.

15.     Mandak, E.; Zhu, D.; Godany, T. A.; Nyström, L. Fourier transform infrared spectroscopy and Raman spectroscopy as tools for identification of steryl ferulates. *J. Agric. Food Chem.* **2013**, *61*, 2446-2452.

16.     Cheng, Z.; Zhou, H.; Yin, J.; Yu, L. Electron spin resonance estimation of hydroxyl radical scavenging capacity for lipophilic antioxidants. *J. Agric. Food Chem.* **2007**, *55*, 3325-3333.

17.     Faure, A. M.; Andersen, M. L.; Nyström, L. Ascorbic acid induced degradation of beta-glucan: Hydroxyl radicals as intermediates studied by spin trapping and electron spin resonance spectroscopy. *Carbohydr. Polym.* **2012**, *87*, 2160-2168.

18.     Saint-Cricq De Gaulejac, N.; Provost, C.; Vivas, N. Comparative study of polyphenol scavenging activities assessed by different methods. *J. Agric. Food Chem.* **1999**, *47*, 425-431.

19.     Zhou, K.; Su, L.; Yu, L. L. Phytochemicals and antioxidant properties in wheat bran. *J. Agric. Food Chem.* **2004**, *52*, 6108-6114.

20.     Akiyama, Y.; Hori, K.; Hata, K.; Kawane, M.; Kawamura, Y.; Yoshiki, Y.; Okubo, K. Screening of chemiluminescence constituents of cereals and DPPH radical scavenging activity of γ-oryzanol. *Luminescence* **2001**, *16*, 237-241.

21.     Islam, M. S.; Yoshida, H.; Matsuki, N.; Ono, K.; Nagasaka, R.; Ushio, H.; Guo, Y.; Hiramatsu, T.; Hosoya, T.; Murata, T.; Hori, M.; Ozaki, H. Antioxidant, free

radical-scavenging, and NF-kappaB-inhibitory activities of phytosteryl ferulates: structure-activity studies. *J. Pharmacol. Sci.* **2009**, *111*, 328-337.

22.    Kikuzaki, H.; Hisamoto, M.; Hirose, K.; Akiyama, K.; Taniguchi, H. Antioxidant properties of ferulic acid and its related compounds. *J. Agric. Food Chem.* **2002**, *50*, 2161-2168.

23.    Winkler-Moser, J. K.; Hwang, H. S.; Bakota, E. L.; Palmquist, D. A. Synthesis of steryl ferulates with various sterol structures and comparison of their antioxidant activity. *Food Chem.* **2015**, *169*, 92-101.

24.    Tan, Z.; Shahidi, F. Chemoenzymatic synthesis of phytosteryl ferulates and evaluation of their antioxidant activity. *J. Agric. Food Chem.* **2011**, *59*, 12375-12383.

25.    Wang, T.; Hicks, K.; Moreau, R. Antioxidant activity of phytosterols, oryzanol, and other phytosterol conjugates. *J. Amer. Oil Chem. Soc.* **2002**, *79*, 1201-1206.

# Effect of Steryl Ferulates on the Kinetics of Methyl Linoleate Autoxidation

Dan Zhu, Eleni Dimitriadou, Laura Nyström. *To be published after additional studies*.

## Abstract

Steryl ferulates are various plant sterols esterified with ferulic acid, belonging to the bioactive lipids that contribute to the health promoting effects of whole grains. This study investigated the effect of steryl ferulates on the kinetics of methyl linoleate autoxidation, by measuring the consumption rate of oxygen in peroxidating methyl linoleate in the presence and absence of different steryl ferulates by electron spin resonance (ESR) spectroscopy. In contrast to α-tocopherol, no induction period was observed for steryl ferulate, even if steryl ferulates were also able to retard the lipid peroxidation. In the applied experimental conditions, In the applied experimental condition, the rate constant for hydrogen-atom transfer from steryl ferulate (specifically cycloartenyl ferulate) to lipid peroxyl radical was determined to be $(1.24 \pm 0.52) \times 10^3$ $M^{-1}$ $s^{-1}$. Furthermore, individual steryl ferulates were also evaluated to investigate the structural influence on the antioxidant effect. However, no significant difference in antioxidant activity was observed among them in the applied reaction system.

## Keywords

Antioxidant activity/ ESR spectroscopy/ Lipid autoxidation/ γ-oryzanol/ Steryl ferulate.

## Abbreviations

AIBN: 2,2′-Azobis(2-methylpropionitrile); ESR: electron spin resonance spectroscopy; TEMPO: 2,2,6,6-tetramethyl-1-piperidinyloxy.

# 1. Introduction

Steryl ferulates are various plant sterols esterified with ferulic acid (Figure 1) that are present in various cereal grains and other seeds [1]. They belong to bioactive lipids contributing to the health promoting effects of whole grains. Steryl ferulates have been shown to possess antioxidant activity and plasma cholesterol lowering effect [2]. Owing to the antioxidant activity, steryl ferulates also show anti-inflammatory, anti-cancer and anti-virus activities [3].

Steryl ferulates exhibit antioxidant activity in many biological systems. There is also some evidence that individual steryl ferulates may vary in their antioxidant activity. For instance, for scavenging DPPH radical, steryl ferulates mixture extracted from rye was effective than the one extracted from wheat, whereas cholesteryl ferulate and sitosteryl ferulate showed similar scavenging effect [4]. In some studies, 4-desmethylsteryl ferulates were observed to be better antioxidants than 4,4'-dimethylsteryl ferulates in an oil model [5, 6]. For the 4,4'-dimethylsteryl ferulates the lower antioxidant activity was suggested to be a relic of the negative effects from the dimethyl groups at C4 as well the cyclopropyl ring as the C9/C19. However, contrary findings suggesting higher antioxidant efficacy of 4,4'-dimethylsteryl ferulates were also reported by Huang in cell model [7] and Xu *et al*. in cholesterol oxidation model [8]. The order of antioxidant activity of different steryl ferulate varies in different systems and the relationship of structure and activity is not fully understood.

To evaluate the antioxidant ability of compounds, their reactivity as H-atom donors toward the peroxyl radicals, which are the chain-carrying species in the autoxidation of lipids, must be evaluated [9]. The autoxidation can be studied either by examining the loss of substrates or the formation of oxidation products (hydroperoxides or their decomposition compounds, conjugated dienes in the case of lipid peroxidation, *etc*.) [10]. Yagi and Ohisi reported that the antioxidant activity decreased from campesteryl ferulate > 24-methylenecycloartanyl ferulate > cycloartenyl ferulate in inhibiting the
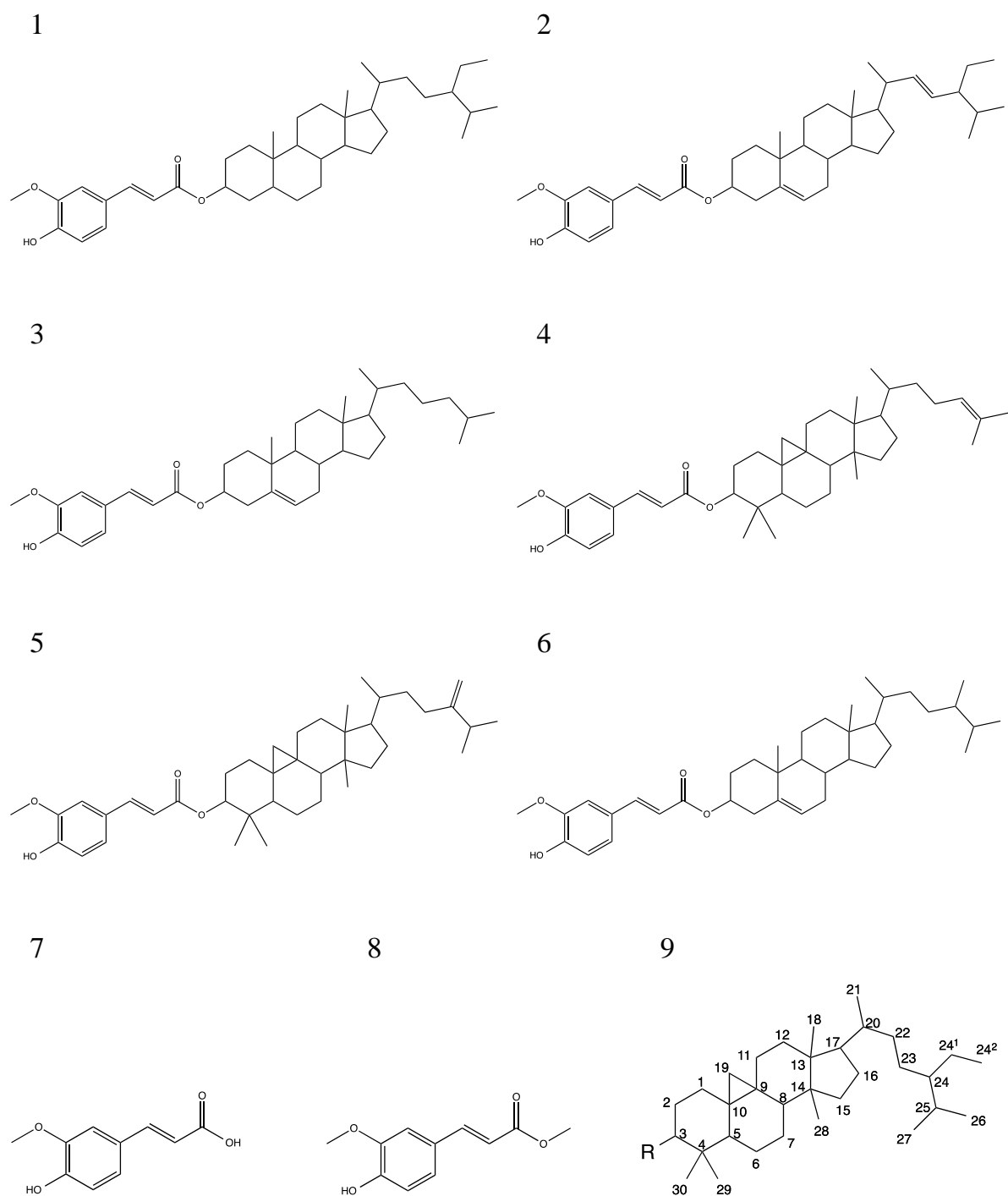
**Figure 1**. Molecular structures of steryl ferulates: sitostanyl ferulate (1); stigmasteryl ferulate (2); cholesteryl ferulate (3); main components of γ-oryzanol: cycloartenyl ferulate (4), 24-methylenecholesteryl ferulate (5) and campesteryl ferulate (6); ferulic acid (7), methyl ferulate (8). A general sterol skeleton (9) was numbered according to IUPAC-IUB 1989.

oxidation of linoleic acid induced by UV irradiation by estimating diene formation at 233 nm [11], whereas Xu and Godber observed that these three steryl ferulates had the same antioxidant effect in autoxidation of linoleic acid by monitoring the formation of hydroperoxide with HPLC [12]. Recently, Winkler-Moser and co-workers reported that the steryl ferulate with saturated sterol group was a better antioxidant than the one with double bond at C5 position in frying oil by determining the formation of PTAGs (one of the major products of oil oxidation, triacylglycerol polymers) with HPLC and the double bond loss in fatty acids with NMR [5]. The formation of lipid oxidation products is often difficult to determine since the products are complicated mixtures and may decompose easily. The consumption of oxygen is on the other hand a comprehensive indicator of lipid oxidation [10] and is well applicable also for kinetic studies.

The aim of this study is to investigate the effect of steryl ferulates on the kinetics of methyl linoleate autoxidation, by measuring the consumption rate of oxygen in peroxidating methyl linoleate in the presence and absence of different steryl ferulates in the hydrogen-bond-accepting ("water-like") solvent *tert*-butanol. The autoxidation of methyl linoleate was started by an azo initiator, 2,2′-Azobis(2-methylpropionitrile) (AIBN). The oxygen concentration in the reaction system was investigated by electron spin resonance (ESR) spectroscopy with the oxygen probe 2,2,6,6-tetramethyl-1-piperidinyloxy (TEMPO). The antioxidant effects of cycloartenyl ferulate, stigmasteryl ferulate, cholesteryl ferulate, sitostanyl ferulate as well as the steryl ferulates mixture from rice (γ-oryzanol) were evaluated. For comparison, ferulic acid and methyl ferulate were also analyzed in this study. As far as we know, this work is the first to study the kinetics and antioxidant mechanism of steryl ferulates in lipid autoxidation by means of oxygen consumption.

## 2. Materials and Methods

### 2.1. Materials

2,2′-Azobis(2-methylpropionitrile) (AIBN; 98%), *trans*-ferulic acid (≥ 99%), *tert*-butanol (≥ 99.5%), 2,2,6,6-tetramethyl-1-piperidinyloxy (TEMPO; ≥ 99%) and α-tocopherol (≥ 96%) were purchased from Sigma Aldrich (Buchs, Switzerland). Methyl linoleate (99%) was bought from NuChek Prep (Elysian, MN, USA). Methyl ferulate (99%) was from Alfa Aesar (Ward Hill, MA, USA). γ-oryzanol (≥ 95% purity) was obtained from CTC Organics (Atlanta, GA, USA). Cycloartenyl ferulate (≥ 99%) was purchased from Wako (Osaka, Japan).

Stigmasteryl ferulate (99%) and cholesteryl ferulate (97%) were synthesized by Dr. Antoni Sánchez-Ferrer (Laboratory of Food and Soft Materials, ETH Zurich, Switzerland) as reported in an earlier study (Zhu et al. manuscript submitted for publication). Sitostanyl ferulate (98%) was extracted and purified from wheat bran according to a method previously described [13].

## 2.2. Oxygen consumption measurement

The measurement of oxygen consumption rate was according previous studies [9, 14]. All the solutions were prepared in *tert*-butanol. The autoxidation of 0.242 M methyl linoleate was initiated by the thermal decomposition of 0.034 M AIBN at 50 °C with 35 µM TEMPO as oxygen spin probe. The measurements were conducted both in the absence (blank) and presence of different antioxidants. The reference antioxidant α-tocopherol was analyzed at a final concentration of 80 µM in the reaction system. For the evaluation of the inhibition rate constant, cycloartenyl ferulate was investigated as model compound of steryl ferulate, with final concentrations of 140, 280, 350, 420, 490 and 560 µM. For the comparison of the antioxidant effects of various ferulates, methyl ferulate, stigmasteryl ferulate, cholesteryl ferulate, sitostanyl ferulate, γ-oryzanol and ferulic acid, were also conducted in reaction system with final concentrations of 280, 420 and 560 µM.

The reaction mixture was first saturated with air at room temperature and then 110 µL of the solution was transfered in a 200 µL micropipette (Brand GMBH, Wertheim,

Germany). A second micropipette (50 µL, Brand GMBH, Wertheim, Germany) with smaller diameter and sealed at one end, was introduced into the sample tube (200 µL) to leave very little dead volume space. Parafilm was used to close the system. Then the tube was inserted in the cavity of ESR (kept at 50 °C throughout the measurement). The first spectrum was recorded after 1 min to allow the temperature equilibration time. The peak-to-peak-amplitude of the first singlet in the ESR signal of the TEMPO was used for the calculations. The parameters of ESR were set as follows: B0-field, 3350 G; sweep width, 100 G; steps, 4096; sweep time, 30 s; number of passes 2; modulation frequency, 1000 mG; microwave attenuation, 10 dB; and receiver gain, 90. All analyses were carried out in triplicate.

## 2.3 Calculation of inhibition rate constant of steryl ferulate

The inhibition rate constant of steryl ferulate was determined by a method from Darley-Usmar et al. [15]. This method is based on determination of the ratio of $(-d[O_2]/dt)_{inh}$ (the rate of oxygen consumption in lipid autoxidation inhibited by different concentrations of the antioxidant steryl ferulate $[SF]$) and $(-d[O_2]/dt)_{ox}$ (the rate of oxygen consumption in autoxidation without antioxidant) with constant concentration of methyl linoleate ($[RH]$) and initiation rate of lipid autoxidation $R_i$:

$$\frac{(-d[O_2]/dt)_{inh}}{(-d[O_2]/dt)_{ox}} = 1 - \beta\left\{(k_{SF}[SF]+1) - \sqrt{(k_{SF}^2[SF]^2+1)}\right\}$$

(1)

where

$$\beta = \frac{k_p[RH]}{\sqrt{2k_t R_i} + k_p[RH]}$$

(2)

$$\text{and } k_{SF} = \frac{k_{inh}}{\sqrt{2k_t R_i}}$$

(3)

The composite rate constant $k_{SF}$ contains the information of rate constant ($k_{inh}$) of inhibiting the autoxidation of methyl linoleate by steryl ferulate. $k_p$ and $k_t$ are the rate

constants of propagation reaction (in supporting info, reaction S3) and termination reaction (in supporting info, reaction S4) of lipid autoxidation, respectively. The $k_t$ value is estimated from literature as $8.5 \times 10^6 \, \text{M}^{-1} \, \text{s}^{-1}$ [16]. Since the decomposition of AIBN is temperature-dependent and the reaction system is maintained at 50°C, the rate of initiation of lipid autoxidation $R_i$ is constant. $R_i$ is determined from the reference antioxidant α-tocopherol, according to the formula with its concentration, stoichiometric factor $n$ and induction period $\tau$ [9, 17]:

$$R_i = n \frac{[\alpha TOH]}{\tau} \qquad (4)$$

## 2.4. Data analysis

Nonparametric test with Kruskal-Wallis analysis of variance and subsequent post-hoc analysis (pairwise comparisons) was performed with IBM SPSS Statistics 19.0 (IBM Corp., Armonk, NY, USA) in order to determine significant differences between samples. The differences were considered significant for $p$ value $< 0.05$.

# 3. Results and discussion

## 3.1. Reaction mechanism

This oximetry for lipid autoxidation studies by ESR was introduced by Cipollone *et al.* [18] and Pedulli *et al.* [10], and was applied in this study to evaluate the kinetics of methyl linoleate autoxidation in the presence of steryl ferulates. In the oxidation system applied, oxygen concentration ($[O_2]$) is negatively proportional to the square root of the ESR signal intensity ($I^{-1/2}$) of the spin probe TEMPO [19]. Details of the reactions in this system are described in supporting information S1-2. The time traces of oxygen consumption during the autoxidation of methyl linoleate in the absence (blank) and presence of α-tocopherol (80 μM) or cycloartenyl ferulate (*e.g.*, 280, 420 and 560 μM) are shown in Figure 2. Values for rates of oxygen consumption ($-d[O_2]/dt$), obtained from a liner regression of the experimental data, are reported in Table 1.
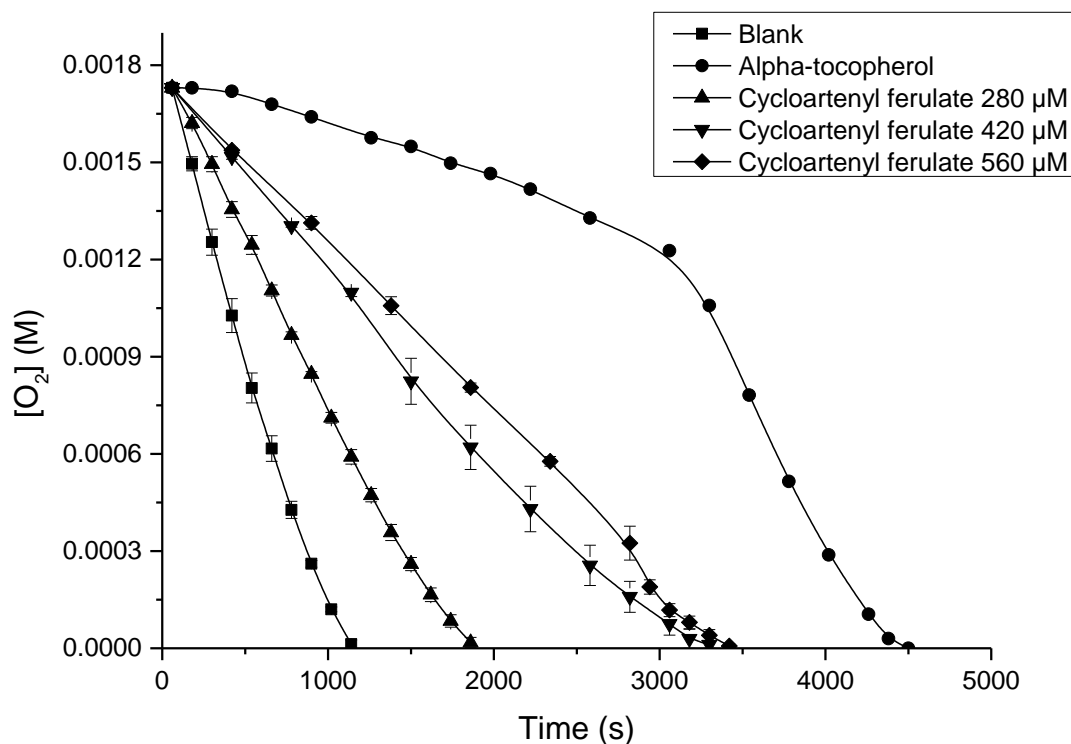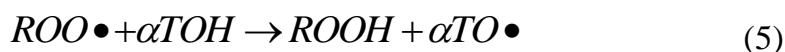
**Figure 2**. Oxygen consumption in autoxidation of methyl linoleate initiated by AIBN at 50 °C in presence of cycloartenyl ferulate or α-tocopherol.

**Table 1** Rate of oxygen consumption ($-d[O_2]/dt$) in autoxidation of methyl linoleate in presence of cycloartenyl ferulate or α-tocopherol.

| Antioxidant | Concentration (μM) | $R_i$ ($10^{-8}$ M s$^{-1}$) | $R_{ox}$ ($10^{-7}$ M s$^{-1}$) | $R_{inh}$ ($10^{-7}$ M s$^{-1}$) | $R_{inh}/R_{ox}$ |
|---|---|---|---|---|---|
| Cycloartenyl ferulate | 140 | 5.23 | 16.20 | 11.70 | 0.72 |
| | 280 | | | 9.58 | 0.59 |
| | 350 | | | 8.25 | 0.51 |
| | 420 | | | 5.28 | 0.33 |
| | 490 | | | 5.35 | 0.33 |
| | 560 | | | 4.67 | 0.29 |
| α-tocopherol | 80 | 5.23 | 16.20 | 1.69 | 0.10 |

Effective antioxidant α-tocopherol shows a clear induction period $τ$ of 3060 s (time for antioxidant inhibits the lipid oxidation). A rapid change in the slope of the curve

indicates the point (at 3060 s) at which all α-tocopherol is consumed and the rate of oxygen consumption is no longer inhibited. The value $(-d[O_2]/dt)_{inh}$ of α-tocopherol in Table 1 is obtained from the regression of $[O_2]$ vs. time from 0-3060 s. The $\tau$ value depends on the antioxidant concentration and the number of peroxyl radicals interrupted by each molecular of antioxidant (stoichiometric factor $n$) [17]. In the case of α-tocopherol, the $n$ value is 2 [9, 16], indicating that one molecule of α-tocopherol (αTOH) is able to inactivate two peroxyl radicals (ROO•), as shown in reaction (5) and (6). Thus, α-tocopherol is a chain-breaking antioxidant. Moreover, the rate of initiation of lipid autoxidation $R_i$ could be determined as $5.23 \times 10^{-8}$ M s$^{-1}$ based on the equation (4).

$$ROO \bullet + \alpha TOH \rightarrow ROOH + \alpha TO \bullet \qquad (5)$$

$$ROO \bullet + \alpha TO \bullet \rightarrow adducts \qquad (6)$$

Cycloartenyl ferulate was also able to slow down the oxidation of methyl linoleate although less than α-tocopherol (Figure 2). The mechanism of antioxidant activity of ferulates results from the phenolic proton in the ferulic acid moiety, which can be abstracted by any radical present in the media, and the resulting ferulate radical is stabilized by resonance along the π-electron system constituted by the aromatic ring and the carboxylate in *para* position to the phenol group [20, 21]. However, cycloartenyl ferulate at different concentrations was only able to retard oxidation, and no definite induction period could be detected, suggesting that it could not break the chain reactions completely [9, 16]. Thus its stoichiometric factor cannot be determined. In this case the kinetic constant of inhibition was determined by the method (section 2.3) proposed by Darley-Usmar et al. [15]. The numerical values of $k_{SF}$ and $\beta$ can be obtained from fitting the data to equation (1) with different concentrations of cycloartenyl ferulate under same experimental condition by software Origin 9.0 (Figure 3). From the obtained $k_{SF}$ $((1.32 \pm 0.55) \times 10^3$ M$^{-1})$ and $\beta$ $(1.47 \pm 0.42)$ values, the inhibition rate constant of cycloartenyl ferulate in autoxidation of methyl linoleate is determined as $(1.24 \pm 0.52) \times 10^3$ M$^{-1}$ s$^{-1}$ in this method.
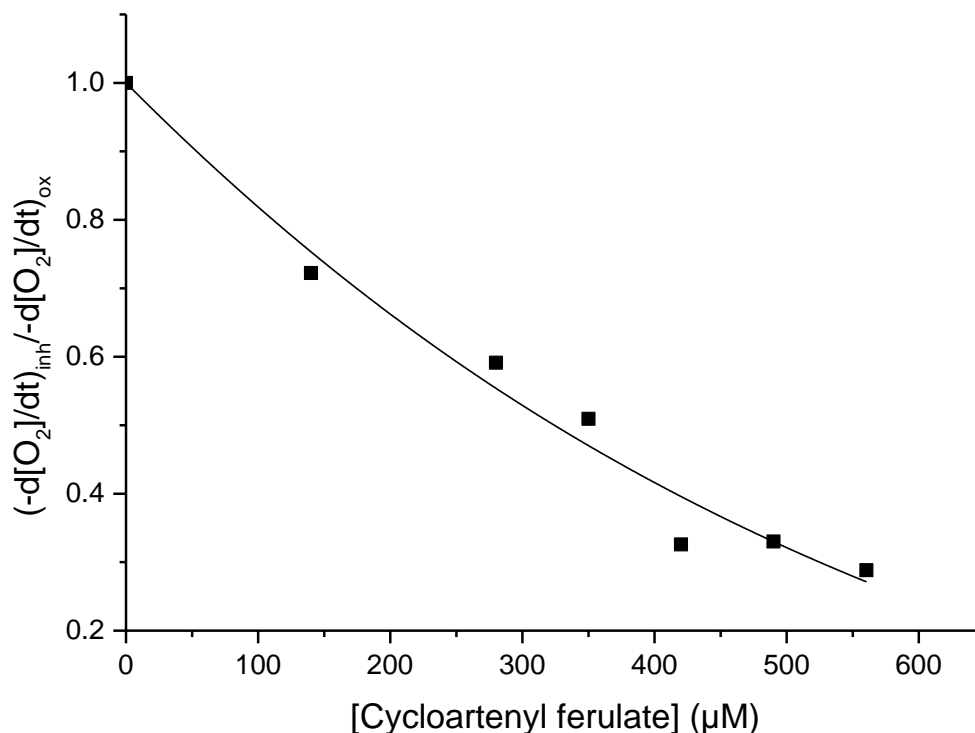
**Figure 3** Ratio of the rates of oxygen consumption in the presence of cycloartenyl ferulate at different concentrations in autoxidation of methyl linoleate initiated by AIBN at 50 °C.

This is the first study regarding the inhibition rate constant of steryl ferulate (specifically cycloartenyl ferulate) in autoxidation of methyl linoleate showing that cycloartenyl ferulate behaves as a retarder of the lipid peroxidation in *tert*-butanol. Some literature values for inhibition rate constants of other natural antioxidants under the same experimental conditions have been reported. For example, α-tocopherol which is one of the most efficient natural antioxidants, had an inhibition rate constant of $6.28 \times 10^5$ $M^{-1}$ $s^{-1}$ [9, 16, 22], which is nearly 500 times more effective than cycloartenyl ferulate. Furthermore, cycloartenyl ferulate is approximately 10-20 times less effective than quercetin ($k_{inh}=2.1 \times 10^4$ $M^{-1}$ $s^{-1}$) [9], epicatechin ($k_{inh}=1.7 \times 10^4$ $M^{-1}$ $s^{-1}$) [9], (+)-catechin ($k_{inh}=1.5 \times 10^4$ $M^{-1}$ $s^{-1}$) [18] and commercially used antioxidant BHT ($k_{inh}=1.8 \times 10^4$ $M^{-1}$ $s^{-1}$) [16]. Therefore, cycloartenyl ferulate possesses an antioxidant activity, however, less effective than the other commonly used antioxidants.

## 3.2. Comparison of antioxidant effect of various steryl ferulates

126

For comparing the antioxidant effects of various ferulates, stigmasteryl ferulate, cholesteryl ferulate, sitostanyl ferulate, γ-oryzanol, methyl ferulate as well as ferulic acid were also investigated in this study. Like cycloartenyl ferulate, all of the ferulates including ferulic acid induce only a retardation of oxidation and no definite induction period could be detected, indicating that these ferulates also cannot break the chain reactions completely. The rate of oxygen consumption in autoxidation of methyl linoleate in presence of different ferulates and ferulic acid is shown in Figure 4.

However, overall individual steryl ferulates, methyl ferulate and ferulic acid show similar effects and there are no significant differences between compounds at each analysed concentration ($p > 0.05$). Generally, all the compounds in this study retarded the autoxidation of methyl linoleate dose-dependently. The oxygen consumption rates decrease by approximately 40%, 60% and 70% when the antioxidants are at 280, 420 and 560 μM in the reaction system, respectively.

In the tested steryl ferulates, 4,4'-dimethylsteryl ferulate (cycloartenyl ferulate), unsaturated 4-desmethylsteryl ferulate (stigmasteryl ferulate and cholesteryl ferulate, with the only structural differences at the side chain), saturated 4-desmethylsteryl ferulate (sitostanyl ferulate) and steryl ferulate mixture γ-oryzanol (containing 32% cycloartenyl ferulate, 40% 24-methylenecycloartanyl ferulate, 14% campesteryl ferulate and other steryl ferulates) exhibit the similar behaviour in this reaction system, suggesting that the different sterol moieties have no influence on the hydrogen donating ability from the ferulic acid moiety. The same antioxidant effect in lipid oxidation model between 4,4'-dimethylsteryl ferulate and 4-desmethylsteryl ferulate was also observed by Xu and Godber [12], but not by the study from Yagi and Ohishi [11] and Winkler-Moser *et al.* [5, 23]. Furthermore, ferulic acid and methyl ferulate show the same effect as steryl ferulate, indicating that the steric hindrance from the sterol moiety is not shown in our study, also suggesting that the esterification of ferulic acid has no influence on the inhibition effect in lipid autoxidation model. Moreover, steryl ferulate shows less antioxidant activity than α-tocopherol, which is in agreement with the observation by Xu and Godber [12]. Overall, the individual steryl ferulates behave as a

127

retarder of the lipid peroxidation, and no difference in antioxidant activity has been found among them.
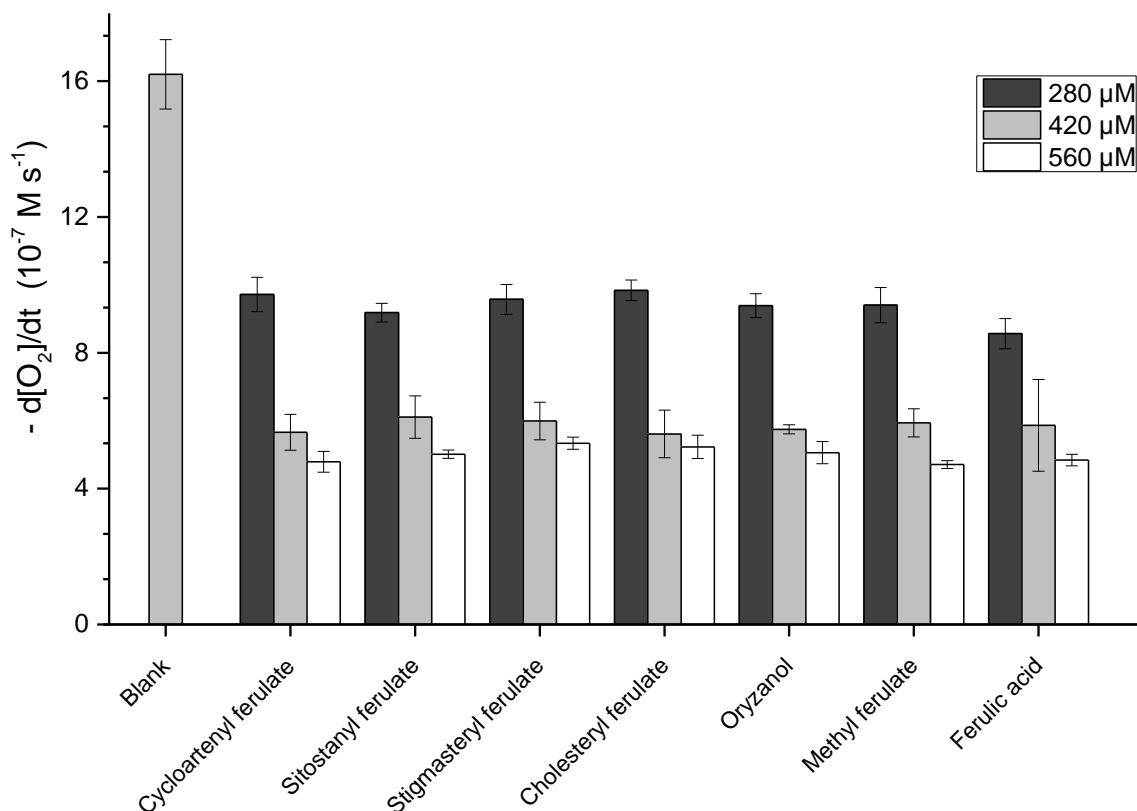


**Figure 4** Comparison of the rate of oxygen consumption in autoxidation of methyl linoleate in presence of different ferulates and ferulic acid

# Acknowledgements

# References

[1] Seitz, L. M., Stanol and sterol esters of ferulic and p-coumaric acids in wheat, corn, rye, and triticale. *Journal of Agricultural and Food Chemistry* 1989, *37*, 662-667.

[2] Lemus, C., Angelis, A., Halabalaki, M., Leandros, A., in: Watson, R. R., Preedy, V. R., Zibadi, S. (Eds.), *Wheat and Rice in Disease Prevention and Health: Benefits, risks and mechanisms of whole grains in health promotion*, Academic Press, London, UK 2014, pp. 409-430.

[3] Ghatak, S. B., Panchal, S. J., Gamma-oryzanol-A multi-purpose steryl ferulate. *Current Nutrition and Food science* 2011, *7*, 10-20.

[4] Nyström, L., Mäkinen, M., Lampi, A. M., Piironen, V., Antioxidant activity of steryl ferulate extracts from rye and wheat bran. *Journal of Agricultural and Food Chemistry* 2005, *53*, 2503-2510.

[5] Winkler-Moser, J. K., Hwang, H. S., Bakota, E. L., Palmquist, D. A., Synthesis of steryl ferulates with various sterol structures and comparison of their antioxidant activity. *Food Chemistry* 2015, *169*, 92-101.

[6] Wang, T., Hicks, K., Moreau, R., Antioxidant activity of phytosterols, oryzanol, and other phytosterol conjugates. *Journal of the American Oil Chemists Society* 2002, *79*, 1201-1206.

[7] Huang, C. J., Potential functionality and digestibility of oryzanol as determined using in vitro cell culture models. PhD Thesis, Louisiana State University, 2003.

[8] Xu, Z., Hua, N., Godber, J. S., Antioxidant activity of tocopherols, tocotrienols, and γ-oryzanol components from rice bran against cholesterol oxidation accelerated by 2,2'-azobis(2-methylpropionamidine) dihydrochloride. *Journal of Agricultural and Food Chemistry* 2001, *49*, 2077-2081.

[9] Pedrielli, P., Pedulli, G. F., Skibsted, L. H., Antioxidant mechanism of flavonoids. Solvent effect on rate constant for chain-breaking reaction of quercetin and epicatechin in autoxidation of methyl linoleate. *Journal of Agricultural and Food Chemistry* 2001, *49*, 3034-3040.

[10] Pedulli, G. F., Lucarini, M., Pedrielli, P., Sagrini, M., Cipollone, M., The determination of the oxygen consumption in autoxidation studies by means of EPR spectroscopy. *Research on Chemical Intermediates* 1996, *22*, 1-14.

[11] Yagi, K., Ohishi, N., Action of ferulic acid and Its derivatives as antioxidants. *Journal of Nutritional Science and Vitaminology* 1979, *25*, 127-130.

[12] Xu, Z., Godber, J. S., Antioxidant activities of major components of γ-oryzanol from rice bran using a linoleic acid model. *Journal of the American Oil Chemists Society* 2001, *78*, 645-649.

[13] Mandak, E., Zhu, D., Godany, T. A., Nyström, L., Fourier transform infrared spectroscopy and Raman spectroscopy as tools for identification of steryl ferulates. *Journal of Agricultural and Food Chemistry* 2013, *61*, 2446-2452.

[14] Pedrielli, P., Skibsted, L. H., Antioxidant synergy and regeneration effect of quercetin, (-)-epicatechin, and (+)-catechin on alpha-tocopherol in homogeneous solutions of peroxidating methyl linoleate. *Journal of Agricultural and Food Chemistry* 2002, *50*, 7138-7144.

[15] Darley-Usmar, V. M., Hersey, A., Garland, L. G., A Method for the Comparative-Assessment of Antioxidants as Peroxyl Radical Scavengers. *Biochemical pharmacology* 1989, 38, 1465-1469.

[16] Pedrielli, P., Holkeri, L., Skibsted, L., Antioxidant activity of (+)-catechin. Rate constant for hydrogen-atom transfer to peroxyl radicals. *European Food Research and Technology* 2001, *213*, 405-408.

[17] Burton, G. W., Ingold, K. U., Autoxidation of biological molecules. 1. Antioxidant activity of vitamin E and related chain-breaking phenolic antioxidants in vitro. *Journal of the American Chemical Society* 1981, *103*, 6472-6477.

[18] Cipollone, M., di Palma, C., Pedulli, G. F., A New Method for the Determination of Oxygen Solubilities by EPR. *Applied Magnetic Resonance* 1992, *3*, 99-106.

[19] Akihisa, T., Ogihara, J., Kato, J., Yasukawa, K.*, et al.*, Inhibitory effects of triterpenoids and sterols on human immunodeficiency virus-1 reverse transcriptase. *Lipids* 2001, *36*, 507-512.

[20] Nyström, L., in: Xu, Z., Howard, L. R. (Eds.), *Analysis of Antioxidant-Rich Phytochemicals*, Wiley-Blackwell, Oxford, UK 2012, pp. 313-351.

[21] Graf, E., Antioxidant potential of ferulic acid. *Free Radical Biology and Medicine* 1992, *13*, 435-448.

[22] Niki, E., Saito, T., Kawakami, A., Kamiya, Y., Inhibition of oxidation of methyl linoleate in solution by vitamin E and vitamin C. *Journal of Biological Chemistry* 1984, *259*, 4177-4182.

[23] Winkler-Moser, J. K., Rennick, K. A., Palmquist, D. A., Berhow, M. A., Vaughn, S. F., Comparison of the impact of gamma-oryzanol and corn steryl ferulates on the polymerization of soybean oil during frying. *Journal of the American Oil Chemists Society* 2011, *89*, 243-252.

# Supporting information

## S1. Lipid autoxidation

The lipid autoxidation is a free radical chain reaction between atmospheric oxygen and the substrate. The simplified scheme of autoxidation of unsaturated fatty acid (RH) is as follows:

*Initiation:*

$$RH \xrightarrow{\;Ri\;} R\bullet + H\bullet \qquad\qquad (S1)$$

*Propagation:*

$$R\bullet + O_2 \rightarrow ROO\bullet \qquad\qquad (S2)$$

$$ROO\bullet + RH \rightarrow ROOH + R\bullet \qquad\qquad (S3)$$

*Termination:*

$$2ROO\bullet \rightarrow more\ stable\ products \qquad\qquad (S4)$$
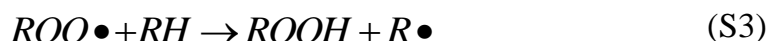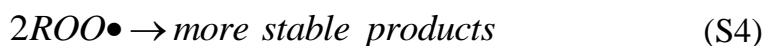
Initiation is the step in which an alkyl radical (R•) is produced (reaction S1). In the propagation step (reactions S2-S3), the alkyl radical reacts with oxygen and forms a peroxyl radical (ROO•), which then can draw a hydrogen atom from another fatty acid and the reaction chain continues. Hydroperoxides (ROOH) are primary products of autoxidation that may further decompose. The chain is terminated when lipid peroxyl radicals react together and form more stable compounds (reactions S4). Quantitative autoxidation studies can be performed only if the $R_i$ (reaction S1) is constant, which can be achieved by thermal decomposition of the azo initiator [1].

## S2. Reaction system

This oximetry for lipid autoxidation studies by ESR was introduced by Cipollone et al. [2] and Pedulli et al. [1]. It is based on measuring the change in ESR signal intensity of a nitroxyl radical probe TEMPO in a closed system containing an initiator and an easily

oxidized substrate, such as methyl linoleate. TEMPO is very stable and gives a spectrum of three singlets with intensity ratio 1:1:1 (Figure S1). The oxygen solubility in the above experimental environment is $1.73 \times 10^{-3}$ M [3]. When the oxygen is saturated in the system, the ESR signal is broad and the amplitude is low; during autoxidation, the amount of oxygen in a closed sample system decreases, resulting in an increase of the intensity and decrease of the width of EPR signal. The oxygen concentration is positively proportional to the width of ESR signal and negatively proportional to the square root of the signal intensity ($I^{-1/2}$) [4]. At the beginning of the experiment, the width is difficult to be measured accurately due to relatively low signal:noise ratio, thus, it is more convenient to measure the peak-to-peak amplitude of the signal (intensity).
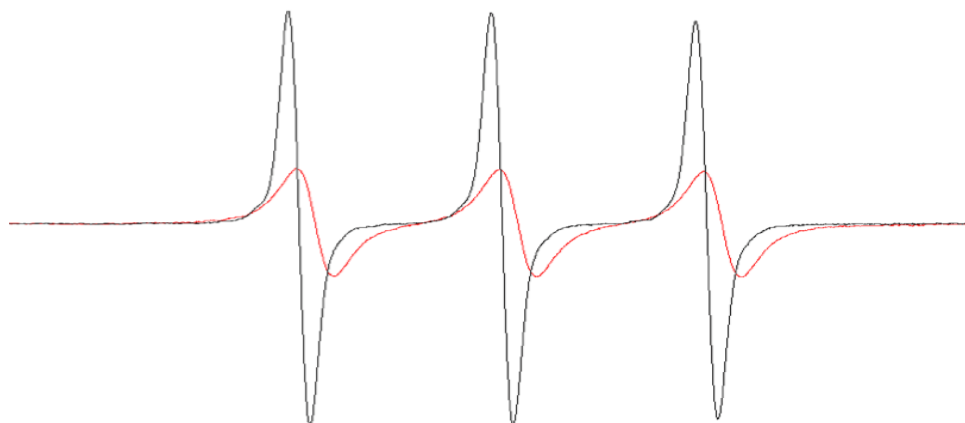


**Figure S1**. EPR spectra of nitroxyl radical TEMPO in *tert*-butanol in presence ($1.73 \times 10^{-3}$ M; red) or absence (black) of oxygen.

When adding an extra radical (TEMPO•) into the sample system, two potential reactions (S5-S6) might happen in the autoxidation and interfere the reaction chain as well as the oxygen consumption measurement.

$$TEMPO \bullet + R \bullet \rightarrow products \qquad (S5)$$

$$TEMPO \bullet + ROO \bullet \rightarrow products \qquad (S6)$$

The reaction S6 can be neglected since peroxyl radicals do not react with aliphatic nitroxides. However, the reaction S5 between the alkyl radical and the nitroxyl radical can take place to compete with reaction S2. To solve this problem, the concentration of TEMPO is at least one magnitude lower than the concentration of oxygen in system ($<$ $10^{-4}$ M), then the alkyl radical preferably reacts with oxygen (reaction S2) than with TEMPO due to the lower kinetics constant of reaction S6 compared to reaction S2 [1]. TEMPO can only interfere in the chain reaction in the end. As shown the blank sample in Figure S2, at 1140 s, the oxygen is consumed, the ESR intensity reaches highest (lowest $I^{-1/2}$); then the TEMPO reacts with the alkyl radical (reaction S5) and the ESR intensity drops and eventually disappears.
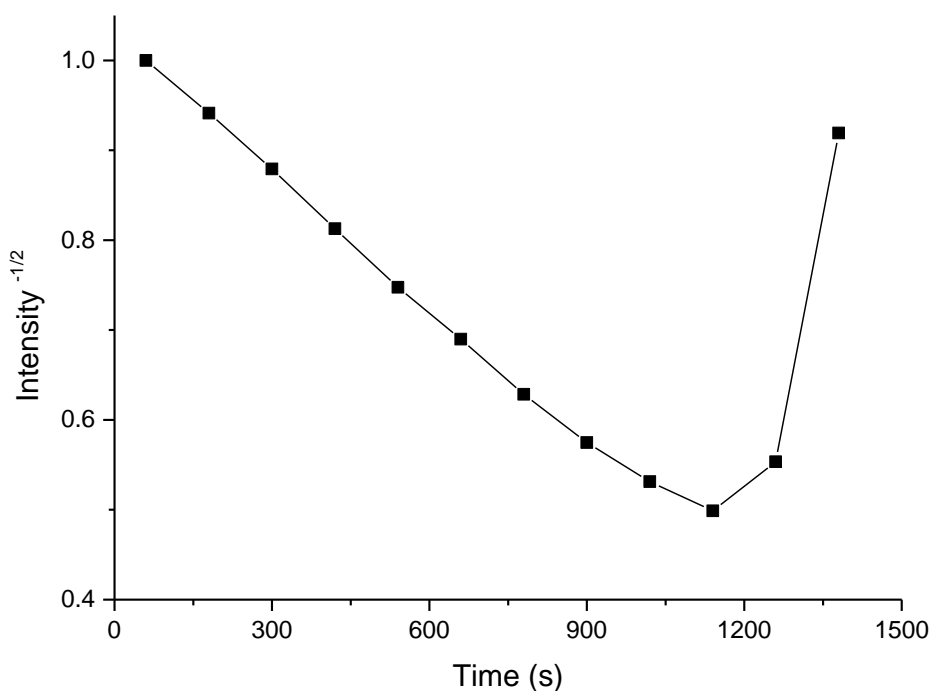


**Figure S2** Time dependent of the square root of intensity of EPR spectra of TEMPO during autoxidation of methyl linoleate initiated by AIBN at 50 °C in the absence of antioxidant (blank).

Primary antioxidants (AH), *e.g.*, the reference antioxidant α-tocopherol in our study, react through their hydrogen atoms with the free radicals and further form more stable products in the reaction system. Since the bond dissociation energy of the O-H bond in phenolic compounds is lower than that of the weaker C-H bond in the alkyl compound,

the reaction between the peroxyl radical (ROO•) and the antioxidant (reaction 5 in main text) is faster than that of peroxyl radical and another lipid molecule (reaction S3). Further, the phenoxiradical (A•) may continue to react with lipid peroxyl radical to form lipid-antioxidant complex [5]. By these reactions in the system, the autoxidation of lipid is inhibited by the antioxidant.

## References of supporting information

[1] Pedulli, G. F., Lucarini, M., Pedrielli, P., Sagrini, M., Cipollone, M., The determination of the oxygen consumption in autoxidation studies by means of EPR spectroscopy. *Research on Chemical Intermediates* 1996, *22*, 1-14.

[2] Cipollone, M., di Palma, C., Pedulli, G. F., A New Method for the Determination of Oxygen Solubilities by EPR. *Applied Magnetic Resonance* 1992, *3*, 99-106.

[3] Pedrielli, P., Skibsted, L. H., Antioxidant synergy and regeneration effect of quercetin, (-)-epicatechin, and (+)-catechin on alpha-tocopherol in homogeneous solutions of peroxidating methyl linoleate. *Journal of Agricultural and Food Chemistry* 2002, *50*, 7138-7144.

[4] Akihisa, T., Ogihara, J., Kato, J., Yasukawa, K., *et al.*, Inhibitory effects of triterpenoids and sterols on human immunodeficiency virus-1 reverse transcriptase. *Lipids* 2001, *36*, 507-512.

[5] Jorgensen, L. V., Flavonoids and other naturally occuring antioxidants. Physico-chemical aspects of their antioxidant mode of action. PhD thesis. *Food Chemistery Department*, The Rayal Veterinary and Agriculatural University, Frederiksberg, Denmark, 1998.

# Permeation of Steryl Ferulates Through an in vitro Intestinal Barrier Model

## Abstract

**Scope:** Steryl ferulates (SFs) belong to the bioactive lipids contributing to the health promoting effects of whole grains. However, their intestinal absorption remains unclear. We investigated the permeation of individual SFs using an *in vitro* intestinal barrier model.

**Methods and results:** An *in vitro* Caco-2 cell monolayer, mimicking the intestinal barrier, was used to evaluate the permeation of eight SFs from different sources. A method based on ultra performance liquid chromatography with high-resolution mass spectrometric detection was developed for their quantification. Although only a negligible amount ($< 0.5\%$) permeated across the Caco-2 cell monolayer, some differences in the permeability coefficients were observed between individual SFs. Permeation mechanism was mainly passive diffusion.

**Conclusion:** This work indicates that the permeation of SFs across the gut is very low. Therefore, cholesterol lowering and antioxidant activity related health benefits of SFs most likely occur in the gut independently from absorption.

## Keywords

## Abbreviations

GI, gastrointestinal; HBSS, Hank's balanced salt solutions; LY, Lucifer yellow; $P_{app}$, apparent permeability coefficient; SF, steryl ferulate; TEER, transepithelial electrical resistance; UPLC-MS, ultra performance liquid chromatography with high-resolution mass spectrometric detection.

## 1 Introduction

Steryl ferulates (SFs), esters of ferulic acid and phytosterols, are secondary plant metabolites present in the bran layers of grains [1]. While the mixture of SFs in rice, γ-oryzanol, is by far the most studied, SFs have also been identified in barley, corn, rye, triticale, wheat and wild rice [2]. SFs are known for a variety of beneficial health effects, such as cholesterol lowering activity, reduction of serum thyroid stimulating hormone levels, and attenuation of gastric hypersecretive disorder [3, 4]. Additionally, SFs are recognized as antioxidants, through the hydrogen donating capacity of their ferulic acid moiety [5].

The sterol moieties (Fig. 1) integrated into the SFs vary between grain species and varieties, as well as environmental factors [6]. Differences in the bioactive properties of SFs have been reported earlier: for example SFs from rice (γ-oryzanol, rich in SF **1-2**) had inferior antioxidant potential compared to other SFs (SF **3-6**), originating from wheat bran [7]. Additionally, SFs from rye and wheat (SF **3-6**) were hydrolysed more effectively than γ-oryzanol by steryl esterase *in vitro* [8]. Hence, these studies reveal a different biological behaviour for the individual SFs.
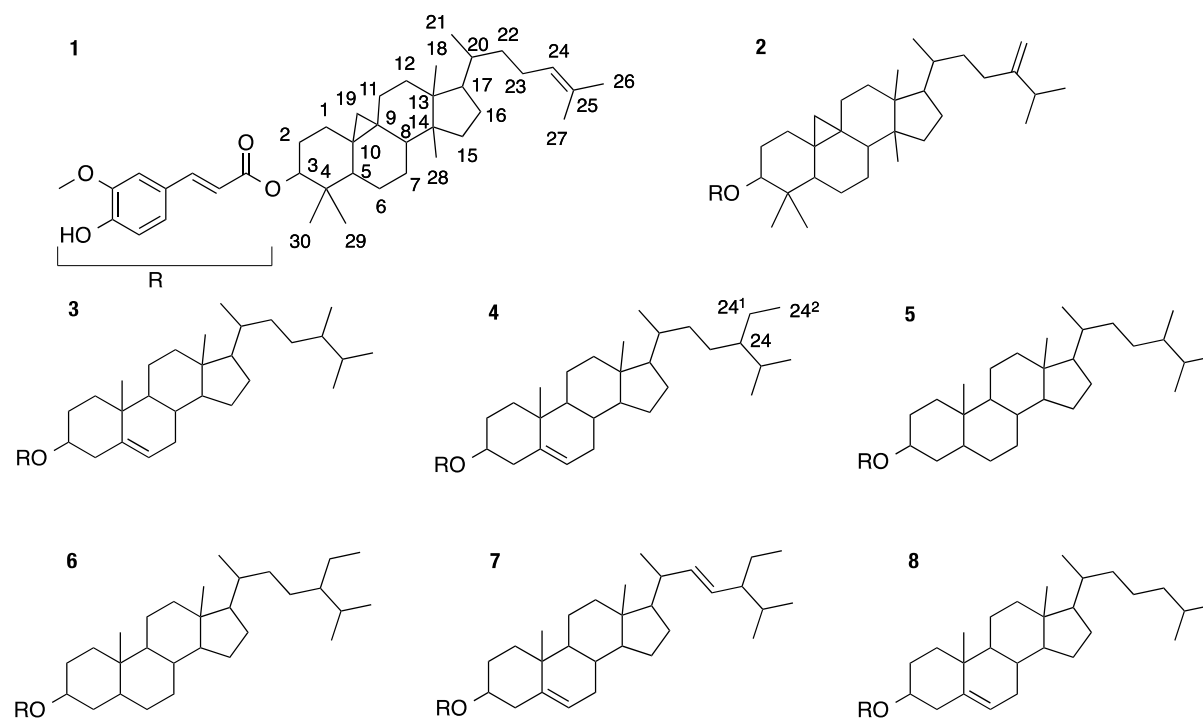
**Figure 1**. Chemical structures of (**1**) cycloartenyl ferulate; (**2**) 24-methylenecycloartanyl ferulate; (**3**) campesteryl ferulate; (**4**) sitosteryl ferulate; (**5**) campestanyl ferulate; (**6**) sitostanyl ferulate; (**7**) stigmasteryl ferulate; (**8**) cholesteryl ferulate.

γ-Oryzanol has been reported to be poorly absorbed in rat [9] and rabbit [10]. Moreover, no cellular uptake of SFs was observed in human intestinal cells C2BBe1 [11]. In a recent clinical study, volunteers took a daily dose of 5% γ-oryzanol for 3 days in skimmed milk yogurt and showed that nearly 80% of intact γ-oryzanol was recovered in the feces [12]. Nevertheless, none of these studies provide clear evidence regarding the exact intestinal absorption of individual SFs.

Due to SFs' hydrophobicity, their absorption necessitates initial release from the food matrix followed by emulsification and/or micellar solubilization by biological surfactants during digestion. The resulting oil droplets, liposomes or micelles function as reservoir and/or transport vehicle across the unstirred water layer until they reach the brush border membrane of enterocytes [13]. The use of *in vitro* cell model monolayer provides a good starting point to investigate the permeation of SFs through the intestinal epithelium. Caco-2 human colon carcinoma cells, form monolayers with tight junctions,

and can be used to mimic the intestinal barrier and study food components or drugs intestinal absorption [14].

The aim of this study was to investigate the permeation of eight individual SFs (Fig. 1) through Caco-2 cell monolayers. Cycloartenyl ferulate (SF **1**) is the only single SF commercially available, and is often used as model compound of individual SFs. A highly sensitive quantification method of the individual SF species based on ultra performance liquid chromatography with high-resolution mass spectrometric detection (UPLC-MS) was developed. To the best of our knowledge, this study is the first to provide an investigation of permeability of individual SFs in a human intestinal barrier model.

# 2 Materials and methods

## 2.1 Materials

Acetic acid, acetonitrile (HPLC grade), ammonium hydroxide solution ($NH_4OH$), 1-butanol, bovine serum albumin (BSA), hexane, isopropanol, Lucifer yellow (LY), 1-monoolein, oleic acid, L-α-phosphatidylcholine and sodium taurocholate were purchased from Sigma-Aldrich (St. Louis, MO, USA). SF **1** (99%) was purchased from Wako (Osaka, Japan). Acetonitrile and isopropanol (MS grade) were purchased from Biosolve (Dieuze, France). γ-oryzanol was obtained from CTC Organics (Atlanta, GA, USA). Wheat bran was milled fraction from Swissmill (Zurich, Switzerland). Stigmasteryl ferulate (SF **7**; 99%) and cholesteryl ferulate (SF **8**; 97%) were synthesized (manuscript submitted for publication) by Dr. Antoni Sánchez-Ferrer (Laboratory of Food and Soft Materials, ETH Zurich, Switzerland).

Caco-2 cells were obtained from ATCC (Rockville, MD, USA). Dulbecco's Modified Eagle Medium (DMEM), fetal bovine serum, nonessential amino acids, Hank's balanced salt solutions (HBSS) and 89 units/mL penicillin and 89 μg/mL streptomycin were purchased from Invitrogen (Paisley, UK). Cell culture PET transwell membranes

(pore size, 3.0 µm, effective growth area, 0.9 cm$^2$) and companion 12 well plates were from BD Biosciences (Franklin Lakes, NJ, USA). Cell Counting Kit-8 (CCK-8) was from Dojindo (Kumamoto, Japan).

## 2.2 Maintenance of Caco-2 cell culture

Caco-2 cells were cultured in DMEM supplemented with 1% nonessential amino acids, 15% fetal bovine serum and 0.8% penicillin-streptomycin at 37 °C in a humidified atmosphere with 5% $CO_2$. For maintenance, the medium was changed every second day and the cells were passaged every week. Cells of passage 49-64 were used in this study.

## 2.3 Sample preparation

### 2.3.1 Extraction and purification of SFs

The extraction and purification of individual SFs were performed according to a method previously described [15]. Briefly, total lipids were extracted from wheat bran and then neutral lipids were eliminated by base-acid wash. The residue or γ-oryzanol was separated and purified by preparative HPLC (Merck-Hitachi, Japan) using an Xbridge Prep Shield RP C18 column (Waters, Ireland) with detection at 325 nm. Mobile phase was acetonitrile:$H_2O$:butanol:acetic acid 88:6:4:2 at 6.6 mL/min, 25°C. SF **2** (96% purity as area percentage) was collected from γ-oryzanol. SF **3** (98%) and **4** (96%) were collected from both γ-oryzanol and wheat bran. SF **5** (95%) and **6** (98%) were from wheat bran. Quantification of SFs was performed by analytical RP-HPLC (Agilent 1100, Germany) with an XBridge Shield C18 column (Waters, Ireland), and using the same mobile phase as for preparative-HPLC with 1 mL/min flow and detection at 325 nm. SF **1** was used as an external standard for RP-HPLC quantification.

### 2.3.2 Preparation of SF solution

The preparation method of SF in HBSS was adapted from previous studies [11, 16]. Firstly, 0.1 mM SF, 0.5 mM oleic acid, 0.25 mM 1-monoolein and 0.3 mM phosphatidylcholine were dissolved in hexane and isopropanol (3:1, v/v). After solvent evaporation under nitrogen stream at 45°C, the samples were redissolved in 6.6 mM sodium taurocholate in HBSS. The mixture was sonicated (Sonorex Super RK510, Germany) in an ice bath for 1 h, and was observed to be free of precipitation. The solution was stored overnight at room temperature and centrifuged for 15 min at 3220 $g$. The supernatant was collected and passed through a 0.2-µm PVDF syringe filter (BGB, Switzerland). For quantification in the final preparation, SF was extracted with 2-fold amount of hexane/isopropanol/ethyl acetate (2:1:1, v/v/v) (×2) and 2-fold amount of hexane/isopropanol/ethyl acetate (10:1:1, v/v/v) (×4). The organic layers were combined and redissolved in acetonitrile for quantification by RP-HPLC. SF solubilization at concentration of 70 µM was achieved with the above-described method. Furthermore, the highest SF concentration in HBSS was 190 µM, achieved by doubling the amount of surfactants.

## 2.4 Caco-2 cell viability after SF treatment

Caco-2 cell viability was evaluated by a tetrazolium salt (WST-8)-based colorimetric assay with the Cell Counting Kit-8. WST-8 is reduced by dehydrogenases in cells to give an orange colored formazan, directly proportional to the number of living cells. Briefly, Caco-2 cells were seeded in 96-well plates at an initial density of 5,800 cells/well and grown for 2 weeks to develop a confluent monolayer. The cells were treated with 100 µL of individual SF in HBSS, vehicle in HBSS (mixture of oleic acid, 1-monoolein, phosphatidylcholine and sodium taurocholate, with the same preparation procedure without SF), as well as HBSS alone for 3 h at 37 °C, 5% $CO_2$. The samples were removed and the cells were incubated with 100 µL complete medium for 2 h. After this, the incubation solvent was exchanged to 10 µL of CCK-8 solution and 100 µL complete medium, and was incubated for another 2 h. Finally, cell viability was determined by measuring absorbance at 450 nm using a plate reader (TECAN

infinite M200 Reader, Switzerland). Data are expressed as follows: viability (%) = $A_{sample}/A_{control} \times 100$.

## 2.5 Permeability experiments across Caco-2 cell monolayer

### 2.5.1 Quality control of Caco-2 cell monolayer

To generate Caco-2 cell monolayer on the transwell membrane supports, 0.5 mL cell suspension was placed in the apical chamber at density of 180,000 cells/well, and 1.5 mL culture medium was added in the basolateral chamber. Medium was carefully changed every second day.  To monitor the growth of Caco-2 monolayer, transepithelial electrical resistance (TEER) value was measured using an EVOM epithelial voltmeter with STX2 electrode (World Precision Instruments, Sarasota, FL, USA) every second day. The TEER increased with time in culture, reaching a maximum at 10-14 days, and then stabilized at 21-25 days. Only monolayers with TEER > 500 $\Omega \bullet cm^2$ were used [14, 17].

### 2.5.2 Transport assay

The permeability assay was performed according to a previously reported protocol [14, 17]. The medium was removed from the transwell, and cell monolayer was washed with HBSS and incubated in HBSS for 20 min. 1.5 mL HBSS including 4% BSA (for desorption of SF from acceptor wells) was loaded in the basolateral chamber, and 0.5 mL sample solution was put in the apical side followed by immediate sampling 50 μL from apical side for quantification at time 0. The sample was incubated for 3 h on a rocker (Gasser Apparatebau, Switzerland) at frequency of 46 swings/min. 750-μL sample was taken from basolateral chamber at 1 and 2 h, and replaced by the same volume of HBSS with 4% BSA. After 3 h, the total volumes from both apical and basolateral sides were collected. After transport study, Caco-2 cell monolayers were post-incubated with medium for additional 15 h. TEER was measured before every sampling during the whole experiment. To verify passage of SF through the membrane

support, a control analysis of each SF was studied in the same manner without Caco-2 cell monolayer. All the collected samples were stored at -20°C for further quantification.

The integrity of the cell monolayers was also assessed by monitoring Lucifer Yellow (LY, molecular weight 521.6 Da) permeation [18]. Quantification of LY was performed using a fluorescence plate reader at $\lambda_{Ex}/\lambda_{Em}$ 430/530 nm. The analyzed solutions were: (a) LY alone (1 mg/mL) at 37°C; (b) LY and vehicle at 37°C; (c) SF **1** (70 µM, 190 µM) with and without LY at 37°C and at 4°C; (d) eight individual SF solutions (70 µM) at 37°C.

## 2.6 UPLC-MS analysis of SFs

Since the concentration of SF collected from the basolateral chamber after transport assay was found to be near or below the limit of quantification of RP-HPLC with UV detector, UPLC-MS method based on high sensitivity and mass accuracy was developed for SF quantification. Internal standard solution was directly added to the samples collected from transport study, after which SFs were extracted with solvent as previously described (in 2.3.2). The separation was performed with a Waters ACQUITY UPLC® system with an ACQUITY UPLC BEH C18 column (50 mm × 2.1 mm, 1.7 µm particle size) using mobile phase at 0.5 mL/min, 40ºC. The detection was performed with a MS system (Synapt G2) with an electrospray ionization source (negative ion mode) and a Q-TOF analyser (Waters Corp., Milford, MA, USA). Identification of SFs was according to previous studies by Mandak and Nyström [2] and Fang et al. [19]. For quantification of permeated SF **8**, SF **1** in acetonitrile was used as internal standard, with LOD of 1.35 ng/mL and LOQ of 4.5 ng/mL. For the quantification of other SFs, SF **8** was used as internal standard, with LOD of 1.56 ng/mL and LOQ of 5.2 ng/mL. Details of quantification are described in supporting information S1.

## 2.7 Data analysis

The apparent permeability coefficient ($P_{app}$, cm/s) was calculated using the equation:

$P_{app} = \Delta Q/(\Delta t \times A \times C_0)$

where $\Delta Q/\Delta t$ is the rate of the compound across the monolayer, $A$ is the surface area of the insert and $C_0$ is the initial compound concentration in the apical chamber.

All analyses were carried out at least in triplicate. Data are presented as means $\pm$ SEM. Nonparametric test with Kruskal–Wallis analysis of variance and subsequent post-hoc analysis (pairwise comparisons) was performed with IBM SPSS Statistics 19.0 (IBM Corp., Armonk, NY, USA) in order to determine significant differences between samples. The differences were considered significant for $p$-value $< 0.05$.

# 3 Results

## 3.1 Effect of steryl ferulate on Caco-2 cell monolayer viability

In our study, to investigate the effect of concentration on cell viability, the cytotoxicity of steryl ferulate (SF) was studied at 70 µM and 190 µM with the model compound cycloartenyl ferulate (SF 1) after solubilization with bile salt (sodium taurocholate) and food components (oleic acid, 1-monoolein and phosphatidylcholine) in HBSS (Fig. 2). The cytotoxicity difference of SF 1 both at 70 µM and 190 µM was not statistically significant compared to the control (HBSS alone) (p > 0.05). However, there seemed to be a trend that the viability of Caco-2 cells was slightly impaired when increasing the SF concentration to 190 µM as well as with the vehicle alone, suggesting that the observed effect is due to the greater amount of vehicle used to deliver this higher concentration of SF 1 rather than SF 1 itself. Further, the cytotoxicity of the other SFs (2-8) prepared in HBSS was studied at a concentration of 70 µM. Measurement of the dehydrogenase activity after incubation with individual SFs for 3 h, also did not show statistically significant cytotoxicity to the Caco-2 cell compared to the control (p > 0.05).
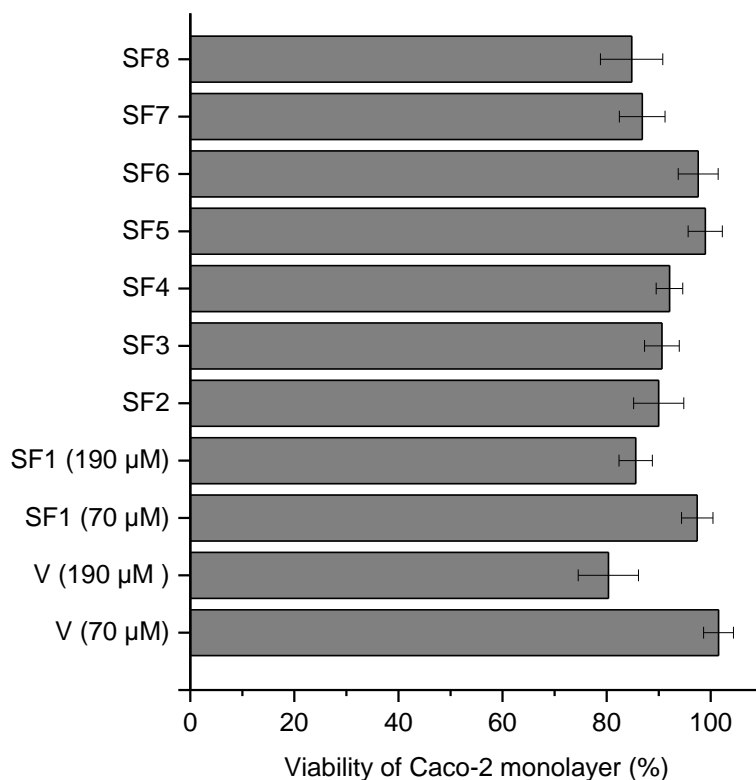
**Figure 2.** Effects of individual SFs on viability of Caco-2 monolayer cells after apical exposure (SF **2** - **8**, 70 μM; SF**1** at 70 and 190 μM; vehicle (**V**), mixture of oleic acid, 1-monoolein, phosphatidylcholine and sodium taurocholate, amount equals to the one in the solutions of SF at 70 μM and 190 μM. Data are expressed as mean ± SEM (n = 3 - 6).

## 3.2 Effect of SF 1 on Caco-2 monolayer integrity

SF 1 served as a model compound to assess permeation of individual SFs. To characterize its transepithelial transport, different incubation conditions were investigated on Caco-2 monolayer. Transport at 37°C, but not at 4°C, is indicative of active-transport; while transport occurring at both temperatures suggests a passive diffusion mechanism [17, 20]. The low temperature can significantly decrease the fluidity of cell membrane and cell metabolism including the ATPases activity that is involved in the energy-dependent transport process [21, 22]. The effect of SF 1 on the tight junction of Caco-2 cell monolayer was investigated by measuring the TEER values and co-transport with fluorescent probe LY. Two concentrations of SF 1 were used, 70 μM and 190 μM.

TEER value is temperature-dependent, thus the temperature should be well controlled [17]. In our study, TEER values were constant (around 550 $\Omega \bullet cm^2$ at 37°C, 900 $\Omega \bullet cm^2$ at 4°C) during the incubation with SF **1** at 70 μM, as well as its co-incubation with LY (Fig. 3, A and B). The used vehicle had no effect on the TEER. This suggests that the integrity of Caco-2 cell monolayers was not impaired during the transport studies. When increasing the concentration to 190 μM, the membrane integrity was transiently compromised, as indicated by the significant decrease of TEER values by ≈ 25% at 37°C. This was likely due to the higher amount of vehicle required rather than the SFs themselves. Nevertheless, the cells regained their integrity within 18 h (Fig. 3A). Similar behavior in TEER values were also observed when performed at 4 °C (Fig. 3B).

LY is known to cross Caco-2 cell monolayer exclusively through passive paracellular diffusion [18]. When the $P_{app}$ of LY is smaller than $1 \times 10^{-6}$ cm/s, Caco-2 cell monolayers are suitable for the permeation study [18]. In our study, $P_{app}$ of LY alone in monolayer was $5.4 \times 10^{-8}$ cm/s. No significant changes for $P_{app}$ of LY were observed with SF **1** at 70 μM both at 4 and 37°C (Fig. 3C, calculation in supporting information S3). When the concentration of SF **1** was raised to 190 μM, the $P_{app}$ value of LY was slightly increased at 37°C, $P_{app}$ was increased even further by reducing the temperature to 4°C, suggesting some toxic effect at high concentration of SF **1**. These observations are in well agreement with cytotoxicity and TEER results; nevertheless, although the toxicity was observed, the $P_{app}$ value of LY was still low ($< 1 \times 10^{-6}$ cm/s).
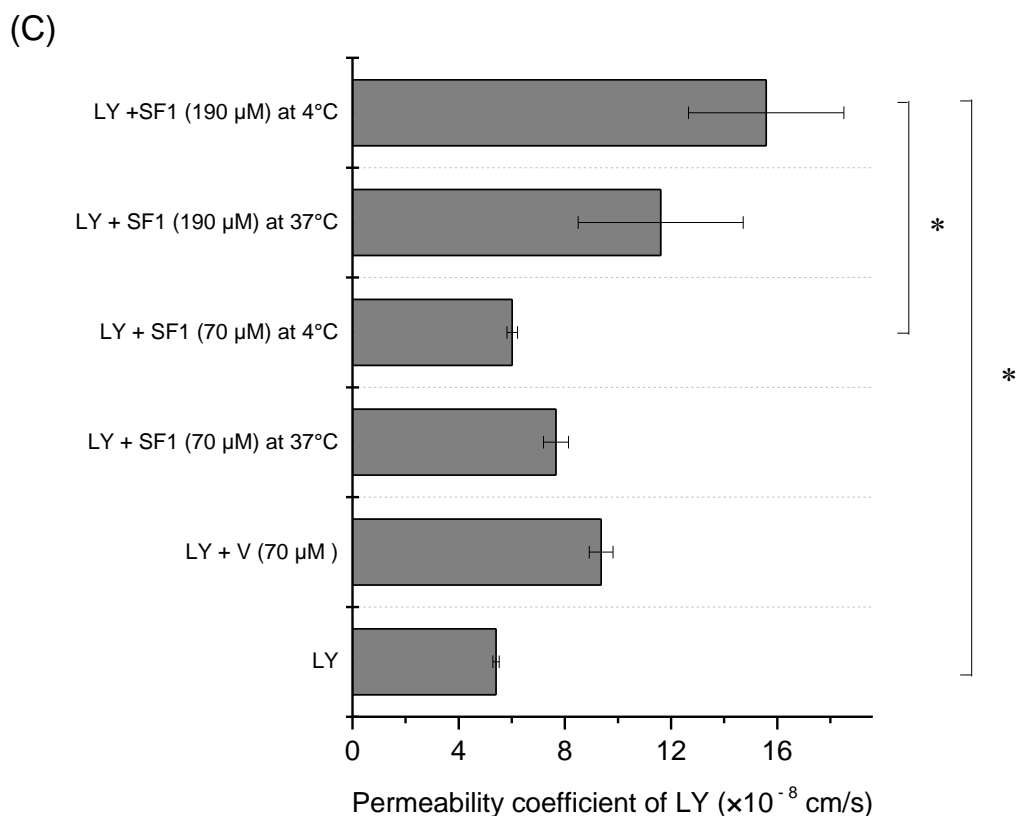
(A)



(B)

(C)
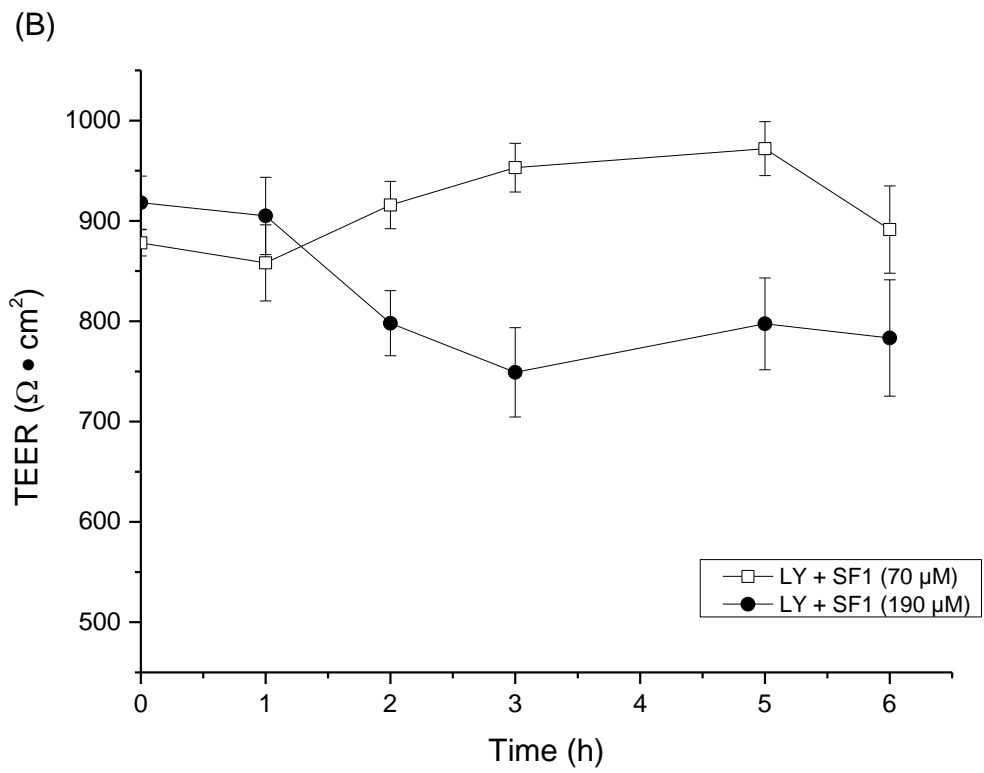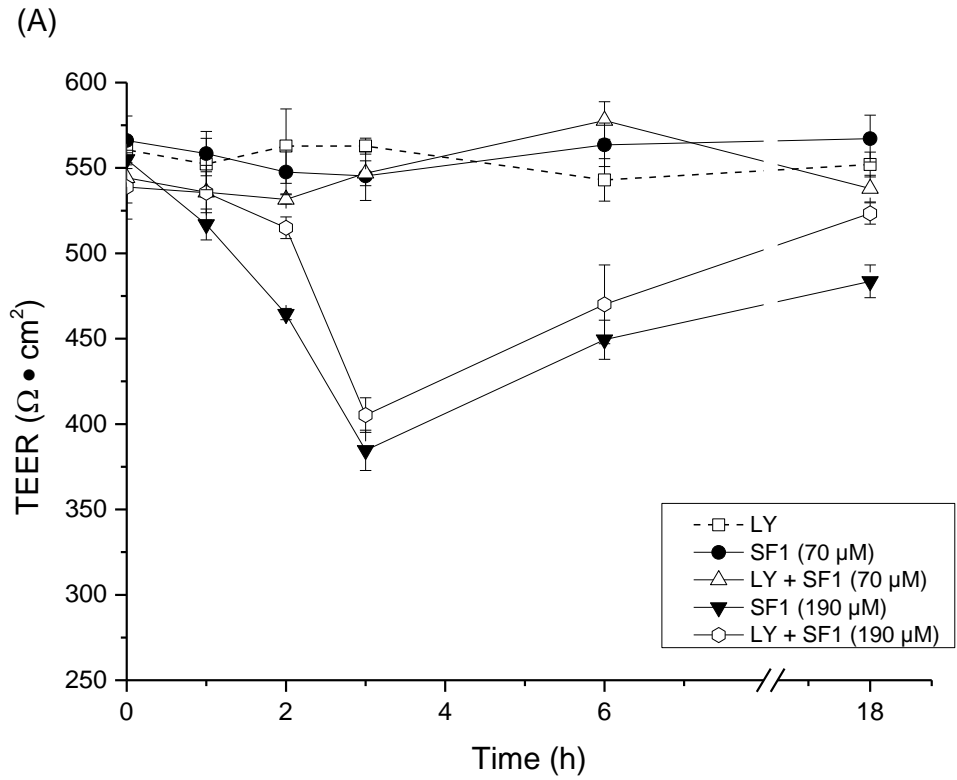


**Figure 3.** Effects of apical exposure of cycloartenyl ferulate (SF **1**) in different conditions on the tight junction of Caco-2 monolayer: (A) Variation of TEER of Caco-2 monolayer at 37°C. (B) Variation of TEER of Caco-2 monolayer at 4°C. (C) Permeability coefficient of LY in Caco-2 monolayer. Data are expressed as mean ± SEM (n = 3 - 6). An asterisk indicates a significant difference between groups ($p < 0.05$).

The cumulative percentage of SF **1** transported into receiving chamber increased linearly over time (Fig. 4A). The permeation ratios of SF **1** with donor concentrations of 70 and 190 μM in 3 h were only 0.15-0.23% and 0.26-0.29%, respectively. In our study, high mass recovery in both chambers (around 100%) of intact SF **1** indicated that no significant metabolism or degradation occurred in Caco-2 cell monolayer. SF **1** had $P_{app}$ values ranging from $0.81 \times 10^{-7}$ - $1.12 \times 10^{-7}$ cm/s at 70 μM and $1.31 \times 10^{-7}$ - $1.43 \times 10^{-7}$ cm/s at 190 μM, without significant difference between different concentrations (Fig. 4B, calculation in supporting information S4). Highly bioavailable drugs are known to have $P_{app}$ values $> 1 \times 10^{-6}$ cm/s, whereas poorly absorbed drugs have $P_{app}$ values $< 1 \times 10^{-7}$ cm/s [23]. The low $P_{app}$ value indicates that SF **1** is a poorly absorbed

compound. Moreover, SF **1** had similar $P_{app}$ values at 4°C and 37°C, and no significant inhibition of permeation of SF **1** at 4°C, suggesting that the permeation of SF **1** is mainly through passive diffusion; nevertheless, it remains unknown whether the paracellular or transcellular diffusion occurs in the Caco-2 cell monolayer.
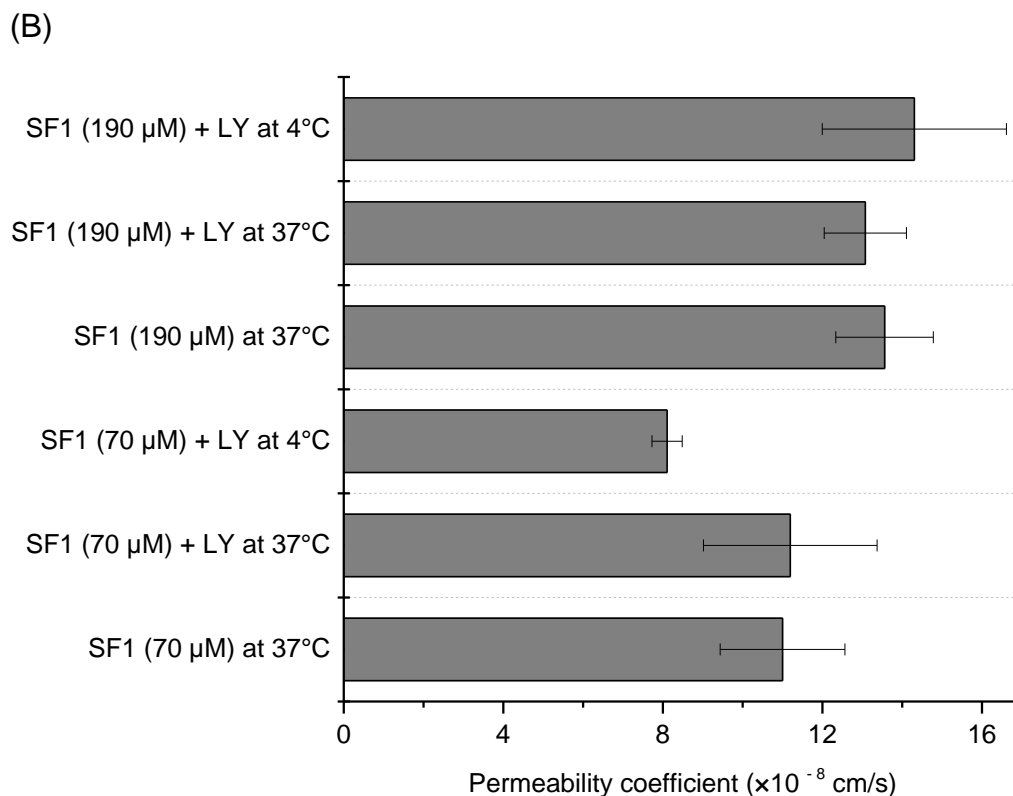
(A)

(B)
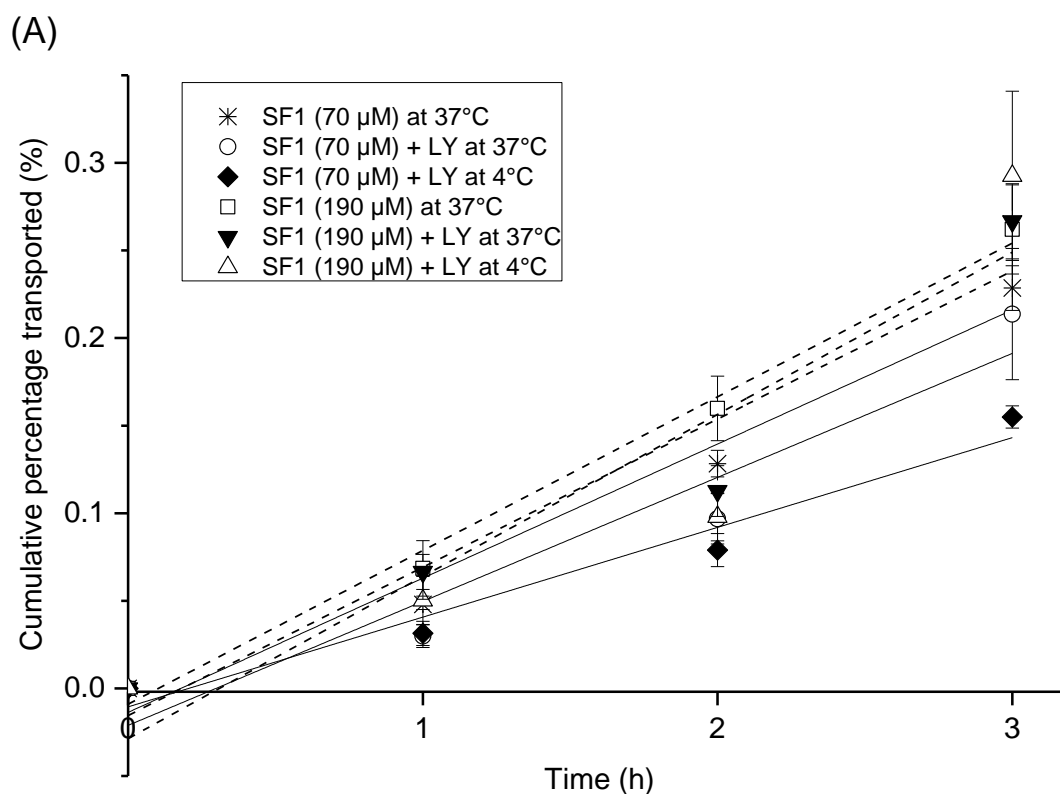


**Figure 4.** Permeation of cycloartenyl ferulate (SF **1**) in different conditions in Caco-2 monolayer: (A) transport percentage of SF **1** (solid line for 70 μM, dashed line for 190 μM) over time; (B) comparison of the permeability coefficients of SF **1**. Data are expressed as mean $\pm$ SEM (n = 6 - 9).

## 3.3 Individual SFs

The ability of individual SFs to permeate was investigated using Caco-2 cell monolayer. Given that 190 μM of SFs showed some cytotoxicity, likely due to the higher amount of vehicle, all additional SFs were tested at 70 μM. Monitoring the integrity of the monolayer (through TEER measurements) suggests no significant cytotoxicity or compromise of the monolayer, being the resistance consistently at 550 $\Omega \bullet cm^2$ (supporting information S5).

Although their transport ratios were very low, all the individual SFs showed a time-dependent passage across the model (Fig. 5A). Only 0.23% of SF **1** and 0.22% of SF **6**

permeated to the receiver chamber, while for SF **8,** the permeation ratio was only 0.04%. In this study, mass recovery was consistently around 100% for all individual SFs, which indicates no significant metabolism or degradation of SFs in monolayer. Generally, all of these SFs had very low $P_{app}$ value ($1.69 \times 10^{-8}$-$1.10 \times 10^{-7}$ cm/s), suggesting they are poorly absorbed compounds (Fig. 5B; calculation in supporting information S5); nevertheless, up to a 6.5 fold difference was observed between the highest and lowest $P_{app}$ values (SF **1** versus **8**). Statistically, $P_{app}$ of SF **1** was significantly higher than SF **7** and **8**, as well as SF **5** was significantly higher than **8.** This study confirmed that individual SFs have very low permeation, while still having significant differences in their permeation values between SF species.
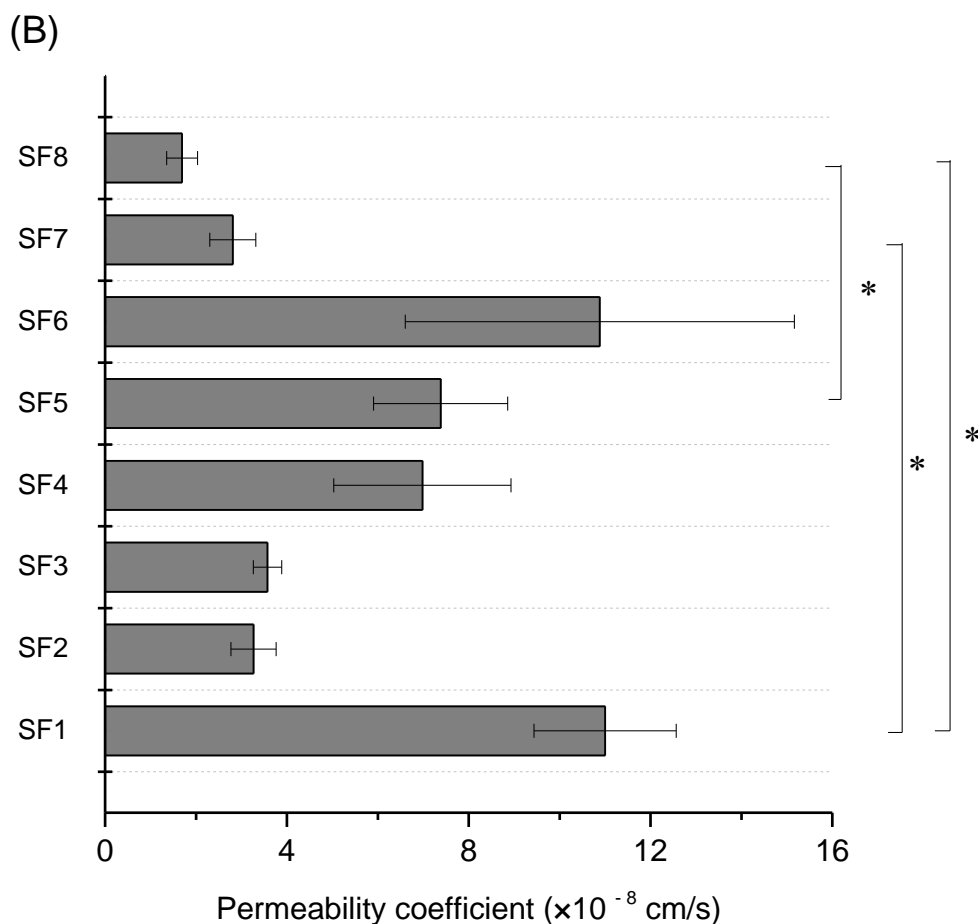
(A)
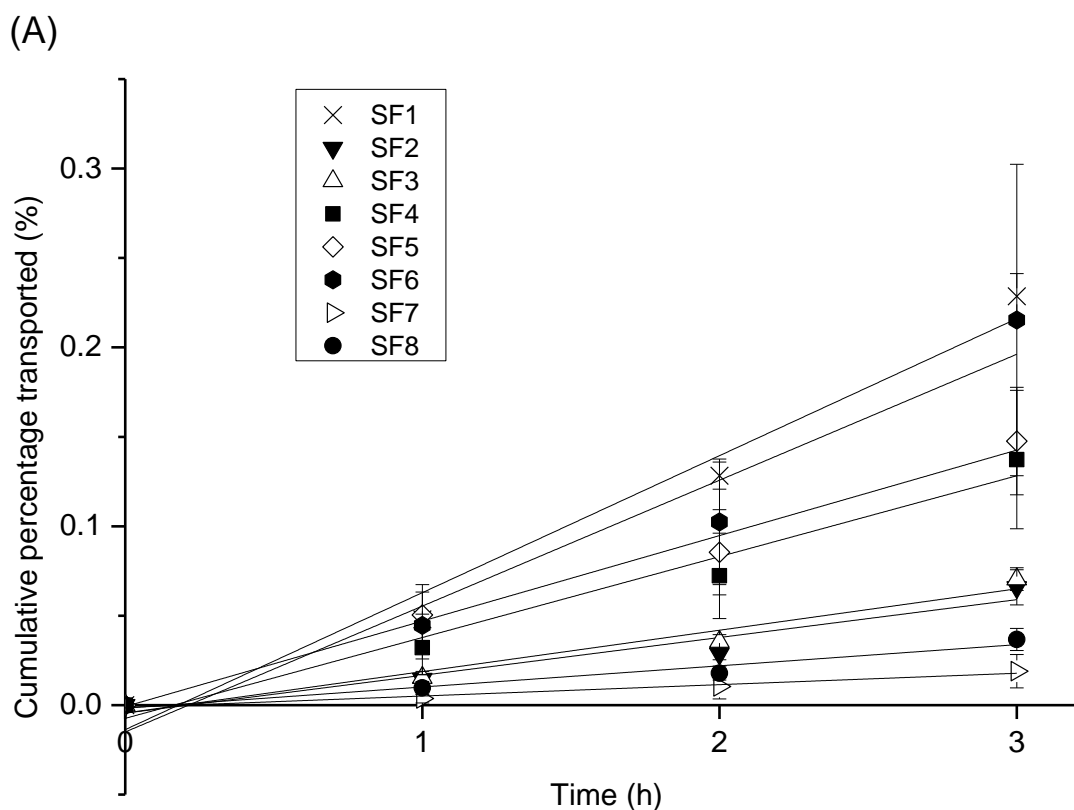
**Figure 5.** Permeation of individual SFs (SF **1** - **8**, 70 μM) in Caco-2 monolayer at 37°C: (A) transport percentage of SFs over time; (B) comparison of the permeability coefficients of SFs. Data are expressed as mean ± SEM (n = 6 - 9). An asterisk indicates a significant difference between groups ($p < 0.05$).

## 4 Discussions

Previous *in vivo* studies suggested the low absorption behavior of SFs. Fujiwara and co-workers reported that after oral administration of radiolabeled SF to rats, only a small fraction of radioactivity transferred to blood, with a peak concentration corresponding to 0.06% of the dose 4h after administration [9]. From the available clinical human study by Lubinus and co-workers, no intact SF was reported in the blood sample after consumption of SFs enriched yogurt, and only cycloartenol, which was thought as the product from SF **1**, was significantly increased by 23.7% compared on day 3 and day 0

[12]. This suggested that metabolism or degradation of SF **1** might have occurred in the gastrointestinal (GI) tract. Furthermore, Umehara and co-workers reported that in healthy volunteers the peak plasma concentration of SFs was 21 to 107 ng/mL (equivalent to 0.01-0.05% of the total administered dose) after an oral dose of 600 mg, and 112 ng/mL (< 0.3% of the dose) after repetitive oral dose of 100 mg three times a day for 10 days [24]. However, no information was so far available about the intestinal absorption of individual SFs, hence a different behaviour between individual SFs cannot be excluded.

In this study, we optimized the permeation conditions using a model compound SF **1**, to investigate the permeation of an array of naturally occurring SFs. Although very small amount (less than 0.5%) of individual SFs permeated across the Caco-2 cell monolayer, we still observed that some differences of $P_{app}$ were found between individual SFs, $P_{app}$ of SF **1** > **7**, **1** > **8**, and **3** > **7**. Examining the structural differences between these pairs of compounds lead us to believe that SF structures may influence their ability to permeate across the monolayer. SF **1** and **7** or **8** differ in both their sterol rings and side chains, SF **3** and **7** only differ in the presence and absence of one carbon at C-24 position. There is some evidence within literature that various sterols have different absorptions in the animal model, which was associated to the variation in their side chain (campesterol > sitosterol > stigmasterol) and saturation of double bond (sitosterol > sitostanol) [25]. In the view of physicochemical properties of eight SFs, we applied semi-empirical quantum mechanics method (AM1) for molecular simulation to explain their $P_{app}$ differences. The dipole moment and quantitative structure-activity relationship parameters (logP, surface area, volume, hydration energy, etc.) were obtained from the quantum mechanics simulations. However, we could not identify a distinct trend between their physicochemical properties and permeability (supporting information S6). Moreover, high mass recovery after permeation in this study suggested there was no significant hydrolysis, metabolism or degradation of SF by the cells. SFs were initially hypothesized to be hydrolysed to free ferulic acid and phytosterol, and could subsequently be absorbed [26]. Indeed, some *in vitro* studies have shown that SFs are substrate for cholesteryl esterase from animal pancreas and microorganism, and

cholesteryl esterase has strong preference for desmethylsteryl ferulate [8, 27, 28]. However, Huang found that the decrease in SFs concentration was not accompanied by either an increase in free phytosterols or in ferulic acid in *in vitro* cell model, indicating that hydrolysis of SF is still unclear [11]. Moreover, the hydrolysis is still possibly present by pancreatic and microbial cholesteryl esterase *in vivo* [12]. The Caco-2 cell model lacks gut microorganisms that may secrete cholesterol esterase; the significant hydrolysis of SF is not expected. Without additional analysis we cannot entirely exclude the possibility of SF degradation or hydrolysis occurring to a minor degree. Furthermore, the similar permeation of SF **1** both at 4°C and 37°C indicated that the transport mechanism functions primarily through passive diffusion. Nevertheless, it remains to be determined whether it occurs through paracellular or transcellular diffusion. The similar behaviours in permeation between SFs (SF **2** - **8**) to SF **1** (*e.g.* the similar TEER recording or low $P_{app}$ values) lead us to conclude that they also permeate through an analogous passive diffusion mechanism. Still, active transport cannot be fully excluded within this study. In our study, the low $P_{app}$ values resulted in extremely low levels of transported SFs and therefore in an analytical limitation. This hinders further analysis of potential hydrolytic products of SFs, as well as the analysis of a possible active transport.

SFs are primarily found in the bran of certain cereal grains and seeds. Their biosynthetic pathway as well as location within the plant cells remains unknown. Their function in plants may be related to protection against environmental stress [29], antioxidant property [30] and regulation of microbial activity in the grains [1]. Dietary intake of SFs usually comes from cereal grains like rice, wheat and corn. However, according to our previous study, the bioaccessibility of SFs was found to be almost negligible (0.1%) from a grain matrix [2], which indicates that SFs do not need to be highly absorbable from the complex grain matrix to provide their functional effect. Furthermore, the low absorption behaviour, confirmed in this study, suggests that the cholesterol-lowering and antioxidant activity related health benefits associated with SFs most likely occur in the gut independently from absorption. For instance, a recent work by Mäkynen and co-workers showed that SFs (γ-oryzanol) significantly inhibited incorporation of

cholesterol into synthetic micelles, and also SFs had ability to significantly decrease the apical uptake of cholesterol into Caco-2 cells [31]. Moreover, many of the poorly absorbed dietary antioxidants indeed play an important role in protecting the GI tract from oxidative damage without necessarily being absorbed [32]. Their concentration can be much higher in the lumen of GI tract than are ever achieved in plasma or tissues, and their antioxidant action in the GI tract can delay the development of inflammation and related disease (e.g. cancer) in stomach or colon [33]. SFs showed the potential to ameliorate colonic inflammation in colitis mice model by inhibiting NF-κB activity and decreasing pro-inflammatory cytokines and COX-2 levels due to their antioxidant effects [34]. Furthermore, they may act as antioxidants against reactive oxygen species produced by intestinal microflora. Little is known about the bioactivities of SFs in the digesta, an area which remains to be explored. The results of this work confirm that all the individual SFs share the same behavior: they are poorly absorbed compounds and their health benefits most likely occur in the gut independently from absorption.

## Acknowledgements

The authors declare no competing financial interest.

# 5 References

[1] Seitz, L. M., Stanol and sterol esters of ferulic and p-coumaric acids in wheat, corn, rye, and triticale. *J. Agric. Food Chem.* 1989, *37*, 662-667.

[2] Mandak, E., Nyström, L., The effect of in vitro digestion on steryl ferulates from rice (Oryza sativa L.) and other grains. *J. Agric. Food Chem.* 2012, *60*, 6123-6130.

[3] Ghatak, S. B., Panchal, S. J., Gamma-oryzanol-A multi-purpose steryl ferulate. *Curr. Nutr. Food Sci.* 2011, *7*, 10-20.

[4] Cicero, A., Derosa, G., Rice bran and its main components: potential role in the management of coronary risk factors. *Curr. Top. Nutraceutical Res.* 2005, *3*, 29-46.

[5] Nyström, L., in: Xu, Z., Howard, L. R. (Eds.), *Analysis of Antioxidant-Rich Phytochemicals*, Wiley-Blackwell, Oxford, UK 2012, pp. 313-351.

[6] Bergman, C. J., Xu, Z., Genotype and environment effects on tocopherol, tocotrienol, and γ-oryzanol contents of southern U.S. rice. *Cereal Chem.* 2003, *80*, 446-449.

[7] Nyström, L., Mäkinen, M., Lampi, A. M., Piironen, V., Antioxidant activity of steryl ferulate extracts from rye and wheat bran. *J. Agric. Food Chem.* 2005, *53*, 2503-2510.

[8] Nyström, L., Moreau, R. A., Lampi, A.-M., Hicks, K. B., Piironen, V., Enzymatic hydrolysis of steryl ferulates and steryl glycosides. *Eur. Food Res. Technol.* 2008, *227*, 727-733.

[9] Fujiwara, S., Sakurai, S., Sugimoto, I., Awata, N., Absorption and metabolism of gamma-oryzanol in rats. *Chem. Pharm. Bull.* 1983, *31*, 645-652.

[10] Fujiwara, S., Sakurai, S., Noumi, K., Sugimoto, I., Awata, N., Metabolism of gamma-oryzanol in rabbit. *Yakugaku zasshi* 1980, *100*, 1011-1018.

[11] Huang, C. J., Potential functionality and digestibility of oryzanol as determined using in vitro cell culture models. PhD thesis. Louisiana State University 2003.

[12] Lubinus, T., Barnsteiner, A., Skurk, T., Hauner, H., Engel, K. H., Fate of dietary phytosteryl/-stanyl esters: analysis of individual intact esters in human feces. *Eur. J. Nutr.* 2013, *52*, 997-1013.

[13] Carey, M. C., Small, D. M., Bliss, C. M., Lipid digestion and absorption. *Annu. Rev. Physiol.* 1983, *45*, 651-677.

[14] Hubatsch, I., Ragnarsson, E. G., Artursson, P., Determination of drug permeability and prediction of drug absorption in Caco-2 monolayers. *Nat. Protoc.* 2007, *2*, 2111-2119.

[15] Mandak, E., Zhu, D., Godany, T. A., Nyström, L., Fourier transform infrared spectroscopy and Raman spectroscopy as tools for identification of steryl ferulates. *J. Agric. Food Chem.* 2013, *61*, 2446-2452.

[16] Hamada, T., Goto, H., Yamahira, T., Sugawara, T.*, et al.*, Solubility in and affinity for the bile salt micelle of plant sterols are important determinants of their intestinal absorption in rats. *Lipids* 2006, *41*, 551-556.

[17] Tavelin, S., Gråsjö, J., Taipalensuu, J., Ocklind, G., Artursson, P., in: Wise, C. (Ed.), *Epithelial Cell Culture Protocols*, Humana Press, Totowa 2002, pp. 233-272.

[18] Yu, H., Huang, Q., Investigation of the absorption mechanism of solubilized curcumin using Caco-2 cell monolayers. *J. Agric. Food Chem.* 2011, *59*, 9120-9126.

[19] Fang, N., Yu, S., Badger, T. M., Characterization of triterpene alcohol and sterol ferulates in rice bran using LC-MS/MS. *J. Agric. Food Chem.* 2003, *51*, 3260-3267.

[20] Rieux, A. d., Ragnarsson, E. G. E., Gullberg, E., Préat, V.*, et al.*, Transport of nanoparticles across an in vitro model of the human intestinal follicle associated epithelium. *Eur. J. Pharm. Sci.* 2005, *25*, 455-465.

[21] Los, D. A., Murata, N., Membrane fluidity and its roles in the perception of environmental signals. *Biochim. Biophys. Acta - Biomembranes* 2004, *1666*, 142-157.

[22] Holtzman, E., in: Holtzman, E. (Ed.), *Lysosomes*, Springer US 1989, pp. 25-92.

[23] Artursson, P., Palm, K., Luthman, K., Caco-2 monolayers in experimental and theoretical predictions of drug transport. *Adv. Drug Deliv. Rev.* 2001, *46*, 27-43.

[24] Umehara, K., Shimokawa, Y., Miyamoto, G., Effect of gamma-oryzanol on cytochrome P450 activities in human liver microsomes. *Biol. Pharm. Bull.* 2004, *27*, 1151-1153.

[25] Ling, W. H., Jones, P. J., Dietary phytosterols: a review of metabolism, benefits and side effects. *Life Sci.* 1995, *57*, 195-206.

[26] Berger, A., Rein, D., Schafer, A., Monnard, I.*, et al.*, Similar cholesterol-lowering properties of rice bran oil, with varied gamma-oryzanol, in mildly hypercholesterolemic men. *Eur. J. Nutr.* 2005, *44*, 163-173.

[27] Miller, A., Majauskaite, L., Engel, K.-H., Enzyme-catalyzed hydrolysis of γ-oryzanol. *Eur. Food Res. Technol.* 2004, *218*, 349-354.

[28] Moreau, R. A., Hicks, K. B., The in vitro hydrolysis of phytosterol conjugates in food matrices by mammalian digestive enzymes. *Lipids* 2004, *39*, 769-776.

[29] Britz, S. J., Prasad, P. V., Moreau, R. A., Allen, L. H. J.*, et al.*, Influence of growth temperature on the amounts of tocopherols, tocotrienols, and gamma-oryzanol in brown rice. *J. Agric. Food Chem.* 2007, *55*, 7559-7565.

[30] Nantiyakul, N., Furse, S., Fisk, I., Foster, T.*, et al.*, Phytochemical composition of Oryza sativa (rice) bran oil bodies in crude and purified Isolates. *J. Amer. Oil Chem. Soc.* 2012, *89*, 1867-1872.

[31] Mäkynen, K., Chitchumroonchokchai, C., Adisakwattana, S., Failla, M., Ariyapitipun, T., Effect of gamma-oryzanol on the bioaccessibility and synthesis of cholesterol. *Eur. Rev. Med. Pharmacol. Sci.* 2012, *16*, 49-56.

[32] Stahl, W., van den Berg, H., Arthur, J., Bast, A.*, et al.*, Bioavailability and metabolism. *Mol. Aspects Med.* 2002, *23*, 39-100.

[33] Halliwell, B., Zhao, K., Whiteman, M., The gastrointestinal tract: a major site of antioxidant action? *Free Radic. Res.* 2000, *33*, 819-830.

[34] Islam, M. S., Murata, T., Fujisawa, M., Nagasaka, R.*, et al.*, Anti-inflammatory effects of phytosteryl ferulates in colitis induced by dextran sulphate sodium in mice. *Br. J. Pharmacol.* 2008, *154*, 812-824.

# Supporting Information

## S1. Quantification of SFs by ultra performance liquid chromatography with high-resolution mass spectrometric detection (UPLC-MS)

Most of the absorption studies regarding γ-oryzanol, cholesterol, phytosterols or other type of steryl conjugates were performed with radiolabeled components due to the limit of traditional detection technique [1, 2]. Importantly, this highly sensitive and accurate UPLC-MS quantification method represents a useful tool to investigate individual SFs in extremely low concentrations, bypassing the requirement of radioactivity handling.

### S1.1. Instrument parameters

The analysis was performed with a Waters ACQUITY UPLC® system with an ACQUITY UPLC BEH C18 column (50 mm × 2.1 mm, 1.7 μm particle size) connected to a MS system (Synapt G2) with an electrospray ionization source (ESI) and a quadrupole time-of-flight (Q-TOF) analyser (Waters Corp., Milford, MA, USA). For a precise injection volume, 10 μL of the sample was injected in full loop mode. To separate SFs in UPLC, the mobile phase was composed of A ($H_2O$ + 0.05% $NH_4OH$, v/v) and B (acetonitrile: isopropanol 90:10), with a gradient from 20% A to 8% A in the first 1 min, followed by isocratic condition of 8% A until 8.8 min, then in the last 0.2 min back to 20% A. The column temperature was 40°C and flow rate of 0.5 mL/min. For SF detection, the MS conditions were as follows: the voltages of capillary, sampling cone and extraction cone 2.5 kV, 60 V and 4 V in ESI negative ion mode, respectively. The temperature for source was 120 °C and 550°C for desolvation. The cone and desolvation gas (nitrogen) flow rates were 20 and 800 L/h, respectively. Mass spectra were acquired from m/z 50-1200 at a scan rate of 0.5 s in continuum mode. The fragment ion information was gained by setting collision energy ramp from 40 to 60 eV in the trap region. Peaks were identified based on the mass to charge ratio (m/z) of the compounds and relative retention time (RRT) compared with internal standard. Data acquisition and processing were performed using MassLynx 4.1 and Quanlynx software

(Waters Corp.) with automatic Savitzky-Golay smoothing (interactions = 1 and width = 2) and chromatogram mass window of 0.02 Da.

## S1.2. Internal standard and method validation

First, internal standard solution was added directly into the samples collected from transport study, and then SFs were extracted with solvent as previously described (in 2.3.2).

For the quantification of cholesteryl ferulate (SF **8**), internal standard was cycloartenyl ferulate (SF **1**) in acetonitrile, with levels of addition from 9 ng to 20.25 ng for the samples from basolateral chamber during different incubation time. The limit of detection (LOD) and the limit of quantification (LOQ) were defined as 3 and 10 times of the signal-to-noise ratio (S/N) in the region of internal standard in the chromatogram, respectively. The linear range of SF **1** was 4.5 to 405 ng/mL with the correlation coefficient $R^2 \geq 0.967$. The lowest point of calibration curve (4.5 ng/mL) was used as the LOQ. LOD was 1.35 ng/mL. Internal standard recovery for the samples collected from the basolateral chamber was mainly 60% to 110%.

And for the other SFs (SF**1**-**7**), SF **8** was used as internal standard, with levels of addition from 7.8 to 60.75 ng for the samples from basolateral chamber according to the different incubation time and transport assay conditions. Linear range of SF **8** was 5.2 to 312 ng/mL, $R^2 \geq 0.996$. LOQ was 5.2 ng/mL and LOD was 1.56 ng/mL. Internal standard recovery from basolateral chamber was mainly 70%-110%.

## S2. Validation of SF solution

SFs in this study were dissolved in HBSS with oleic acid, 1-monoolein, phosphatidylcholine and sodium taurocholate. The "micelle" size was determined by dynamic light scattering with a Delsa Nano C Particle Analyzer (Beckman Coulter,

USA). Individual SFs had the similar particle sizes and no significant difference among them was observed (Table S1).

**Table S1** Micelle size in HBSS. Data are expressed as mean ± SEM (n=6).

| Compounds | Diameters (nm) |
| --- | --- |
| V (70 μM) [a] | 105±5 |
| V (190 μM) [b] | 110±3 |
| SF **1** (70 μM) | 101±4 |
| SF **1** (190 μM) | 109±4 |
| SF **2** [c] | 96±6 |
| SF **3** [c] | 98±3 |
| SF **4** [c] | 99±5 |
| SF **5** [c] | 105±4 |
| SF **6** [c] | 93±4 |
| SF **7** [c] | 99±4 |
| SF **8** [c] | 94±3 |

[a]: vehicle, amount equals to the one in the solutions of SF **1** - **8** at 70 μM.
[b]: vehicle, amount equals to the one in the solution of SF **1** at 190 μM.
[c]: The concentration of SF in solution is 70 μM.

## S3. Permeability coefficient calculation of Lucifer Yellow (LY) in different conditions

The calculation procedure of permeability coefficient (Papp) was according to protocol by Hubatsch et al. [3] and Tavelin et al. [4].

**Table S2** Concentrations, cumulative amount and fraction transported of LY in different conditions over time (Data are expressed as mean ± SEM (n=3-6).

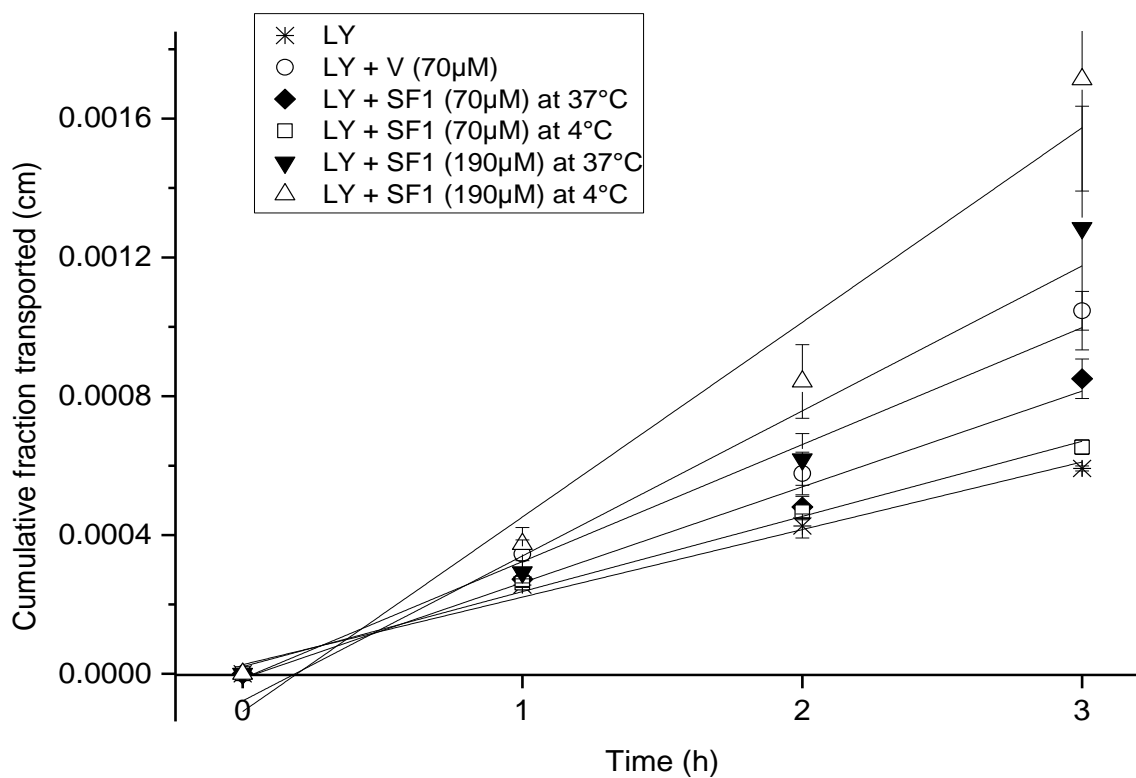| | Concentration in receiver (μM) | | | Cumulative amount transported (nmol) | | | Cumulative fraction transported ($10^{-4}$ cm) | | |
|---|---|---|---|---|---|---|---|---|---|
| | 1 h | 2 h | 3 h | 1 h | 2 h | 3 h | 1 h | 2 h | 3 h |
| LY | 0.31±0.01 | 0.37±0.07 | 0.39±0.05 | 0.47±0.01 | 0.78±0.05 | 1.09±0.03 | 2.6±0.1 | 4.3±0.3 | 5.9±0.1 |
| LY + V (70μM) | 0.46±0.17 | 0.54±0.17 | 0.86±0.17 | 0.69±0.10 | 1.16±0.16 | 2.05±0.07 | 3.5±0.4 | 5.8±0.6 | 10.5±0.6 |
| LY + SF**1** (70 μM) at 37 °C | 0.31±0.05 | 0.40±0.06 | 0.63±0.22 | 0.47±0.03 | 0.83±0.04 | 1.48±0.12 | 2.7±0.2 | 4.8±0.3 | 8.5±0.6 |
| LY + SF**1** (70 μM) at 4 °C | 0.31±0.03 | 0.40±0.05 | 0.42±0.05 | 0.47±0.02 | 0.84±0.04 | 1.17±0.04 | 2.6±0.1 | 4.7±0.2 | 6.5±0.2 |
| LY + SF**1** (190 μM) at 37 °C | 0.33±0.03 | 0.53±0.18 | 1.01±0.84 | 0.50±0.02 | 1.04±0.12 | 2.16±0.57 | 2.9±0.1 | 6.2±0.7 | 12.8±3.5 |
| LY + SF**1** (190 μM) at 4 °C | 0.44±0.13 | 0.77±0.28 | 1.41±0.81 | 0.65±0.08 | 1.48±0.19 | 3.01±0.59 | 3.7±0.5 | 8.4±1.1 | 17.1±3.2 |

**Figure S1** Cumulative fraction transported of LY in different conditions over time. The slope of linear-fit was $P_{app}$.

## S4. Permeability coefficient calculation of SF 1 in different conditions

**Table S3** Concentrations, cumulative amount and fraction transported of SF **1** in different conditions over time. Data are expressed as

mean ± SEM (n=6 - 9).

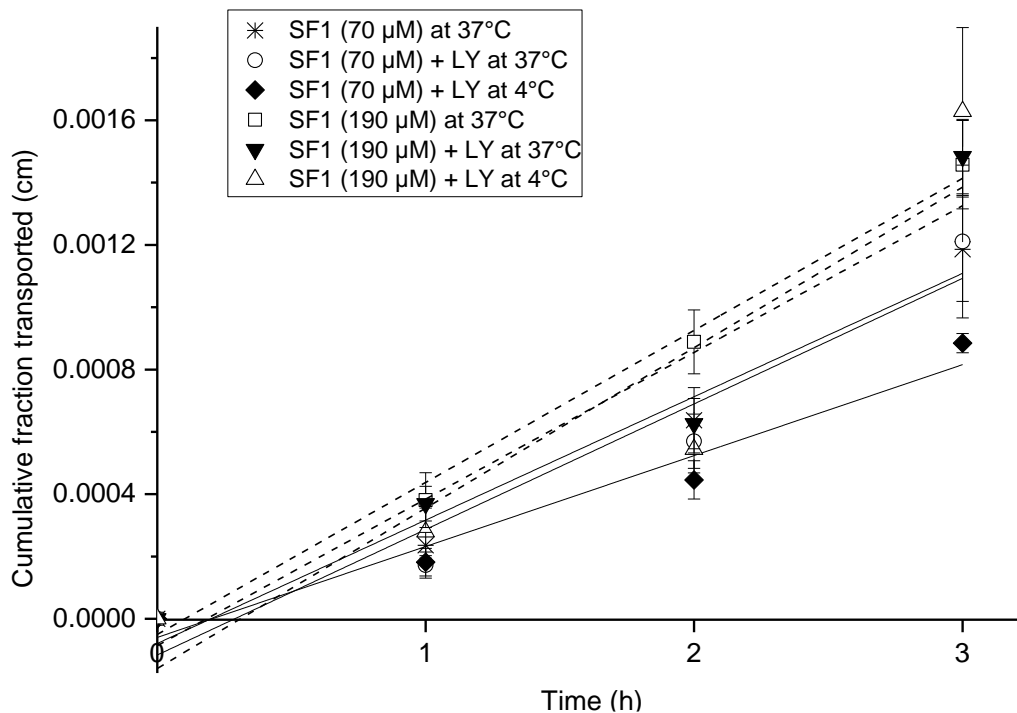| | Concentration in receiver (µM) | | | Cumulative amount transported (nmol) | | | Cumulative fraction transported ($10^{-4}$ cm) | | |
|---|---|---|---|---|---|---|---|---|---|
| | 1 h | 2 h | 3 h | 1 h | 2 h | 3 h | 1 h | 2 h | 3 h |
| SF**1** (70µM) at 37°C | 0.010 ± 0.002 | 0.022 ± 0.004 | 0.034 ± 0.005 | 0.015 ± 0.003 | 0.040 ± 0.007 | 0.075 ± 0.011 | 2.4 ± 0.4 | 6.4 ± 1.0 | 11.9 ± 1.7 |
| SF**1** (70µM) + LY at 37°C | 0.007 ± 0.002 | 0.020 ± 0.003 | 0.037 ± 0.008 | 0.011 ± 0.003 | 0.036 ± 0.005 | 0.076 ± 0.015 | 1.7 ± 0.4 | 5.7 ± 0.9 | 12.1 ± 2.5 |
| SF**1** (70µM) + LY at 4°C | 0.008 ± 0.002 | 0.015 ± 0.002 | 0.026 ± 0.002 | 0.011 ± 0.003 | 0.028 ± 0.004 | 0.056 ± 0.002 | 1.8 ± 0.4 | 4.5 ± 0.6 | 8.8 ± 0.3 |
| SF**1** (190µM) at 37°C | 0.043 ± 0.010 | 0.080 ± 0.009 | 0.104 ± 0.009 | 0.065 ± 0.015 | 0.152 ± 0.017 | 0.249 ± 0.024 | 3.8 ± 0.9 | 8.9 ± 1.0 | 14.6 ± 1.4 |
| SF**1** (190µM) + LY at 37°C | 0.042 ± 0.006 | 0.050 ± 0.007 | 0.123 ± 0.013 | 0.063 ± 0.010 | 0.107 ± 0.014 | 0.253 ± 0.020 | 3.7 ± 0.6 | 6.3 ± 0.8 | 14.8 ± 1.2 |
| SF**1** (190µM) + LY at 4°C | 0.032 ± 0.009 | 0.046 ± 0.008 | 0.146 ± 0.032 | 0.048 ± 0.013 | 0.093 ± 0.013 | 0.278 ± 0.046 | 2.8 ± 0.8 | 5.4 ± 0.8 | 16.3 ± 2.7 |

**Figure S2** Cumulative fraction transported of SF **1** in different conditions over time (solid line for 70 μM, dashed line for 190 μM). The slope of linear-fit was $P_{app}$.
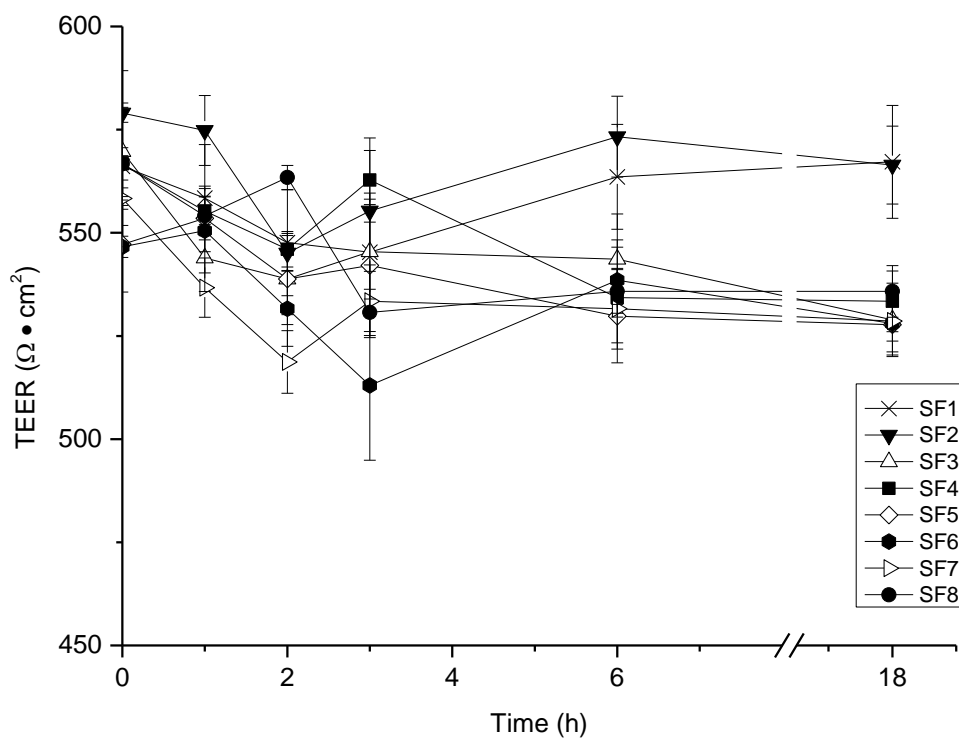
## S5. Permeability coefficient calculation of SFs



**Figure S3** Variation of TEER of Caco-2 monolayer as a function of apical exposure of individual SFs (SF **1** - **8**, 70 μM) at 37°C. Data are expressed as mean ± SEM (n = 6 - 9).

**Table S4** Concentrations, cumulative amount and fraction transported of SF **1 - 8** over time. Data are expressed as mean ± SEM (n=6 - 9).

| | Concentration in receiver (µM) | | | Cumulative amount transported (nmol) | | | Cumulative fraction transported ($10^{-4}$ cm) | | |
|---|---|---|---|---|---|---|---|---|---|
| | 1 h | 2 h | 3 h | 1 h | 2 h | 3 h | 1 h | 2 h | 3 h |
| SF**1** | 0.010±0.002 | 0.022±0.004 | 0.034±0.005 | 0.015±0.003 | 0.040±0.007 | 0.075±0.011 | 2.4±0.4 | 6.4±1.0 | 11.9±1.7 |
| SF**2** | 0.003±0.001 | 0.005±0.001 | 0.011±0.002 | 0.005±0.001 | 0.010±0.001 | 0.023±0.003 | 0.8±0.1 | 1.6±0.2 | 3.7±0.5 |
| SF**3** | 0.004±0.001 | 0.006±0.001 | 0.011±0.001 | 0.005±0.001 | 0.012±0.001 | 0.025±0.002 | 0.9±0.2 | 2.0±0.2 | 3.9±0.4 |
| SF**4** | 0.007±0.003 | 0.013±0.004 | 0.022±0.005 | 0.011±0.005 | 0.025±0.008 | 0.048±0.014 | 1.8±0.8 | 4.0±1.3 | 7.6±2.2 |
| SF**5** | 0.012±0.004 | 0.014±0.004 | 0.022±0.004 | 0.018±0.006 | 0.030±0.008 | 0.052±0.011 | 2.8±0.9 | 4.8±1.3 | 8.2±1.7 |
| SF**6** | 0.010±0.004 | 0.019±0.006 | 0.036±0.015 | 0.016±0.007 | 0.036±0.012 | 0.075±0.030 | 2.5±1.0 | 5.7±2.0 | 12.0±4.9 |
| SF**7** | 0.002±0.001 | 0.006±0.001 | 0.009±0.001 | 0.004±0.001 | 0.010±0.002 | 0.019±0.003 | 0.6±0.1 | 1.7±0.4 | 3.0±0.5 |
| SF**8** | 0.002±0.001 | 0.003±0.001 | 0.006±0.001 | 0.003±0.001 | 0.006±0.001 | 0.013±0.002 | 0.5±0.2 | 1.0±0.2 | 2.0±0.3 |

Note: Nonparametric test with Kruskal–Wallis analysis of variance and subsequent post-hoc analysis (pairwise comparisons) was performed with SPSS on the cumulative amount transported of individual SFs over time. The cumulative amount transported of SF **1** is significantly higher than SF **8** at 1 h, 2 h and 3 h. Moreover, at 3 h, SF **5** is significantly higher than SF **8**; SF **1** is significantly higher than SF **7**. Other cumulative amounts transported of individual SFs over time are not statistically significantly different.
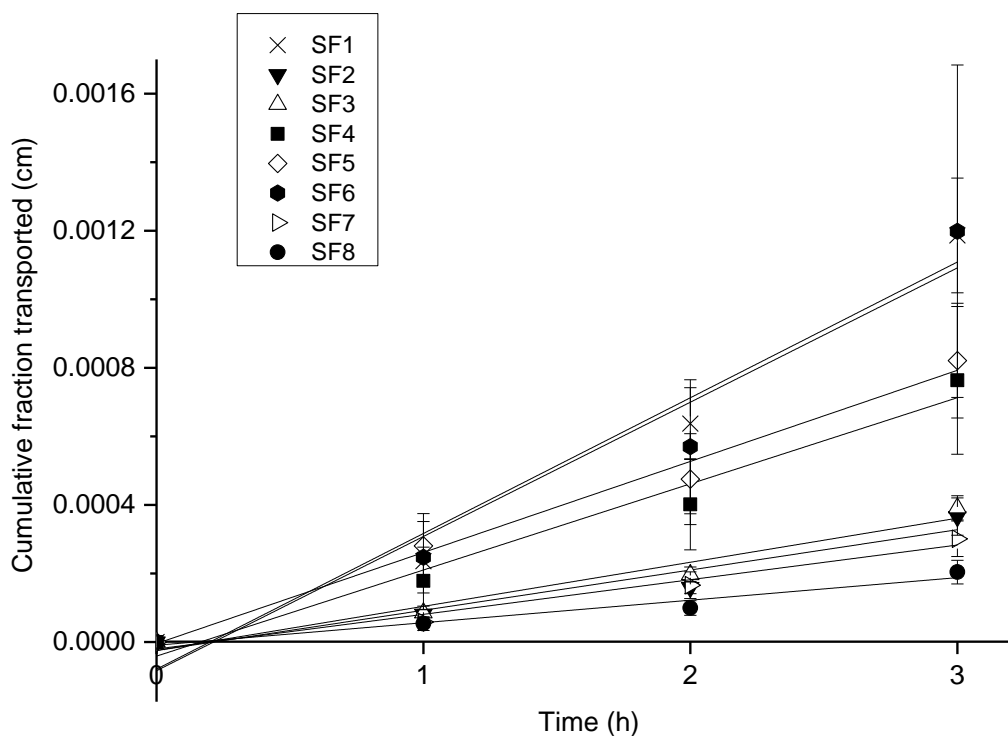
**Figure S4** Cumulative fraction transported of individual SFs (SF **1** - **8**, 70 μM) over time. The slope of linear-fit was $P_{app}$.

## S6. Correlation between permeability coefficient and physicochemical properties of SFs

Molecular simulation of eight SFs was conducted by HyperChem 8.0.3 software. There was no significant correlation between their physicochemical properties and permeability. Correlation was analysed by IBM SPSS Statistics 19.0 based on Pearson's correlation coefficients ($p < 0.05$, 2-tailed).

**Table S5** Correlation between permeability coefficient and physicochemical properties of SFs

| Physicochemical properties | Pearson's Correlation | |
|---|---|---|
| | Coefficient | $p$ value |
| Connolly surface area ($\text{Å}^2$) | 0.050 | 0.907 |
| Connolly volume ($\text{Å}^3$) | 0.297 | 0.474 |
| Hydration energy (kcal/mol) | 0.586 | 0.127 |
| logP | 0.599 | 0.117 |
| Refractivity ($\text{Å}^3$) | 0.269 | 0.520 |
| Polarizability ($\text{Å}^3$) | 0.444 | 0.270 |
| Dipole Moment (D) | -0.001 | 0.998 |
| Mass (Da) | 0.336 | 0.416 |
| Density ($\text{kg/m}^3$) | -0.498 | 0.209 |

## References of supporting information

[1] Fujiwara, S., Sakurai, S., Sugimoto, I., Awata, N., Absorption and metabolism of gamma-oryzanol in rats. *Chem. Pharm. Bull.* 1983, *31*, 645-652.

[2] Yamanashi, Y., Takada, T., Suzuki, H., Niemann-Pick C1-like 1 overexpression facilitates ezetimibe-sensitive cholesterol and β-sitosterol uptake in CaCo-2 cells. *J. Pharmacol. Exp. Ther.* 2007, *320*, 559-564.

[3] Hubatsch, I., Ragnarsson, E. G., Artursson, P., Determination of drug permeability and prediction of drug absorption in Caco-2 monolayers. *Nat. Protoc.* 2007, *2*, 2111-2119.

[4] Tavelin, S., Gråsjö, J., Taipalensuu, J., Ocklind, G., Artursson, P., in: Wise, C. (Ed.), *Epithelial Cell Culture Protocols*, Humana Press, Totowa 2002, pp. 233-272.

# PART 3 - Conclusions and Outlook

## Conclusions

In the present study, it was demonstrated that profiles of individual steryl ferulates varied depending on the rice varieties. The analysis of steryl ferulates by UPLC-HR-Q-TOF-MS method was newly developed. With OMIC approach, the differentiation of rice varieties was achieved with characteristic markers based on their steryl ferulate profiles and other potential small lipids. In addition to steryl ferulates, this sensitive analytical technique could also reveal several new compounds of bioactive lipids in rice, *e.g.*, steryl *p*-coumarate and sinapate. Furthermore, this method could potentially be applied for rice authentication.

Individual steryl ferulates exhibited DPPH radical, hydroxyl radical and superoxide anion radical scavenging abilities. Generally, the difference in their antioxidant activity was very small and depended greatly on the reaction models. In addition to the intra-molecular variations, intermolecular interactions, as well as interactions with the solvent (environment), should also be considered. Thus, the same steryl ferulate compound could show different scavenging properties depending on the substrate studied, as well as the kind of radical scavenging process taking place. The solvation energy was observed to significantly influence the antioxidant activity, and the trend was that the higher the solvation energy, the better the antioxidant activity.

In the model of methyl linoleate autoxidation, steryl ferulates induced a retarding of oxidation and no definite induction period was detected, indicating that steryl ferulates could not break the chain reactions completely. Furthermore, there was no significant difference in antioxidant effect among individual steryl ferulates in this model. Steryl ferulates possessed antioxidant activity, however, less effective than the other commonly used antioxidants, such as α-tocopherol.

Steryl ferulates had very low apparent permeability coefficients in Caco-2 cell monolayer, indicating that their permeation across the gut is very low. Although only a negligible amount of steryl ferulates permeated across the monolayer, still some significant differences were observed between different steryl ferulate species, *e.g.*, cycloartenyl ferulate > stigmasteryl and cholesteryl ferulates, as well as campesteryl ferulate > stigmasteryl ferulate. No direct trend between their physicochemical properties and permeability was observed. Furthermore, the permeation mechanism of steryl ferulate was mainly through passive diffusion. High mass recovery after permeation in this study suggested that there was no significant hydrolysis, metabolism or degradation of steryl ferulates by the cells. Moreover, the results of this work confirmed that all the individual SFs are poorly absorbed compounds and their health benefits most likely occur in the gut independently from absorption.

Results of this project provide better insight into the occurrence and bioactivities of individual steryl ferulates and understanding of the health benefits of whole grains that are the main sources of these bioactive compounds. Once the potential beneficial health effects of individual steryl ferulates are clearly understood, more efficient crop selection and processing methods can be employed to enhance the steryl ferulate quality of edible grains.

## Outlook

The UPLC-HR-Q-TOF-MS method together with OMIC approach might reveal several new compounds of bioactive lipids in rice; however, due to the limited identification performed in this study, these small lipids need further characterization and identification. Moreover, more rice varieties should be investigated to enlarge the database of small bioactive lipids (markers) and further to create the prediction model to be applied for unknown samples, which need to be identified and differentiated.

The antioxidant activity of steryl ferulates should be reconsidered based on the reaction occurring, and with respect to the food product to be studied, along with other synergistic processes that might happen in natural settings. The subtle differences of their antioxidant activity were from the intra-molecular variations, the intermolecular interactions as well as the interactions with the solvent (environment), to better understand the reasons underlying the differences in activities, simulation and experiments concerning these factors could be carried out. Furthermore, to date, antioxidant studies of steryl ferulates have mostly been performed in oil systems and radical scavenging systems *in vitro*; to gain more information on their antioxidant activity *in vivo*, cell models, animal models and clinical studies should be applied.

The permeation study indicated that the transport mechanism functions primarily through passive diffusion. Nevertheless, it remains to be determined whether it occurs through paracellular or transcellular diffusion. The low $P_{app}$ values resulted in extremely low levels of transported steryl ferulates, and no metabolic products generated from steryl ferulates could be detected. Still, active transport and potential hydrolysis to a small extent cannot be fully excluded with this study. To date, there is no clear evidence to explain the possible hydrolysis, metabolism and degradation *in vivo*. Furthermore, although only a negligible amount permeated across the monolayer, still some significant differences were observed between different steryl ferulate species. The reason of this phenomenon remains unknown. Therefore, more research is required in order to clarify these questions.

For health humans, the absorption ratio of cholesterol is more than 40%, and that of phytosterols is usually less than 5%, whereas for steryl ferulates, the ratio is negligible. It will be interesting to explore the roles of certain influx transporter or efflux pump on/in the enterocyte in the absorption of steryl ferulates. Furthermore, their low absorption behaviour confirmed in this study, suggests that their cholesterol-lowering and antioxidant activity related health benefits most likely occur in the gut independently from absorption. Little is known about the bioactivities of steryl ferulates in the digesta, an area that remains to be studied. Once the bioactivities of steryl

ferulates *in vivo* as well as their absorption behaviour are clearly understood, the recommendation dosage could be well suggested and the supplementation or formulation of steryl ferulates could be developed to enhance their bioactivity.